



Studies of Biological Active Peptides

(Structure determination, Synthesis and Activity)

A thesis submitted in fulfilment of the requirements for the degree of

Doctor of Philosophy

by

Pinmanee Boontheung

Master of Science (Chemistry)

Bachelor of Pharmacy

Department of Chemistry

The University of Adelaide



**THE UNIVERSITY
OF ADELAIDE**
AUSTRALIA

January, 2003

CONTENTS

Acknowledgements	vi
Statement of Originality	viii
List of Figures	ix
List of Tables	xiii
Abstract	xv
Chapter One. Introduction	
1.1 Peptide Chemistry	1
1.2 The Structure of a Peptide	2
1.3 Types of Peptide Mediators	3
1.3.1 Hormones	4
1.3.2 Neuropeptides	5
1.4 Peptide Biosynthesis	5
1.5 Biological Properties of Peptides	7
1.6 Mass Spectrometry	7
1.6.1 General	7
1.6.2 Mass spectrometric determination of the peptide	8
1.6.3 Electrospray ionisation (ESI)	9
1.6.4 Finnigan LCQ electrospray mass spectrometer	12
1.6.5 QTOF 2 hybrid quadrupole time of flight mass spectrometer	14
1.7 Peptide Sequencing	15
1.7.1 Mass spectrometry	15
1.7.2 Automated Edman sequencing	17
1.7.3 Enzyme digestion	18
1.7.4 Determination of C-terminal end group	19
1.8 Bioactivity Testing	19
1.9 References	21

Chapter Two. Bioactive Peptides from Amphibians

2.1	Amphibians	25
2.2	Amphibian Skin and its Secretions	26
	2.2.1 Glandular characteristics	26
	2.2.2 Production of peptides	28
2.3	Amphibian Peptides and their Physiological Functions	29
2.4	Peptides from the Genus <i>Litoria</i>	31
	2.4.1 Smooth muscle active neuropeptides	32
	2.4.2 Neuronal nitric oxide synthase (NOS) inhibitors	33
	2.4.3 Antibiotic and anticancer active peptides	35
	2.4.4 Pheromones	42
	2.4.5 Other functions	43
2.5	Collection of Frog Peptides	44
2.6	References	46

Chapter Three. Peptides from *Litoria alboguttata* and *Cyclorana australis*

3.1	General	52
3.2	Results and Discussion	55
	3.2.1 Isolation and identification of peptides from the glandular secretion of <i>Litoria alboguttata</i>	55
	3.2.2 The genus <i>Cyclorana</i> -The particular case of <i>C. australis</i>	60
3.3	Conclusions	63
3.4	Experimental	64
	3.4.1 Collection and preparation of <i>Litoria alboguttata</i> secretions	64
	3.4.2 HPLC separation	65
	3.4.3 Mass spectrometry analysis	65
	3.4.4 Automated Edman sequencing	66
3.5	References	67

Chapter Four. The Isolation and Structure Determination of Eugenin, a neuropeptide isolated from the pouch of the pregnant female Tammar wallaby (*Macropus eugenii*)

4.1	Introduction	69
4.2	Tammar Wallaby (<i>Macropus eugenii</i>)	71
4.3	Brush-tailed Rock Wallaby (<i>Petrogale penicillata</i>)	73

4.4	Yellow-footed Rock Wallaby (<i>Petrogale xanthopus</i>)	75
4.5	Results and Discussion	76
4.5.1	Isolation of eugenin from the pouch of the Tammar wallaby (<i>Macropus eugenii</i>)	77
4.5.2	Other components isolated from the HPLC separations	82
4.6	Conclusions	87
4.7	Experimental	88
4.7.1	Collection and preparation of samples	88
4.7.2	Analytical and preparative HPLC	88
4.7.3	Mass spectrometry analysis	89
4.8	References	91
Chapter Five. Discovery of New Caerulein-like Peptides		
5.1	General	94
5.2	Caerulein-like Peptides from <i>Litoria citropa</i>	95
5.3	Caerulein-like Peptides from <i>Litoria splendida</i>	98
5.4	References	102
Chapter Six. Peptide Synthesis		
6.1	Introduction	104
6.2	Solid-phase Peptide Synthesis (SPPS)	105
6.2.1	Solid supports	107
6.2.2	Role of the resin support	112
6.2.3	The protecting group	114
6.2.4	Peptide bond formation	116
6.2.5	Determination of chain assembly	117
6.2.6	Deprotection and cleavage from the resin support	118
6.3	Synthesis of Tyrosine Sulfated Containing Peptides	120
6.4	Results and Discussion	122
6.4.1	Synthesis of desulfated caerulein and eugenin peptides	123
6.4.2	Synthesis of caerulein analogues and eugenin peptides	124
6.5	Conclusions	127
6.6	Experimental	127
6.6.1	General procedure	127

6.6.2	HPLC analysis	130
6.6.3	Mass spectrometry (MS)	131
6.7	Solid-phase Synthesis of Caerulein 1.2Y ⁴	131
6.8	Solid-phase Synthesis of Caerulein 3.1Y ⁴	132
6.9	Solid-phase Synthesis of Eugenin Y ⁴	133
6.10	Solid-phase Synthesis of Caerulein 1.2	134
6.11	Solid-phase Synthesis of Caerulein 2.1	135
6.12	Solid-phase Synthesis of Caerulein 2.2	136
6.13	Solid-phase Synthesis of Caerulein 3.1	137
6.14	Solid-phase Synthesis of Caerulein 3.2	138
6.15	Solid-phase Synthesis of Caerulein 4.1	139
6.16	Solid-phase Synthesis of Caerulein 4.2	140
6.17	Solid-phase Synthesis of Eugenin	141
6.18	Abbreviations	142
6.19	References	144

Chapter Seven. Bioactivity of Eugenin and Caerulein-like Peptides

7.1	Introduction	152
7.2	Characterisation of Tyrosine Sulfation Sites	153
7.2.1	Occurrence	153
7.2.2	Roles of tyrosine sulfation	154
7.2.3	Tyrosine sulfation and bioactivity	155
7.3	Caerulein-like Peptides	156
7.3.1	General	156
7.3.2	Pharmacological action	157
7.3.3	Target receptors	158
7.3.4	Caerulein and contraction activity	159
7.3.5	Caerulein and analgaesic activity	159
7.4	Structure-activity Relationship of Caerulein-like Peptides	161
7.5	Results and Discussion	162
7.6	Conclusions	164
7.7	Experimental	165
7.7.1	Antimicrobial testing	165
7.7.2	Contraction studies of eugenin	165

7.7.3	Contraction studies of caerulein analogues	167
7.8	References	169
Chapter Eight. Comparison of the Positive and Negative Ion Electrospray Mass Spectra of Small Peptides Containing Pyroglutamate		
8.1	Comparison of Positive and Negative Ion Mass Spectra of Peptides Containing Pyroglutamate	177
8.1.1	General	177
8.1.2	Results and discussion	178
8.2	Negative Ion Spectra of Caerulein-like Peptides	187
8.2.1	General	187
8.2.2	Results and discussion	189
8.3	Conclusions	194
8.4	Experimental	195
8.4.1	Preparation of synthetic peptides	195
8.4.2	Mass spectrometry	195
8.5	References	196
Summary and Conclusions		197
Publications		199

Acknowledgements

Whilst the thesis has been written under my name, many people have contributed in many ways to its completion. I would like to take this opportunity to express my sincere gratitude to them.

Foremost among those to be thanked is my supervisor, Professor John H. Bowie, who initiated this project. Over the years he has displayed a great deal of patience and tolerance whilst providing encouragement, guidance and insight throughout the project. His ability and willingness to collaborate with various individuals have been a great inspiration to me.

I would also like to thank Professor Paul Alewood, from Drug Design and Development Centre, University of Queensland, for his help and advice regarding solid-phase peptide synthesis techniques and Dr. Paramjit Bansal for continuous assistance in various aspects of the solid-phase synthesis of tyrosine sulfated containing peptides.

I would also like to thank the following people for their direct input into this thesis. Professor Russell Baudinette and Jane Skinner, from the Department of Environmental Biology, University of Adelaide, for providing the wallaby secretions. Associate Professor Mike Tyler and Ben Smith, from the Department of Environmental Biology, University of Adelaide, for providing the amphibian secretions. Associate Professor John C. Wallace, from the Department of Molecular Biosciences, University of Adelaide, for providing the automated Edman sequencing data. Thanks also to Dr. Ian Musgrave, from the Department of Pharmacology, University of Adelaide, for his help with the muscle contraction studies of eugenin and the Institute for Molecular Bioscience, University of Queensland, for conducting the contraction studies of caerulein analogues.

Thanks are also extended to all the academic, research and technical staff at the University of Adelaide for their help and advice – particularly Dr. Paul Wabnitz, Dr. Tom Rozek and Andrew McAnoy for mass spectrometry advice and Craig Brinkworth for his great help with the QTOF 2 mass spectrometer and Edman sequencing. Thanks also to the members

of the Bowie research group, especially Craig Brinkworth and Dr. Kate Wegener for the friendship, expert advice and comic relief in the last four years.

I am thankful to Craig Brinkworth, Margit Apponyi and Tara Pukala for their helping with proof reading this thesis.

I offer my very special thanks to my dear, Narongsak Tonmukayakul, for his encouragement, companionship and constant love. During the years we shared the emotional hardships and the happiness of my progress.

I would especially like to thank my parents for all the support they have given me throughout my life; without their sacrifices and devotion, I could never have achieved this much. *To my parents, I sincerely dedicate this thesis.*

Statement of Originality

This thesis contains no material that has been accepted for the award of any other degree or diploma in any university or other tertiary institution and, to the best of my knowledge and belief, contains no material previously published or written by another person except where due reference has been made in the text.

I give consent for this copy of my thesis, when deposited in the University Library, to be available for loan and photocopying.

Pinmanee Boontheung

31/1/03

Date

List of Figures

<i>Figure 1.1: The peptide bond</i>	2
<i>Figure 1.2: A schematic of the two canonical forms of the peptide bonds</i>	3
<i>Figure 1.3: Geometry of the peptide bond</i>	3
<i>Figure 1.4: Synthesis of a peptide mediator</i>	6
<i>Figure 1.5: The ESI process in the positive ion polarity mode</i>	11
<i>Figure 1.6: Finnigan LCQ mass spectrometer</i>	12
<i>Figure 1.7: Diagram of the LCQ</i>	13
<i>Figure 1.8: Schematic diagram of the QTOF 2 mass spectrometer</i>	14
<i>Figure 1.9: A diagram of the fragment ions produced in positive mode</i>	16
<i>Figure 1.10: Illustration of the Edman degradation cycle</i>	17
<i>Figure 1.11: Lys-C digestion</i>	18
<i>Figure 1.12: Determination of the C-terminal end group by methylation</i>	19
<i>Figure 2.1: Litoria splendida</i>	27
<i>Figure 2.2: Litoria caerulea</i>	27
<i>Figure 2.3: The granular gland of a frog</i>	28
<i>Figure 2.4: Schematic diagram showing the biosynthesis route of a active peptide formation</i>	29
<i>Figure 2.5: Edman helical wheel projection</i>	36
<i>Figure 2.6: A picture illustrating the 'barrel-stave' model suggested for membrane permeation</i>	37
<i>Figure 2.7: A picture illustrating the 'carpet-like' model suggested for membrane permeation</i>	38
<i>Figure 2.8: The 3D structure of caerin 1.1</i>	40
<i>Figure 2.9: The 3D structure of maculatin 1.1</i>	40
<i>Figure 2.10: The 3D structure of aurein 1.2</i>	41
<i>Figure 2.11: The 3D structure of citropin 1.1</i>	42

Figure 3.1: <i>L. alboguttata</i>	53
Figure 3.2: <i>C. australis</i>	53
Figure 3.3: Diagram of the geographic distribution of <i>Litoria alboguttata</i>	54
Figure 3.4: Diagram of the geographic distribution of <i>Cyclorana australis</i>	55
Figure 3.5: HPLC chromatogram from the crude secretions of <i>L. alboguttata</i>	56
Figure 3.6: MS/MS data of guttatin 1	57
Figure 3.7: MS/MS data of guttatin 2	58
Figure 3.8: MS/MS data of guttatin 3	59
Figure 3.9: HPLC chromatogram from the crude secretions of <i>Cyclorana australis</i>	61
Figure 3.10: MS/MS data of (MH ⁺) 715 from <i>C. australis</i>	62
Figure 3.11: MS/MS data of (MH ⁺) 786 from <i>C. australis</i>	63
Figure 4.1: The development processes of the young marsupial	70
Figure 4.2: Picture of a Tammar wallaby (<i>Macropus eugenii</i>)	72
Figure 4.3: Diagram of the geographic distribution of the Tammar wallaby	72
Figure 4.4: Picture of a Brush-tailed Rock wallaby (<i>Petrogale penicillata</i>)	74
Figure 4.5: Diagram of the geographic distribution of the Brush-tailed Rock wallaby	74
Figure 4.6: Picture of a Yellow-footed Rock wallaby (<i>Petrogale xanthopus</i>)	75
Figure 4.7: Diagram of the geographic distribution of the Yellow-footed Rock wallaby	76
Figure 4.8: HPLC separation of the pouch secretion of female <i>M. eugenii</i>	78
Figure 4.9: CID electrospray mass spectrum (MS/MS) of [(MH ⁺)-SO ₃] ⁺ ion of eugenin	80
Figure 4.10: CID electrospray mass spectrum (MS/MS) of [(MH)-SO ₃] ⁻ ion of eugenin	81
Figure 4.11: HPLC separation of the pouch secretion of female <i>P. xanthopus</i>	83
Figure 4.12: HPLC separation of the pouch secretion of female <i>P. penicillata</i>	84
Figure 4.13: MS/MS data of m/z 453	85
Figure 4.14: MS/MS data of (MH ⁺) ion m/z 679	86
Figure 4.15: MS/MS data of (M-H) ⁻ ion of m/z 677	86
Figure 5.1: Picture of <i>Litoria citropa</i>	95
Figure 5.2: Diagram of the geographic distribution of <i>Litoria citropa</i>	96
Figure 5.3: HPLC separation of the crude secretions from <i>Litoria citropa</i>	97

Figure 5.4: <i>Litoria splendida</i>	99
Figure 5.5: Geographic distribution of <i>Litoria splendida</i>	99
Figure 5.6: HPLC separation of glandular secretion of male <i>L. splendida</i> , obtained in January	100
Figure 5.7: HPLC separation of glandular secretion of male <i>L. splendida</i> , obtained in July	100
Figure 6.1: Initial idea for SPPS	106
Figure 6.2: The structure of polymer network of the gel type resin	108
Figure 6.3: The structure of a functionalised surface particle	110
Figure 6.4: The physical structure of a supported soft gel polymer network	111
Figure 6.5: Structure of a grafted polystyrene brush polymer on polyethylene	112
Figure 6.6: The peptide-resin support used in solid phase synthesis	113
Figure 6.7: Chain assembly of stepwise SPPS	115
Figure 7.1: Sulfotransferases pathway	154
Figure 7.2: The location of the tyrosine sulfated residue from the C-terminus of CCK, caerulein and gastrin	156
Figure 7.3: Hypothetical model of the interactions between CCK, via CCK-A and CCK-B receptors and the opioid system via δ -opioid and μ -opioid receptors	160
Figure 8.1a: CID electrospray mass spectrum (MS/MS) of the (MH^+) ion of <i>pGlu Pro Gln Val-OH</i>	179
Figure 8.1b: CID electrospray mass spectrum (MS/MS) of the $(M-H)^-$ ion of <i>pGlu Pro Gln Val-OH</i>	180
Figure 8.2: CID electrospray mass spectrum (MS/MS) of the $(M-H)^-$ ion of <i>pGlu Pro Gln Val Gln Val-OH</i>	183
Figure 8.3a: CID electrospray mass spectrum (MS/MS) of the (MH^+) ion of <i>pGlu Pro Gln Val Phe Val-NH₂</i>	185
Figure 8.3b: CID electrospray mass spectrum (MS/MS) of the $(M-H)^-$ ion of <i>pGlu Pro Gln Val Phe Val-NH₂</i>	185
Figure 8.4: Positive ion electrospray mass spectrum (MS/MS) of the $[(MH^+)-SO_3]^+$ ion of caerulein 2.2	189

Figure 8.5a: Negative ion electrospray mass spectrum (MS/MS) of the $[(M-H)^-SO_3]^-$ ion of caerulein 2.2	190
Figure 8.5b: Negative ion electrospray mass spectrum (MS/MS) of the $(M-H)^-$ ion of caerulein 2.2	190
Figure 8.6: Negative ion electrospray mass spectrum (MS/MS) of the $(M-H)^-$ ion of caerulein 3.1Y ^A	192
Figure 8.7: Negative ion electrospray mass spectrum (MS/MS) of the $(M-H)^-$ ion of caerulein 4.1Y ^A	193

List of Tables

<i>Table 1.1: Biological properties of some peptides</i>	7
<i>Table 2.1: Classifications of the various glands present on the frog</i>	27
<i>Table 2.2: Physiological functions of amphibian peptides</i>	31
<i>Table 2.3: Sequences of the caerulein peptides from Litoria species</i>	32
<i>Table 2.4: Examples of nNOS inhibitors</i>	34
<i>Table 2.5: The caerin and related peptides from Litoria species</i>	39
<i>Table 2.6: The citropin type peptides</i>	41
<i>Table 2.7: Tryptophyllin peptides from L. rubella and L. electrica</i>	44
<i>Table 3.1: Caeridin type peptides from frogs of the genus Litoria</i>	60
<i>Table 4.1: Components that lose 84, 94 and 114 Da</i>	85
<i>Table 4.2: 'High resolution' data for peaks shown in Figure 4.13</i>	86
<i>Table 4.3: ESMS spectra of other components, which lose 99, 110 and 226 Da</i>	87
<i>Table 5.1: Sequence of the caerulein-type peptides</i>	95
<i>Table 5.2: Caerulein-like peptides from Litoria citropa</i>	97
<i>Table 5.3: Desulfated caeruleins from Litoria citropa</i>	98
<i>Table 6.1: Sequencing of tyrosine sulfate containing peptides</i>	123
<i>Table 6.2: Molecular weight and yield obtained of caerulein analogues and eugenin peptides</i>	126
<i>Table 7.1: Some Tyr(SO₃)-containing peptides found in nature</i>	153
<i>Table 7.2: Examples of biological effects of desulfated tyrosine peptides</i>	155
<i>Table 7.3: Location and characteristics of the CCK-A and CCK-B receptors</i>	158
<i>Table 7.4: Sequencing of eugenin and caerulein analogues</i>	162

Table 8.1: <i>Characteristic negative ion fragmentations of side-chain of amino acid residue from (M-H)⁻ ions of small peptides</i>	174
Table 8.2: <i>Positive and negative ion mass spectra of peptide (2), (3) and (4)</i>	181
Table 8.3: <i>Sequences of caerulein peptides used in this study</i>	188
Table 8.4: <i>Negative ion mass spectra of caerulein 3.2 and 4.2</i>	192

Abstract

The research presented in this thesis involves three main areas: (i) the investigation of the biologically active peptides from Australian animals including the green tree frog (*Litoria alboguttata*), the Tammar wallaby (*Macropus eugenii*), the Brush-tailed Rock wallaby (*Petrogale penicillata*) and the Yellow-footed Rock wallaby (*Petrogale xanthopus*), (ii) the establishment of a facile synthetic method for caerulein-like peptides and eugenin via solid phase peptide synthesis, and (iii) the comparison of the positive and negative ion electrospray mass spectra of pyroglutamate containing peptides.

The skin secretion of the Australian tree frog, *Litoria alboguttata* has been investigated, with three novel peptides identified. These are guttatin 1 [GLLDSVL-NH₂], guttatin 2 [GLLDNVL-NH₂] and guttatin 3 [GLLDTVKGLN-NH₂]. These peptides have no antibacterial activity. Guttatin 1 from *Litoria alboguttata* shows a similar sequence to a peptide (MH⁺) 715 previously obtained from *Cyclorana australis*. This suggests the possibility that *Litoria alboguttata* should be reclassified within the *Cyclorana* genus.

The secretions from the pouch of the pregnant Tammar wallaby, Brush-tailed Rock wallaby and Yellow-footed Rock wallaby have been investigated. Eugenin [pEQDY(SO₃)VFMHPF-NH₂] was found in the pouch secretion of pregnant Tammar wallabies. This peptide was not identified in pouch secretions of the Brush-tailed Rock wallaby or the Yellow-footed Rock wallaby. Eugenin shows a contractile response on smooth muscle cell at a concentration of 10⁻⁹ M. It seems to be atropine-dependent, perhaps acting on a CCK-B receptor site.

An efficient Fmoc-based solid-phase method for the synthesis of tyrosine sulfate containing peptides was developed and successfully applied to caerulein analogues and to eugenin. Caerulein analogues and eugenin were synthesised using this method in 14-24% yields.

Seven caerulein-like peptides have been synthesised and investigated for contractile response. Only caerulein 1.2 [pEQDY(SO₃)TGWFDN-NH₂] and caerulein 3.1 [pEQDY(SO₃)GTGWMDN-NH₂] caused contraction of the smooth muscle cell at a concentration of 10⁻⁹ M.

The positive ion electrospray mass spectra of (MH⁺) and the negative ion electrospray mass spectra of (M-H)⁻ ions of selected pyroglutamate containing peptides both provide sequencing data. The negative ion electrospray mass spectra provide significant sequencing information from a combination of α , β and γ backbone cleavage ions. The negative ion spectra also indicate the presence of specific amino acid side chains (e.g. Ser and Thr) by side-chain cleavages, of which there are no counterparts in positive ion spectra.

Chapter One

Introduction

1.1 Peptide Chemistry

Peptides are key regulators of the vast majority of cellular, intercellular and other physiological processes. These peptides show enormous potential for the treatment and cure of many diseases that plague humans and other animals. Despite this potential, peptides have received relatively little attention for their development as drugs. The major reason for this is that endoproteases can degrade these peptides following their introduction into the body. Even so, a number of peptides are used in medicine (see *section 2.3*).

Peptide chemistry has been a major area of science since the nineteenth century¹. A number of uncharacterised peptide mediators have been discovered, including substance P, bradykinin and angiotensin. To date, advancing technology including nuclear magnetic resonance (NMR) spectroscopy, mass spectrometry, X-ray diffraction and circular

dichroism (CD) spectroscopy have allowed many peptides and proteins to be fully characterised.

1.2 The Structure of a Peptide

A peptide consists of a number of amino acids linked together by condensation of the carboxyl group of one amino acid and the amino group of another, via a peptide bond (*Figure 1.1*).

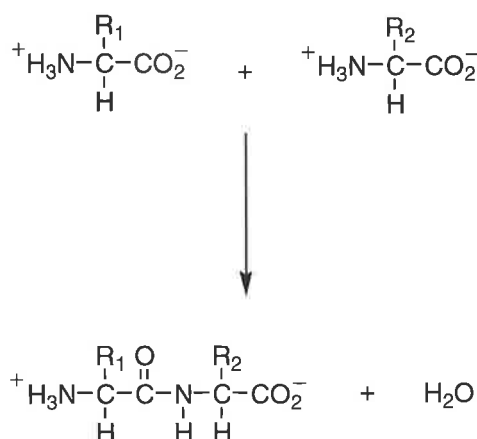


Figure 1.1: The peptide bond

A peptide generally consists of 5-20 amino acid residues, while a protein is a polypeptide, often containing thousands of amino acids. The peptide bond is a rigid unit due to the double bond character that results from delocalisation of the lone pair of electrons on the nitrogen atom (*Figure 1.2*). X-ray studies of peptides indicate that the amide moiety is planar: the carbonyl carbon, nitrogen and the atoms attached to them lie in a plane² (*Figure 1.3*).

An examiner has requested that a section on chirality and a list of common amino acids be included here. These are appended as appendices 1 and 2 at the end of the thesis.

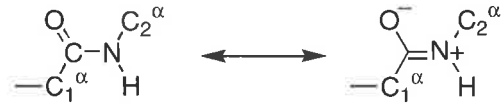


Figure 1.2: A schematic of the two canonical forms of the peptide bond

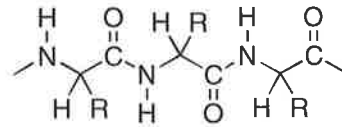


Figure 1.3: Geometry of the peptide link

Initially, a peptide has a C-terminal CO_2H group, but this can be post-translationally modified to CONH_2 . Other post-translational modifications that can occur include glycosylation, acetylation, carboxylation, sulphation or phosphorylation³. Peptides may contain intramolecular disulphide bonds, which means that the molecule adopts a (partially) cyclic structure.

Peptides are often difficult to crystallise and in these cases, X-ray diffraction cannot be used. Nuclear magnetic resonance spectroscopy has been applied widely to determine the 3D structures of peptides and proteins.

1.3 Types of Peptide Mediators

Many mammalian peptides come from the central nervous system (CNS) and the endocrine glands. However, some are formed in the plasma and other sites such as the vascular endothelium, the heart and in cells of the immune system. It is not unusual for the same peptide to be present in several locations in the body, and to have more than one function.

Peptides bind to specific receptors. For example, some small peptides act on the G-protein-coupled receptor^{*3}. Peptides also act on the nervous system as co-transmitters with other peptides or with non-peptide transmitters⁴. Peptides may be hormones and/or neuropeptides.

1.3.1 Hormones

Hormones are chemical messengers, secreted by specific cells of the endocrine glands, such as the pancreas, pituitary or adrenal cortex. Peptide hormones are transmitted via the blood to stimulate specific functions of other tissues or organs, including many critical functions like growth, reproduction, lactation, water balance and adrenal function⁵. For example, the hormone insulin is secreted by the B cells of the pancreas, and is a chemical messenger carried by the blood to other organs. The insulin binds to receptors on cell surfaces and stimulates these cells to use glucose as metabolic fuel. Other peptide hormones include (i) oxytocin (1), a hormone that stimulates uterine contraction and is secreted by the posterior pituitary glands, (ii) bradykinin (2), a hormone that inhibits inflammation of tissue, (iii) thyrotropin-releasing factor (3), which is formed in the hypothalamus and stimulates the release of thyrotrophin hormone and

* G-protein is a middle management protein in the organisational ladder, able to communicate between the receptors and enzymes and/or ion channels. They are called G-proteins because of their interactions with guanine of nucleotides.

(iv), enkephalin (4), which is formed in the central nervous system and induces an analgaesic effect⁵.

(1) Oxytocin	$\begin{array}{c} \text{S} \text{---} \text{S} \\ \quad \\ \text{CYIQNCPLG-NH}_2 \end{array}$
(2) Bradykinin	RPPGFSPFR-OH
(3) Thyrotropin-releasing factor	pEHP-NH ₂
(4) Enkephalin	YGGFL-OH or YGGFM-OH

1.3.2 Neuropeptides

Neuropeptides are endogenous substances present in nerve cells that are involved in nervous function. Some neuropeptides have been found in the mammalian central nervous system. Neuropeptides usually produce their effects by interacting with specific receptor recognition sites. Certain neuropeptides activate a second messenger system, producing an intracellular effect that alters the synaptic activity of particular neurons⁶. Neuropeptides can act on either presynaptic or postsynaptic sites and are normally released from sensory neurons. For example, substance P (RPKPQQFFGLM-NH₂) mediates pain transmission in primary sensory neurons by interacting with substance P receptors in the spinal cord.

1.4 Peptide Biosynthesis

Peptide structure is directly coded in the genome. A peptide is often produced from a precursor protein, from which proteolytic enzymes excise the active peptide. The precursor protein is packaged into vesicles at the point of synthesis and the active peptide is

produced intracellularly following selective enzymic cleavage. A schematic diagram of this process is shown in *Figure 1.4*.

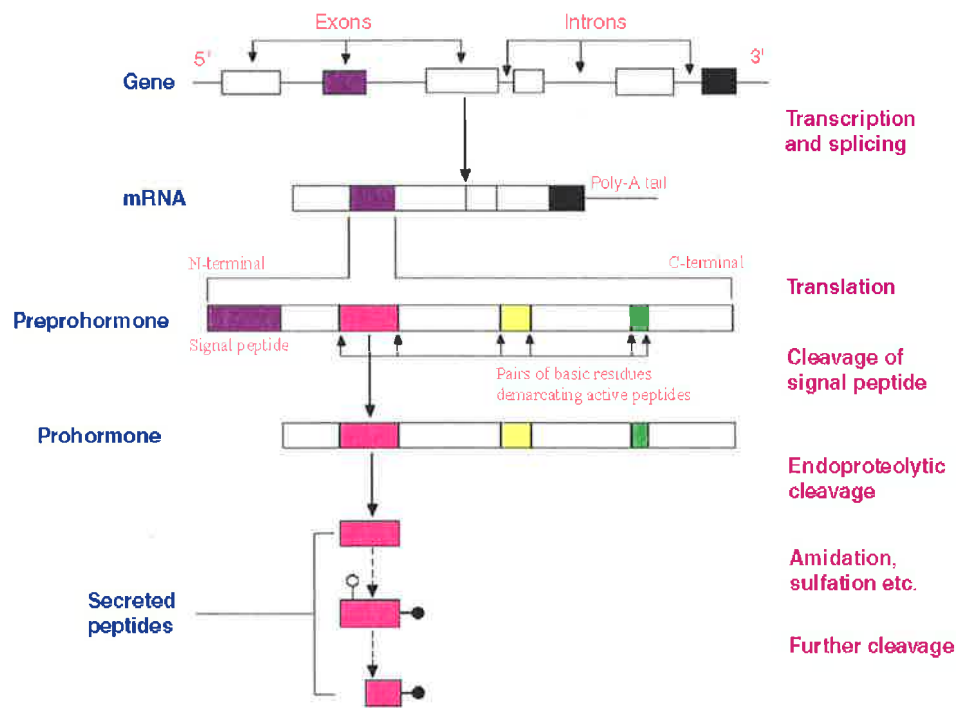


Figure 1.4: Synthesis of a peptide mediator (from³)

A single precursor gene may give rise to several peptides either by selective DNA splicing before transcription, by selective cleavage of the prohormone, or by post-translational modification³. The signal peptide is normally cleaved off at an early stage to form a prohormone. The active peptides are usually separated within the prohormone sequence by pairs of basic amino acids (Lys-Lys or Lys-Arg), which are cleavage points for the various trypsin-like proteases that act to release the peptides³.

1.5 Biological Properties of Peptides

Peptides exhibit a remarkable range of biological properties: peptides can be used as antibiotics, hormones, food additives, poisons or painkillers. Examples of the biological properties of some peptides are listed in *Table 1.1*.

Table 1.1: *Biological properties of some peptides*⁷

Name	Biological properties
Aspartame	An artificial sweetener about 100 times sweeter than sugar
Angiotensin II	Used by the body to increase blood pressure, this peptide is known as a hypertensive agent
Enkephalins	Found in the brain, these peptides are involved in the control of pain
Gramicidin S	A cyclic decapeptide that is a powerful antibiotic
Oxytocin	A hormone cyclic nonapeptide, which among other things, can be used to induce labour in pregnancy
Phalloin	An extremely poisonous bicyclic peptide found in the Deathcap toadstool
TRH	A hormone that controls the release of another hormone (thyrotrophin) in the body and also affects the CNS

1.6 Mass Spectrometry

1.6.1 General

Mass spectrometry is an analytical technique used to measure the molecular weight of a molecule and also to give structural information about that molecule.

There are three phases in obtaining a mass spectrum.

- (i) Ionisation, to produce ions from the vaporised compound.

- (ii) Analysis, to separate ions according to their mass to charge ratios.
- (iii) Detection of ions and observation of their fragmentation patterns.

Thompson carried out the first mass spectrometry experiment in 1886⁸. Since that time, the sector mass spectrometer has developed from a single to a double⁹; and later to three¹⁰ and four sectors¹¹ in order to achieve higher resolution and more advanced analytical capability. Initially, ionisation techniques involved electron impact (EI)¹², chemical ionisation (CI)¹³ and field ionisation and desorption¹⁴. Further techniques were required to introduce and analyse larger and more polar sample molecules in the gas phase. Softer ionisation techniques were developed including plasma desorption ionisation¹⁵, secondary ion mass spectrometry (SIMS)¹⁶, fast atom bombardment (FAB)¹⁷, laser desorption^{18,19} and electrospray ionisation²⁰. In addition, new mass analysers were developed including quadrupole^{21,22}, time of flight^{23,24}, ion-cyclotron resonance (ICR)^{25,26}, ion-trap^{27,28}, flowing afterglow²⁹ and Fourier Transform (ICR) mass spectrometers³⁰⁻³².

1.6.2 Mass spectrometric determination of the peptide

Recently, mass spectrometry has become a very helpful tool for determining the amino acid sequences of peptides and proteins.

In the 1980s, Barber and co-workers introduced fast atom bombardment (FAB) ionisation^{17,33,34}. Variants of secondary ion mass spectrometry (SIMS) such as liquid SIMS³⁵ and dynamic SIMS³⁶ were also developed for peptide analysis. These techniques eliminate the time consuming chemical derivatisations necessary to make the peptide volatile enough for electron ionisation (EI) or chemical ionisation (CI)³⁷. The possibility of

ionising large peptides by FABMS opened the way for new strategies in peptide sequencing. FABMS was used to great effect in the period 1980-1995. Since then, new ionisation techniques have been developed such as matrix assisted laser desorption-ionisation (MALDI)³⁸ and electrospray ionisation (ESI)³⁹. These new techniques have significantly enhanced the applicability of mass spectrometry for the analysis of biological macromolecules. Because of its sensitivity, speed and high degree of molecular specificity, mass spectrometry has become a vital part of those analytical protocols used for peptide characterisation.

In this thesis, reported peptides were characterised using either a Finnigan LCQ electrospray mass spectrometer or a QTOF 2 hybrid quadrupole time of flight mass spectrometer.

1.6.3 Electrospray ionisation (ESI)

1) General

Electrospray ionisation was reported early in last century by Zeleny⁴⁰. In 1968, Dole and co-workers^{41,42} reported the use of the electrospray technique as an ionisation method for macromolecules. The combination of ESI and mass spectrometry (ESMS) was reported by Yamashita and Fenn⁴³ and Aleksandros *et al.*^{44,45} in 1984. Fenn and coworkers⁴³ further demonstrated the applicability of ESMS in the negative ion mode. Aleksandrov *et al.* showed the online combination of ESMS with liquid chromatography⁴⁵, and applied ESMS to the study of oligosaccharides⁴⁶, and intact polypeptides of molecular weight to 1500 Da⁴⁷.

Dole reported the multiple charging of macromolecules by ESI on the basis of ion mobility measurements⁴⁸, but had difficulties with the interpretation of the data. In 1985, both Aleksandrov *et al.*^{46,47} and Fenn and coworkers⁴⁹ reported the formation of doubly charged ions of peptides such as bradykinin and gramicidin.

In 1988, Aleksandrov *et al.* successfully analysed a polypeptide of molecular weight 3492 that produced intense doubly and triply protonated molecular ions⁵⁰.

Also in 1988, Fenn and coworkers reported the analysis of polyethylene glycols with molecular weights up to 17,500 Da and as many as 23 charges⁵¹, as well as ESMS spectra of intact multiply protonated proteins molecules up to molecular weight 40,000 Da, having as many as 45 charges⁵². Since then, the use of ESMS for the study of large biomolecules has become a standard analytical technique.

2) Characteristics of electrospray ionisation

Electrospray ionisation is a soft ionisation process, which transforms ions from solution into the gas phase²⁰. The ESI technique can be used for high molecular weight material, heat-labile compounds and polar compounds that had not previously proven suitable to produce mass spectra. The mass range for analysis by ESI is now greater than 100,000 Da: principally because the multiple charging of ions reduces the mass range [e.g. an ion $(50,000+50H^+)^{50+}$ will show a peak at m/z 1001].

The ESI technique produces ions from molecules in solution by spraying the solution from a sharp tip in the presence of a high electric field (4000 V). The spray produces small charged droplets. As the droplets evaporate, the surface charge density of the droplets

increases. The droplets divide into smaller droplets as the electrostatic repulsion becomes greater than the surface tension²⁰. As the ions move from atmospheric pressure to the high vacuum of the mass spectrometer through a series of capillaries, nozzles and the skimmer, the ions collide with residual gas molecules at an intermediate pressure to remove residual solvent molecules (*Figure 1.5*).

The charge of an ion is simple to determine. Every multiply charged ion has an envelope of peaks produced by the various isotopes. The difference between the peaks is a function of the charge state of that particular system. For example, if the difference between the peaks is 0.5 Da, then the charge state of that ion is 2. For multiply charged ions, a software package determines the MW using an algorithm.

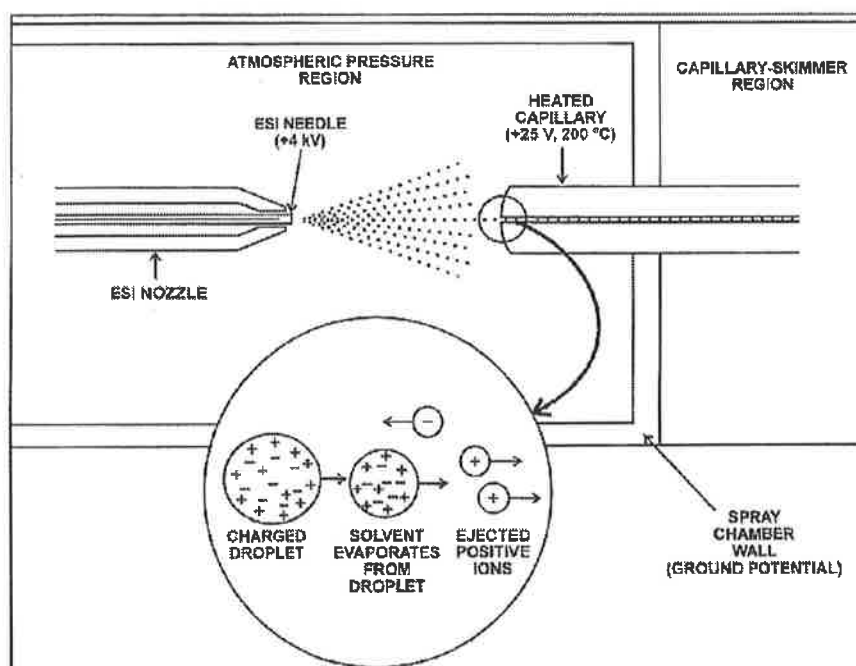


Figure 1.5: The ESI process in the positive ion polarity mode (from 20)

When compared with other ionisation techniques, ESI offers the advantages of relatively low cost, convenient automation and ease of interfacing on-line with chromatography or capillary electrophoresis systems.

1.6.4 Finnigan LCQ electropray mass spectrometer

The Finnigan LCQ electropray mass spectrometer is an ^{Quadrupole} octapole ion trap mass spectrometer ^{with octapoles used to transmit ions} (Figure 1.6) equipped with an LC system.



Figure 1.6: Finnigan LCQ mass spectrometer (from Finnigan LCQ manual)

The mass range of the LCQ is 50-4000 Da. The charge state of the ion is determined with the aid of a zoomscan that allows the m/z values of the peaks of the multiply charged ion to be closely examined. The other capabilities of the LCQ are its $MS^{n\dagger 53}$ and on-line liquid chromatography techniques. The inside schematic setting of the Finnigan LCQ mass spectrometer is shown in *Figure 1.7*.

[†] The chosen ion is first isolated in the ion trap. The internal energy of the ion is increased such that it will undergo rapid collisions with helium gas and effect fragmentation. The daughter ions produced are then sequentially ejected from the ion trap and detected. This is called an MS/MS experiment (or MS^2). MS^n experiments use the same procedures. For example the daughter ion of an MS/MS experiment is isolated, excited, and fragmented giving MS/MS/MS (MS^3) data, etc.

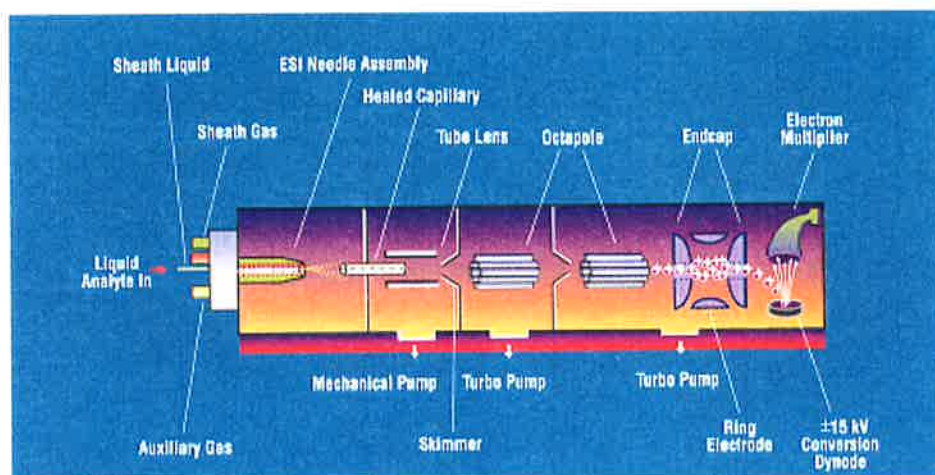


Figure 1.7: Diagram of the LCQ (from Finnigan LCQ manual)

LC/MS analysis involves the sample being introduced into an HPLC instrument coupled to the mass spectrometer. After the sample has entered the HPLC, components move through the column. The separated chemical components pass through a transfer line and then enter the mass spectrometer to be analysed.

The LC/MS detector consists of an atmospheric pressure ionisation (API) source, ion optics, mass analyser and ion detector system. The ions are produced in the API source and then transmitted into the mass analyser. The polarity of the potentials applied to the lenses in the API source and ion optics determines whether negative or positive ions are transmitted to the mass analyser. The lenses in the API source and ion optics also act as a gate to start and stop the transmission of the optimum number of ions from the API source to the mass analyser. The mass to charge ratios of the ions produced in the API source are then measured by the mass analyser.

1.6.5 QTOF 2 hybrid quadrupole time of flight mass spectrometer

Gas phase ions are produced by electrospray ionisation (ESI) in the Z-spray source. A large voltage (3-6 kV) is applied to the liquid flowing through a capillary (1-10 $\mu\text{L}/\text{min}$). The free ions produced by ESI are drawn through the sample cone aperture and into the ion block before being extracted into the analyser. In the QTOF 2, the analyser consists of a quadrupole mass analyser and an orthogonal acceleration time of flight (TOF) mass spectrometer, separated by a hexapole collision cell, as shown in *Figure 1.8*.

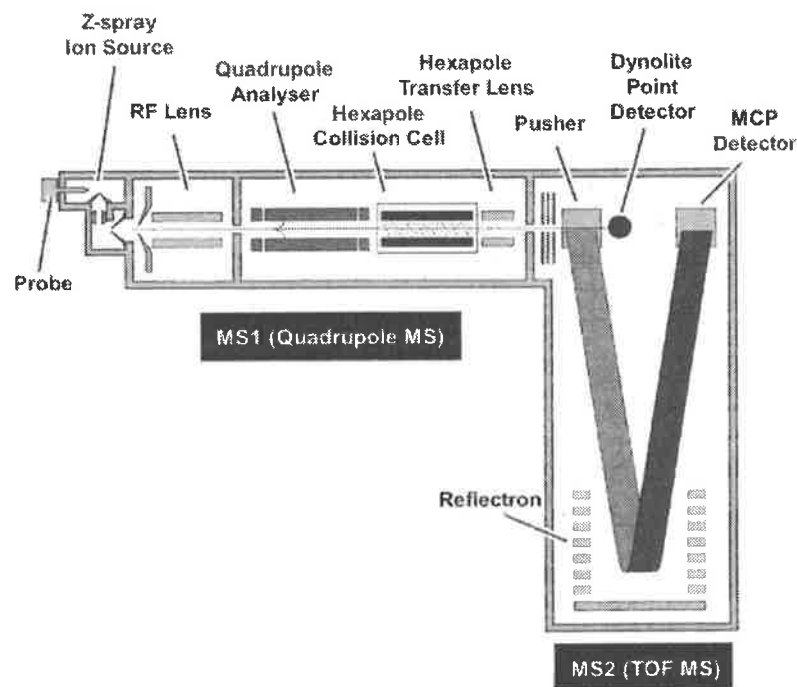


Figure 1.8: Schematic diagram of the QTOF 2 mass spectrometer (from Micromass QTOF 2 manual)

In the TOF ^{analyser} sector, ions are accelerated by a positive voltage to the same kinetic energy before being pushed toward the reflectron and reflected back to the detector. At the same kinetic energy, the ions' velocity is inversely proportional to the square root of their

mass²⁴. Thus the ions can be separated according to their flight times, with ions of large mass taking longer to reach the detector.

Ions can be selected by the quadrupole mass analyser and fragmented in the hexapole collision cell. Fragmentation of the chosen ions is carried out by collision-induced decomposition (CID). The resulting daughter ions can be scanned by the TOF mass sector.

The QTOF 2 has a microchannel plate (MCP) detector, which can record a full spectrum every 50 μ s. The spectra are added up in the memory of the time to digital converter and the resulting spectrum is transferred to the connected computer. Each spectrum on the computer will be a sum of 20,000 individually detected spectra for an acquisition rate of 1 spectrum per second.

The QTOF 2 records spectra with a very high sensitivity and a high mass range (up to 10,000 Da), which is suitable for the analysis of small quantities of peptides.

1.7 Peptide Sequencing

1.7.1 Mass spectrometry

The sequences of peptides are determined by analysis of their characteristic mass spectral fragmentations, principally in the positive mode. A number of positive ion fragmentations of peptides have been reported^{37,54}. We use B and Y+2 cleavage ions for sequencing purposes, as they generally produce the most abundant fragment ions. B cleavages give

sequence information from the C-terminal end of the peptide, and Y+2 cleavages give sequence information about the N-terminal end (*Figure 1.9*).

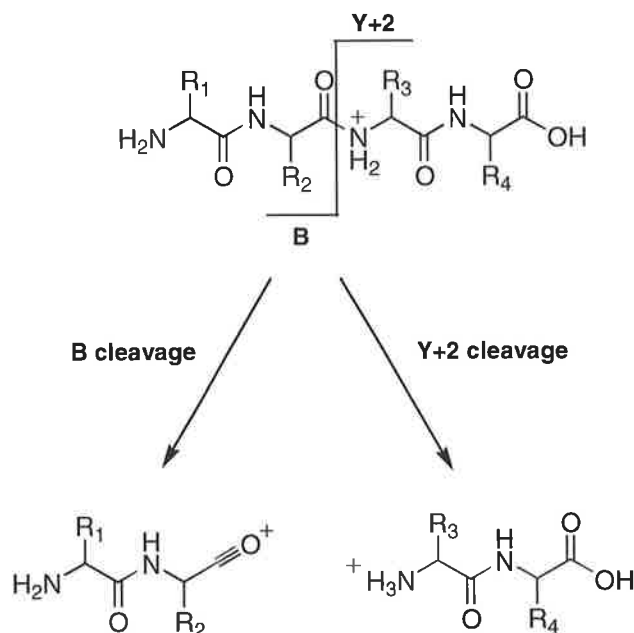


Figure 1.9: A diagram of the fragment ions produced in positive mode

In addition to B and Y+2 fragmentations, there are A and Z fragmentations which can also occur along the peptide backbone. These are not discussed further in this thesis (for more explanation of these fragmentations see Biemann *et al.*³⁷).

The limitation of the MS technique is that it cannot readily differentiate between isomeric or isobaric amino acid residues unless the instrument has high-resolution capabilities. These residues are the isomers Ile (113 Da) and Leu (113 Da) and the isobaric Lys (128 Da) and Gln (128 Da) residues. Leu and Ile isomers can be distinguished using the automated Edman sequencing technique⁵⁵, while the isobaric isomers can be distinguished by enzymic digestion (e.g. using the enzyme Lys-C) or automated Edman sequencing.

1.7.2 Automated Edman sequencing

Edman degradation determines the sequence of amino acids in a peptide or protein by sequential chemical degradation from the N-terminus of the peptide. Edman degradation was first reported during the 1950s⁵⁶ and developed to automated sequencing in 1967⁵⁷. In preparation for Edman degradation, the purified peptide must be immobilised on a support. Typically the sample is either adsorbed to a chemically modified glass fibre disc or electroblotted from a gel onto a porous polyvinylidene fluoride (PVDF) membrane. Edman degradation is then performed. The key reagent used in this process is phenyl isothiocyanate (PITC). The steps of the Edman chemistry cycle are shown in *Figure 1.10*.

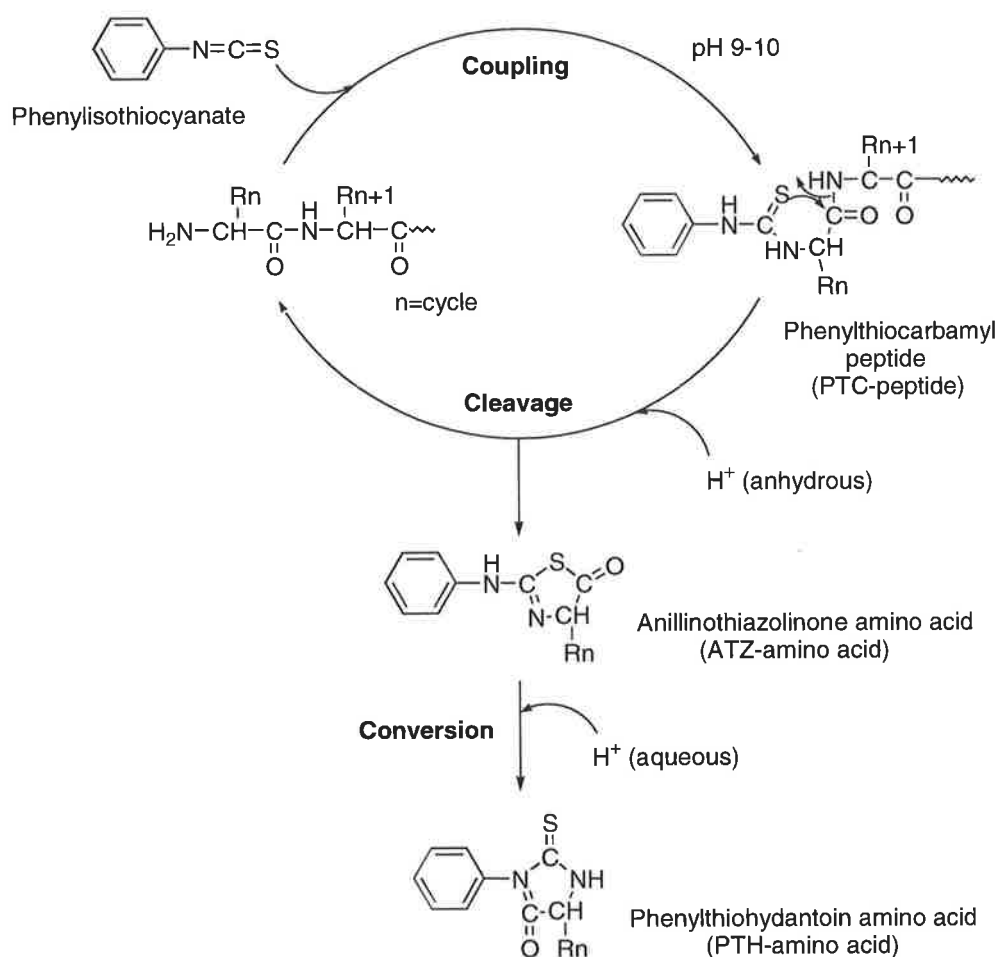


Figure 1.10: Illustration of the Edman degradation cycle

The Edman method is an effective technique that can routinely sequence proteins of up to 100 residues. There are some limitations including:

- (i) A peptide with a blocked N-terminus, for example a peptide containing pyroglutamate at the N-terminal, cannot be sequenced using this technique. The blocked end group prohibits coupling with phenyl isothiocyanate.
- (ii) Uncommon or modified amino acids may be difficult to identify by automated Edman degradation. This is because the chromatographic behaviour of the phenyl thiohydantoin (PTH) derivative may be unknown or the PTH derivative may be insoluble in the organic solvent and thus unable to be detected.
- (iii) As the peptide is cleaved, its size decreases and it becomes more soluble and therefore may be washed from the solid support. This may lead to loss of the remaining portion of the peptide before the full sequence is determined.

1.7.3 Enzyme digestion

Enzyme digestion will cleave a particular amide bond to produce smaller peptides that can be sequenced by mass spectrometry. For example, the enzyme Lys-C is often used because many peptides contain lysine residues. ^{*}Cleavage occurs at the carboxyl side of the lysine residue as shown in *Figure 1.11*.

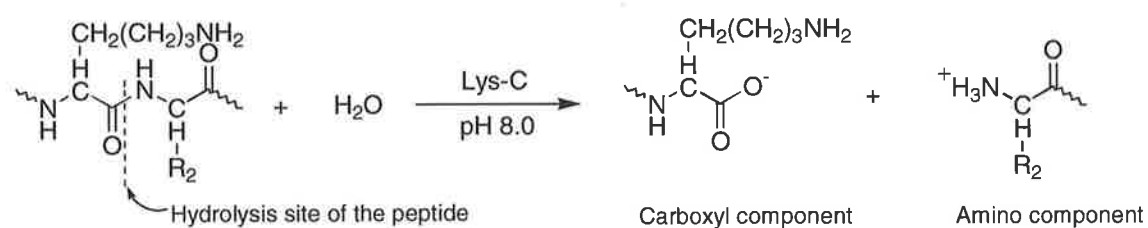


Figure 1.11: Lys-C digestion

* Trypsin is also commonly used for protein digestion.

1.7.4 Determination of C-terminal end group

Peptides usually have either C-terminal CO_2H or CONH_2 groups. Converting the C-terminal end group into the methyl ester allows differentiation between these possibilities. The resulting methyl ester is analysed using mass spectrometry. The C-terminal end group, either CO_2H or CONH_2 , is identified by the mass difference between the parent ion of the methyl ester and the original peptide as shown in *Figure 1.12*.

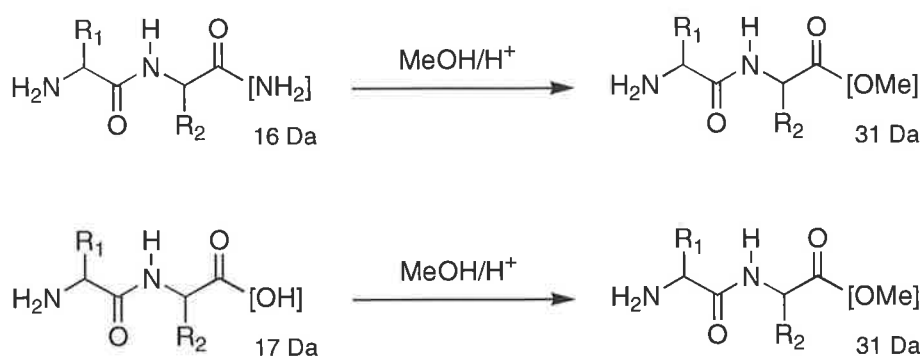


Figure 1.12: Determination of the C-terminal end group by methylation

1.8 Bioactivity Testing

The natural peptides described in this thesis are only available in microgram quantities in the pure state. We require up to 50 mg to enable biological testing (antimicrobial, anticancer, nNOS and various neuropeptide tests), so we either have the peptides synthesised commercially (Mimotopes, Melbourne) or prepare them ourselves (see *Chapter 6*).

Antibacterial testing is conducted by the Institute of Medical and Veterinary Science (IMVS), Adelaide, South Australia. The procedure involves introducing varying concentrations of peptide into cultures of bacterial colonies in a petri dish. The results are reported as a minimum inhibitory concentration (MIC, $\mu\text{g/mL}$)⁵⁸. If no inhibition is detected at concentrations less than 100 $\mu\text{g/mL}$, the peptide is deemed to be “inactive” against the organism.

Anticancer activity is also examined. This is carried out by the National Cancer Institute (Washington DC, USA) by assessing the *in vitro* chemosensitivity of a number of human tumour cell lines to the synthetic peptide⁵⁹. Results for each test agent are reported as the percentage growth of the treated cells, when compared to the untreated control cells. Peptides that reduced the growth of any one of the cell lines to 32% or less are passed on for evaluation in a full panel of 60 human tumour cell lines.

It has recently been reported that certain amphibian host-defence peptides inhibit the formation of nitric oxide by the enzyme neuronal nitric oxide synthase (nNOS)⁶⁰. As a consequence, all new peptides are screened for this activity. The assay used involves measuring the nNOS catalysed conversion of [³H]arginine to [³H]citrulline and determining the concentration of peptide that inhibits this reaction by 50%⁶¹. These activity tests are carried out by the Australian Institute of Marine Science (Queensland, Australia).

1.9 References

- 1) Ward, D. J. *Peptide Pharmaceutical*; Hrubby, V. J., Kazmierski, W., Kawasaki, A. M. and Matsunaga, A. M., Ed.; Open University Press: Milton Keynes, 1991, p 135.
- 2) Boyd, M. *Organic Chemistry*; Joraanstad, D., Ed.; Prentice-Hall Inc.: New Jersey, 1992; Vol. 6, p 1215.
- 3) Rang, H. P.; Dale, M. M.; Ritter, J. M. *Pharmacology*; 2 ed.; Churchill Livingstone: London, 1992, p 191.
- 4) Yanagisawa, M.; Kurihara, H.; Kimura, S.; Tomobe, Y.; Kobayashi, M. *Nature* **1988**, *332*, 411.
- 5) Ward, D. J. *Peptide Pharmaceuticals*; Knapp, R. J., Davis, T. P., Burks, T. F. and Yamamura, H. I., Ed.; Open University Press: Milton Keynes, 1991, p 210.
- 6) Iversen, L. L. *Trends Neurosci.* **1983**, *6*, 291.
- 7) Bailey, P. D. *An Introduction to Peptide Chemistry*; John Wiley and Sons: New York, USA, 1990, p 6.
- 8) Thompson, J. J. *Philos. Mag.* **1907**, *13*, 561.
- 9) Beynon, J. H.; Cooks, R. G.; Amy, J. W.; Baitinger, W. E.; Ridley, T. Y. *Anal. Chem.* **1973**, *45*, 1023.
- 10) Gross, M. L.; Chess, E. K.; Lyon, P. A.; Crow, F. W.; Evans, S.; Tudge, H. *Int. J. Mass Spectrom. Ion. Phys.* **1982**, *42*, 243.
- 11) Gross, M. L. *Methods Enzymol.* **1990**, *193*, 131.
- 12) Chapman, J. R. *Practical Organic Mass Spectrometry. A guide for chemical and biochemical analysis.*; John Wiley & Son: Chichester, 1993, p 1.
- 13) Munson, M. S. B.; Field, F. H. *J. Am. Chem. Soc.* **1966**, *88*, 2621.
- 14) Winkler, H. U.; Beckey, H. D. *Biochem. Biophys. Res. Commun.* **1970**, *46*, 391.

- 15) Cotter, R. J. *Anal. Chem.* **1988**, *60*, 781A.
- 16) Pachuta, S. J.; Cooks, R. G. *Desorption Mass Spectrometry*; American Chemical Society: Washington D. C., 1985, p 1.
- 17) Barber, M.; Bordoli, R. S.; Sedgwick, R. D.; Tyler, A. N. *J. Chem. Soc. Chem. Commun.* **1981**, 325.
- 18) Karas, M.; Bachmann, D.; Bahr, U.; Hillenkamp, F. *Int. J. Mass Spectrom. Ion Phys.* **1987**, *78*, 53.
- 19) Karas, M.; Bahr, U.; Hillenkamp, F. *Int. J. Mass Spectrom. Ion Phys.* **1989**, *92*, 231.
- 20) Fenn, J. B.; Mann, M.; Mang, C. K.; Wong, S. F.; Whitehouse, C. M. *Mass Spectrom. Rev.* **1990**, *9*, 37.
- 21) Yost, R. A.; Enke, C. G. *Anal. Chem.* **1979**, *51*, 1251A.
- 22) Schwartz, J. C.; Schey, K. L.; Cooks, R. G. *Int. J. Mass Spectrom. Ion Phys.* **1990**, *101*, 1.
- 23) Cotter, R. J. *Anal. Chem.* **1992**, *64*, 1027A.
- 24) Cotter, R. J. *Time of Flight Mass Spectrometry*; American Chemical Society: Washington D. C., 1994, p 16.
- 25) Gross, M. L.; Wilkins, C. L. *Anal. Chem.* **1971**, *43*, 65A.
- 26) Wanczek, K. P. *Int. J. Mass Spectrom. Ion Phys.* **1984**, *60*, 11.
- 27) Cooks, R. G.; Kaiser, R. E. *Acc. Chem. Res.* **1990**, *23*, 213.
- 28) McLuckey, S. A.; Van Berkel, G. L.; Goeringer, D. E.; Glish, G. L. *Anal. Chem.* **1994**, *66*, 689A.
- 29) Ferguson, E. F.; Fehsenfeld, F. C.; Schmeltekopf, A. L. *Adv. Atom. Mol. Phys.* **1969**, *5*, 1.
- 30) Comisarow, M. B.; Marshall, A. G. *Chem. Phys. Lett.* **1979**, *25*, 282.
- 31) Russell, D. H. *Mass Spectrom. Rev.* **1986**, *5*, 167.

- 32) Holliman, C. L.; Rempel, D. L.; Gross, M. L. *Mass Spectrom. Rev.* **1994**, *13*, 105.
- 33) Barber, M.; Bordoli, R. S.; Garner, G. V.; Gordon, D. B.; Sedgwick, R. D.; Tetler, L. W.; Tyler, A. N. *Biochem. J.* **1981**, *197*, 401.
- 34) Barber, M.; Bordoli, R. S.; Elliot, G. J.; Sedgwick, R. D.; Tyler, A. N. *Anal. Chem.* **1982**, *54*, 645A.
- 35) Aberth, W.; Straub, K. M.; Burlingame, A. L. *Anal. Chem.* **1982**, *54*, 2029.
- 36) Benninghoven, A.; Jasper, D.; Sichtermann, W. *Appl. Phys.* **1976**, *11*, 35.
- 37) Biemann, K.; Martin, S. A. *Mass Spectrom. Rev.* **1987**, *6*, 1.
- 38) Karas, M.; Hillenkamp, F. *Anal. Chem.* **1988**, *60*, 2299.
- 39) Yamashita, M.; Fenn, J. B. *J. Phys. Chem.* **1984**, *88*, 4451.
- 40) Zeleny, J. *J. Phys. Rev.* **1917**, *10*, 1.
- 41) Dole, M.; Mack, L. L.; Hines, R. L.; Mobley, R. C.; Ferguson, L. D.; Alice, M. B. *J. Chem. Phys.* **1968**, *49*, 2240.
- 42) Mack, L. L.; Kralik, P.; Rheude, A.; Dole, M. *J. Chem. Phys.* **1970**, *52*, 4977.
- 43) Yamashita, M.; Fenn, J. B. *J. Phys. Chem.* **1984**, *88*, 4671.
- 44) Aleksandrov, M. L.; Gall, L. N.; Krasnov, V. N.; Nikolaev, V. I.; Pavlenko, V. A.; Shkurov, V. A. *Dokl. Akad. Nauk. SSSR* **1984**, *277*, 379.
- 45) Aleksandrov, M. L.; Gall, L. N.; Krasnov, V. N.; Nikolaev, V. I.; Pavlenko, V. A.; Shkurov, V. A.; Baram, G. I.; Gracher, M. A.; Knorre, V. D.; Kusner, Y. S. *Bioorg. Kim.* **1984**, *10*, 710.
- 46) Aleksandrov, M. L.; Besuklandnikov, P. V.; Grachev, M. A.; Elyakova, L. A.; Zyyaginsteva, T. N.; Kondratser, V. M.; Kusner, Y. S.; Mirgorodskaya, O. A.; Fridlyansky, G. V. *Bioorg. Kim.* **1986**, *12*, 1689.
- 47) Aleksandrov, M. L.; Baram, G. I.; Gall, L. N.; Krasnov, N. V.; Kusner, Y. S.; Mirgorodskaya, O. A.; Nikolaev, V. I.; Shkurov, V. A. *Bioorg. Kim.* **1985**, *11*, 700.

- 48) Gieniec, J.; Mack, L. L.; Nakamac, K.; Gupta, C.; Kumar, V.; Dole, M. *Biomed. Mass Spectrom.* **1984**, *11*, 259.
- 49) Whitehouse, C. M.; Dreyer, R. N.; Yamashita, M.; Fenn, J. B. *Anal. Chem.* **1985**, *57*, 675.
- 50) Aleksandrov, M. L.; Kondratsev, V. M.; Kusner, Y. S.; Mirgorodskaya, O. A.; Podtelezchnikov, A. V.; Fridlyansku, G. V. *Bioorg. Kim.* **1988**, *14*, 852.
- 51) Wong, S. F.; Meng, C. K.; Fenn, J. B. *J. Phys. Chem.* **1988**, *92*, 546.
- 52) Meng, C. K.; Mann, M.; Fenn, J. B. *Z. Phys. D.* **1988**, *10*, 361.
- 53) Jonscher, K. R.; Yates, J. R. *Anal. Biochem.* **1997**, *244*, 1.
- 54) Roepstorff, P.; Fohlman, J. *J. Biomed. Mass Spectrom.* **1984**, *11*, 601.
- 55) Hunkapiller, M. W.; Hewick, R. M.; Drewer, W. J.; Hood, L. E. *Methods Enzymol* **1983**, *91*, 399.
- 56) Edman, P. *Acta. Chem. Scand.* **1950**, *4*, 283.
- 57) Edman, P.; Begg, G. *Eur. J. Biochem.* **1967**, *1*, 80.
- 58) Jorgensen, J. H.; Cleeland, R.; Craig, W. A.; Doern, G.; Ferraro, M. J.; Finegold, S. M.; Hansen, S. L.; Jenkins, S. G.; Novick, W. J.; Pfaller, M. A.; Preston, D. A.; Reller, L. B.; Swenson, J. M. *National Committee for Clinical Laboratory Standards Doc. M7-A3* **1993**, *13*, 1.
- 59) Monks, A.; Scudiero, D.; Skehan, P.; Shoemaker, R.; Paul, K.; Vistica, D.; Hose, C.; Langley, J.; Cronise, P.; Cambell, H.; Mayo, J. *J. Natl. Cancer Inst.* **1991**, *83*, 757.
- 60) Doyle, J.; Llewellyn, L. E.; Brinkworth, C. S.; Bowie, J. H.; Wegener, K. L.; Rozek, T.; Wabnitz, P. A.; Wallace, J. C.; Tyler, M. J. *Eur. J. Biochem.* **2002**, *269*, 100.
- 61) Ichida, S.; Wada, T.; Sekiguchi, M.; Kishino, H.; Okazaki, Y.; Akimoto, T. *Neurochem. Res.* **1993**, *18*, 1137.

Chapter Two

Bioactive Peptides from Amphibians

2.1 Amphibians

Amphibians are animals that are both terrestrial and aquatic. Most anurans (frogs and toads) live on land but breed in water. Amphibians evolved from fresh-water fishes in Devonian times some 300 million years ago. Changes in environment since that time led to physical and behavioural adaptation. A major evolutionary development was the formation of a dermal layer, which produced active secretions from the skin to retard desiccation¹. In frogs, the secretion has evolved further to help the general homeostasis²⁻⁵ and to protect it from a variety of predators and microbial pathogens.

2.2 Amphibian Skin and its Secretions

2.2.1 Glandular characteristics

Amphibians live in environments where there are numerous microbial pathogens. They have evolved a variety of host defence compounds to protect themselves from such pathogens. Many of these host defence compounds are peptides but there are also amines, steroid derivatives and toxic alkaloids in the glandular secretions^{1,4,6,7}.

The defense compounds are produced in specialised cells in both the gut and the skin. These secretions contain host defense compounds that represent a spectacular array of bio-organic chemicals.

The skin has two types of glands, the granular glands and the mucosal glands⁶. The active compounds are produced in the granular glands located on the dorsal surface and dispersed throughout the dermal layer of the frog. In some species of anuran, the glands are localised and enlarged, strategically concentrated in areas that are most exposed to predatory attack⁸. For example, the magnificent tree frog *Litoria splendida* has large parotoid and rostral glands at the back and front of the head respectively (*Figure 2.1*), while the common green tree frog of Australia (*Litoria caerulea*) has granular glands visible as small lumps all over the dorsal surface (*Figure 2.2*). The glands are classified by their anatomical position⁹ and are listed in *Table 2.1*.

Table 2.1: Classifications of the various glands present on the frog.

Type of glands	Anatomical position
Rostral	On the dorsal surface of the head
Supralibial	On the upper lip extending beyond the jaw
Parotoid	On the shoulders
Submandibular	Adjacent to the lower jaw
Coccygeal	Flanks on each side of the coccyx
Inguinal	On each side of the groin region
Femoral	On the postural surface of each femur
Tibial	On the dorsal surface of each calf

**Figure 2.1:** *Litoria splendida***Figure 2.2:** *Litoria caerulea*

Photographs by courtesy of Assoc. Prof. M J. Tyler

The action of the glands is controlled by the central nervous system, with the release of secretion occurring under stress¹⁰. For example, when attacked by a snake, the South African clawed frog will secrete particular chemicals to induce a yawning reflex in the predator, often allowing the frog to escape¹¹. Many of these defence agents are peptides, released onto the skin following stimulation or physical injury, and can kill bacteria, fungi, protozoa and cancerous cells¹².

2.2.2 Production of peptides

The granular glands are located below the epidermis (*Figure 2.3*) and consist of a myoepithelial cell envelope with the nuclei, endoplasmic reticulum and Golgi complexes located inside the cell. The lumen of the gland contains the secretory granules where the peptides are stored¹¹.

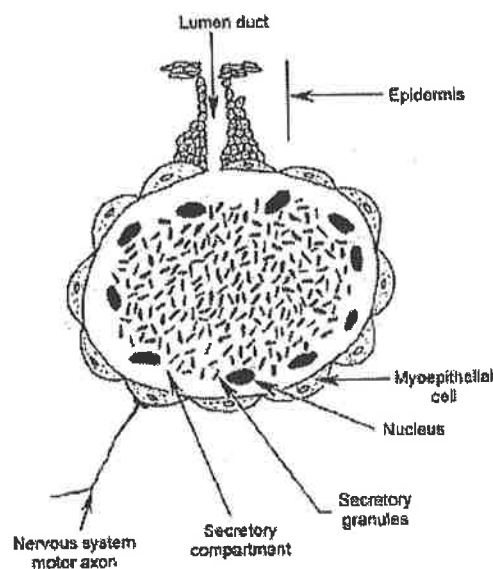


Figure 2.3: The granular gland of a frog (from¹¹)

The peptides are produced by transcription of the DNA to mRNA in the cell nucleus, followed by translation of the mRNA to produce a species called ‘the prepropeptide’ (signal-spacer-active peptide). An endoprotease cleaves off the signal peptide, and the inactive propeptide (spacer peptide-active peptide) is transported to the glands of the skin and gut as required.

The spacer peptide is normally anionic with its negative charge counteracting the positive charge of the active peptide^{13,14}. Following stimulation, another endoprotease cleaves off the spacer peptide and the active peptide is then released from the glands onto the skin and into the gut (*Figure 2.4*)^{15,16}.

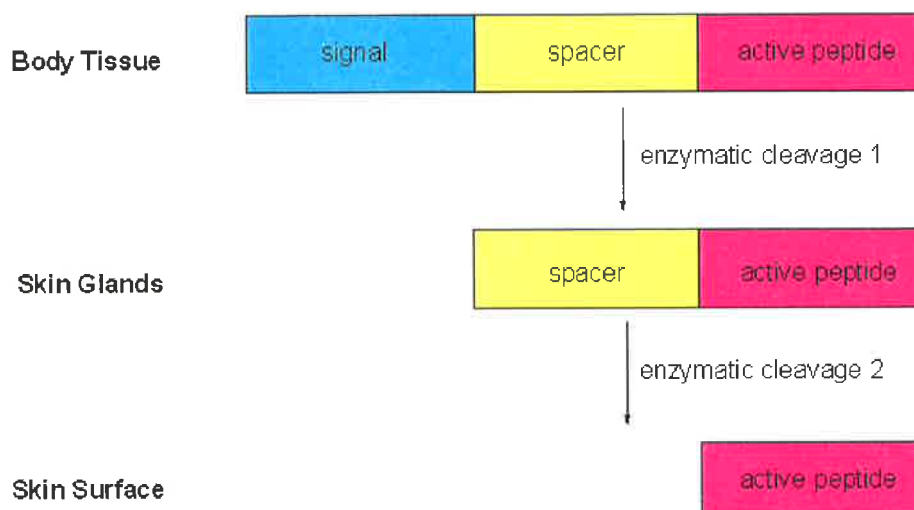


Figure 2.4: Schematic diagram showing the biosynthesis route of active peptide formation.

2.3 Amphibian Peptides and their Physiological Functions

Secretions from amphibian skin have been used by humans for medicinal and therapeutic purposes for over 2000 years. Traditional Chinese medicines used frog and toad skin secretions to regulate internal bodily functions and increase fertility^{1,17} while the Peruvian

Indians used the secretions to increase their physical strength, awareness and resistance to hunger¹⁸. As well as making the most of therapeutic agents secreted by the poison dart frog, Columbian Indians traditionally used its toxic secretions to tip their darts for hunting¹⁹. A poison dart frog contains nearly 200 micrograms of principally alkaloid toxins in its skin; the lethal dose for humans is only a few micrograms²⁰. Medical researchers have exploited the properties of these toxins to develop muscle relaxing and muscle stimulating agents²¹. Since then, particular frog-skin secretions have been used to develop several very useful medicines including heart stimulants, diuretics and antibacterials²².

Erspamer and his colleagues initiated studies on the isolation of amphibian peptides in the early 1960s²³. They first identified physalaemin as a potent hypotensive agent from South American frog *Physalaemus fuscumaculatus*^{23,24}. They reported that amphibian skin was a rich source of biologically active peptides⁴, and noted that many of these skin peptides were similar or identical to peptide hormones present in mammals²⁵. For example, crina-angiotensin II from *Crinia georgiana*²⁶ and xenopsin from *Xenopus laevis*^{27,28} are similar to the angiotensin and neurotensin mammalian hormones respectively. Since then, many families of amphibian peptides have been identified, including the bombesins, bradykinins, caeruleins, dermorphins, tachykinins, magainins and bombinins¹. Many of these peptides may have potential medical applications as drugs (*Table 2.2*).

Table 2.2: Physiological functions of amphibian peptides

Peptide	Sequence	Physiological function	Amphibian
Angiotensin	APGDRIYVHPF-OH	Vasodilator	<i>Crinia georgiana</i> ²⁹
Bombesin	pEQRLGNQWAVGH LM-NH ₂	Muscle stimulant	<i>Bombina bombina</i> ³⁰
Bombinin	GIGALSAKGALKGLA KGLAEHFAN-NH ₂	Antibacterial	<i>Bombina variegata</i> ³¹
Bradykinin	RPPGFSPFR-OH	Vasodilator	<i>Rana temporaria</i> ³²
Caerulein	YAFGYPS-NH ₂	Hypotensive	<i>Hyla caerulea</i> ³³
Dermorphin	pEQDY(SO ₃)TGWMDF- NH ₂	Analgaesic	<i>Phyllomedusa sauvagii</i> ²¹
Magainin	GIGKFLHSAGKFGKAF VGEIMKS-OH	Antibacterial	<i>Xenopus laevis</i> ^{34,35}
Tachykinin	pEADPNKFYGLM-NH ₂	Hypotensive	<i>Phyllomedusa bicolor</i> ¹⁸
Xenopsin	pEGKRPWIL-OH	Hypotensive	<i>Xenopus laevis</i> ^{27,28}

2.4 Peptides from the Genus *Litoria*

The Adelaide research group has investigated the host defence peptides from 34 species of Australian frogs and toads over the past fifteen years, isolating more than 150 biologically active peptides. The genera examined so far include are *Litoria*, *Uperoleia*, *Limnodynastes*, *Crinia* and *Cyclorana*³⁶⁻³⁸. Frogs of the genus *Litoria* however, have been studied the most, with the following species being investigated: *L. splendida*³⁹⁻⁴¹, *L. caerulea*^{42,43}, *L. gillini*⁴⁴, *L. ewingi*⁴⁵, *L. xanthomera*⁴⁶, *L. chloris*⁴⁷, *L. genimaculata*^{48,49}, *L. eucnemis*⁵⁰, *L. infrafronata*⁵¹, *L. citropa*^{52,53}, *L. subglandulosa*⁵⁰, *L. aurea*⁵⁴, *L. raniformis*⁵⁴ and *L. dahlii*⁵⁵.

The majority of frogs studied excrete a variety of peptides from the skin glands. The following types of host-defence peptides have been identified:- (a) neuropeptides falling

into two groups; (i) smooth muscle active compounds that lower blood pressure and sometimes also act as analgesics, and (ii) peptides that inhibit the formation of nitric oxide (NO) by neuronal nitric oxide synthase, (b) wide-spectrum antibiotic peptides, which often also act as antiviral, antifungal and anticancer agents, (c) narrow spectrum antibiotic peptides and (d) pheromone peptides.

2.4.1 Smooth muscle active neuropeptides

All species of the genus *Litoria* contain at least one neuropeptide from the caerulein family of peptides, a feature they have in common with a number of frogs and toads of other genera⁶. Caerulein exhibits a spectrum of activity similar to that of the mammalian intestinal peptides gastrin and CCK8 [DY(SO₃)TGWMFDF-NH₂]; it modifies satiety, sedation and thermoregulation, and is an analgesic several thousand times more active than morphine. A number of caerulein type peptides have been isolated from frogs of the *Litoria* genus: these are listed in Table 2.3. They all contain a tyrosine sulfate residue at position ⁴_β. Frogs may change their neuropeptide content depending on the time of year. For example *Litoria splendida* produces caerulein 1.1 in the summer months (the reproductive season), and caerulein 1.2 (Met8 to Phe8) in the winter (hibernation period)⁵⁶.

Table 2.3: Sequences of the caerulein peptides from *Litoria* species

Caerulein	Sequence	M.W. ^a	References
1.1	pEQDY(SO ₃)TGWMDF-NH ₂	1351	39-51,53-55,57
1.2	pEQDY(SO ₃)TGWDFDF-NH ₂	1367	41,53
2.1	pEQDY(SO ₃)TGAHMDF-NH ₂	1373	53
2.2	pEQDY(SO ₃)TGAHFDF-NH ₂	1389	53

3.1	pEQDY(SO ₃)GTGWMDf-NH ₂	1408	53
3.2	pEQDY(SO ₃)GTGWFDF-NH ₂	1424	53
4.1	pEQDY(SO ₃)TGSHMDf-NH ₂	1389	53
4.2	pEQDY(SO ₃)TGSHFDF-NH ₂	1405	53

Note: (a) nominal masses. The sum of the integral masses of all amino acid residues.

2.4.2 Neuronal nitric oxide synthase (NOS) inhibitors

The three oxide synthases, namely neuronal, endothelial and inducible, are highly regulated enzymes responsible for the synthesis of the signal molecule nitric oxide. They are among the most complex enzymes known (for nNOS see^{58,59}), and a complex sequence involving binding sites for a number of co-factors including heme, tetrahydrobiopterin, flavin mononucleotide (FMN), flavin adenine dinucleotide (FAD) and nicotinamide adenine dinucleotide (NADPH), nNOS, converts arginine to citrulline, releasing the short-lived but reactive radical NO^{60,61}. Nitric oxide synthases are composed of two domains: (i) the catalytic oxygenase domain that binds heme, tetrahydrobiopterin and the substrate arginine, and (ii) the electron-supplying reductase domain that binds NADPH, FAD and FMN. Communication between the oxygenase and reductase domains is determined by the regulatory enzyme calmodulin, which interacts at a specific site between the two domains. In the cases of nNOS and eNOS isoforms, the calmodulin is regulated by intracellular Ca²⁺, but not for iNOS⁶²⁻⁶⁵. Dimerisation of the oxygenase domain is necessary for catalytic activity^{60,61}.

All tree frogs of the genus *Litoria* have at least one peptide in their glandular skin secretion that inhibits the operation of nNOS. These peptides, which are often major components of the skin secretions, are usually active at a concentration of 10⁻⁶ molar. The peptides, which

inhibit the formation of NO from nNOS, either play a role in the fundamental physiology of the animal and/or are part of the defence arsenal used to combat attack by predators.

Table 2.4: Examples of nNOS inhibitors⁶⁶

Name	Source	Sequence	IC ₅₀ (µg/mL)
Inhibitor Group 1			
Citropin 1.1	<i>L. citropa</i>	GLFDVIKKVASVIGGL-NH ₂	8.2
Aurein 2.2	<i>L. aurea</i>	GLFDIVKKVVGALGSL-NH ₂	4.3
Inhibitor Group 2			
Frenatin 3	<i>L. infrafrenata</i>	GLMSVLGHAVGNVLGGLFKPKS-OH	6.8
Splendipherin	<i>L. splendida</i>	GLVSSIGKALGGLLADVVKSKGQPA-OH	8.5
Inhibitor Group 3			
Caerin 1.8	<i>L. chloris</i>	GLFKVLGSVAKHLLPHVVPVIAEKL-NH ₂	1.7
Caerin 1.9	<i>L. chloris</i>	GLFGVLGSIAKHVLPVVPVIAEKL-NH ₂	6.2

Amphibian peptide nNOS inhibitors fit into three structural types: i) short basic amphipathic peptides, which terminate in an amide group and are capable of adopting α -helical structure, ii) basic peptides, which terminate with carboxylic acid groups; and iii) peptides with a helix-hinge-helix type structure. Examples of these inhibitors are listed in *Table 2.4*. Although these three types of peptide have few structural features in common, it is thought that they operate in the same manner. Each of these peptides inhibits the operation of nNOS by interacting with the regulatory protein Ca²⁺ calmodulin to change its shape. As a consequence, the modified calmodulin is unable to attach to the calmodulin binding domain of nNOS⁶⁶.

2.4.3 Antibiotic and anticancer active peptides

The primary structures of antibacterial peptides can vary significantly, but the peptides generally interact directly with the membrane surface. The secondary structures of antibacterial peptides are crucial for their activity⁶⁷.

Antibacterial peptides normally have an excess of positive charge due to the presence of more basic amino acid residues (e.g. arginine and lysine) than acidic residues (aspartic acid and glutamic acid). They often have amphipathic, α -helical structures⁶⁸, containing 13-30 amino acid residues. Antibacterial peptides bind to the bacterial membrane by electrostatic interactions⁶⁹⁻⁷². The positively charged residues bind to the negatively charged lipid head group⁶⁹. The all D-isomers of selected antibiotic peptides have been shown to have equivalent activity to the natural L form, a characteristic of membrane active peptides^{38,73}.

An antibacterial peptide is often conformationally random in extracellular fluid but may adopt an α -helical formation in the vicinity of a membrane. The α -helical structure can be represented using an Edmundson helical wheel projection⁷⁴. This is a two-dimensional representation of the three dimensional structure of an α -helix. The perimeter of the wheel corresponds to the backbone of the polypeptide chain. The α -side chains are projected onto the plane, which is perpendicular to the axis of the helix. Adjacent residues are spaced 100° apart around the circumference and one turn of an α -helix is 3.6 residues long. This corresponds to 18 residues per revolution of a helix. The α -carbon atoms of the residues in the peptide are numbered from 1 to 18 for a complete helix starting at the N-terminal end as shown in *Figure 2.5*.

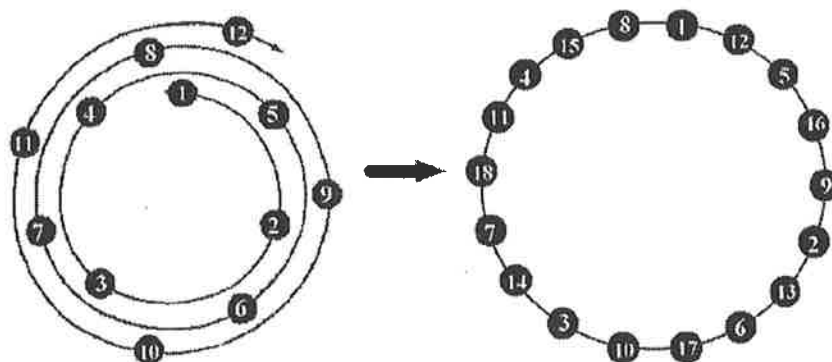


Figure 2.5: Edmundson helical wheel projection

Basic antibacterial peptides will bind to negatively charged phospholipid head groups of the lipid bilayer in a bacterial membrane⁶⁹. This interaction does not occur with normal cells since they have mainly zwitterionic phospholipids on their outer membrane. The lipid environment of the bacterial membrane induces the peptide to form an α -helical structure. The antibacterial peptides arrange themselves in a parallel manner on the membrane allowing the hydrophobic region to be buried in the lipid environment whereas the hydrophilic region is exposed to the aqueous environment and the polar lipid head groups.

A bacterial cell membrane is normally formed from a phospholipid bilayer, which provides a natural barrier to confine the flow of ions and other solutes between the bacterial cell and its environment. Disruption of the bilayer will cause cell death. Antibacterial peptides are thought to act by disrupting the integrity of the cytoplasmic membrane.

The mechanism of antibiotic action of the peptide involves penetration of the membrane^{75,76} resulting in the formation of water-filled pores⁷⁷, causing lysis of the cell.

The exact details of how this occurs are still unclear, but there are two major mechanisms proposed to explain penetration of a membrane. The first involves penetration through the membrane by the 'barrel-stave' mechanism. For this, the peptide must have a minimum of

20 residues to effect full penetration of the membrane⁷⁸ as shown in *Figure 2.6*. This process involves the unstructured cationic peptides binding to the membrane surface. The cationic residues of the peptide are electrostatically attracted to the anionic head groups of the membrane, and upon this interaction the peptides adopt amphipathic α -helical structure. The peptides aggregate on the surface, before inserting vertically into the bilayer to form a transmembrane pore, with their hydrophobic surfaces facing the core. These interact with the hydrophobic alkyl chains of the phospholipid bilayer. The polar hydrophilic surfaces are arrayed in the central pore allowing the passive flux of ions and small molecules across the membrane, disrupting the osmotic gradient of the cell, ultimately lysing the cell.

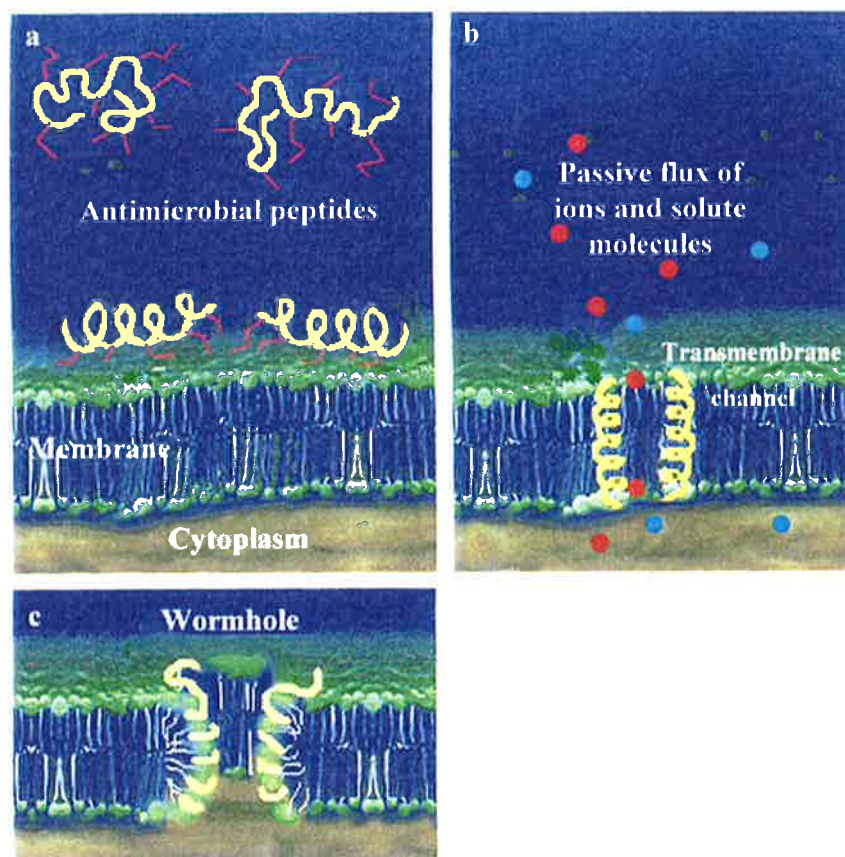


Figure 2.6: A picture illustrating the 'barrel-stave' model suggested for membrane permeation, (a) interaction of peptides with membrane followed by (b) transmembrane channel formation resulting in the passive flux of ions and solute and (c) a worm hole.
(from⁷⁸)

The second mechanism is known as the ‘carpet’ mechanism⁷⁹⁻⁸¹. The initial stages of this mechanism involve the unstructured peptide binding to the lipid membrane, where it adopts an amphipathic structure before intercalating into the membrane surface. A carpet is formed as additional monomers cover the surface. Once a threshold concentration is reached, the membrane disintegrates. At this stage transmembrane pores may form allowing peptides to cross the membrane and membrane segments may break off as micelles.

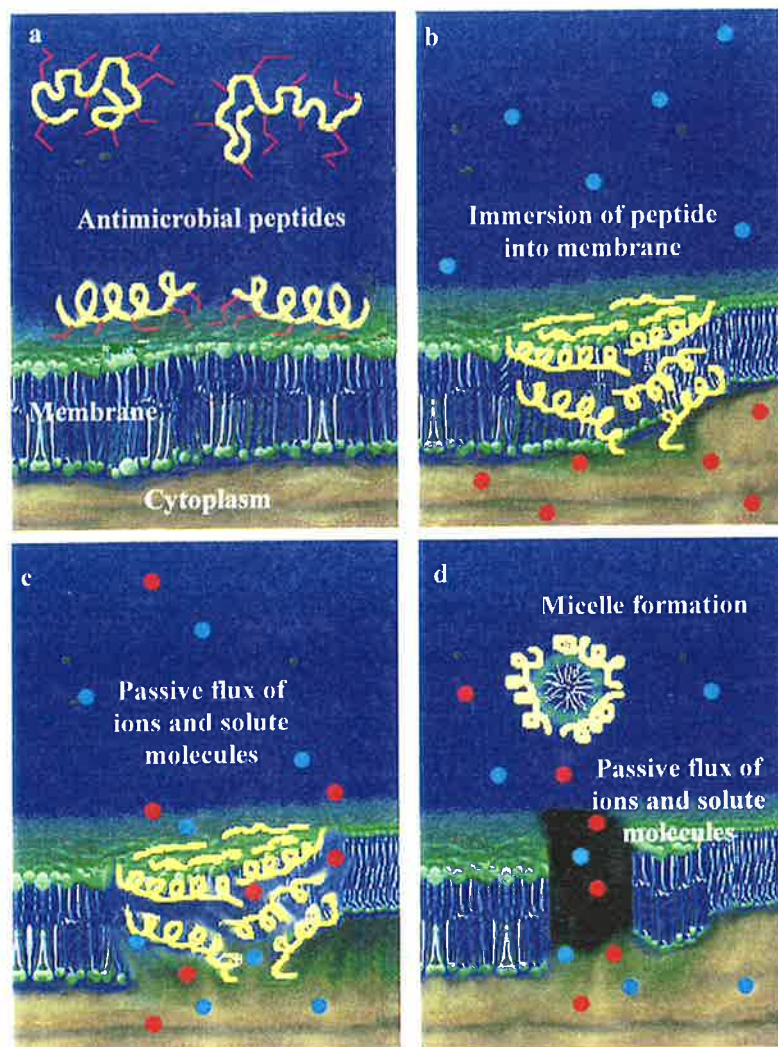


Figure 2.7: A picture illustrating the ‘carpet-like’ model suggested for membrane permeation, (a) peptides-membrane interaction followed by (b) immersion of peptides into phospholipid bilayer and, the last step could be either (c) membrane disintegration or (d) peptide-lipid micelle formation. (from⁷⁸)

The antibiotic and anticancer active peptides from the *Litoria* species have been divided into two general groups: (i) the caerin type peptides (ii) the citropin type peptides.

1) *The caerin type antibiotic and anticancer active peptides*

Tree frogs of the genus *Litoria* have a cocktail of antibacterial peptides including both wide-spectrum and narrow spectrum antibiotics. The wide spectrum antibiotics also show wide spectrum anticancer activity in tests carried out by the National Cancer Institute (Washington, DC). The wide spectrum active peptides show antibiotic and anticancer activity in the 1-100 $\mu\text{g}/\text{mL}$ range. Some of these active peptides are listed in *Table 2.5*.

Table 2.5: *The caerin and related peptides from Litoria species*

Name	Sequence	Species
Caerin 1.1	GLLSVLGSAKHVLPVVPVIAEHL-NH ₂	a, b, c, d
Caerin 1.2	GLLGVLGSAKHVLPVVPVIAEHL-NH ₂	a
Caerin 1.3	GLLSVLGSAQHVLPHVVPVIAEHL-NH ₂	a
Caerin 1.4	GLLSSLSSVAKHVLPVVPVIAEHL-NH ₂	a
Caerin 1.5	GLLSVLGSVVKHVIPVVPVIAEHL-NH ₂	a
Caerin 1.6	GLFSVLGAVAKHVLPVVPVIAEKL-NH ₂	e, f
Caerin 1.7	GLFKVLGSAKHLLPHVAPVIAEKL-NH ₂	e, f
Caerin 1.8	GLFKVLGSAKHLLPHVVPVIAEKL-NH ₂	f
Caerin 1.9	GLFGVLGSIAKHVLPVVPVIAEKL-NH ₂	f
Caerin 1.10	GLLSVLGDVAKHVLPVVPVIAEKL-NH ₂	b
Maculatin 1.1	GLFGVLAKVAAHVPAIAEHF-NH ₂	g

Note: (a) *Litoria caerulea*^{42,43}, (b) *Litoria splendida*³⁹⁻⁴¹, (c) *Litoria gilleni*⁴⁴, (d) *Litoria ewingi*⁴⁵, (e) *Litoria xanthomera*⁴⁶, (f) *Litoria chloris*⁴⁷, and (g) *Litoria genimaculata*^{48,49}

All the caerin 1 peptides are basic peptides with similar sequences, and NMR studies show that they have two α helical regions separated by a central hinge region of higher flexibility. The 3D structure of caerin 1.1 is shown in *Figure 2.8*. Maculatin 1.1 is a

modified caerin 1.1, which has four residues missing from the central hinge region. The 3D structure of maculatin 1.1 is shown in *Figure 2.9*.

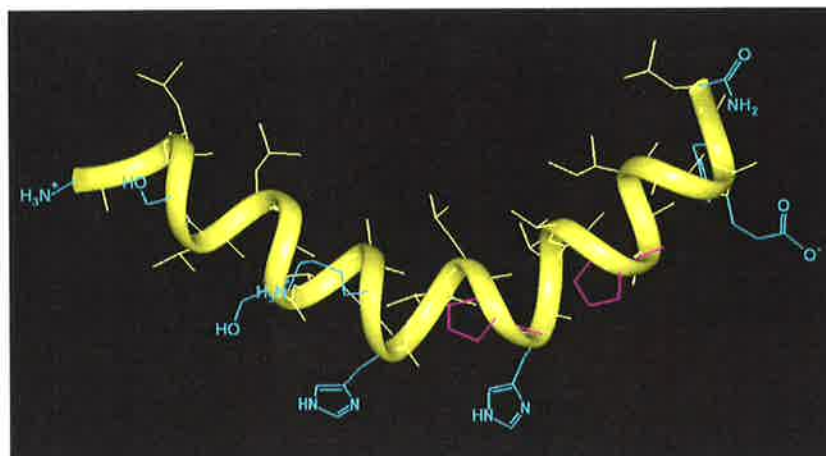


Figure 2.8: The 3D structure of caerin 1.1

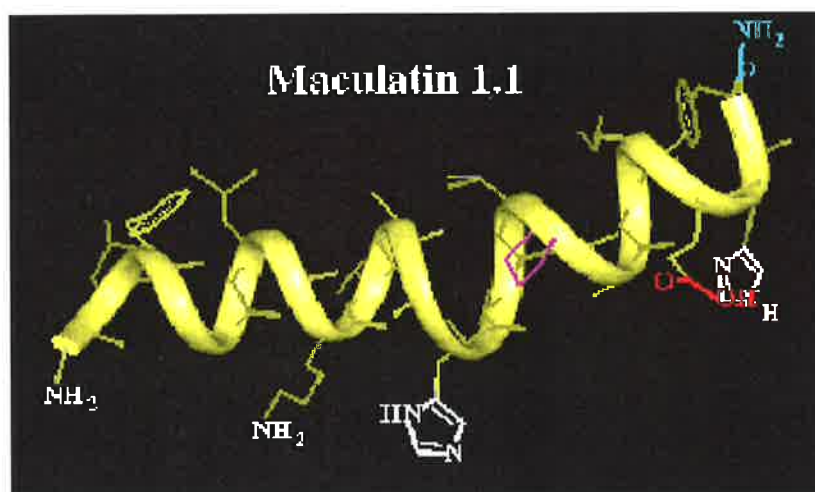


Figure 2.9: The 3D structure of maculatin 1.1

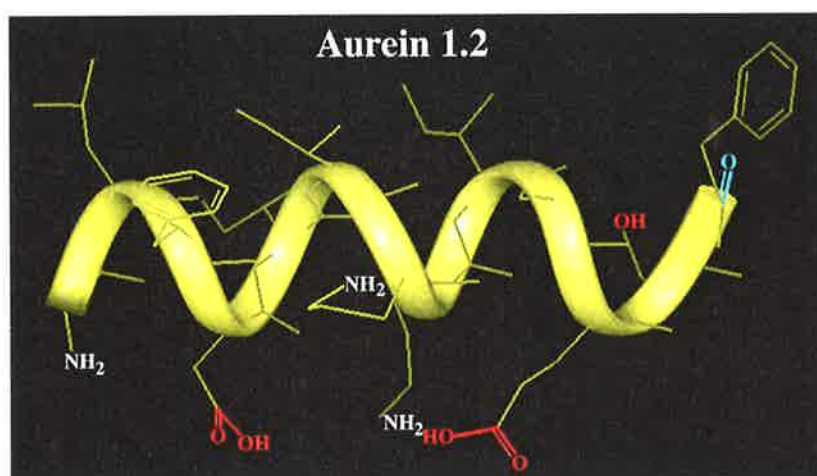
2) The citropin type antibiotic and anticancer active peptides

There are a number of species of the genera *Litoria* that do not produce hinged antibiotic and anticancer active peptides of the caerin or maculatin families. The most abundant peptides in these glandular secretions are simple basic amphipathic peptides of the type shown in *Table 2.6*.

Table 2.6: The citropin type peptides

Name	Sequence	Species
Aurein 1.1	GLFDILKKLAQSL-NH ₂	<i>L. aurea</i> ⁵⁴
Aurein 3.1	GLFDIVKKLKLAGHIAGST-NH ₂	<i>L. aurea</i> ⁵⁴
Citropin 1.1	GLFDVIKKVASVIGGL-NH ₂	<i>L. citropa</i> ⁵³
Citropin 1.2	GLFDIIKKVASVVGGL-NH ₂	<i>L. citropa</i> ⁵³
Citropin 1.3	GLFDIIKKVASVIGGL-NH ₂	<i>L. citropa</i> ⁵³
Maculatin 2.1	GFVDLKKVAGTIANVVT-NH ₂	<i>L. genimaculata</i> ⁴⁸

The smallest of the peptides shown in *Table 2.6* is the thirteen residue aurein 1 peptide: this is one of the smallest amphibian peptides to show significant antimicrobial and anticancer activity⁵⁴. Most of these peptides, like the citropins 1, contain sixteen amino acid residues. All of these basic peptides have Lys residues at positions 7 and 8. The 3D structures of aurein 1.2 and citropin 1.1 are shown in *Figures 2.10* and *Figure 2.11* respectively: both structures are simple α helices with well defined hydrophobic and hydrophilic zones.

**Figure 2.10:** The 3D structure of aurein 1.2

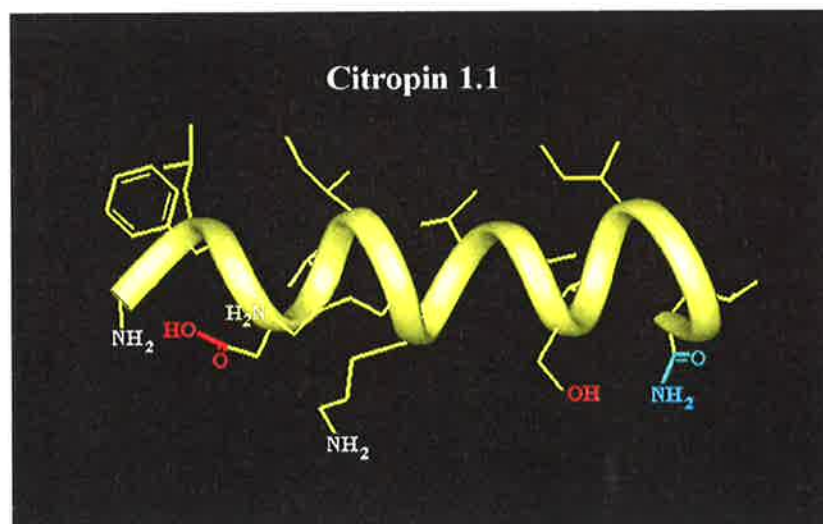


Figure 2.11: The 3D structure of citropin 1.1

2.4.4 Pheromones

Pheromones are chemical signals that members of a particular species use to communicate with one another⁸². They are generally active in minute quantities and may evoke a behavioural response as a signal compound or as part of a complex mixture⁸³. The behavioural response is dependent on the type of signal or message that the pheromone is carrying. There are several types of pheromones including recognition, aggregation, dispersion, aggression and sex pheromones.

Typical communication by a pheromone consists of three components: (i) message emission; this process involves a glandular organ associated with a specialised mechanism that transfers the chemical molecules into the surrounding system⁸⁴, (ii) message transmission; pheromones are transmitted and dispersed throughout the water/air, (iii) message reception; this pheromone is perceived by an olfactory (the sense of smell) process. This process involves the absorption of pheromone into the specialised sensory

neurons that extend into either a cavity or sensory fibers⁸⁵, and then move to the receptor sites within the neurons by diffusion⁸⁶.

A peptide isolated from males of *Litoria splendida* during the breeding season has been shown to act as a sex pheromone. This peptide, named splendipherin (GLVSSIGKALGGLLADVVKSKGQPA-OH), attracts the female frog in water at a concentration of 10^{-11} - 10^{-9} M and is species specific. Peptides from other species, which have similar sequences to splendipherin, for example aurein 5.2 (GLMSSIGKALGGLIVDVLKPKTPAS-OH) from *L. aurea*, may also have some kind of pheromone role. However, this needs to be determined through further experimentation⁵⁴.

2.4.5 Other functions

The majority of *Litoria* species have host defence peptides of the type outlined above, namely, neuropeptides and antimicrobial peptides. However, there are some species that are exceptions to this scenario and have apparently evolved differently. The red tree frog *Litoria rubella* is widespread throughout central and northern Australia, and a related species *Litoria electrica* is found only in northern Australia. Both of these frogs produce abundant secretions, which contain no antimicrobial peptides, but yield the small peptides shown in *Table 2.7*. The actual role of these peptides in amphibian skin is not fully understood. Similar peptides are known to have a sedative effect and it is possible that they may turn out to be neuromodulators or neurotransmitters.

Table 2.7: Tryptophyllin peptides from *L. rubella* and *L. electrica*

Name	Sequence	Species
Tryptophyllin 1.1	PWL-NH ₂	<i>L. rubella</i> ⁸⁷
Tryptophyllin 1.2	FPWL-NH ₂	<i>L. rubella</i> ⁸⁷ and <i>L. electrica</i> ⁸⁸
Tryptophyllin 1.3	pEFPWL-NH ₂	<i>L. rubella</i> ⁸⁷
Tryptophyllin 1.4	FPPFWL-NH ₂	<i>L. rubella</i> ⁸⁷

2.5 Collection of Frog Peptides

Previously, the isolation of amphibian peptides required killing large numbers of anurans and extracting the dried skin. The skins were removed, dried and the peptides extracted using methanol. Sometimes more than 1000 specimens were required to provide enough material for identification⁸⁹. Since many frogs are now endangered species, several non-harmful methods of extraction have been developed. Injection of adrenaline or noradrenaline into the frog affects the release of the secretion without harming the animal⁹⁰. More recently, a benign method of extraction involving surface electrical stimulation (SES) has been reported⁹¹. The frog is held and its skin moistened with distilled water. A platinum electrode is attached to an electrical stimulator and is rubbed over the glandular region. This mild electrical stimulation induces the release of the secretion. The stimulus strength varies with the size of the frog. After a short delay, the secretion is discharged and the entire process is completed in 30-40 seconds. The crude secretion is washed from the skin with distilled water and diluted with an equivalent volume of methanol to deactivate any enzymes. The secretion is immediately worked up (by centrifuging followed by lyophilization) as the active peptides risk being degraded by any enzymes left in the secretion. The same animal can be stimulated monthly, which allows sufficient time for the glands to replenish their secretions.

Once secretions have been collected, they are concentrated and subjected to high performance liquid chromatography to separate and purify the peptide components. The primary amino acid sequences are identified using the complementary methods of electrospray mass spectrometry and Edman sequencing as described in *Chapter 1, Section 1.7*.

2.6 References

- 1) Lazarus, L. H.; Attila, M. *Prog. Neurobiol.* **1993**, *41*, 473.
- 2) Wygoda, M. *Herpetologica* **1988**, *44*, 251.
- 3) Naidu, K. A. *Indian J. Exp. Biology* **1988**, *26*, 37.
- 4) Bevin, C. L.; Zasloff, M. *Ann. Rev. Biochem.* **1990**, *59*, 395.
- 5) Amey, A. P.; Grigg, G. C. *Comp. Biochem. Physiol.* **1995**, *111A*, 283.
- 6) Erspamer, V. *Amphibian Biology: The integument*; Surrey Beatty and Sons: Norton, NSW, Australia, 1994; Vol. 1, p 178.
- 7) Barra, D.; Simmaco, M. *Trends Biochem.* **1995**, *13*, 205.
- 8) Toledo, R. C.; Jared, C. *Comp. Biochem. Physiol.* **1995**, *111A*, 1.
- 9) Tyler, M. J. *Encyclopaedia of Australian Animals*; Strahan, R., Ed.; Harper Collins: London, U. K., 1992, p 3.
- 10) Jackson, I. M.; Reichlin, S. *Science* **1977**, *198*, 414.
- 11) Barthalmus, G. T.; Zielinski, W. J. *Pharmacol. Biochem. Behav.* **1988**, *30*, 957.
- 12) Boman, H. G. *Cell* **1991**, *65*, 205.
- 13) Dockary, G. J.; Hopkins, C. R. *J. Cell. Biol.* **1975**, *64*, 724.
- 14) Terry, A. S.; Poulter, L.; Williams, J. C.; Hutkins, M.; Giovannini, C. H. *J. Biol. Chem.* **1988**, *263*, 5745.
- 15) Hauser, F.; Hoffman, W. *J. Biol. Chem.* **1992**, *34*, 24620.
- 16) Hernandez, C.; Mor, A.; Dunia, I. *Eur. J. Cell* **1992**, *59*, 414.
- 17) Tyler, M. J. *Toxic Plants and Animals: A guide for Australia*; Covacevich, J., Davie, P. and Pearn, J., Ed.; Queensland Museum: Brisbane, 1987, p 329.
- 18) Erspamer, V.; Erspamer, G. F.; Severini, C.; Potenza, R. L.; Barra, D.; Mignogna, G.; Bianchi, A. *Toxicon.* **1993**, *31*, 1099.

- 19) Carraway, R. E.; Cochrane, D. E. *J. Biol. Chem.* **1987**, *261*, 15886.
- 20) Labler, L.; Keilova, H.; Sorm, F.; Styblova, S. *Toxicon* **1968**, *5*, 247.
- 21) Negri, L.; Lattanzi, R.; Melchiorri, P. *Brit. J. Pharm.* **1995**, *114*, 57.
- 22) Daly, J. W.; Caceres, J.; Moni, R. W.; Gusovsky, F.; Moos, M.; Seamon, K. B.; Milton, K.; Myers, C. W. *Proc. Natl. Acad. Sci. USA* **1992**, *89*, 10960.
- 23) Erspamer, V.; Bertaccini, G.; Cei, J. M. *Experientia* **1962**, *18*, 562.
- 24) Erspamer, V.; Anastasi, A.; Bertaccini, G.; Cei, J. M. *Experientia* **1964**, *20*, 489.
- 25) Erspamer, V.; Melchiorri, P. *Pure Appl. Chem.* **1973**, *35*, 463.
- 26) Erspamer, V.; Melchiorri, P.; Nakajima, T.; Yasuhara, T.; Enden, R. *Experientia* **1979**, *35*, 1132.
- 27) Araki, K.; Tachibana, S.; Uchiyama, M.; Nakajima, T.; Yasuhara, T. *Chem. Pharm. Bull.* **1973**, *21*, 2801.
- 28) Araki, K.; Tachibana, S.; Uchiyama, M.; Nakajima, T.; Yasuhara, T. *Chem. Pharm. Bull.* **1975**, *23*, 3132.
- 29) Erspamer, V.; Melchiorri, P.; Nakajima, T.; Yasuhara, T.; Endean, R. *Experientia* **1979**, *35*, 1132.
- 30) Erspamer, V.; Erspamer, G. F.; Inselvini, M.; Negri, L. *Brit. J. Pharmacol.* **1972**, *45*, 333.
- 31) Simmaco, M.; Barra, D.; Chiarini, F.; Noviello, L.; Melchiorri, P.; Kreil, G.; Richter, K. *Eur. J. Biochem.* **1991**, *199*, 217.
- 32) Anastasi, A.; Erspamer, V.; Bertaccini, G. *Comp. Biochem. Physiol.* **1965**, *14*, 43.
- 33) Gibson, B. W.; Poulter, L.; Williams, D. H.; Maggio, J. E. *J. Biol. Chem.* **1986**, *261*, 5341.
- 34) Soravia, E.; Martini, G.; Zasloff, M. *FEBS Lett.* **1988**, *228*, 337.
- 35) Berkowitz, B. A.; Bevins, C. L.; Zasloff, M. *Biochem. Pharmacol.* **1990**, *39*, 625.

- 36) Bowie, J. H.; Tyler, M. J.; Chia, B. C. S.; Carver, J. A.; Wallace, J. C. *Chem. Aust.* **1998**, *9*, 45.
- 37) Bowie, J. H.; Chia, B. S. C.; Tyler, M. J. *Pharm. News.* **1998**, *5*, 16.
- 38) Bowie, J. H.; Wegener, K. L.; Wabnitz, P. A.; Chia, B. C. S.; Carver, J. A.; Wallace, J. C.; Tyler, M. J. *Protein and Peptide Letts.* **1999**, *6*, 259.
- 39) Stone, D. J. M.; Bowie, J. H.; Tyler, M. J.; Wallace, J. C. *Chem. Commun.* **1992**, 1224.
- 40) Stone, D. J. M.; Waugh, R. J.; Bowie, J. H.; Wallace, J. C.; Tyler, M. J. *J. Chem. Soc. Perkin. Trans. 1* **1992**, *1*, 3173.
- 41) Wong, H.; Bowie, J. H.; Carver, J. A. *Eur. J. Biochem.* **1997**, *247*, 545.
- 42) Waugh, R. J.; Stone, D. J. M.; Bowie, J. H.; Wallace, J. C.; Tyler, M. J. *J. Chem. Soc. Perkin. Trans. 1* **1993**, 573.
- 43) Stone, D. J. M.; Waugh, R. J.; Bowie, J. H.; Wallace, J. C.; Tyler, M. J. *J. Chem. Res. S* **1993**, 138.
- 44) Waugh, R. J.; Stone, D. J. M.; Bowie, J. H.; Wallace, J. C.; Tyler, M. J. *J. Chem. Res. S* **1993**, 139.
- 45) Steinborner, S. T.; Bowie, J. H.; Tyler, M. J.; Wallace, J. C. *Aust. J. Chem.* **1997**, *50*, 889.
- 46) Steinborner, S. T.; Waugh, R. J.; Bowie, J. H.; Wallace, J. C.; Tyler, M. J.; Ramsay, S. L. *J. Peptide Sci.* **1997**, *3*, 181.
- 47) Steinborner, S. T.; Currie, G. J.; Bowie, J. H.; Wallace, J. C.; Tyler, M. J. *J. Peptide Res.* **1998**, *51*, 121.
- 48) Rozek, T.; Waugh, R. J.; Steinborner, S. T.; Bowie, J. H.; Wallace, J. C.; Tyler, M. J. *J. Peptide Sci.* **1998**, *4*, 111.
- 49) Chia, B. C. S.; Bowie, J. H.; Carver, J. A.; Mulhern, T. D. *Eur. J. Biochem.* **2000**, *267*, 1894.

- 50) Brinkworth, C. S.; Bowie, J. H.; Wallace, J. C.; Tyler, M. J. *unpublished work* .
- 51) Waugh, R. J.; Raftery, M. J.; Bowie, J. H.; Tyler, M. J.; Wallace, J. C. *J. Peptide Sci.* **1996**, *10*, 92.
- 52) Wabnitz, P. A.; Bowie, J. H.; Tyler, M. J. *Rapid Commun. Mass Spectrom.* **1999**, *13*, 2498.
- 53) Wegener, K. L.; Wabnitz, P. A.; Carver, J. A.; Bowie, J. H.; Chia, B. C. S.; Wallace, J. C.; Tyler, M. J. *Eur. J. Biochem.* **1999**, *265*, 627.
- 54) Rozek, T.; Wegener, K. L.; Bowie, J. H.; Olver, I. N.; Carver, J. A.; Wallace, J. C.; Tyler, M. J. *Eur. J. Biochem.* **2000**, *267*, 5330.
- 55) Wegener, K. L.; Brinkworth, C. S.; Bowie, J. H.; Wallace, J. C.; Tyler, M. J. *Rapid Commun. Mass Spectrom.* **2001**, *15*, 1726.
- 56) Wabnitz, P. A.; Bowie, J. H.; Tyler, M. J.; Wallace, J. C.; Smith, B. P. *Eur. J. Biochem.* **2000**, *267*, 269.
- 57) Wabnitz, P. A.; Bowie, J. H.; Tyler, M. J. *Rapid Commun. Mass Spectrom.* **1999**, *13*, 2498.
- 58) Bredt, D. S.; Hwang, P. M.; Glatt, C. L.; Lowenstein, C.; Reed, R. R.; Snyder, S. H. *Nature* **1991**, *351*, 714.
- 59) Marletta, M. A. *J. Biol. Chem.* **1993**, *268*, 12231.
- 60) Marletta, M. A. *Cell* **1994**, *78*, 927.
- 61) Pfeiffer, S.; Mayer, B.; Hemmens, B. *Angew. Chem. Intl. Ed. Engl.* **1999**, *38*, 1715.
- 62) Forsen, S. *Nat. Struct. Biol.* **1995**, *2*, 777.
- 63) Venema, R. C.; Sayegh, H. S.; Kent, J. D.; Harrison, D. G. *J. Biol. Chem.* **1996**, *271*, 6435.
- 64) Lee, S. J.; Stull, J. T. *J. Biol. Chem.* **1998**, *273*, 27430.
- 65) Matsuda, H.; Iyanagi, T. *Biochem. Biophys. Acta* **1999**, *1473*, 345.

- 66) Doyle, J.; Llewellyn, L. E.; Brinkworth, C. S.; Bowie, J. H.; Wegener, K. L.; Rozek, T.; Wabnitz, P. A.; Wallace, J. C.; Tyler, M. J. *Eur. J. Biochem.* **2002**, *269*, 100.
- 67) Saberwal, G.; Nagaraj, R. *Biochem. et. Biophys. Acta* **1994**, *1197*, 109.
- 68) Marion, D.; Zasloff, M.; Bax, A. *FEBS Lett.* **1988**, *227*, 21.
- 69) Nakajima, Y.; Qu, X. M.; Natori, S. *J. Biol. Chem.* **1987**, *262*, 1165.
- 70) Hoffman, W. *J. Biol. Chem.* **1988**, *263*, 7686.
- 71) Williams, R. W.; Starman, R.; Taylor, K. P.; Beeler, T.; Covell, D.; Zasloff, M. *Biochemistry* **1990**, *29*, 4490.
- 72) Jacob, L.; Zasloff, M. *Antimicrobial Peptides: Ciba Foundation Symposium 186*; Marsh, J. and Goode, J. A., Ed.; John Wiley & Sons: London, 1994, p 197.
- 73) Wade, D.; Boman, A.; Wahlen, B.; Drain, C. M.; Andreu, D.; Boman, H. G.; Merrifield, R. B. *Proc. Natl. Acad. Sci. USA* **1990**, *87*, 4761.
- 74) Schiffer, M.; Edmundson, A. B. *J. Biophys.* **1967**, *7*, 121.
- 75) Waal, A.; Gomes, A. V.; Mensick, A.; Grootegoed, J. A. *FEBS Lett.* **1991**, *293*, 219.
- 76) Cruciani, R. A.; Barker, J. L.; Zasloff, M.; Chen, H. C.; Colamonici, O. *Proc. Natl. Acad. Sci. USA* **1991**, *88*, 3792.
- 77) Cruciani, R. A.; Barker, J. L.; Durell, S. R.; Raghunathan, G.; Guy, H. R.; Zasloff, M.; Stanley, F. *Eur. J. Pharmacol.* **1992**, *226*, 287.
- 78) Ojcius, D. M.; Young, J. D. E. *Trends. Biochem. Sci.* **1991**, *16*, 225.
- 79) Shai, Y. C. *Trends Biochem.* **1995**, *20*, 460.
- 80) Bechinger, B. *J. Membr. Biol.* **1997**, *156*, 197.
- 81) Matsuzaki, K. *Biochem. Biophys. Acta* **1998**, *1376*, 391.
- 82) Guerin, P.; Arn, H.; Buser, H. R. *Semiochemistry Flavours and Pheromones*; Acree, T. and Soderlund, D., Ed.; Proceedings American Chemical Society Symposium: Washington, DC, 1983, p 239.

- 83) Birch, M. C. *Pheromones*; Neuberger, A. and Tatum, E. L., Ed.; Northholland Research Monographs, Frontiers of Biology: Amsterdam, The Netherlands, 1974, p 1.
- 84) Shorey, H. H. *Animal Communication by Pheromones*; Academic Press: New York, 1976, p 2.
- 85) Scott, J. W. *J. Steroid Biochem. Mol. Biol.* **1991**, *39*, 593.
- 86) Pace, U.; Hanski, E.; Solomon, Y.; Lancet, D. *Nature* **1985**, *316*, 255.
- 87) Steinborner, S. T.; Gao, C.; Raftery, M. J.; Waugh, R. J.; Blumenthal, T.; Bowie, J. H.; Wallace, J. C.; Tyler, M. J. *Aust. J. Chem.* **1994**, *47*, 2099.
- 88) Wabnitz, P. A.; Bowie, J. H.; Wallace, J. C.; Tyler, M. J. *Aust. J. Chem.* **1999**, *52*, 639.
- 89) Roseghini, M.; Erspamer, V.; Endean, R. *Comp. Biochem. Physiol.* **1976**, *54*, 31.
- 90) Nakajima, T. *Trends. Pharmacol. Sci.* **1981**, *2*, 202.
- 91) Tyler, M. J.; Stone, D. J.; Bowie, J. H. *J. Pharm. Toxicol. Methods* **1992**, *28*, 199.

Chapter Three

Peptides from *Litoria alboguttata* and *Cyclorana australis*

3.1 General

Closely related species of frogs contain similar host defence peptides in their glandular secretions, e.g. related tree frogs of the genus *Litoria* most produce caerin peptides (see *Chapter 2, Table 2.5*), the *L. citropa* group produce citropin type peptides (see *Chapter 2, Table 2.6*), while the *L. rubella* group of frogs all produce tryptophyllin peptides (see *Chapter 2, Table 2.7*).

There is a frog called the Striped Burrowing Frog (*Litoria alboguttata*) which has been very difficult to classify. It is the only species of the genus *Litoria* which is able to burrow, and it has a marked resemblance to burrowing frogs of the genus *Cyclorana*. A preliminary survey of the peptides of several species of the genus *Cyclorana* was carried out in

1993/1994; they have very different peptides from anything we have outlined in *Chapter 2* for frogs of the genus *Litoria*. The purpose of the present project is to determine the structures of peptides from the glandular secretion of *Litoria alboguttata* to see whether the peptides are similar to those isolated from *Litoria* species, or if these peptides are similar to those previously isolated from *Cyclorana* species. The two species we have investigated, *L. alboguttata* and *C. australis* are compared in *Figures 3.1* and *3.2*.



Figure 3.1: L. alboguttata



Figure 3.2: C. australis

Photographs provided through the
courtesy of Assoc. Prof. M. J. Tyler

Litoria alboguttata is shown in *Figure 3.1*. The back is olive to pale green with brown patches and a pale yellow/green mid-vertebral stripe. The ventral surface is a dull white with darker mottling, particularly upon the throat. Males are 54-67 mm long; females 61-

83 mm. This species inhabits inundated grasslands and open forest. It ranges from the north-eastern coastal region of the Northern Territory around the east coast of Queensland into northern New South Wales¹ as shown in *Figure 3.3*. The Giant Frog *Cyclorana australis* is shown in *Figure 3.2*. The dorsum varies from pale grey to brown, with or without small darker markings through to bright green. Dark brown or chocolate head stripes extend from the tip of the snout to the flanks, and there is often a pale mid-dorsal stripe. Males are 70-77 mm long; females 71-105 mm. This ground dwelling frog is found in northern Australia, from Broome in Western Australia across to the western edge of Cape York in Queensland as shown in *Figure 3.4*. In the wet season it basks near temporary pools².

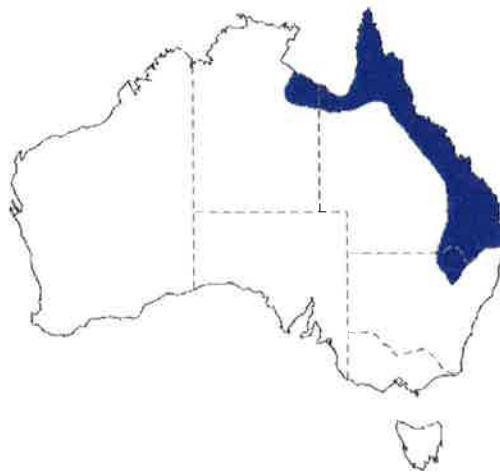


Figure 3.3: Diagram of the geographic distribution of *Litoria alboguttata*

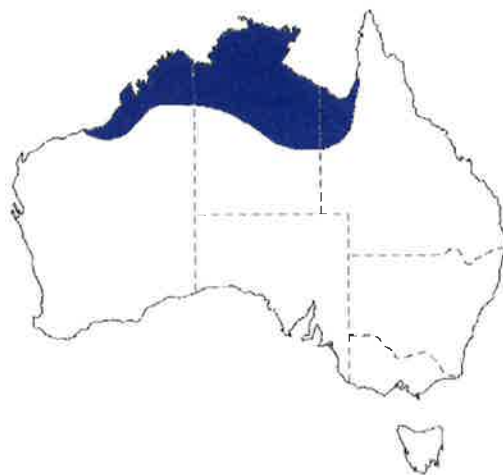


Figure 3.4: Diagram of the geographic distribution of Cyclorana australis

3.2 Results and Discussion

3.2.1 Isolation and identification of peptides from the glandular secretion of *Litoria alboguttata*

Litoria alboguttata has granular glands across the entire dorsal surface. These glands can be seen as protuberances on the back of the animal, as shown in *Figure 3.1*. We use the benign method of electrical stimulation on the dorsal surface of the animal to force it to exude its glandular secretion³. This is immediately washed from the skin with distilled and deionised water. The aqueous extract is then diluted with methanol (1:1), to precipitate and deactivate any proteases which might degrade the active peptides. The mixture is centrifuged, and the remaining liquid taken down under vacuum until there is only 1 mL left. This material is then subjected to HPLC separation. ^{See Section 3.4 for details.} The analytical HPLC profile of this secretion is shown in *Figure 3.5*. A number of HPLC runs were carried out, individual fractions were collected from each HPLC experiment and the same fractions from each experiment combined in order to provide sufficient material (generally about 25 µg) for

mass spectrometric investigations. Each combined fraction was lyophilised and subjected to electrospray mass spectrometry (ESMS) using either a Finnigan LCQ or a Micromass QTOF 2 mass spectrometer. The spectra shown in *Figures 3.6-3.8* were determined using the QTOF 2 spectrometer.

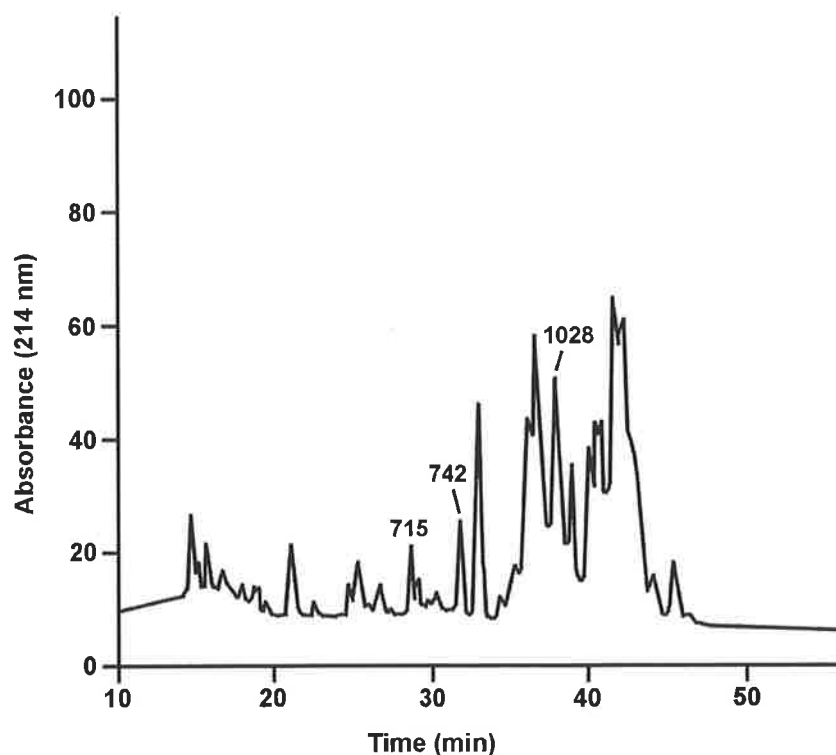


Figure 3.5: HPLC chromatogram from the crude secretions of L. alboguttata

Although the HPLC trace shown in *Figure 3.5* is complex, only three peptide fractions were identified using ESMS. This is most unusual. Normally for *Litoria* species, most of the HPLC fractions contain peptide material. This immediately singles out *L. alboguttata* as being unusual among *Litoria* species. The three peptides have $(MH^+) = 715, 742$ and 1028 Da, and we name the peptides the guttatins 1-3. The electrospray mass spectra are shown in *Figures 3.6-3.8*.

ESMS of guttatin 1 shows an (MH^+) species at m/z 715 (Figure 3.6). Data from B cleavages are drawn schematically above the spectrum while those from Y+2 cleavages are shown underneath the spectrum. The B cleavages give the partial sequence Leu/Ile Asp Ser Val Leu/Ile (NH_2) . The first B cleavage ion $[(MH^+)-17 (NH_3)]$ identifies the C-terminal $CONH_2$. The Y+2 cleavages give the partial sequence (Gly Leu/Ile) Leu/Ile Asp (Ser Val). This gives the sequence of guttatin 1 as:- [Gly (Leu/Ile)] Leu/Ile Asp Ser Val Leu/Ile (NH_2) . Automated Edman sequencing⁴ gives the sequence Gly Leu Leu Asp Ser Val Leu (NH_2) .

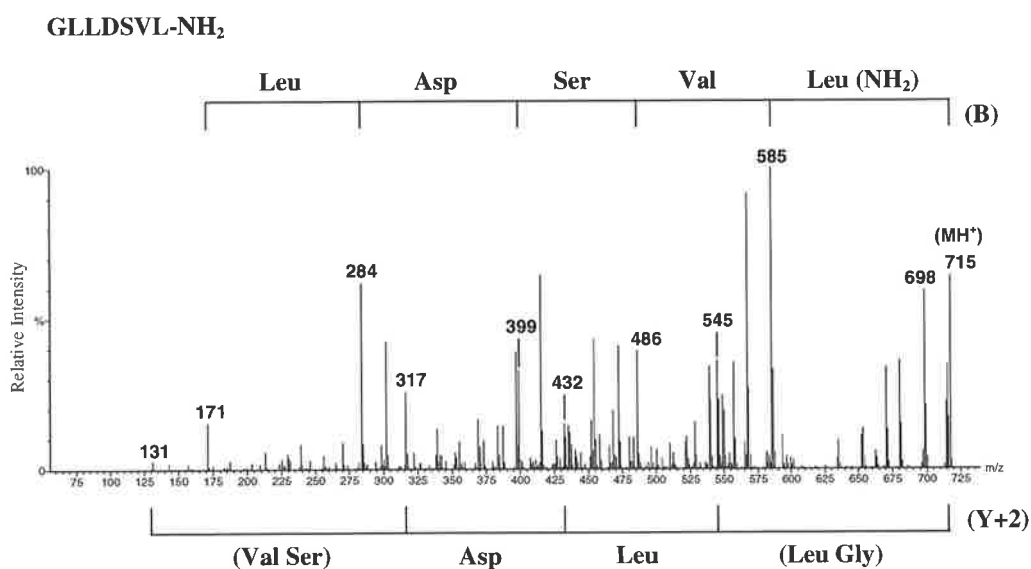


Figure 3.6: MS/MS data of guttatin 1 (m/z 715)

The ESMS of guttatin 2 gives (MH^+) m/z 742 (Figure 3.7). Data from B cleavages give the partial sequence Leu/Ile Asp Asn Val Leu/Ile (NH_2) . The first B cleavage $[(MH^+)-17 (NH_3)]$ identifies a C-terminal $CONH_2$. The Y+2 cleavages give the partial sequence [Gly (Leu/Ile)] [(Leu/Ile) Asp] Asn. The sequence of guttatin 2 from mass spectrometry is therefore [Gly (Leu/Ile)] Leu/Ile Asp Asn Val Leu/Ile (NH_2) . Automated Edman sequencing⁴ gives the sequence Gly Leu Leu Asp Asn Val Leu (NH_2) .

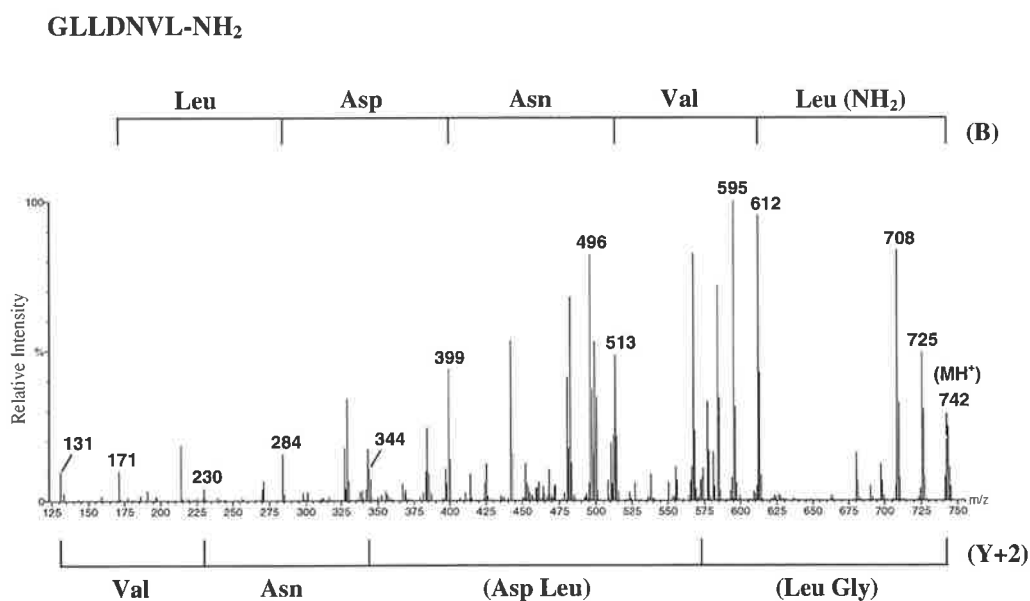


Figure 3.7: MS/MS data of guttatin 2 (m/z 742)

ESMS of guttatin 3 shows the (MH^+) peak at m/z 1028 (*Figure 3.8*). The B cleavages give the partial sequence Leu/Ile Asp Thr Val Lys/Gln Gly Leu/Ile Asn (NH_2). Y+2 cleavages identify the partial sequence [(Gly Leu/Ile Leu/Ile)]. The MS sequence is therefore [Gly Leu/Ile] Leu/Ile Asp Thr Val Lys/Gln Gly Leu/Ile (NH_2). Automated Edman sequencing⁴ gives the sequence of guttatin 3 as Gly Leu Leu Asp Thr Val Lys Gly Leu Asn (NH_2).

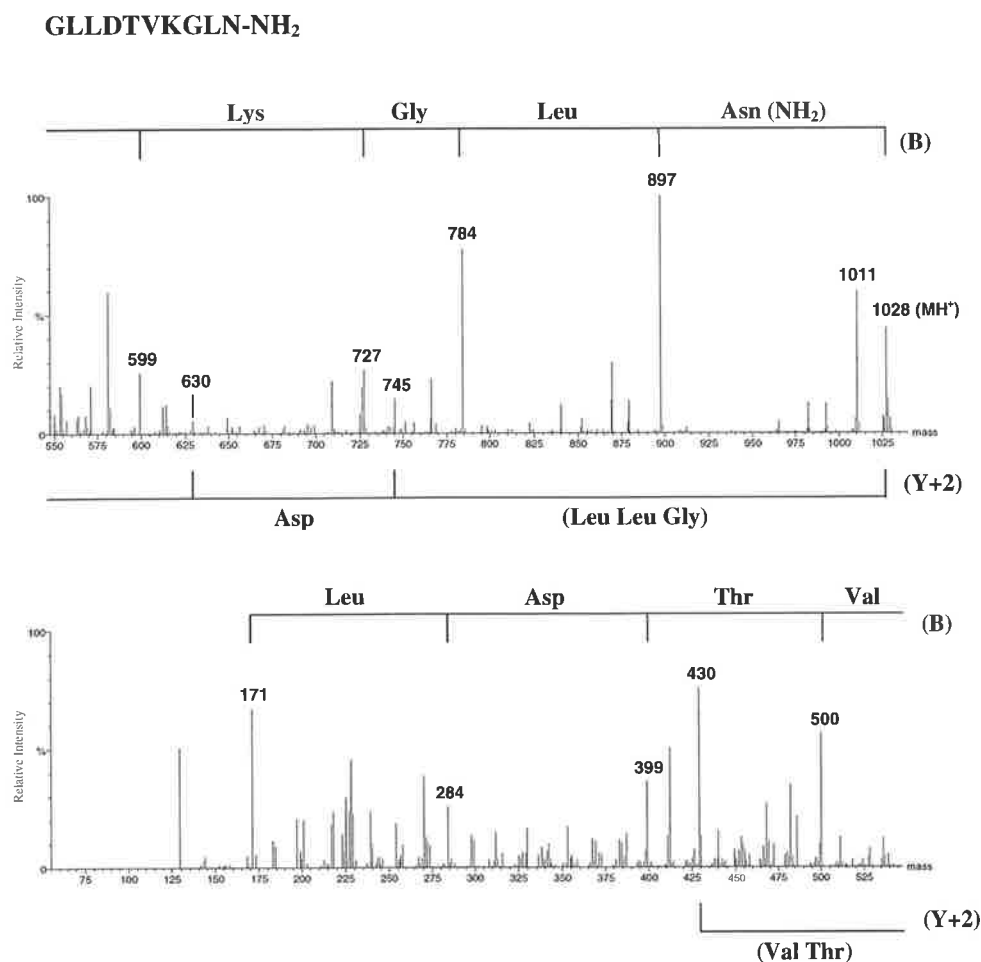


Figure 3.8: MS/MS data of guttatin 3 (m/z 1028)

Litoria albobuttata has neither antibiotic peptides nor neuropeptides in its glandular secretion. Nor does it have any tryptophyllin neuromodulators like those found in *Litoria rubella* and *Litoria electrica*. Thus it is unlike any other species of the genus that we have studied. The three guttatin peptides do have some sequence correspondence with inactive caeridin peptides isolated together with active peptides from tree frogs of the genus *Litoria*^{5-10,12,13}.

Table 3.1: Caeridin type peptides from frogs of the genus *Litoria*

Name	Sequence	Species
Guttatin 1	GLLDSVL-NH ₂	<i>L. alboguttata</i>
Guttatin 2	GLLDNVL-NH ₂	<i>L. alboguttata</i>
Guttatin 3	GLLDTVKGLN-NH ₂	<i>L. alboguttata</i>
Caeridin 1.1	GLLDGLLGTGL-NH ₂	a, b, c, d, e
Caeridin 1.4	GLLDGLLGGLGL-NH ₂	c, d
Caeridin 1.5	GLLDGLLGGLGL-NH ₂	d
Caeridin 2	GLLDVVGNNLLGGLGL-NH ₂	e
Caeridin 3	GLFDAIGNLLGGLGL-NH ₂	e
Caeridin 4	GLLDVVGNVLHSGGL-NH ₂	e

Note: (a) *Litoria splendida*⁵⁻⁷; (b) *Litoria caerulea*^{8,9}; (c) *Litoria gilleni*¹⁰; (d) *Litoria xanthomera*¹¹; (e) *Litoria chloris*¹²

The caeridin structures are listed in *Table 3.1* for comparison with the guttatins. The roles of the caeridin peptides have not been determined. Perhaps they are spacer peptides from the Pro caerin peptides, but if this is so, why do they have post-translational modification of the C-terminal group?

3.2.2 The genus *Cyclorana*-the particular case of *C. australis*

A variety of species of the genus *Cyclorana* was studied in 1993/1994 as part of the Adelaide amphibian survey¹⁴. This work was not continued because HPLC investigations showed that the amounts of peptide material in the glands were miniscule. The only species for which an MS study was initiated was *Cyclorana australis*. The HPLC profile of the glandular skin secretion of *Cyclorana australis* is shown in *Figure 3.9*.

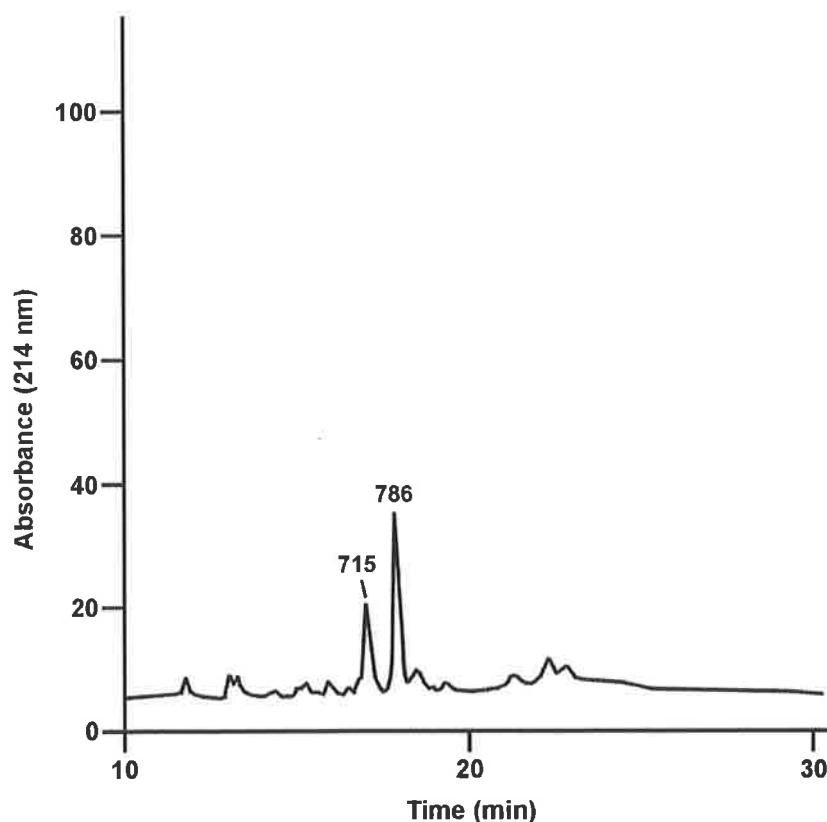


*Figure 3.9: HPLC chromatogram from the crude secretions of *Cyclorana australis* (provided by Prof. D.H. Bowie)*

There are only two peptide components present in the HPLC separation and there was less than 5 μg of each component available for study. Fast atom bombardment (FAB) mass spectra were determined on a VG ZAB 2HF mass spectrometer. The two components have $(\text{MH}^+) = 715$ and 786 respectively. Neither the energy resolution, nor the sensitivity of the ZAB approaches that of our modern instruments, and the ZAB was then being used at maximum sensitivity. The MS/MS data for the two components are shown in *Figures 3.10* and *3.11*.

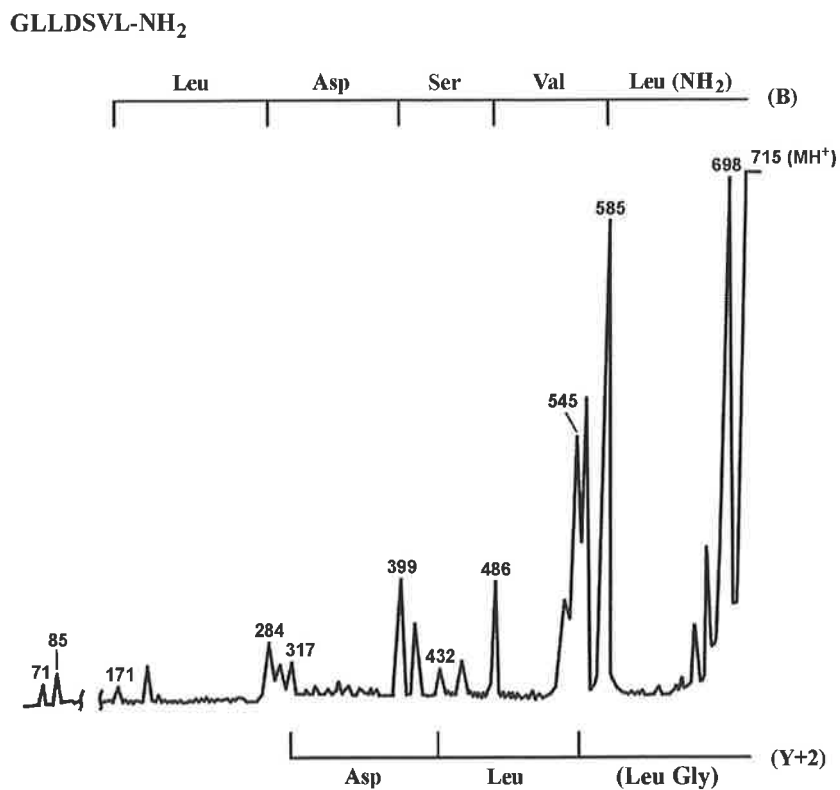


Figure 3.10: MS/MS data of (MH⁺) 715 from *C. australis*

The MS/MS data shown in *Figure 3.10*, although crude, suggest that m/z 715 is either the same as guttatin 1 or an Ile isomer of it. There is no component corresponding to m/z 786 from *Litoria alboguttata* but the likelihood is that the spectrum shown in *Figure 3.11* is that of GLLDGTVL-NH₂ or an Ile isomer.

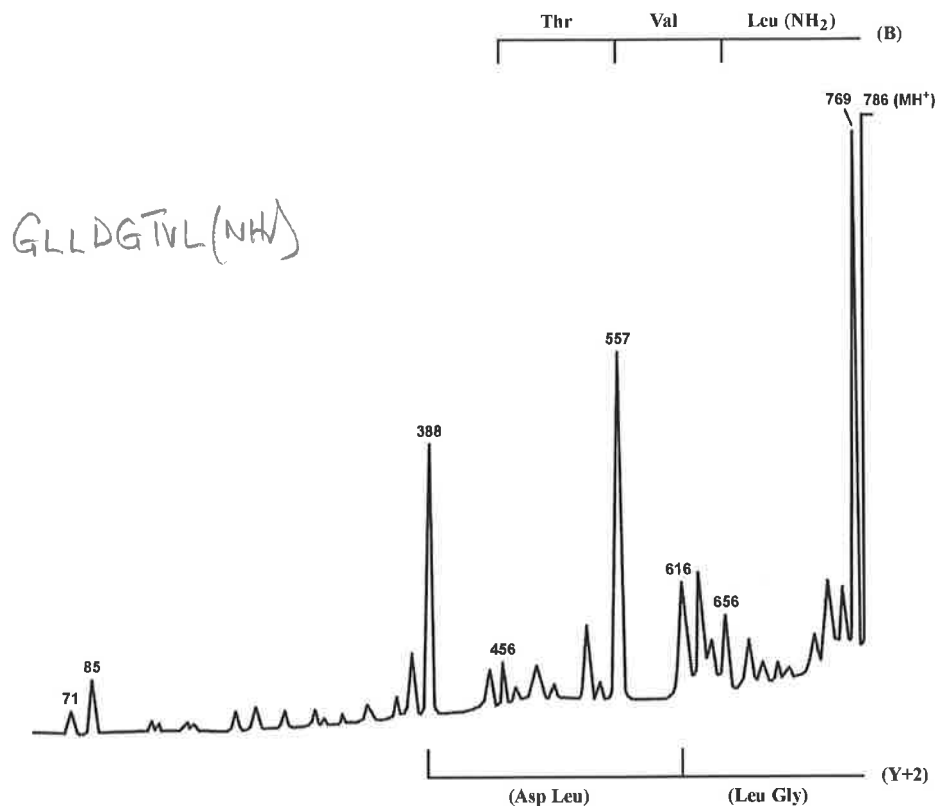


Figure 3.11: MS/MS data of (MH^+) 786 from *C. australis*

Obviously, we need further samples of the glandular secretion of *Cyclorana australis* to confirm (or refute) that m/z 715 corresponds to guttatin 1. Unfortunately we have been unable to obtain live samples of this animal from the Northern Territory over the last two seasons because the government of the Northern Territory has refused to provide us with a licence to collect the animals. They are concerned that we will use the animals for “commercial” purposes in spite of our explanations to the contrary.

3.3 Conclusions

In conclusion, there is no doubt that *Litoria alboguttata* has a peptide content in its glandular secretion unlike that of any other species of the genus *Litoria* that we have studied. The fact that it is also the only burrowing frog of the genus *Litoria* suggests that it

may have been wrongly classified, and that it would be better classified as a member of the genus of *Cyclorana* burrowing frogs. If the peptide (MH⁺) 715 of *Cyclorana australis* really does correspond to guttatin 1 from *Litoria alboguttata*, that should provide circumstantial evidence to warrant the consideration of reclassification of *Litoria alboguttata* as *Cyclorana alboguttata*.

3.4 Experimental

3.4.1 Collection and preparation of *Litoria alboguttata* secretions

The skin secretions from adult *Litoria alboguttata* were obtained courtesy of Associate Professor Michael Tyler, Department of Zoology, University of Adelaide. The secretion was obtained by the surface electrical stimulation (SES) method³. The frogs were held by the back legs, the skin moistened with distilled water and the area stimulated by means of a bipolar electrode of 21G platinum attached to a C.F Palmer student model electrical stimulator. The electrode was rubbed in a circular manner over the entire dorsal surface of the frog. The operating conditions used were pulse duration of 2.5 milliseconds; pulse repetition of 50 Hz and a voltage of 10 volts. After stimulation, the crude secretion was rinsed off the skin with distilled water into a sterile container. An equal volume of methanol was added to the aqueous solution, which was then centrifuged (to remove any particular or insoluble matter) at 3000 rpm for 5 minutes using a Clements GS 100 centrifuge. The supernatant liquid was decanted off and reduced in volume to 1 mL using a Savant SC 100A Speedvac[®] concentrator. The resulting extract was filtered using 0.45 µm Miller filters. This extract can be stored for up to 1 month at -10°C without any alteration in the peptide composition.

3.4.2 HPLC separation

Secretions were separated by high performance liquid chromatography (HPLC) using the following system components: Waters Millipore Lambda Max 481 LC spectrophotometer (214 nm), Waters Millipore 501 and 510 pumps, ICI DP 800 data interface and ICI DP 800 data station.

HPLC separation was achieved for each crude secretion by using a VYDAC 218TP54 C₁₈ protein and peptide reverse phase column with a VYDAC 218TP 300 A° guard column preceding the analytical column. The column was equilibrated with 10% acetonitrile/aqueous 0.1% trifluoroacetic acid as the ion-pairing agent. The lyophilised sample (250 µL) was injected into the column. The typical procedure used for obtaining a 'peptide profile' was operating a linear gradient of 10-75% acetonitrile over a period of 30 minutes with a flow rate of 1 mL/min. The analytical column was also used to further purify individual peptide fractions using a maximum gradient change of 5% acetonitrile over 30 minutes.

3.4.3 Mass spectrometry analysis

The molecular weights of individual peptides and their amino acid sequences were determined using a Finnigan LCQ ion trap mass spectrometer. The sample was dissolved in methanol/water (1:1, v/v) and infused into the electrospray source via a rheodyne injector with a 5 µL loop at 5 µL/min. The electrospray conditions were: source voltage 4.2 kV, source current 17 µA, heated capillary 200°C and capillary voltage 3 V, sheath gas flow 30 psi. Mass spectra were acquired with the automatic gain control on, a maximum

time of 400 milliseconds and using a 3 microscan, averaging over approximately 20 scans. Molecular weights of peptides were determined from (MH⁺) ions.

The Micromass QTOF 2 hybrid orthogonal acceleration time of flight mass spectrometer was used to determine the amino acid sequences of the peptides. The QTOF 2 is fitted with an electrospray source in an orthogonal configuration with the ZSPRAY interface. Samples were dissolved in methanol/water (1:1, v/v) and infused into the electrospray source with a flow rate of 5 μ L/min. Conditions were as follows: capillary voltage 3 kV, source temperature 80°C, desolvation temperature 150°C and cone voltage 50-110 V. MS/MS data were acquired with the argon collision gas energy set to ~50 eV to give optimal fragmentation. Peptides were analysed in the positive mode.

3.4.4 Automated Edman sequencing

Automated Edman sequencing was carried out by the Department of Molecular Biosciences, University of Adelaide, using an applied Biosystem 470A Sequencer equipped with a 900A data analysis module. The Edman sequencing was used to distinguish between the isomeric residues isoleucine and leucine and isobaric residues glutamine and lysine, and also to confirm sequences determined by mass spectrometry.

3.5 References

- 1) Barker, J.; Grigg, G. C.; Tyler, M. J. *A Field Guide to Australian Frogs*; Surrey Beatty and Sons: NSW, 1995, p 142.
- 2) Barker, J.; Grigg, G. C.; Tyler, M. J. *A Field Guide to Australian Frogs*; Surrey Beatty and Sons: NSW, 1995, p 155.
- 3) Tyler, M. J.; Stone, D. J. M.; Bowie, J. H. *J. Pharm. Toxicol. Methods* **1992**, 6, 400.
- 4) Hunkapiller, M. W.; Hewick, R. M.; Drewer, W. J.; Hood, L. E. *Methods Enzymol* **1983**, 91, 399.
- 5) Stone, D. J. M.; Bowie, J. H.; Tyler, M. J.; Wallace, J. C. *Chem. Commun.* **1992**, 1224.
- 6) Stone, D. J. M.; Waugh, R. J.; Bowie, J. H.; Wallace, J. C.; Tyler, M. J. *J. Chem. Soc. Perkin. Trans. 1* **1992**, 3173.
- 7) Wong, H.; Bowie, J. H.; Carver, J. A. *Eur. J. Biochem.* **1997**, 247, 545.
- 8) Waugh, R. J.; Stone, D. J. M.; Bowie, J. H.; Wallace, J. C.; Tyler, M. J. *J. Chem. Soc. Perkin. Trans. 1* **1993**, 573.
- 9) Stone, D. J. M.; Waugh, R. J.; Bowie, J. H.; Wallace, J. C.; Tyler, M. J. *J. Chem. Res. S* **1993**, 138.
- 10) Waugh, R. J.; Stone, D. J. M.; Bowie, J. H.; Wallace, J. C.; Tyler, M. J. *J. Chem. Res. S* **1993**, 139.
- 11) Steinborner, S. T.; Waugh, R. J.; Bowie, J. H.; Wallace, J. C.; Tyler, M. J.; Ramsay, S. L. *J. Peptide Sci.* **1997**, 3, 181.
- 12) Steinborner, S. T.; Currie, G. J.; Bowie, J. H.; Wallace, J. C.; Tyler, M. J. *J. Peptide Res.* **1998**, 51, 121.
- 13) Steinborner, S. T.; Bowie, J. H.; Tyler, M. J.; Wallace, J. C. *Aust. J. Chem.* **1997**, 50, 889.

14) Raftery, M. J.; Bowie, J. H.; Tyler, M. J. *unpublished observations* .

Chapter Four

The Isolation and Structure Determination of Eugenin, a neuropeptide isolated from the pouch of the pregnant female Tammar wallaby (*Macropus eugenii*)

4.1 Introduction

The young of marsupials are born at an early stage of development of the fetus. Many of the developmental processes that occur *in utero*, in eutherian mammals take place during the pouch life of marsupials¹. Examples of marsupials are the koala, kangaroo, wallaby and wombat ~~etc.~~

After a short period of intra-uterine development, the young marsupial crawls unaided to the mother's pouch, attaches to a teat and undergoes further development² (*Figure 4.1*).



Figure 4.1: The developmental processes of the young marsupial

High humidity together with a constant temperature close to the maternal body temperature³ characterise the pouch microclimate. The pouch is slightly warm and the conditions produce a suitable environment for microorganisms. It has been shown that many gram-positive bacilli are present in the marsupial pouch, but few gram-negative bacilli are detected⁴⁻⁶. The bacterial content of the pouch decreases upon arrival and occupancy of the young marsupial⁷, almost certainly a consequence of the mother providing immune protection for the young in the pouch.

When the newborn wallaby first climbs into the mother's pouch, it has no immune system¹. It seems likely that the mother wallaby produces an anti-microbial compound which protects the young in the pouch until it can develop its own immune system. There are two possible sources that explain how the female wallaby protects its young during the early period of occupancy of the pouch. Either it has antimicrobial and other biologically active agents in the milk, or the secretions in the pouch contains host defence compounds. There are a variety of antimicrobially active proteins and peptides present in the milk of marsupials, including lysozyme and other antibacterial enzymes⁸⁻¹³, and whey proteins¹⁴⁻²³. There is also evidence that wallabies produce immunoglobulins in the pouch²⁴.

Baudinette⁷ has shown that the female Tammar wallaby produces a waxy secretion in the pouch, and the constituency of this secretion appears to depend on the oestrus cycle. Bioactive peptides have been shown to be part of the host defence systems of a variety of animals²⁵. Perhaps the mother marsupial may produce active peptides in the pouch to protect their young when they are high risk of infection during the first few weeks of their occupancy of the mother's pouch?

The aims of the research presented in this chapter are:

- (i) To isolate and determine the structures of any active peptides from the pouch secretion of females from three species of wallabies *Macropus eugenii*, *Petrogale penicillata* and *Petrogale xanthopus*.
- (ii) To compare the peptide profiles of those three species.
- (iii) To determine the bioactivity of any isolated peptide, e.g. neuropeptides and/or antimicrobial activity.

4.2 Tammar Wallaby (*Macropus eugenii*)

The Tammar wallaby is found on the SA and WA mainland and on some associated offshore islands including Kangaroo Island off the coast of South Australia²⁶. The Tammar wallaby is distributed in at least a dozen areas, many of them isolated for more than 10,000 years²⁷.

The Tammar wallaby requires dense low vegetation for daytime shelter, and open grassy areas for feeding. It lives in coastal scrub, heath, dry forest and thickets in mallee and woodland.



Photograph provided
by Prof R.W. Baudinette

Figure 4.2: Picture of a Tammar wallaby (*Macropus eugenii*)



Figure 4.3: Diagram of the geographic distribution of the Tammar wallaby

Most wallaby young are born in the period of late January to March. Within a few hours of birth, the female mates again, and this embryo remains passive during the lactation period. The passive embryo is not reactivated when the previous young leave the pouch in September to October. The passive embryos are reactivated in mid December and the

young are born about 40 days later. The young stay in the pouch for 8 to 9 months and leave the pouch in September or October.

The population of the Tammar wallaby has been reduced since European settlement. It was formerly abundant in some regions of mainland South Australia, but it survives today only in a small area near Cleve. The population has also been greatly reduced by the clearing of land for wheat growing in South-western Western Australia. The Flinders Island population is almost certainly extinct, its numbers having been severely reduced by loss of habitat and bushfires. None now survive on St Francis, St Peter or Thistle Islands. Introduced populations are thriving on Greenly Island, South Australia. The species continues to be abundant on Kangaroo Island, despite ongoing persecution outside the Flinders Chase National Park. It is also found on North Twin Peaks Island and Middle Island in the Recherche Archipelago; Garden Island, off Fremantle; and East and West Wallaby Island, in the Abrolhos²⁶.

4.3 Brush-tailed Rock Wallaby (*Petrogale penicillata*)

The Brush-tailed Rock wallaby inhabits rocky areas in inland and subcoastal regions of South-eastern Australia. Inhabited rock slopes usually receive direct sunlight for a part of the day and have windblown caves, rock cracks or tumbled boulders that are used by the wallabies for shelter. Although colonies may occupy sites where grass does not grow, these sites are always close to areas of native or introduced grasslands²⁸.



Figure 4.4: Picture of a Brush-tailed Rock wallaby (*Petrogale penicillata*)
(ex Prof. R.W. Baudinette)

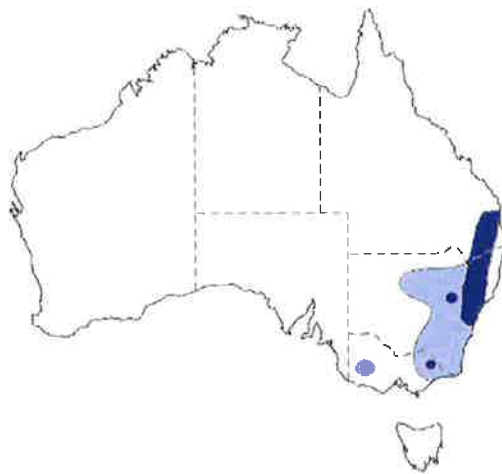


Figure 4.5: Diagram of the geographic distribution of the Brush-tailed Rock wallaby

Petrogale penicillata appears to be fairly common in South-eastern Queensland and northern New South Wales. This species declined dramatically in Victoria in the early 1900s, and was thought to be extinct until 1953 when a few colonies were rediscovered in East Gippsland. In 1970, additional remnant populations were located in the Grampians. In New South Wales, it has declined west of the Great Divide where sheep grazing is the major land use.

4.4 Yellow-footed Rock Wallaby (*Petrogale xanthopus*)

The Yellow-footed Rock wallaby is found mainly in the Flinders Ranges of South Australia, and in the Adavale Basin in South-western Queensland. Smaller populations are found in the Gawler Ranges and Olary Hills, South Australia, the Gap and Coturaundee Ranges, New South Wales, and the Caraway Ranges, Queensland²⁹.



Figure 4.6: Picture of a Yellow-footed Rock wallaby (*Petrogale xanthopus*)
(ex Prof R.W. Baudinette)

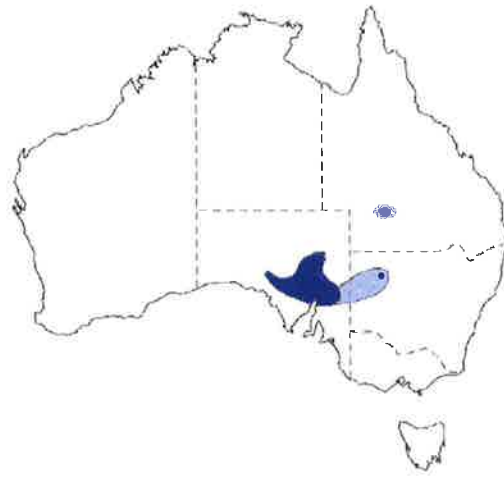


Figure 4.7: Diagram of the geographic distribution of the Yellow-footed Rock wallaby

These animals inhabit arid and rocky areas. Some populations are found in association with permanent fresh water, others may be restricted to wet areas at the edges of rock faces. The gestation period occurs over 31 to 32 days, and the pouch life of the young is about 194 days. The diet of the Yellow-footed Rock wallaby is mainly grass³⁰.

The Yellow-footed Rock wallaby has become rarer since the settlement of South Australia in the 1830s by Europeans. However, most of the land which it now inhabits is useless for agricultural purposes, so only mining ventures have a direct impact on the population of this species.

4.5 Results and Discussion

Cotton wool swabs of the pouch of several female Tammar wallabies were obtained over a period of six weeks as described in the experimental section. On average, several milligrams of solid material was obtained from each swab after work up. Swabs were also taken from the pouch of a female wallaby that was not pregnant, and from several females

of both Yellow-footed Rock and Brush-tailed Rock wallabies with young during the first two weeks of lactation. The swab samples from each wallaby species were worked up as described in the experimental section. Each swab sample was subjected to HPLC analysis, with individual fractions being collected. Each fraction was lyophilised and subjected to examination by electrospray mass spectrometry (ESMS) using either a Finnigan LCQ or Micromass QTOF 2 mass spectrometer. Only one peptide was identified from swabs taken from Tammar wallabies, and this has been called eugenin. Other components including some small peptides were also found in swabs from the pouches of the three wallabies. These fractions showed no antibiotic activity, and were not investigated further.

4.5.1 Isolation of eugenin from the pouch of the Tammar wallaby (*Macropus eugenii*)

The HPLC profile of the pouch secretion for a lactating female of the species *M. eugenii* is shown in *Figure 4.8*.

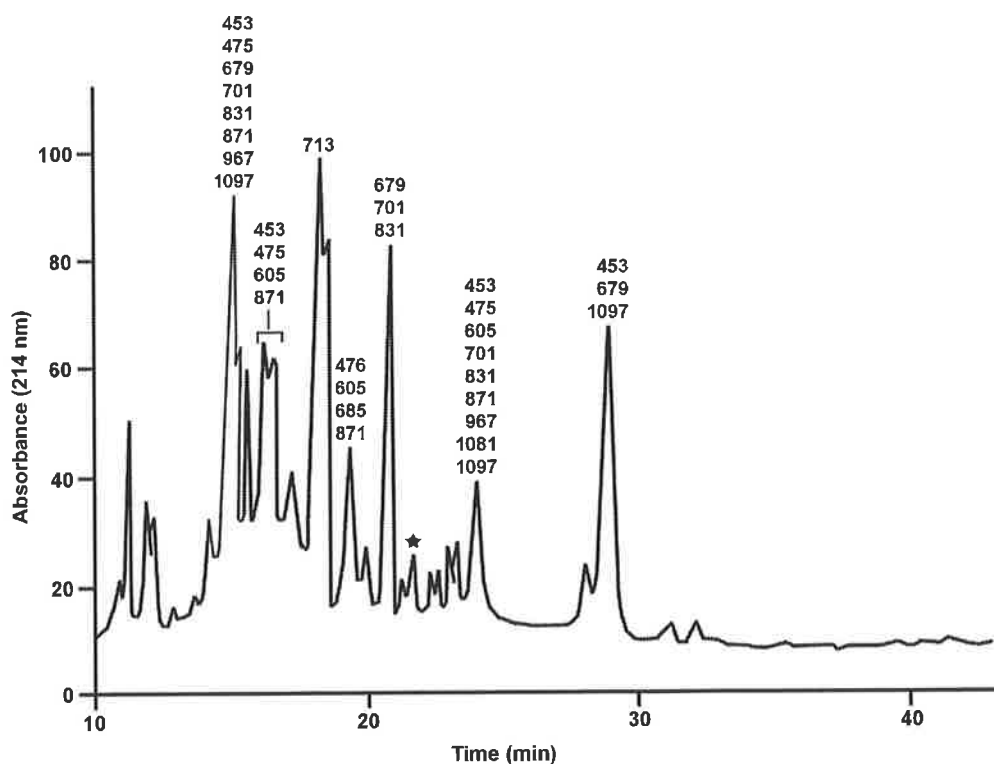


Figure 4.8: HPLC separation of the pouch secretion of female *M. eugenii*. * indicates eugenin

All components were monitored by electrospray mass spectrometry, but only eugenin was characterised as a bioactive peptide. Eugenin was isolated from HPLC traces of Tammar wallaby only in the first two weeks of lactation. It was not detected in the pouch secretions of females that were not pregnant nor was it detected in the pouch secretions of females carrying young after two weeks of occupancy of the pouch. Since the young have no immune system in the first two weeks of pouch occupancy, there is a distinct possibility that eugenin is involved in some way in the protection of the young.

Further HPLC separation was required of the eugenin fractions in order to obtain a pure component. The eugenin fraction was collected, concentrated and dried *in vacuo*. Only 5 μg of pure eugenin was available for study.

Eugenin is a post translationally modified peptide, with pGlu at the N-terminal end and a CONH₂ moiety at the C-terminal end of the peptide. The sequence of eugenin is pGlu Gln Asp Tyr(SO₃) Val Phe Met His Pro Phe-NH₂. Since eugenin has a N-terminal pGlu residue, automated Edman sequencing³¹ cannot be used for this compound. The sequence of eugenin was determined using a combination of negative ion and positive ion electrospray mass spectra. The negative ion mass spectrum of eugenin gives peaks corresponding to (M-H)⁻ and [(M-H)⁻-SO₃]⁻ at *m/z* 1371 and 1291 respectively, indicating that eugenin has a molecular weight of 1372 Da, and contains a sulfate group. The positive ion mass spectrum shows no (MH⁺) ion, but shows a pronounced peak corresponding to an [MH⁺-SO₃]⁺ species at *m/z* 1293. The collision induced mass spectrum (MS/MS) of the [MH⁺-SO₃]⁺ ion is recorded in *Figure 4.9*. A partial amino acid sequence for eugenin is provided, as determined using B and Y+2 fragmentations³².

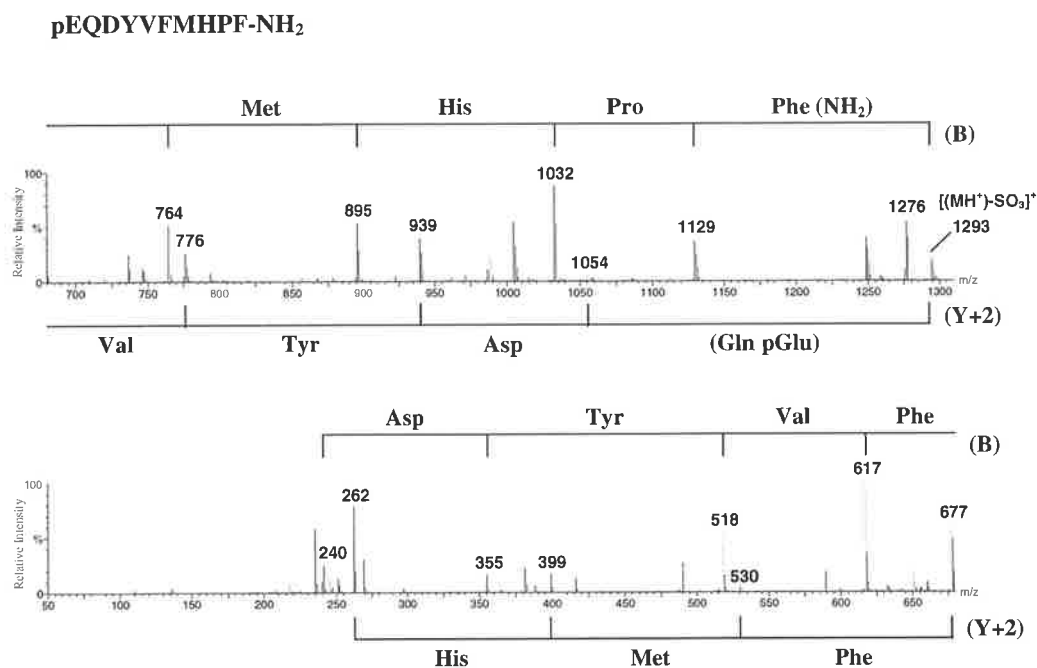


Figure 4.9: CID electrospray mass spectrum (MS/MS) of [(MH⁺)-SO₃]⁺ ion of eugenin. The B fragmentations are indicated schematically above the spectrum and provide information concerning the sequence from the C-terminal end of the peptide, while the Y+2 fragmentations (shown schematically underneath the spectrum) provide sequencing data from the N-terminal end of the peptide.

The positive ion mass spectrum provides the majority of the sequence except for a definite assignment of the first two residues at the N-terminal end of the peptide.

The collision induced negative ion mass spectrum (MS/MS) of the [(M-H)⁻-SO₃]⁻ ion of eugenin is shown in *Figure 4.10*. Negative ion spectra are considered in detail in *Chapter 8*. There are four backbone cleavages in negative ion spectra, which provide sequencing information. These have been previously reported³³. Two of these (α and β cleavages) are fragmentations of amide moieties, and give information analogous to that provided by B and Y+2 cleavages in the corresponding positive ion spectra. The other two backbone cleavage (δ and γ cleavages) originate from any Asp, Asn, Glu or Gln side chains and provide specific information concerning the positions of these four residues in the sequence. The δ and γ fragmentations are particularly important in identifying Gln

residues, since isobaric Gln and Lys cannot be differentiated by low-resolution positive ion mass spectrometry (except by using Lys-C digestion)³³.

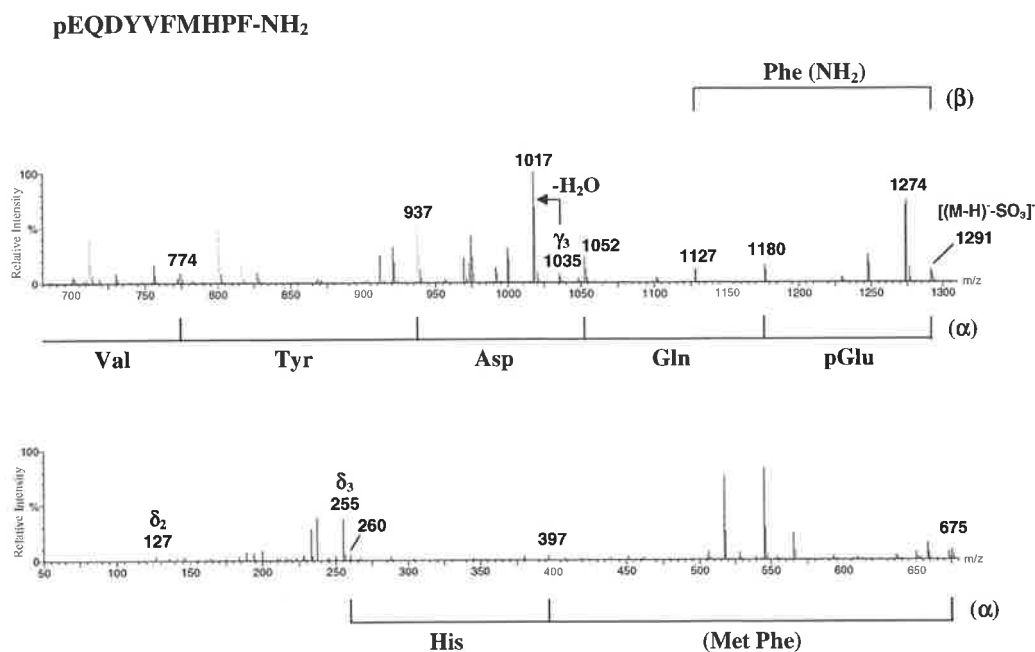


Figure 4.10: CID electrospray mass spectrum (MS/MS) of $[(M-H)^-SO_3]$ ion of eugenin: The α and β derived sequences are indicated schematically above and below the spectrum respectively, while δ and γ cleavages are indicated on the spectrum.*

The data shown in *Figures 4.9 and 4.10* give the full sequence of eugenin: in particular, the negative ion spectrum identifies pGlu as residue 1, Gln2 rather than Lys2 and Asp3. Synthetic[‡] and natural eugenin were shown to be identical by comparison of their HPLC behaviour and their positive and negative ion mass spectra.

* For details of negative ion cleavages - see Chapter 8

[‡] See Chapter 6 for the synthesis of eugenin

Eugenin has a sequence partially related to those of the mammalian gastrin-like neuropeptide CCK-8³⁴ and gastrin³⁵ (see below). Eugenin also shows sequence similarity to the amphibian neuropeptide caerulein³⁶⁻³⁸.

Eugenin	pGlu Gln Asp Tyr(SO ₃) Val Phe Met His Pro Phe-NH ₂
CCK-8	Asp Tyr(SO ₃) Thr Gly Trp Met Asp Phe-NH ₂
Hexagastrin	Tyr(SO ₃) Gly Trp Met Asp Phe-NH ₂
Caerulein	pGlu Gln Asp Tyr(SO ₃) Thr Gly Trp Met Asp Phe-NH ₂

CCK-8 and caerulein have similar physiological activity: they both show smooth muscle activity, gastrin-like activity and reduce blood pressure at the ng/kg of body weight, while caerulein is an analgaesic several thousand times more potent than morphine³⁷.

CCK-8 and caerulein both contain a tyrosine sulfate: the bioactivity is significantly diminished if the tyrosine sulfate group is hydrolysed³⁷. Eugenin contains the same first four residues as caerulein, but the sequence after the Tyr(SO₃) residue of eugenin is different from those of the other mammalian and amphibian analogues. What is the role of eugenin in the wallaby pouch? It is certain that it is present in the wallaby pouch for some biological purpose. The investigation of the biological activity of eugenin and related peptides is described later in *Chapter 7*.

4.5.2 Other components isolated from the HPLC separations

The HPLC profiles of females of the three wallaby species were monitored prior to and during pregnancy as described in the experimental section. The HPLC profiles do not show

significant change over the monitoring period. Representative HPLC profiles from swabs taken from the studied wallaby species are shown in *Figure 4.8*, *4.11* and *4.12*, with components of each HPLC fraction shown in those figures.

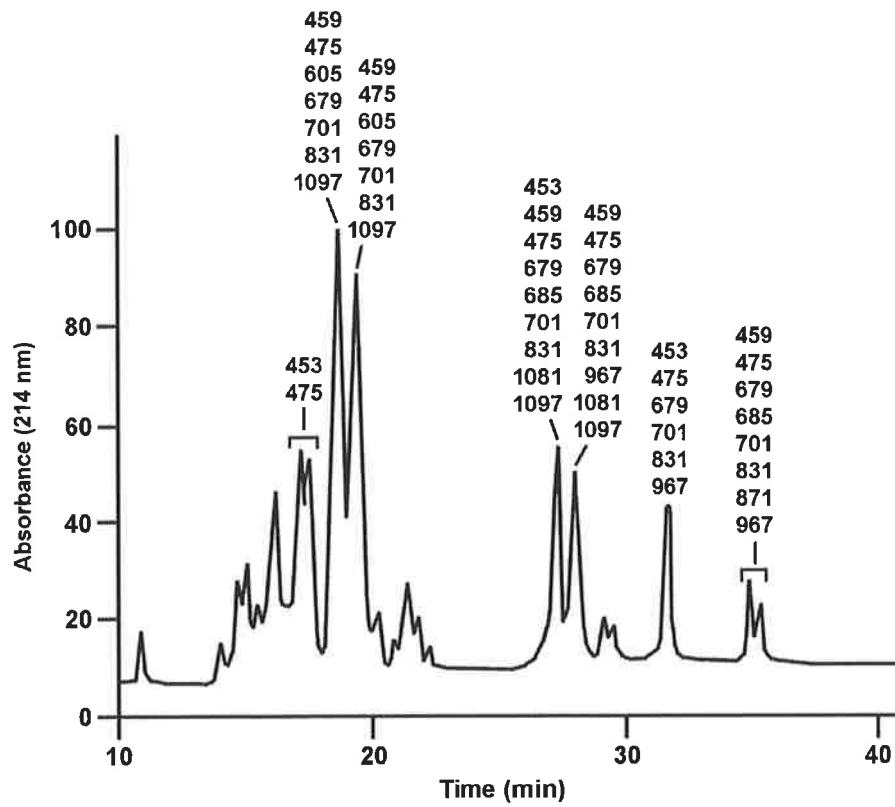


Figure 4.11: HPLC separation of the pouch secretion of female P. xanthopus

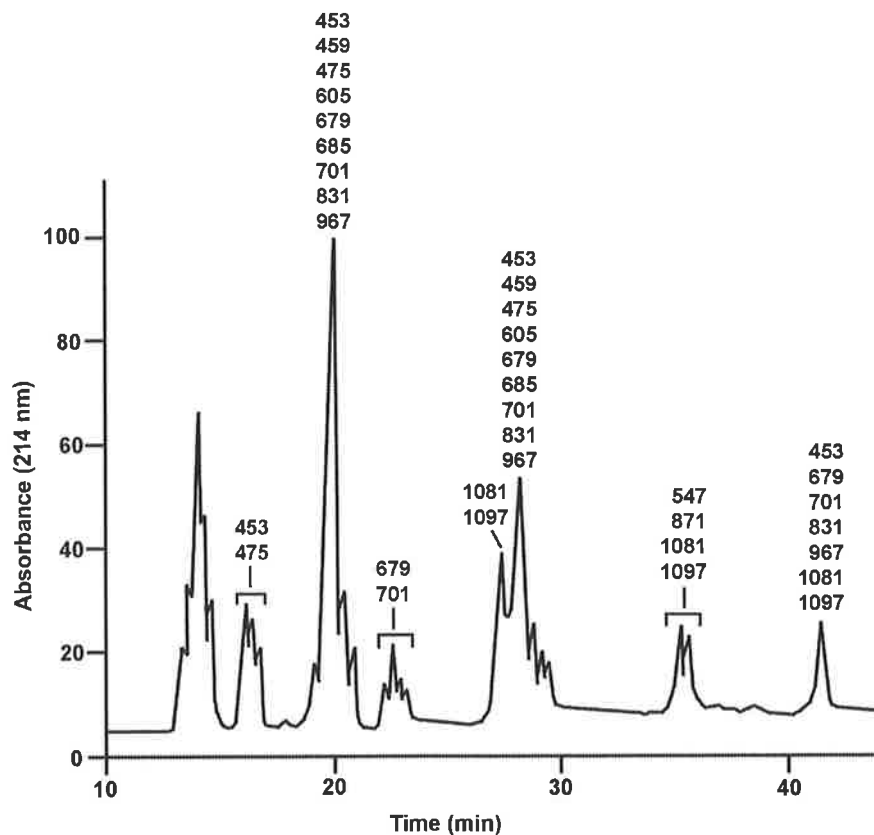


Figure 4.12: HPLC separation of the pouch secretion of female *P. penicillata*

Apart from eugenin there are two major types of component present in the aqueous extract of the pouch secretion; these are common to all three wallaby species. None show any antibiotic activity. We have measured the electrospray mass spectra of these components and although we have not determined their structures, we include a brief summary of the components here.

At no stage did we have more than 5 μg of any component. The first of these compounds are those (MH^+) ions which undergo successive and competitive losses of 84, 94 and 114 Da. The spectra of these compounds are listed in *Table 4.1*.

Table 4.1: Components that lose 84, 94 and 114 Da (only peaks greater than 15% of the base peak are listed). LCQ mass spectrometer

Parent (m/z)	Fragment peaks (m/z)
605	511, 491
714	630, 616, 572, 558, 548, 516, 496, 454, 402
831	813, 717, 699, 633, 615, 604, 517, 491, 381
871	777, 757, 683, 643, 605, 491
967	873, 853, 831, 815, 717, 633, 615, 517, 491
1081	1045, 1037, 997, 967, 853, 739
1097	1079, 1013, 983, 869, 755

The other types of compounds are those with (MH^+) values at m/z 453, 459, 475, 547, 679, 685 and 701. The positive ion spectra of two of these, m/z 453 and 679 are shown in *Figure 4.13* and *4.14*. “High resolution” data for m/z 453 is listed in *Table 4.2*. The negative ion spectrum of the compound of molecular weight 678 Da is shown in *Figure 4.15*: this should be compared with the corresponding positive ion spectrum shown in *Figure 4.14*. The spectra of the other compounds in this group are listed in *Table 4.3*.

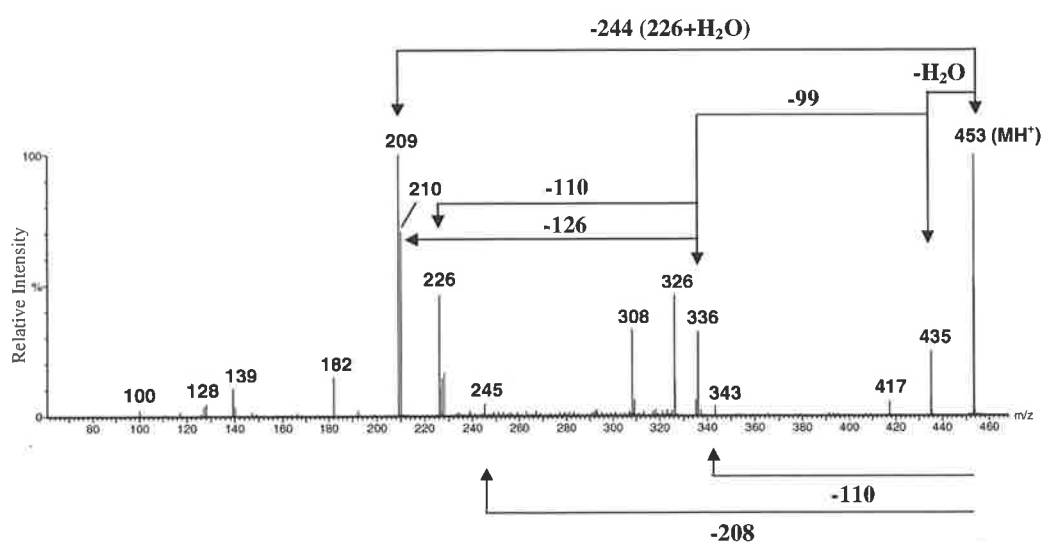


Figure 4.13: MS/MS data of m/z 453 (QTOF 2 instrument)

Table 4.3: ESMS spectra of other components, which lose 99, 110 and 226 Da

Parents (m/z)	Fragment peaks (m/z)
459	441, 415, 360, 349, 239
475	457, 376, 365, 277, 258
685	667, 575, 479, 459, 441, 349, 239
701	683, 591, 492, 475, 393, 376, 365, 294

When we first obtained the data shown in *Figure 4.13-4.15* and *Table 4.3*, we thought that these related compounds might contain N-terminal pGlu and C-terminal Val-OH units. The peak at *m/z* 209 (*Figure 4.13* and *4.14*) might be pGlu Pro (calculated 209.0926) and the loss of 99 Da might be Val (calculated 99.063). Comparison of these values with those listed in *Table 4.2* show these proposals to be incorrect. In addition, the positive and negative ion spectra of the component of MW 678 Da (*Figure 4.14* and *4.15*) are not consistent with a peptide structure.

Although we have not identified the structures of any of these compounds, they show no antibiotic activity, and we have not considered them further.

4.6 Conclusions

The secretion from the pouch of the pregnant Tammar wallaby contains the peptide eugenin during the first two weeks of occupancy by the young. This peptide is not identified in pouch secretions of the Brush-tailed Rock wallaby or the Yellow-footed Rock wallaby. Eugenin contains an N-terminal pyroglutamic acid residue together with a tyrosine sulfate residue at position 4. The sequence of eugenin is similar to that of human CCK-8 and the amphibian peptide caerulein. It is expected that eugenin will show neuropeptide activity.

The synthesis of eugenin is detailed in *Chapter 6*. The bioactivity of eugenin is described in *Chapter 7*.

4.7 Experimental

4.7.1 Collection and preparation of samples

Marsupials were maintained in captivity by Professor Russell Baudinette; Department of Environmental Biology, University of Adelaide. Swabs were taken from the pouch of the pregnant Tammar wallaby one week before the young enters the pouch, then every second day for the next two weeks, and finally at two-weekly intervals until the young leaves the pouch. Each swab was shaken in a mixture containing distilled water (4 mL), acetonitrile (2 mL) and methanol (2 mL). The resulting solution was centrifuged to remove any particulate or insoluble material at 3000 rpm for 5 minutes using a Clements GS 100 centrifuge. The supernatant liquid was decanted off and concentrated to a volume of 1 mL using a Savant SC 100A Speedvac[®] concentrator. The resulting extract was filtered using a 0.45 μm Miller filters before separation and purification by HPLC.

4.7.2 Analytical and preparative HPLC

HPLC separation was achieved for each crude secretion, using a VYDAC 218TP54 C₁₈ protein and peptide reverse phase column with a VYDAC 218TP 300 A^o guard column preceding the analytical column. The column was equilibrated with 10% acetonitrile/aqueous with 0.1% trifluoroacetic acid as the ion-pairing agent. Lyophilised sample (250 μL) was injected into the column. The typical procedure used for obtaining a

'peptide profile' was operating a linear gradient of 10-75% acetonitrile over a period of 30 minutes with a flow rate of 1 mL/min. The analytical column was also used for further purifying individual peptide fractions using a maximum gradient change of 5% acetonitrile over 30 minutes.

The elution profiles were generated using two HPLC systems,

- (1) The eluant was monitored by Waters Millipore Lambda Max 481 LC spectrophotometer (214 nm). The data was processed through an ICI DP 800 data interface and ICI DP 800 data station. The gradient was programmed through an automated Waters Gradient Controller, which controlled Waters 501 and 510 pumps. Samples were injected into a rheodyne injector fitted with a 1 mL injection loop.
- (2) The eluant was monitored by an ICI LC 1200 UV/VIS detector (214 nm). The data was processed through an ICI DP 800 interface by an ICI DP 800 data station. The gradient was programmed through the ICI DP 800 data station that controlled two ICI LC 1100 HPLC pumps.

Typical HPLC profiles are shown in *Figure 4.8, 4.11 and 4.12.*

4.7.3 Mass spectrometry analysis

The molecular weights of individual peptides and their amino acid sequences (as appropriate) were determined using a Finnigan LCQ ion trap mass spectrometer. The sample was dissolved in methanol/water (1:1, v/v) and infused into the electrospray source via a rheodyne injector with a 5 μ L loop at 5 μ L/min. The electrospray conditions were:

source voltage 4.2 kV, source current 17 μ A, heated capillary 200°C and capillary voltage 3 V, sheath gas flow 30 psi. Mass spectra were acquired with the automatic gain control on, a maximum time of 400 milliseconds and using a 3 microscan, averaging over approximately 20 scans. Molecular weights of peptides were determined by (MH⁺) ions.

ESMS of purified fractions were also measured using a Micromass QTOF 2 orthogonal acceleration time of flight mass spectrometer with a mass range to 10,000 Da. The QTOF 2 is fitted with an electrospray source in an orthogonal configuration with the ZSPRAY interface. Samples were dissolved in acetonitrile/water (1:1) and infused into the electrospray source at a flow rate of 5 μ L/min. Conditions were as follows: capillary voltage 2.43 kV, source temperature 80°C, desolvation temperature 150°C and cone voltage 50-100 V. MS/MS data were acquired with the argon collision gas energy set to ca. 50 eV to give optimal fragmentation.

4.8 References

- 1) Deane, E. M.; Cooper, D. W. *The Developing Marsupial-Models for Biomedical Research*; Tyndale-Biscoe, C. H. and Janssens, P. A., Ed.; Springer Verlag: Berlin, 1988, p 190.
- 2) Deane, E. M.; Cooper, D. W. *Dev. Comp. Immunol.* **1984**, *8*, 863.
- 3) Baudinette, R. V.; Gannon, B. J.; Ryan, R. G.; Frappell, P. B. *Respir. Physiol.* **1988**, *72*, 219.
- 4) Yadav, M. J. *Gen. Microbiol.* **1972**, *70*, 437.
- 5) Russell, E. M.; Giles, D. C. *Behaviour* **1973**, *51*, 19.
- 6) Charlick, J.; Manassis, C.; Stanley, N.; Waring, H.; Cockson, A. *Aust. J. Exp. Biol. Med. Sci.* **1981**, *59*, 743.
- 7) Baudinette, R. V. *Unpublished Observations* .
- 8) Carlsson, A.; Bjorck, L.; Persson, K. *J. Dairy Science* **1989**, *72*, 3166.
- 9) Koldovsky, O. *J. Nutr.* **1989**, *119*, 1542.
- 10) Buts, J. P. *Arch. Pediatr.* **1999**, *5*, 298.
- 11) Kunz, C.; Rodriguez-Palmero, M.; Koletzko, B.; Jensen, R. *Clin. Perinat.* **1999**, *26*, 307.
- 12) Groenink, J.; Walgreen-Weterings, E.; Van't Hof, W.; Veerman, E. C. I.; Amerongen, A. V. N. *FEMS Microbiology Letters* **1999**, *179*, 217.
- 13) Wakabayashi, H.; Matsumoto, H.; Hashimoto, K.; Teraguchi, S.; Takase, M.; Hayasawa, H. *Biosc. Biotech. and Biochem.* **1999**, *63*, 955.
- 14) Bell, K.; McKenzie, H. A.; Muller, V.; Shaw, D. C. *Mol. Cell Biochem.* **1980**, *29*, 3.
- 15) Chauvet, J.; Hurpet, D.; Chauvet, M. T.; Acher, R. *Biosci. Rep.* **1984**, *4*, 245.

- 16) Lazarus, L. H.; Wilson, W. E.; Gaudino, G.; Irons, B. J.; Giglietta, A. *Peptides* **1985**, *6*, 295.
- 17) Nicholas, K. R.; Messer, M.; Elliott, C.; Maher, F.; Shaw, D. C. *Biochem. J.* **1987**, *241*, 899.
- 18) Cowan, P. E. *Reprod. Fert. Dev.* **1989**, *1*, 325.
- 19) Collet, C.; Joseph, R.; Nicholas, K. *Biochem. Biophys. Res. Commun.* **1989**, *164*, 1380.
- 20) Grigor, M. R.; Bennett, B. L.; Carne, A.; Cowan, P. E. *Comp. Biochem. Physiol.* **1991**, *98B*, 451.
- 21) Beg, O. U.; Shaw, D. C. *J. Prot. Chem.* **1994**, *13*, 513.
- 22) Piotte, C. P.; Grigor, M. R. *Arch. Biochem. Biophys.* **1996**, *330*, 59.
- 23) Collet, C.; Joseph, R. *Biochem. Biophys. Acta* **1993**, *1167*, 219.
- 24) Hindes, R. D.; Mizell, M. *Dev. Biol.* **1976**, *53*, 49.
- 25) Boman, H. G.; Marsh, J.; Goode, J. A. *Antimicrobial Peptides: Ciba Foundation Symposium 186*; Marsh, J. and Goode, J. A., Ed.; John Wiley & Sons: London, 1994, p 77.
- 26) Strahan, R. *The mammals of Australia*; Smith, M. J. and Hinds, L., Ed.; Reed Books, The Australian Museum: Chatswood, NSW, 1995; Vol. 2, p 329.
- 27) Poole, W. E.; Wood, J. T.; Simms, N. G. *Wildl. Res.* **1991**, *18*, 625.
- 28) Strahan, R. *The mammals of Australia*; ^{Sharman, G. B., Maynes, G. M.} Eldridge, M. D. B. and Close, R. L., Ed.; Reed Books, The Australian Museum: Chatswood, NSW, 1995; Vol. 2, p 385.
- 29) Strahan, R. *The mammals of Australia*; Sharman, G. B., Maynes, G. M., Eldridge, M. D. B. and Close, R. L., Ed.; Reed Books, The Australian Museum: Chatswood, NSW, 1995; Vol. 2, p 391.
- 30) Copley, P. B.; Robinson, A. C. *Aust. Wildl. Res.* **1983**, *10*, 63.
- 31) Edman, P.; Begg, G. *Eur. J. Biochem.* **1967**, *1*, 80.
- 32) Biemann, K.; Martin, S. A. *Mass Spectrom. Rev.* **1987**, *6*, 1.

- 33) Bowie, J. H.; Brinkworth, C. S.; Dua, S. *Mass Spectrom. Rev.* **2002**, *21*, 87.
- 34) Dockray, G. J.; Gregory, R. A.; Hutchison, J. B.; Harris, J. I.; Runswick, M. J. *Nature* **1978**, *274*, 711.
- 35) Kitagawa, K.; Futaki, S.; Yagami, T.; Sami, S.; Inoue, K. *Int. J. Peptide Protein Res.* **1994**, *43*, 190.
- 36) Anastasi, A.; Erspamer, V.; Endean, R. *Arch. Biochem. Biophys.* **1968**, *125*, 57.
- 37) Erspamer, V. *Amphibian Biology: The integument*; Surrey Beatty and Sons: Norton, NSW, Australia, 1994; Vol. 1, p 178.
- 38) Wabnitz, P. A.; Bowie, J. H.; Tyler, M. J. *Rapid Commun. Mass Spectrom.* **1999**, *13*, 2498.

Chapter Five

Discovery of New Caerulein-like Peptides

5.1 General

Caerulein is an amphibian neuropeptide¹ with smooth muscle, analgaesic and hormone activity². It has been found in numerous species of frog in Central South America, Southeastern Africa and Australia. Caerulein was first isolated from skin extracts of the Australian frog *Litoria caerulea*³ and later from the skin of the African frog *Xenopus laevis*⁴ and the South American leptodactylid frog *Leptodactylus labyrinthicus*⁴. In Australia, caerulein is commonly found in the skin secretion of tree frogs of the genus *Litoria* including *L. caerulea*³, *L. infrafrenata*⁵, *L. xanthomera*⁶ and *L. genimaculata*⁷.

Caerulein analogues have been previously found in the skin secretions of the frog species as shown in *Table 5.1*.

Table 5.1: Sequences of the caerulein-type peptides

Name	Sequence	Source
Phyllocaerulein	pEQEY(SO ₃)TGWMDf-NH ₂	<i>Phyllomedusa sauvagei</i> ⁸
[Asn ² , Leu ⁵] caerulein	pEQNDY(SO ₃)LGWMDf-NH ₂	<i>Kassina maculata</i> ⁹
[Leu ³] caerulein	DY(SO ₃)LGWMDf-NH ₂	<i>Rana erythraea</i> ¹⁰
[Glu(OMe) ²] caerulein	pEQE(OMe)DY(SO ₃)TGWMD F-NH ₂	<i>Nictimystes disrupta</i> ¹¹
Caerulein	pEQDY(SO ₃)TGWMDf-NH ₂	Various <i>Litoria</i> species ^{3,5-7,12,13}

Recently, Wabnitz *et al.* reported the discovery of new caerulein analogs from the skin secretion of *Litoria citropa*¹³ and *Litoria splendida*^{14,15}. All of these peptides closely resemble the structure of the neuropeptide caerulein.

5.2 Caerulein-like Peptides from *Litoria citropa*

Litoria citropa (Figure 5.1), known as “the Australian Blue Mountains tree frog” is found near rocky flowing streams in heavily forested areas from the coast to the Dividing Ranges in eastern Victoria and New South Wales¹³ (Figure 5.2).



Figure 5.1: Picture of *Litoria citropa* (ex Assoc Prof. M.J. Tyler)



Figure 5.2: Diagram of the geographic distribution of *Litoria citropa*

This tree frog is unusual as it secretes host defence peptides from two types of skin glands: namely, (i) dorsal granular glands, which are distributed evenly throughout the dorsal surface, and (ii) the submental gland, a relatively large gland located underneath the throat region.

In 1999, Wabnitz *et. al.*¹³ reported that the secretion from both the dorsal and submental glands of *Litoria citropa* contain the eight caerulein-like peptides listed in *Table 5.2* together with their desulfated counterparts (*Table 5.3*). The HPLC separation of these compounds is shown in *Figure 5.3*.

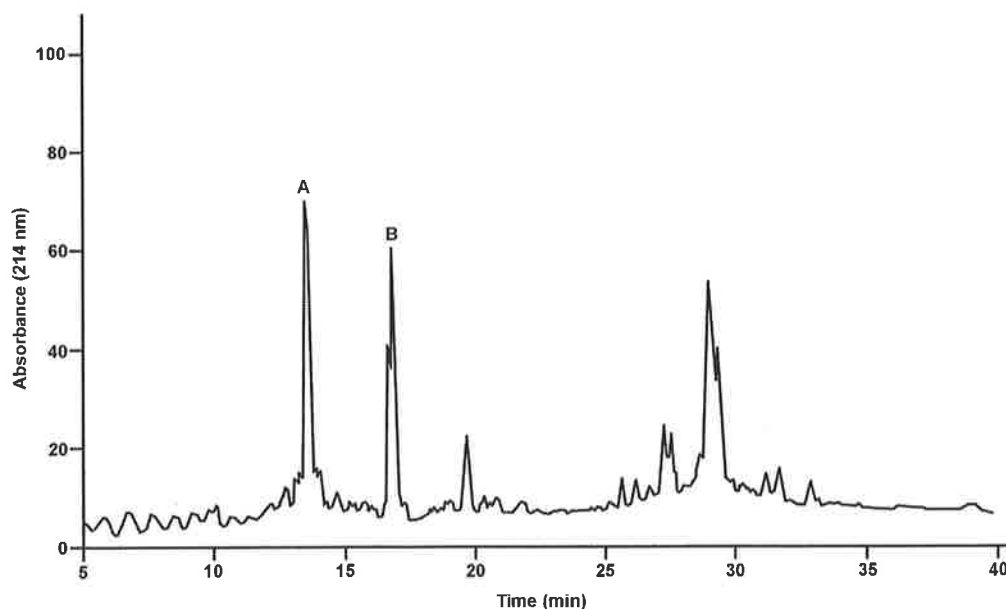


Figure 5.3: HPLC separation of the crude secretions from *Litoria citropa*. (As taken in 1999 by Wabnitz *et al.*¹³). Fraction **A** contains caerulein components (caeruleins 1.2, 2.2, 3.2 and 4.2) and desulfated caerulein components (desulfated caeruleins 1.2Y^A, 2.2Y^A, 3.2Y^A and 4.2Y^A). Fraction **B** contains caerulein components (caeruleins 1.1, 2.1, 3.1 and 4.1) and desulfated caerulein components (desulfated caeruleins 1.1Y^A, 2.1Y^A, 3.1Y^A and 4.1Y^A).

Table 5.2: Caerulein-like peptides from *Litoria citropa*

Caerulein	Sequence
1.1	pEQDY(SO ₃)TGWMDf-NH ₂
1.2	pEQDY(SO ₃)TGWfDF-NH ₂
2.1	pEQDY(SO ₃)TGAHMDF-NH ₂
2.2	pEQDY(SO ₃)TGAHFDF-NH ₂
3.1	pEQDY(SO ₃)GTGWMDf-NH ₂
3.2	pEQDY(SO ₃)GTGWfDF-NH ₂
4.1	pEQDY(SO ₃)TGSHMDF-NH ₂
4.2	pEQDY(SO ₃)TGSHFDF-NH ₂

Caerulein-like peptides may be present in the desulfated form. Examples of desulfated caerulein peptides isolated from *Litoria citropa* are listed *Table 5.3*.

Table 5.3: Desulfated caeruleins from *Litoria citropa*^{13,16}

Name	Sequence
Caerulein Y ⁴	pEQDYTGWMDF-NH ₂
Caerulein 1.2Y ⁴	pEQDYTGWFDF-NH ₂
Caerulein 2.1Y ⁴	pEQDYTGAHMDF-NH ₂
Caerulein 2.2Y ⁴	pEQDYTGAHFDF-NH ₂
Caerulein 3.1Y ⁴	pEQDYGTGWMDF-NH ₂
Caerulein 3.2Y ⁴	pEQDYGTGWFDF-NH ₂
Caerulein 4.1Y ⁴	pEQDYTGSHMDF-NH ₂
Caerulein 4.2Y ⁴	pEQDYTGSHFDF-NH ₂

Non-sulfated caerulein is known to show minimal smooth muscle activity^{2,11}. The desulfated caeruleins isolated from *Litoria citropa* have been shown not to be artefacts formed during extraction or purification procedures. Why *Litoria citropa* produces such an abundance of non-sulfated caerulein derivatives in the glandular secretions is not understood at this time. There must be a specific endoprotease which is effecting this hydrolysis.

5.3 Caerulein-like Peptides from *Litoria splendida*

Litoria splendida is the largest Australian tree frog (*Figure 5.4*). It is located in the Kimberley region of Western Australia (*Figure 5.5*). The peptide secretion can be obtained from the large glands distributed around the front and back of the head. The peptide secretion from the parotoid and rostral gland of *Litoria splendida* has been previously reported^{15,16}.



Figure 5.4: *Litoria splendida* (ex. Assoc. Prof. M. J. Tyler)

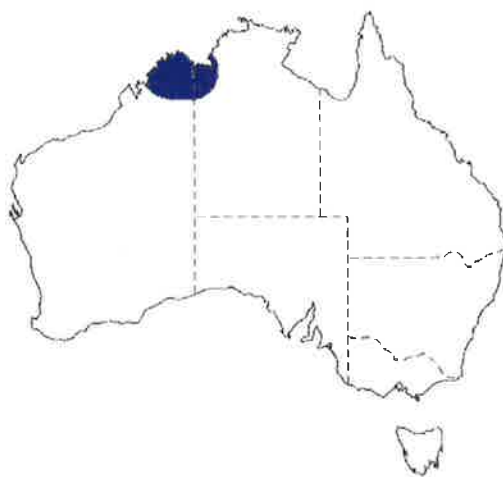


Figure 5.5: Geographic distribution of *Litoria splendida*

Wabnitz *et al.* monitored the components of the glandular secretions of male and female *Litoria splendida* monthly over a three year period¹⁶. He found that the composition of caerulein peptides shows seasonal variations and these variations are identical for the male and female. Examples of HPLC separations are shown for the male frog for January 1998 (Figure 5.6) and July 1998 (Figure 5.7).

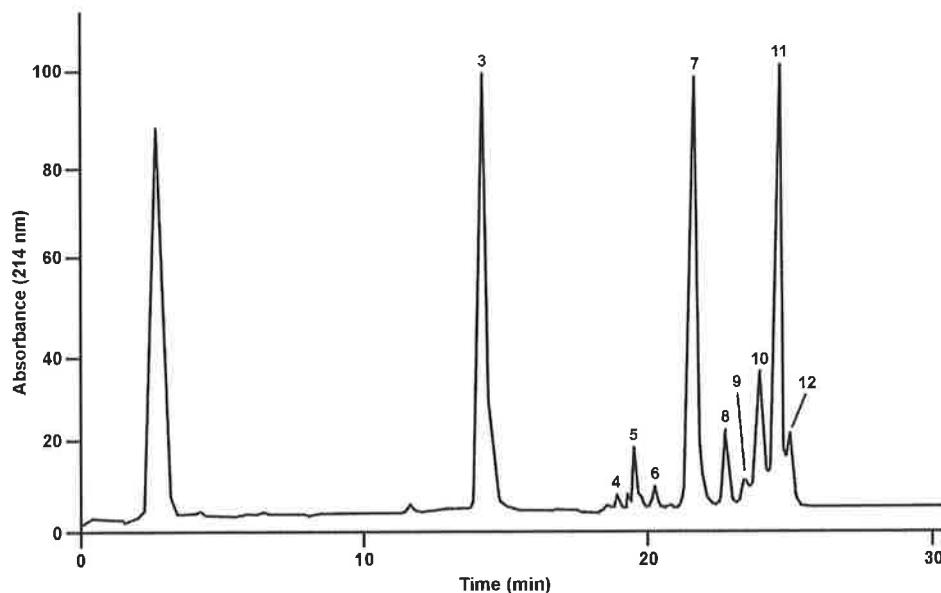


Figure 5.6: HPLC separation of glandular secretion of male *L. splendida*, obtained in January. (As taken in 1998 by Wabnitz et al.¹⁶). Component 3 is caerulein 1.1. Components 4-12 have been previously reported¹⁶.

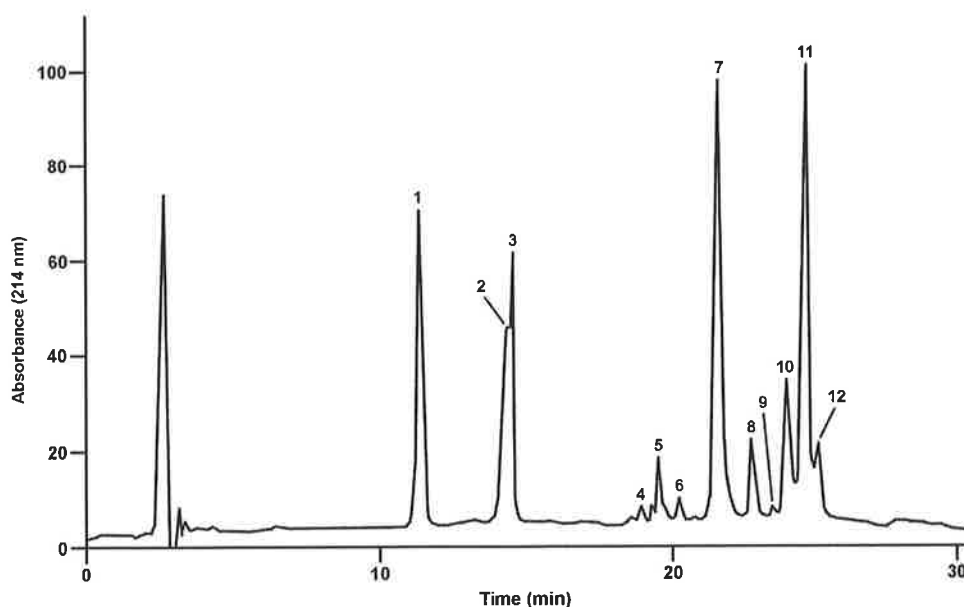


Figure 5.7: HPLC separation of glandular secretion of male *L. splendida*, obtained in July. (As taken in 1998 by Wabnitz et al.¹⁶). Components 1, 2 and 3 are caerulein 1.2, desulfated caerulein 1.2 and caerulein 1.1, respectively. Components 4-12 have been previously reported¹⁶.

Caerulein 1.1 [pEQDY(SO₃)TGWMDF-NH₂] is the sole neuropeptide formed in the period from September to May. During the winter period, more than half of the caerulein is

hydrolysed to the desulfated form, and a new peptide, caerulein 1.2 [pEQDY(SO₃)TGWFDN-NH₂] becomes a major component of the skin secretion. The reasons for these seasonal changes are not known with certainty. It was suggested that this seasonal change might be involved in thermoregulation, i.e. with the initiation and maintenance of the reproductive and hibernation periods of the animal¹⁶.

Caerulein 1.1 is a known neuropeptide which exhibits potent smooth muscle activity². The other seven caerulein-like peptides (*Table 5.2*) have been characterised¹³. However, the commercial synthesis of these peptides was unsuccessful because of the hydrolysis of the tyrosine sulfate residue at position 4 when the synthesised peptides were washed from the support. These peptides need to be synthesised in order to have sufficient material to allow activity testing, because we have less than 1 µg of each of the natural peptides.

The aim of the research presented in the next chapter is to establish a facile synthetic method for tyrosine sulfate containing peptides via solid phase peptide synthesis and to apply this to the caerulein analogues and eugenin.

5.4 References

- 1) Anastasi, A.; Erspamer, V.; Cei, J. M. *Experientia* **1967**, *23*, 699.
- 2) Lazarus, L. H.; Attila, M. *Prog. Neurobiol.* **1993**, *41*, 473.
- 3) Anastasi, A.; Erspamer, V.; Endean, R. *Arch. Biochem. Biophys.* **1968**, *125*, 57.
- 4) Anastasi, A.; Bertaccini, G.; Cei, J. M.; De Caro, G.; Erspamer, V. *Br. J. Pharmacol.* **1970**, *38*, 221.
- 5) Raftery, M. J.; Waugh, R. J.; Bowie, J. H.; Wallace, J. C.; Tyler, M. J. *J. Pept. Sci.* **1996**, *2*, 117.
- 6) Steinborner, S. T.; Waugh, R. J.; Bowie, J. H.; Wallace, J. C.; Tyler, M. J.; Ramsay, S. *L. J. Pept. Sci.* **1997**, *3*, 181.
- 7) Rozek, T.; Waugh, R. J.; Steinborner, S. T.; Bowie, J. H.; Tyler, M. J.; Wallace, J. C. *J. Pept. Sci.* **1998**, *4*, 111.
- 8) Anastasi, A.; Bertaccini, G.; Cei, J. M.; De Caro, G.; Erspamer, V.; Impicciatore, M. *Brit. J. Pharmacol.* **1969**, *37*, 198.
- 9) Montecucchi, P. C.; Falconieri Erspamer, G.; Visser, J. *Experientia* **1977**, *33*, 1138.
- 10) Yasuhara, T.; Nakajima, T.; Erspamer, V.; Falconieri Erspamer, G.; Tukamoto, G. Y.; Mori, M. *Peptide Chemistry 1985*; Kiso, Y., Ed.; Protein Research Foundation: Osaka, 1986, p 363.
- 11) Erspamer, V. *Amphibian Biology*; Heatwole, H., Ed.; Surrey Beatty & Sons Pty. Limited: NSW, 1994; Vol. 1, p 178.
- 12) Wabnitz, P. A.; Walters, H.; Tyler, M. J.; Bowie, J. H. *J. Pept. Res.* **1998**, *52*, 477.
- 13) Wabnitz, P. A.; Bowie, J. H.; Tyler, M. J. *Rapid Commun. Mass Spectrom.* **1999**, *13*, 2498.

- 14) Barker, J.; Grigg, G.; Tyler, M. J. *A Field Guide to Australian Frogs*; Surrey Beatty: Norton, NSW, 1995, p 40.
- 15) Stone, D. J. M.; Bowie, J. H.; Tyler, M. J.; Wallace, J. C. *J. Chem. Soc. Chem. Commun.* **1992**, 400.
- 16) Wabnitz, P. A.; Bowie, J. H.; Tyler, M. J.; Wallace, J. C.; Smith, B. P. *Eur. J. Biochem.* **2000**, 267, 269.

Chapter Six

Peptide Synthesis

6.1 Introduction

Peptide synthesis originated in 1881 with the work of Theodore Curtius¹ who achieved the first synthesis of a protected peptide. In 1901, Emil Fischer² synthesised the first free dipeptide. This work led to the first methods for the formation of “peptide” bonds, amide linkages between α -amino acids, and established the importance of optical purity in synthetic products. Subsequent to this work, progress was slow for the next 30 years. Bergmann and Zervas³ introduced the carbobenzoxy-protecting group for the α -amine of amino acids in 1932. During the 1950s, new methods were developed for the synthesis of small peptides⁴. The older acid azide coupling method of Curtius and the acid chloride method of Fischer were supplemented with the application of mixed anhydrides by Wieland⁵. Meanwhile, active esters were shown to be good coupling reagents, including thiophenyl esters⁶, cyanomethyl esters⁷, nitrophenyl esters⁸ and halogenated phenyl

esters⁹. At this time, the use of carbodiimides as coupling reagents was also introduced¹⁰. Carpino replaced the benzyloxycarbonyl function with the acid-labile tertiary-butylloxycarbonyl group¹¹ and this method was developed by McKay¹² and Anderson¹³. Acid-labile groups such as nitrophenyl sulfenyl¹⁴ and biphenylisopropylloxycarbonyl derivatives¹⁵ were also introduced. Methods of protecting side chain substituents, and the selective removal of protecting groups were also developed during this period⁴.

Poor solubility and low yield were problems with the solution approach to peptide synthesis¹⁶. In addition, the synthetic procedures were very time consuming. In the 1960s, Merrifield¹⁷ introduced a new approach, the “solid phase” method in peptide synthesis. This approach could be used to prepare peptides up to 50 amino acid residues of length. Due to improvements in the solid phase method, the synthesis of bioactive peptides, hormones, antibiotics, growth factors, toxins, etc. are now routine⁴.

6.2 Solid-phase Peptide Synthesis (SPPS)

SPPS involves the initial attachment of the C-terminal amino acid to a “solid” support followed by sequential addition of the subsequent amino acids¹⁷ (*Figure 6.1*).

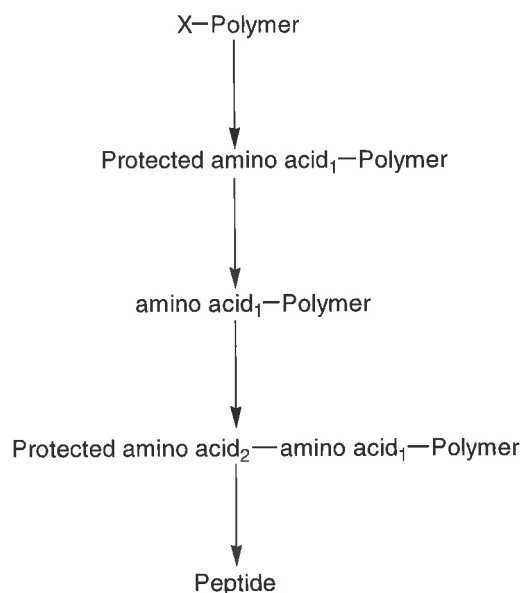


Figure 6.1: Initial idea for SPPS

The SPPS process requires a solid support to hold the C-terminus of the first amino acid in place in order to enable sequential addition of other amino acids. The N-terminus needs to be initially protected during coupling and then deprotected to free the terminal NH_2 for reaction in the next cycle. The three steps, viz, deprotection, neutralisation and coupling, are repeated until the desired sequence is achieved. Finally, the peptide is cleaved from the solid support and the peptide is released into solution.

The support containing the first amino acid is placed in a suitable vessel, and is not transferred or removed until the end of the synthesis. If the solid support is completely insoluble in the solvent used, the peptide will also be insoluble and can be readily filtered and washed without transfer to other containers. Using molar excess and a high concentration of the next protected amino acid produces peptide bond formation. The excess reagent and soluble by-products are removed by washing with solvent. The advantages of the SPPS technique are speed, simplicity and high yield of product. Fundamental aspects of the solid-phase synthesis are¹⁸:

- (i) The peptide is covalently attached to a solid support.
- (ii) “Solid” support: swollen, interpenetrating polymer network.
- (iii) Synthesis occurs within the swollen support.
- (iv) Peptide and resin mutually enhance their solvation.
- (v) Peptide-resin exerts a strong solvating effect on the covalently attached peptide chain.
- (vi) No significant effect of chain length on synthetic efficiency.
- (vii) The reactions are rapid.

6.2.1 Solid supports

The resin support is the key to the solid-phase process. The support must be mechanically robust, swell in the solvents used, show little specific binding to biomolecules and allow non-hindered access of reagents¹⁹.

The first attempts to develop this method involved the use of cellulose⁴. It was reasoned that the synthetic peptide and solid cellulose would be compatible, reactants could enter the matrix, and the peptide product could exit freely. As efforts to esterify cellulose with N-protected or free amino acids were unsatisfactory, the method was abandoned. Materials such as polyvinyl alcohol were also examined but were found to be too soluble in solvents. Ion-exchange resins such as IRC-50 gave the first successful synthesis of a dipeptide using the solid-phase approach. Copolymers of styrene and divinylbenzene were also examined. Originally, 2% of chloromethyl cross-linkers were used on a styrene-divinylbenzene resin bead¹⁷, but this was later modified to 1% cross-linking^{20,21}. This copolymer becomes highly solvated and swollen and may reach a volume 50 fold greater than the dry bead. The

low cross-linking together with use of a good swelling solvent such as dichloromethane or dimethylformamide is particularly effective.

Four major support types have been used in solid-phase synthesis²². These are:

1) Gel type supports

The most used supports are the gel type due to the optimal behaviour of gels for high yield synthesis. Equal distribution of functional groups throughout a highly solvated polymer network is ideal for the assembly of peptides²³. The polymer network is flexible and the resin can either expand or exclude solvent in order to accommodate the growing peptide within the gel (*Figure 6.2*).

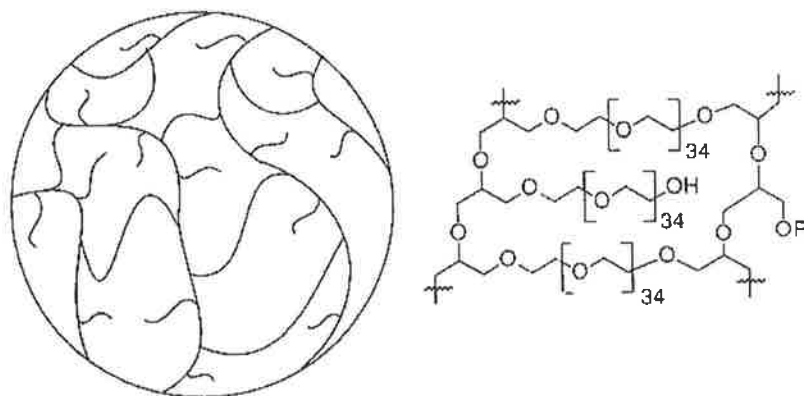


Figure 6.2: The structure of polymer network of the gel type resin.

Four types of gel resins have been developed.

- (i) The hydrophobic polystyrene resins produced from styrene and divinylbenzene and substituted with various forms of functionalities, e.g. for chloromethylation or aminomethylation.

- (ii) Polyacrylamide resins were developed as a hydrophilic alternative to polystyrene resins²⁴. They are obtained by cross-linking poly-*N,N*-dimethylacrylamide with 5% bis-*N,N'*-acryloylethylenediamine, and use *N*-acryloylsarcosine methyl ester as the functional group²⁵.
- (iii) Polyethylene glycol (PEG) grafted resins were introduced as a more stable resin in order to space the site of synthesis from the polymer backbone. They are formed either by grafted polymerisation on polystyrene beads²⁶, or by reaction of preformed oligooxyethylenes with an aminomethylated polystyrene bead²⁷.
- (iv) PEG-based resins are composed of either a PEG/polypropylene glycol (PPG) network or a combination of PEG with a small amount of polyamide or polystyrene. The resin is obtained by partial derivatisation of PEG with epichlorohydrin, chloromethylstyrene or acryloyl chloride. This resin can be mixed with another monomer to give a highly cross-linked polymer with a long cross-linker of PEG²⁸⁻³¹.

2) Surface type supports

These are made from various polymers including polyethylene (*Figure 6.3*), cellulose fibres, porous, highly cross-linked polystyrene or polymethacrylate, or controlled pore glass³².

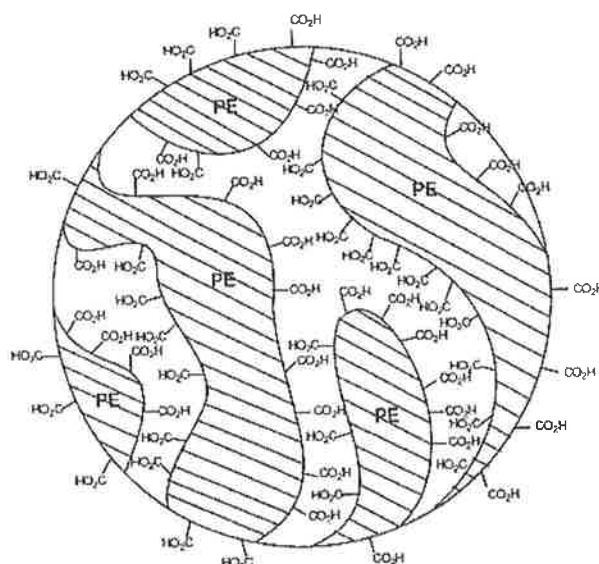


Figure 6.3: The structure of a functionalised surface particle. A chromium trioxide oxidised porous polyethylene (PE)

Some problems are associated with synthesis directly on a functionalised support. The surface area has to be large to give useful loadings for preparative synthesis, and to contain uniform cavities and pores. The surface should not interact with the molecule to be synthesised and should be properly solvated in the solvent. In addition, the distance between the attachment sites should be large enough to allow non-hindered access of reagents and prevent aggregation on the surface.

3) Composites and supported gels

Some polystyrene and polyamide gels are not stable to flow conditions. As a consequence, rigid matrices such as kieselguhr or Teflon were introduced for support^{33,34} (Figure 6.4).

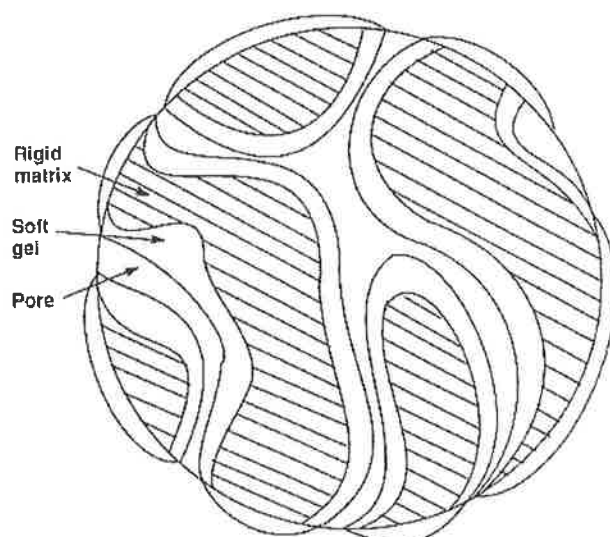


Figure 6.4: *The physical structure of a supported soft gel polymer network*

The use of such matrices for dimethylacrylamide polymerisation achieves a better flow. However, some aggregation of peptide is observed during some peptide syntheses and reaction rates are slower than if unsupported gel polymers are used. This aggregation can result in steric inhibition of reagents to reactive sites¹⁷.

4) Brush polymers

Brush polymers consist of linear chain polymers grafted to a rigid surface. They are often composed of polystyrene attached to polyethylene³⁵. Functionalisation can be achieved along the extending chains, and functional groups can be modified using suitable spacer molecules (*Figure 6.5*).

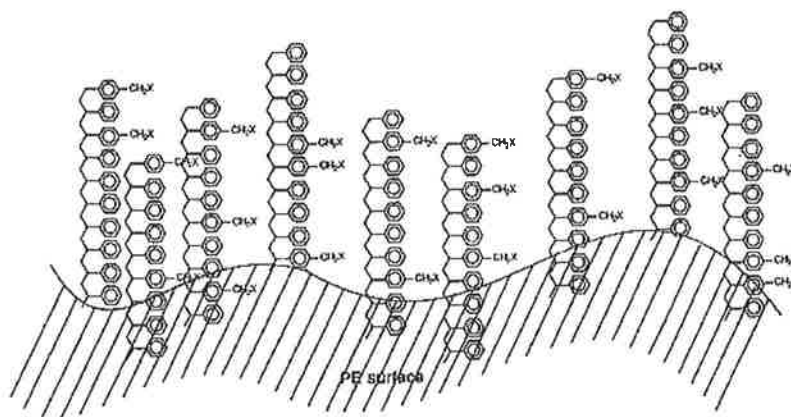


Figure 6.5: Structure of a grafted polystyrene brush polymer on polyethylene

Brush polymers can be modified using polyethylene glycol or polyamide attached to the functional groups, affording a polymer that wets more readily in polar solvents³⁶. The rigid polyethylene surface imposes a one-dimensional restriction on the swelling of the polystyrene chains. This produces difficulties for the synthesis of large and bulky molecules.

Many supports are currently available for solid-phase synthesis. It is important to achieve the optimal performance of the proper support during solid-phase synthesis. For most purposes the mechanically stable beaded gel resins are preferred. However, polystyrene resins or amide bond free PEG-based resins are suited for some organic syntheses³⁷⁻⁴¹.

6.2.2 Role of the resin support

The most commonly used support is a cross-linked polymeric resin¹⁷; a suspension copolymer of styrene divinylbenzene (S-DVB) in the form of beads approximately 50 microns in diameter (*Figure 6.6*).

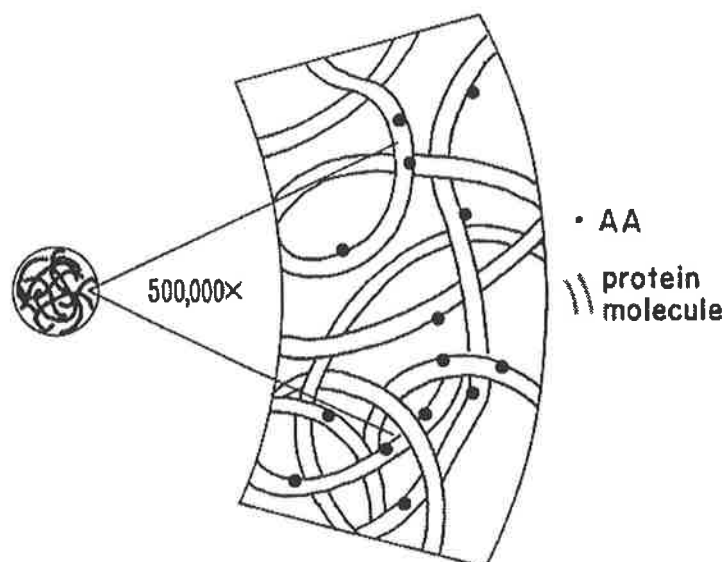


Figure 6.6: The peptide-resin support used in solid phase synthesis

Figure 6.6 shows beads of loosely cross-linked polymer swollen in an organic solvent, with peptide synthesis taking place inside the swollen polymer network. The swollen peptide-resin contains 80-90% of solvent by volume. There are of the order of 10^{12} growing peptide chains per polymer bead⁴².

The swollen peptide-resin exerts a strong solvating effect on the covalently attached peptide chains. One end of the linear peptide is covalently attached to an interpenetrating polymer network⁴³. The peptide-resin beads swell further as the protected peptide chain is elongated. Consequently¹⁸,

- (i) There is no effective limit to the chain length or amount of peptide that can be grown within the swollen resin beads.
- (ii) Only a small amount of solvent is required.
- (iii) High concentrations of reagent for deprotection and coupling can be used.

- (iv) The use of high substitution of the resin in SPPS may lead to increased aggregation of peptide chains within the swollen support, causing difficulty in some syntheses.

It is necessary to maintain the highly solvated state of the peptide-resin throughout the synthetic cycle in order to maximise the reaction yield.

6.2.3 The protecting group

It is necessary to protect reactive substituents of peptides other than those directly involved in amide bond formation. Such protecting groups must be able to be removed without damaging the assembled peptide chain. There are two types of protecting group for SPPS.

1) An α -amino acid protecting group

This protecting group can be removed after formation of each peptide bond, e.g. *tert*-butoxycarbonyl (Boc)-amino acid or 9-fluorenylmethoxycarbonyl (Fmoc)-amino acid strategy. The fundamental operations for one cycle of chain extension in SPPS using Boc or Fmoc-chemistries are illustrated in *Figure 6.7*.

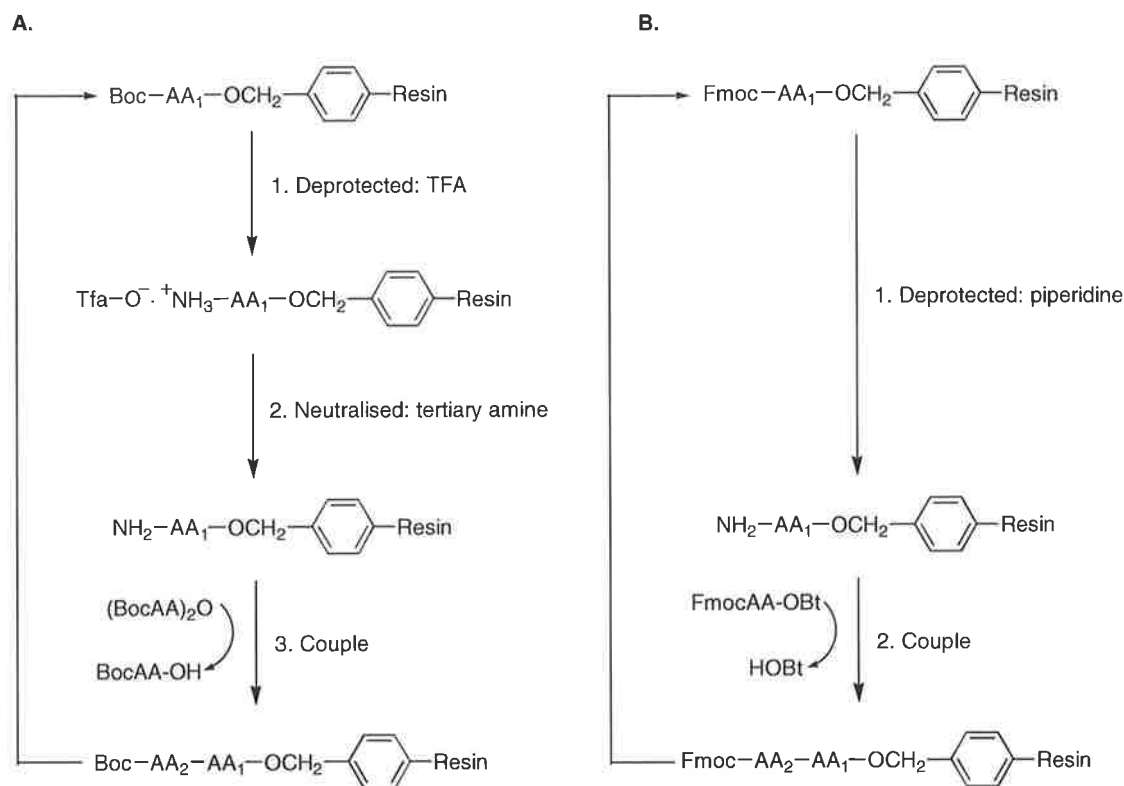


Figure 6.7: Chain assembly of stepwise SPPS. **A** is the Boc process and **B** is the Fmoc process.

Boc-chemistry relies on the acid lability of the protecting groups. The protocol for Boc-chemistry is characterised by the use of dimethylformamide to maintain maximum solvation of the peptide-resin. This ensures swelling of the peptide-resin while potentially aiding the disaggregation of intermolecularly H-bonded aggregates. Neat trifluoroacetic acid is used to remove the N^α -Boc group. After washing with dimethylformamide, the resulting amine salt is neutralised with a tertiary amine. The peptide bond is formed by reaction of the resin-bound peptide with the Boc-amino acid symmetric anhydride¹⁸.

In Fmoc-chemistry, the N^α -Fmoc group is removed (by treatment with a secondary amine such as piperidine) to give a neutral peptide-resin. After washing, the peptide bond is formed by reaction with Fmoc-amino acid hydroxybenzotriazole active ester. This method is operationally simpler than the Boc procedure, and is the method of choice for the solid-

phase syntheses of modified peptide species, e.g. those that have phosphorylated, sulfated or glycosylated units.

2) Side-chain protection

The side-chain protecting groups are removed after completion of the chain assembly. For the N^α-Boc group, the most commonly used side-chain protecting group is a benzyl-based moiety^{18,44-46}. Among these are benzyl (Bzl) for Asp, Glu, Ser, Thr and Tyr; methoxybenzyl (Mob) for Cys; dichlorobenzyl (2ClBz) for Lys; toluenesulfonyl (Tos) for Arg; dinitrophenyl (DNP) for His. Formyl is used for Trp^{18,47}.

Acid-labile side-chain protecting groups are often employed because of the base lability of the Fmoc group: these are based on the *tert*-butyl moiety⁴⁸⁻⁵⁰. For example, *tert*-butyl ethers for Ser, Thr and Tyr; *tert*-butyl esters for Asp and Glu and the *tert*-butyloxycarbonyl (Boc) group for Trp⁵¹ and Lys. The triphenylmethyl (Trt) group has also been used for the protection of Cys⁵², His, Asn and Gln⁵³. The 2,2,5,7,8-pentamethylchroman-6-sulfonyl (Pmc) group commonly protects the guanidino group of Arg⁵⁴.

6.2.4 Peptide bond formation

The formation of an amide bond between two amino acids requires activation of the carboxyl group of one to enable facile reaction with the amino group of the other. It is essential that the coupling method (i) produces the amide in a high yield and (ii) maintains the configurational integrity of the system.

Early methods, which used carbodiimides and 1-hydroxybenzotriazole (HOBt) for activation¹⁸, are now often replaced by the more convenient uronium salt technique⁵⁵. The use of 2-(1*H*-benzotriazol-1-yl)-1,1,3,3-tetramethyl-uroniumhexafluorophosphate (HBTU) in combination with *N,N*-diisopropylethylamine (DIEA) is used for neutralisation and protonation of the protected amino acid prior to use. Coupling reactions carried out in aprotic dipolar solvents (e.g. dimethylformamide) can give dramatic improvement in yield in comparison with reactions carried out in protic solvents⁵⁶.

6.2.5 Determination of chain assembly

The ninhydrin reaction is used for the detection of free amino groups formed during SPPS⁵⁷. This method has been widely used as a guide to the progress of the coupling reaction. The technique involves detection of the ^{chromophore of the} ninhydrin product at 570 nm. The blue chromophore of the ninhydrin reaction product with primary amines is found in solution. It is a sensitive and accurate test, identifying >99% of any residual amine.

The Isatin test⁵⁸ can be used for proline and other secondary amines. Isatin reacts with secondary amines to give a yellow colour on the beads. This can be observed when the supernatant liquid is removed by decantation, and the beads washed by decantation with acetone.

6.2.6 Deprotection and cleavage from the resin support

After completion of the chain assembly, protecting groups are removed and the covalent link between the resin support and the peptide cleaved to remove the free peptide into solution.

In Boc-chemistry, deprotection with trifluoroacetic acid leads to a protonated α -ammonium species, which has to be neutralised with *N,N*-diisopropylethylamine before the next amino acid can be coupled. A benzyl-based side chain is cleaved by treatment with a strong acid such as hydrogen fluoride (HF)⁵⁹. When side chain blocking groups are cleaved by acidolysis, reactive carbonium or acylium ions are formed that can attack alkylatable residues in the peptide. For example, benzyl and *tert*-butyl carbonium ions alkylate Met, Cys, Tyr and Trp residues. This problem can be prevented by adding a large excess of a suitable nucleophilic scavenger in the HF reaction mixture: for example anisole, *m*-cresol, thioanisole, 1,2-dithioethane and methionine have been used for this purpose. Although HF is an inconvenient and toxic reagent, it is still the cleavage reagent of choice in most cases. Once suitable protocols have been established, use of HF is safe, rapid and effective. If equipment for the safe handling of HF is not available, peptide-resins may be cleaved by using trifluoromethanesulfonic acid (TFMSA) or trifluoromethanesulfonic acid trimethylsilyl ester (TMSOTf). However, these reagents may cause side reactions with some peptides⁶⁰.

In the case of Fmoc-chemistry, bases like piperidine are used to remove the Fmoc group. *Tert*-butyl-based side chain protecting groups and peptide-resin are cleaved with trifluoroacetic acid (TFA), resulting in the exposure of vulnerable residues to reactive

carbocation centres. Side-chain deprotection with TFA can generate highly reactive carbocations⁶¹⁻⁶³ and sulfonyl species^{54,64-69} from side-chain protecting groups. These can alkylate or sulfonate susceptible amino acid residues. The amino acids most vulnerable to the consequences of TFA deprotection are Met, Tyr and Trp. The Met residue is susceptible to oxidation^{70,71} or *tert*-butylation^{62,72-74}. Tyr may be *tert*-butyrate^{72,75} or sulfonated by a Pmc group⁶⁶. Trp without Boc side-chain protection is vulnerable to modification by the linker^{76,77} or side-chain protecting groups^{54,62,64,66,72,78-89}. TFA itself can react with *tert*-Bu cations to form *tert*-Bu trifluoroacetate⁶², or it can form an adduct with the scavenger ethanedithiol⁶⁴. Many of the problems mentioned above can be circumvented by the addition of nucleophilic scavengers such as water, phenol, thioanisole and 1,2-dithioethane (EDT) to the trifluoroacetic acid to trap reactive coproducts^{90,91}. There are a number of scavenger mixtures described in the literature. For example, reagent K contains thioanisole, EDT, phenol and water in TFA (5:2.5:5:5:82.5, v/v): this reagent is effective at suppressing side reactions⁶⁵. Addition of thioanisole has been shown to prevent oxidation⁹² and *tert*-butylation of Met⁶⁵, and accelerate the removal of aryl sulfonyl groups⁸⁷. EDT, the second scavenger, ensures complete removal of the Pmc group, linker cations⁷⁷ and *tert*-Bu and *tert*-Bu trifluoroacetate⁶², and also prevents reattachment of *tert*-Bu to Trp, Tyr or Met⁶⁵. Use of EDT will also prevent the reattachment of triphenylmethyl to Cys⁹³⁻⁹⁶. Phenol, the third scavenger, is added to assist in scavenging Pmc cations⁶⁵. When 5% of water is added to the TFA mixture, this will quench the reactivity of *tert*-Bu^{65,72,97}, Pmc ions^{54,65,66,98} and eliminate any side reaction of Pmc⁶⁸.

6.3 Synthesis of Tyrosine Sulfate Containing Peptides

The synthesis of tyrosine sulfate [Tyr(SO₃)]-containing peptides can be challenging. Synthetic methods for Tyr(SO₃)-containing peptides have been reported using either solution-phase⁹⁹⁻¹⁰² or solid-phase methods¹⁰³⁻¹⁰⁹.

Efficient and convenient synthetic strategies for Tyr(SO₃) containing peptides are still being developed. The major difficulty in the synthesis of Tyr(SO₃)-containing peptides lies in the intrinsic acid-lability of the sulfate residue. When Fmoc-based protection of an amide is used during solid-phase peptide synthesis, base catalysed reactions are used. Deprotection of side-chain protecting groups and cleavage of peptides from the resin support are conducted with trifluoroacetic acid at the final stage of synthesis. Tyrosine sulfate derivatives such as Tyr(SO₃-Na) are relatively stable in trifluoroacetic acid¹¹⁰. Thus the preparation of Tyr(SO₃)-containing peptides is normally accomplished using Fmoc-Tyr(SO₃Na)-OH as the building block.

Many acid-labile naturally occurring neuropeptides like caerulein, gastrin II, cholecystokin-8 (CCK-8) have C-terminal CONH₂ groups. Such peptide amides can be synthesised on an amide linkage agent, with the α -amino function protected with the base labile Fmoc group. The initial linkage used with Fmoc utilises 4-hydroxymethylbenzoic acid¹¹¹. This linkage agent is resistant to acids and the acid-labile protecting group can be removed prior to cleavage. To produce peptide amides the deprotected peptide-resin is subjected to treatment with ammonia. The most convenient linker for the synthesis of peptide amides is the rink linker, 4-(Fmoc-amino-2', 4'-dimethoxybenzyl)phenoxyacetic acid¹¹². This is attached to the resin support using common activation methods. The linker

is cleaved with trifluoroacetic acid, while simultaneously removing of the acid-labile side-chain protecting groups to liberate the deprotected peptide amide. Other linker agents such as [5-(4-aminomethyl-3,5-dimethoxyphenoxy)valeric acid] (PAL) linker¹¹³ have been used for producing peptide amides. However, the detachment efficiency of the peptide from the support was less than 40% after cleavage/deprotection conditions using the PAL linker. To improve the detachment efficiency, Kitagawa and co-workers¹⁰⁹ introduced the use of acid-sensitive 2-chlorotrityl resin (Clt-resin)¹¹⁴⁻¹¹⁶ as a solid support.

After chain assembly on the resin, the peptide is side-chain deprotected and removed from the support. The side-chain protecting groups and linkers designed for stepwise synthesis of Tyr(SO₃)-containing peptides are labile to high polarity solvents such as trifluoroethane (TFE) and trifluoroacetic acid (TFA). Removal of the side-chain protecting groups and peptides from the resin support are reported to be favourable with both TFE and TFA at the final stage of synthesis¹⁰⁹. Trifluoroacetic acid is a suitable deprotection reagent for Tyr(SO₃)-containing peptides because of the high-ionised power of TFA. Trifluoroacetic acid can cleave both at the linker-peptide bond and at the attachment point of the linker to the resin. This problem can be circumvented by the addition of nucleophilic scavengers such as water, *m*-cresol, thioanisole or 1,2-dithioethane (EDT) to the trifluoroacetic acid solution. However, the decomposition of Tyr(SO₃) to Tyr in trifluoroacetic acid is accelerated by addition of a sulfur compound such as thioanisole or 1,2-dithioethane as a cation scavenger¹¹⁷. The deprotections therefore have to be promoted without the addition of sulfur-containing soft bases. Water is known to be a good cation scavenger in TFA solution without imparting damage to the Tyr(SO₃) residue. The reaction temperature is also a critical factor in the stability of Tyr(SO₃) in trifluoroacetic acid. The desulfation rate is remarkably retarded at low temperature. Kitagawa *et. al.*¹⁰⁹ examined the effect of water

addition on the rates of both desulfation and deprotection at 0°C. It was found that deprotection was only marginally reduced with increasing water content in the TFA, but the desulfation rate was not affected. Thus, the use of aqueous TFA at low temperature removes most (or all) of the protecting groups with minimum damage to the Tyr(SO₃) residue¹¹⁸. The use of 90-95% aqueous TFA at low temperature are the usual conditions used for Tyr(SO₃) containing peptides¹⁰⁶. Addition of nucleophilic scavengers to the trifluoroacetic acid system such as 90% aqueous TFA/*m*-cresol or 90% aqueous TFA/TIPSi at 4°C have also been used as a deprotection/cleavage agents for the synthesis of tyrosine sulfate containing peptides using the Fmoc-based solid-phase method¹⁰⁶.

6.4 Results and Discussion

Solid-phase chemical synthesis of tyrosine sulfate containing peptides as shown in *Table 6.1* were undertaken to provide sufficient material for biological activity tests to be carried out. Those peptides were synthesised with the Fmoc-SPPS using available Boc-pam resin [*p*-carbamoylmethyl) benzyl resin] as a solid support and rink linker, 4-(Fmoc-amino-2',4'-dimethoxybenzyl) phenoxyacetic acid for the preparation of peptide amides. The Fmoc chemistry-SPPS consists of the following steps in each cycle: i) removal of the Fmoc protecting group of the last coupled amino acid by brief treatment with 50% piperidine in DMF; ii) coupling of the next preactivated Fmoc-amino acid. Between each of these steps a through flow wash with DMF is carried out to remove excess reagents and reaction products not bound to the resin.

eS
Table 6.1: Sequencing of tyrosine sulfate containing peptides

Name	Sequence
Caerulein 1.2Y ⁴	pEQDYTGWFDF-NH ₂
Caerulein 3.1Y ⁴	pEQDYGTGWMDf-NH ₂
Eugenin Y ⁴	pEQDYVFMHPF-NH ₂
Caerulein 1.2	pEQDY(SO ₃)TGWFDF-NH ₂
Caerulein 2.1	pEQDY(SO ₃)TGAHMDF-NH ₂
Caerulein 2.2	pEQDY(SO ₃)TGAHFDF-NH ₂
Caerulein 3.1	pEQDY(SO ₃)GTGWMDf-NH ₂
Caerulein 3.2	pEQDY(SO ₃)GTGWDF-NH ₂
Caerulein 4.1	pEQDY(SO ₃)TGSMDf-NH ₂
Caerulein 4.2	pEQDY(SO ₃)TGSDF-NH ₂

6.4.1 Synthesis of desulfated caerulein and eugenin peptides

Desulfated caerulein 1.2, 3.1 and desulfated eugenin were synthesised by the Fmoc-SPPS. The Boc-pam resin was neutralised and washed before the amide linker was introduced. In this synthesis Fmoc-amino acids were preactivated using HBTU/DIEA. The coupling yields of all syntheses were determined by the quantitative ninhydrin test⁵⁷ (after a coupling time of 10 mins), except for proline which was determined by the isatin test^{58,119}. Coupling efficiencies for each amino acid is dependent upon the primary structure of the peptide. The synthesis of desulfated eugenin was more difficult than desulfated caerulein because eugenin contains an oxidation-susceptible Met residue.

All three peptides were cleaved from the resin and the side chain protecting groups were simultaneously removed by treatment with trifluoroacetic acid (TFA) at the final stage of synthesis. Problems were encountered with the incomplete removal of the *t*Bu protecting group. In order to improve the deprotection efficiency, various scavenger cocktails, such as TFA/H₂O/TIPSi, TFA/TIPSi¹⁰⁶, TFA/H₂O/*m*-cresol¹⁰⁶, TFA/H₂O¹¹⁷,

TFA/phenol/thioanisole/EDT/H₂O⁶⁵ and TFA/TIPSi/EDT/H₂O proved effective. However, the addition of a sulfur compound as a scavenger in the TFA system results in incomplete removal of the *t*Bu protecting group, while scavengers such as H₂O, thioanisole, *m*-cresol and TIPSi are more effective for the removal of this protecting group.

Based on the results obtained here, we chose 90% TFA in TIPSi (for caerulein 1.2Y⁴ and 3.1Y⁴) or 90% aqueous TFA in TIPSi (for eugenin Y⁴) at room temperature, administered within 1.30 hours, as a final deprotection reagent. After purification of the crude peptide by RP-HPLC, caerulein 1.2Y⁴, 3.1Y⁴ and eugenin Y⁴ were obtained. The yields from the protected peptide-resin were poor (8% for caerulein 1.2Y⁴ and 14.3% for caerulein 3.1Y⁴) but these figures are not unreasonable for a total solid-phase synthesis of a short peptide, 10-15 residues in length. The purity of caerulein 3.1Y⁴ and eugenin Y⁴ were confirmed by HPLC and mass analyses. Unfortunately, after several attempts to purify caerulein 1.2Y⁴, the peptide was still impure.

6.4.2 Synthesis of caerulein analogues and eugenin peptides

Various peptides containing tyrosine sulfate [Tyr(SO₃H)] as known caerulein analogues¹²⁰ have been discovered in Australian tree frogs of the *Litoria* species as shown in *Table 6.1*. The roles of these peptides are still unknown. To clarify the significance and biological activity of these peptides, synthetic peptides could serve as useful models. In this regard, much interest has been focused on establishment of a facile synthetic method for Tyr(SO₃H)-containing peptides, overcoming the acid-lability of Tyr(SO₃H). As tyrosine sulfate derivatives are relatively stable in TFA, the preparation of Tyr(SO₃H)-containing peptides is achieved using the Fmoc-SPPS strategy.

For the synthesis of caerulein analogues and eugenin, the C-terminus Fmoc-amide linker was linked to a Pam resin. The resulting amide-resin was treated with 50% piperidine/DMF to remove the N^α-Fmoc group; then each Fmoc-amino acid including Fmoc-Tyr(SO₃Na)-OH was introduced to the peptide chain by the HBTU/DIEA-mediated coupling protocol¹²¹.

The cleavage conditions selected to remove caerulein analogues and eugenin from the resin were a compromise between achieving adequate removal of the *t*Bu side chain protecting groups while preventing undesirable desulfation. The addition of a soft base such as thioanisole or EDT in TFA significantly promotes the desulfation of the Tyr(SO₃H) residue¹⁰⁶. In contrast, scavengers such as H₂O, *m*-cresol and TIPSi have little effect on the decomposition of Tyr(SO₃H)¹⁰⁶. Thus, we tried 90% aqueous TFA/TIPSi, 90% TFA/TIPSi, 90% TFA/*m*-cresol and 90% aqueous TFA in scavenger cocktail trials. In addition, the effect of temperature and time have been examined to compare the desulfation rate from Tyr(SO₃H) with the deprotection rates of the side-chain protecting groups.

Caerulein analogues and eugenin were treated with the four scavenger cocktails mentioned above, at specific temperatures (4°C, 25°C) for a 3-hour period and the degree of desulfation or deprotection was determined by mass spectrometry and HPLC. From these experiments, it found that the deprotection rates of the side-chain protecting group in TFA solution at 25°C for a 3 hour period was satisfactory for completing the removal of the protecting groups. On the other hand, the desulfation rate of Tyr(SO₃H) was dramatically increased by even brief treatment with TFA solution at 25°C. In contrast, the desulfation rate was not affected significantly in TFA solution at 4°C during a period of 3 hours and

the deprotection rate of side-chain protecting groups was also acceptable under such conditions. Thus, by using TFA solution at low temperature, it seems possible to remove a large number of the protecting groups with minimal degradation to the Tyr(SO₃H) residue. TIPSi can also be used in the deprotection system without imparting damage to the Tyr(SO₃H) residue. However, the addition of *m*-cresol and/or water promotes the hydrolysis of Tyr(SO₃H) to Tyr.

Based on the results obtained here, we chose 90% TFA in TIPSi (4°C, 2.5 hours) as the deprotection reagent for the synthesis of caerulein analogues and eugenin peptides. Purification of the crude caerulein analogues and eugenin on RP-HPLC afforded high purity products. The purity of the obtained peptides and the existence of the sulfate ester on Tyr were ascertained by analytical HPLC and TOF-MS. Caerulein analogues and eugenin exhibit pseudo-molecular ions, (MH)⁺ and (M-H)⁻, in the TOF-MS, consistent with the molecular weights calculated for the sulfated peptides as shown in *Table 6.2*.

Table 6.2: Molecular weight and yield obtained of caerulein analogues and eugenin peptides

Name	<i>m/z</i> of (M-H) ⁻ calculated (Da)	<i>m/z</i> of (M-H) ⁻ obtained (Da)	Yield from protected peptide-resin (%)
Caerulein 1.2	1366.4	1366.3	11.4
Caerulein 2.1	1372.4	1372.4	24.0
Caerulein 2.2	1388.4	1388.4	17.4
Caerulein 3.1	1407.5	1407.3	13.3
Caerulein 3.2	1423.5	1423.3	24.0
Caerulein 4.1	1388.4	1388.6	10.3
Caerulein 4.2	1404.4	1404.7	17.4
Eugenin	1371.5	1371.6	14.3

6.5 Conclusions

A facile and efficient strategy for the Fmoc-SPPS of a Tyr(SO₃H)-containing peptide was established and successfully applied to the syntheses of various caerulein analogues and eugenin. The synthetic strategy is follows: i) a sulfated peptide chain is directly constructed on Pam-resin via Fmoc-SPPS; ii) the protected peptide-resin is treated with 90% TFA/TIPSi at 4°C for the appropriate period of time to enable cleavage and deprotection.

6.6 EXPERIMENTAL

6.6.1 General procedure

Material

Manual syntheses were performed with Fmoc-amino acids (Ramage Amide-Resin, tricyclic linker) purchased from BACHEM and Fmoc-L-amino acids were purchased from BACHEM, Nova Biochem and Auspep. Diisopropylcarbodiimide (DIC) was from Aldrich and 2-(1*H*-benzotriazol-1-yl)-1,1,3,3-tetramethyl-uroniumhexafluorophosphate (HBTU) was obtained from Richelieu Biotechnologies (Quebec, Canada). *N,N*-diisopropylethylamine (DIEA), *N,N*-dimethylformamide (DMF), dichloromethane (DCM), piperidine, trifluoroacetic acid and Fmoc-sulfotyrosine (all peptide synthesis grade) were purchased from Auspep (Melbourne, Australia). Acetone (HPLC grade) was obtained from Water Millipore (Milford, MA). High purity water was generated by a Milli-Q™ purification system (Millipore, Bedford, MA).

Chain Assembly

Tyrosine and tyrosine sulfate containing peptides were synthesised by manual solid-phase peptide synthesis using Fmoc-chemistry. The following amino acid side-chain protecting groups were used: Asp(O-*t*Bu), Gln(Trt), His(Trt), Ser(*t*Bu), Thr(*t*Bu) and Trp(Boc). Ala, Gly, Met, Phe, Pro, and Val were used without side-chain protecting groups. pGlu was used without requirement of the α -amino acid and side-chain protection during synthesis. Tyr(SO₃Na) was used for the synthesis of Tyr(SO₃)-containing peptides, while Tyr(*t*Bu) was used for the syntheses of the unsulfated tyrosine containing peptides.

Manual protocol

Syntheses were carried out on a 0.2 mmol scale. The Boc-Phe-OCH₂-Pam resin (substitution value[§] 0.74 mmol/g, 270.3 mg) was swollen in DMF for at least 40 mins and then drained. The N^α-Boc group was removed by treatment with neat TFA (2 x 1 min)** then the resin was flow washed with DMF for 1 min prior to neutralisation with DIEA in DMF (10%, 2 x 1 min)^{††} followed by flow wash with DMF for 1 min. Fmoc-amide linker (0.4 mmol) was dissolved in DCM (1 mL) and DMF (400 μ L). DIC (32 μ L) was added to activate the Fmoc-amide linker, the resulting mixture was left at room temperature for 1 hr.

[§] Substitution value is the number of mmols of the amino acid per gram of the resin.

** The N^α-Boc group was removed by addition of neat TFA (10 mL), shaking for 1 min and then the TFA solution was drained. This process was then repeated.

^{††} The amine salt was neutralised by addition of DIEA in DMF (10%, 10 mL), shaken for 1 min and then drained. This process was then repeated.

The activated linker was then added to the resin, and the mixture shaken for at least 2 hrs at 25°C. Repetitive Fmoc removal was conducted using piperidine in DMF (50%, 2 x 1 min)^{‡‡} and peptide couplings were performed using 4 equivalents of the Fmoc-amino acid derivative. Fmoc-amino acid derivatives were activated in HBTU (0.5 M, 1.6 mL) and DIEA (2.5 mmol, 140 µL) prior to use.

Samples (2 mg) of peptide-resin were removed after each coupling step for determination of residual free α -amino groups by the quantitative Ninhydrin test⁵⁷, except for couplings to proline where a coupling efficiency of >99.5% was achieved as shown by the isatin test^{58,119}. Good couplings (>99.5%) were attained after 10 mins; poor couplings (<99.5%) required double coupling.

After completion of the chain assembly, the peptide-resin was flow washed with DMF (1 min), DCM (1 min) and dried under nitrogen. The manipulations in each elongation cycle of the peptide chain consisted of (i) deprotection of the Fmoc group with piperidine in DMF (50%, 2 x 1 min), (ii) washing with DMF (1 min), (iii) coupling of each activated amino acid derivative (4 eq) for 10 mins and (iv) washing with DMF (1 min). All operations were performed manually in a 20 mL glass reaction vessel with a teflon-lined screw cap. The peptide-resin was agitated with an automatic shaker during the deprotection and coupling steps.

^{‡‡} The Fmoc group was removed using piperidine in DMF (50%, 10 mL), shaken for 1 min and then drained. This process was then repeated.

Deprotection and cleaving trial

Sulfated and desulfated peptides were cleaved from the resin and the side chain protecting groups were removed by treatment using the following trials.

- (i) TFA/H₂O/TIPSi (90:7.5:2.5)
- (ii) TFA/TIPSi (90:10)¹⁰⁶
- (iii) TFA/H₂O/*m*-cresol (90:10:50 eq)¹⁰⁶
- (iv) TFA/H₂O (90:10)¹¹⁷

Reactions were carried out at either 4°C or 25°C. Excess trifluoroacetic acid was removed by blowing with nitrogen, and the crude peptide precipitate was washed with diethyl ether (10 mL), dissolved in a mixture of acetonitrile and water (1:1, 20 mL, containing 0.1% trifluoroacetic acid), and lyophilised.

6.6.2 HPLC analysis

The peptides were purified by preparative HPLC using a Vydac C18 column (10 µm, 2.2 x 25 cm). Chromatographic separations were achieved using linear gradients of buffer B in A at a flow of 8 mL/min with either 0 to 45% B over 60 mins or 25 to 45% B over 40 mins: solvent A, 100% water, 0.05% trifluoroacetic acid; solvent B, 90% aqueous acetonitrile, 0.043% trifluoroacetic acid. The eluant was monitored at 230 nm.

After purification, each fraction was checked for purity using analytical reverse phase HPLC on a Vydac C18 column (5 µm, 0.46 x 25 cm) using a linear gradients of 0 to 45% B over 45 mins. Fractions with the same retention time were combined. Absorbance was monitored at 214 nm.

6.6.3 Mass spectrometry (MS)

Mass spectra were acquired on a TOF Mariner single quadrupole mass spectrometer (PE Biosystem, USA) equipped with an ion spray atmospheric pressure ionisation source. Samples (20 μL) were injected into a moving solvent (30 $\mu\text{L}/\text{min}$; aqueous acetonitrile (50%) containing 0.05% trifluoroacetic acid) coupled directly to the ionisation source via a fused silica capillary interface (50 μm x 50 cm). Sample droplets were analysed in both the positive and negative ionisation modes. The ions enter the analyser through an interface plate and subsequently through an orifice (100-120 μm diameter) at a declustering potential of 60 V in the positive ion mode, and at -40 V in the negative ion mode. Spectra were acquired over the mass range 420-2000 Da in 0.2 Da steps with a total scan time of 3 seconds.

6.7 Solid-phase Synthesis of pEQDYTGWFDF-NH₂ (caerulein 1.2Y⁴)

Solid-phase syntheses were carried out manually on a Boc-Phe-OCH₂-Pam-resin (270.3 mg, 0.2 mmol), which was treated with TFA (2 x 1 min), flow washed with DMF (1 min) and then neutralised with DIEA in DMF (10%, 2 x 1 min). After removal of the Boc group, activated Fmoc-amide linker (226.6 mg, 0.42 mmol) was coupled to the resin overnight. The peptide chain was elongated in a similar manner. All couplings were monitored using the ninhydrin test⁵⁷. The following Fmoc-amino acid derivatives were successively introduced: Phe, Asp(O-*t*Bu), Phe, Trp(Boc), Gly, Thr(*t*Bu), Tyr(*t*Bu), Asp(O-*t*Bu) and Gln(Trt). Finally, amino acid, pGlu was the last introduced into the peptide chain. Double coupling was used to achieve efficient coupling with residues 2 and 10. After final

incorporation of pGlu, the peptide-resin was washed with DMF (1 min), DCM (1 min) and dried under nitrogen respectively. Yield of peptide-resin 599 mg.

The peptide-resin (350 mg) was treated with TFA (50 mL) in triisopropylsilane (5 mL) (9:1, v/v) at 25°C for 1.5 hrs. The resin was removed by filtration and washed with TFA (5 mL). The TFA solution was removed *in vacuo* and the crude peptide precipitate was washed with diethyl ether (10 mL). The precipitate was dissolved with aqueous acetonitrile (50%, 20 mL, containing 0.1% TFA) and lyophilised to give a white powder (37 mg). Purification was attempted several times by preparative HPLC, using an elution gradient of 0 to 45% B over 60 mins with flow rate 8 mL/min but was not successful.

6.8 Solid-phase Synthesis of pEQDYGTGWMDF-NH₂ (caerulein 3.1Y⁴)

The synthesis was carried out using Boc-Phe-OCH₂-Pam-resin (270.3 mg, 0.2 mmol). The peptide chain was synthesised in a similar manner as that outlined above. The following Fmoc-amino acid derivatives were introduced: Phe, Asp(O-*t*Bu), Met, Trp(Boc), Gly, Thr(*t*Bu), Gly, Tyr(*t*Bu), Asp(O-*t*Bu) and Gln(Trt). The amino acid, pGlu was the last introduced into the peptide chain. The presence of free α -amino groups during cycles was monitored using the ninhydrin test⁵⁷. Double coupling was required for residue 11. After chain elongation, the resin was washed with DMF (1 min), DCM (1 min) and then dried under nitrogen, (yield of peptide-resin, 588 mg).

The peptide-resin (290 mg) was cleaved from the resin and the side chain protecting groups were removed by treatment with TFA (52.2 mL) in triisopropylsilane (5.8 mL) (9:1, v/v) at 25°C for 1.5 hr. The resin was filtered and washed with TFA (5 mL). Removal of

the solvent *in vacuo* gave the crude peptide which was washed with diethyl ether (10 mL), dissolved in aqueous acetonitrile (50%, 20 mL, containing 0.1% TFA) and lyophilised to afford a fluffy powder (40 mg). The peptide mixture (25 mg) was separated by preparative HPLC [eluting at 8 mL/min with 0 to 45% B, 60 mins]. This procedure was performed twice. The fractions corresponding to the peak at $t_r = 35.87$ min [as monitored by analytical HPLC, gradient system = 0 to 45% B over 45 mins] were combined and subjected to lyophilization to give a white fluffy powder (2 mg, 8% yield). TOF mass spectrometry gave $(MH^+) = 1329.8$ Da; calculated (average mass) for caerulein 3.1Y⁴, $(MH^+) = 1329.4$ Da.

6.9 Solid-phase Synthesis of pEQDYVFMHPF-NH₂ (eugenin Y⁴)

This synthesis was carried out on a 0.2 mmol scale of Boc-Phe-OCH₂-Pam-resin. The Boc group was removed by treatment with neat TFA (2 x 1 min) followed by a 1 min flow wash with DMF and then neutralised with DIEA in DMF (10%, 2 x 1 min). Activated Fmoc-amide-linker (0.42 mmol) was coupled to the resin after neutralisation of the peptide-resin. The Fmoc-amino acid derivatives were introduced to the peptide chain as follows: Phe, Pro, His(Trt), Met, Phe, Val, Tyr(*t*Bu), Asp(O-*t*Bu) and Gln(Trt). The amino acid, pGlu was the last introduced into the peptide chain. The peptide chain was elongated as outlined above. Couplings were monitored by the ninhydrin test⁵⁷, except for proline, which was determined by the isatin test^{58,119}. Double coupling was required for each of the residues 1, 2, 7, 8 and 10.

After drying, the peptide-resin (180 mg) was treated with aqueous TFA (90%, 18 mL) in triisopropylsilane (2.5%, 0.5 mL) at 25°C for 1.5 hrs. The resin was filtrated and washed

with TFA (5 mL). The TFA solution was collected and concentrated *in vacuo*. The precipitate was washed with diethyl ether (10 mL), dissolved in aqueous acetonitrile (50%, 20 mL, containing 0.1% TFA) and lyophilised to give a white fluffy powder (28 mg). This sample (28 mg) was subjected to reverse phase preparative HPLC [eluting at 8 mL/min with 0 to 45% B over a 60 min period]. The fractions corresponding to the peak at $t_r = 36.33$ min [as monitored by analytical HPLC, gradient system = 0 to 45% B, 45 mins] were combined and lyophilised to afford a white fluffy powder (4 mg, 14.3% yield). TOF mass spectrometry gave $(MH^+) = 1294.7$ Da; calculated (average mass) for eugenin Y⁴, $(MH^+) = 1294.5$ Da.

6.10 Solid-phase Synthesis of pEQDY(SO₃)TGWDFD-NH₂ (caerulein 1.2)

This synthesis was carried out on a 0.2 mmol scale using Boc-Phe-OCH₂-Pam-resin as outlined above. After the Fmoc-amide linker was coupled, the following Fmoc-amino acid derivatives were elongated to the peptide chain: Phe, Asp(O-*t*Bu), Phe, Trp(Boc), Gly, Thr(*t*Bu), Tyr(SO₃Na), Asp(O-*t*Bu), Gln(Trt), followed by the last amino acid, pGlu. Free α -amino groups were determined by the ninhydrin method⁵⁷. Double coupling was required for each of the residues 1, 2, 3, 4, 5 and 10. After the last coupling step, the peptide-resin was washed with DMF (1 min), DCM (1 min) and dried under nitrogen to give 510 mg of material.

The peptide-resin (300 mg) was treated with TFA (63 mL) in triisopropylsilane (7 mL) (9:1, v/v) at 4°C for 2 hrs. The resin was removed by filtration and the TFA solution was concentrated by blowing with nitrogen. The crude peptide mixture was washed with diethyl ether (10 mL), dissolved in aqueous acetonitrile (50%, 20 mL, containing 0.1%

TFA) and lyophilised to give a white powder (40 mg). Crude peptide (35 mg) was purified by preparative HPLC [eluting with gradient 25 to 45% B over 40mins]. The fractions of retention time 38.45 mins [as monitored by analytical HPLC, gradient system = 0 to 45 % B over 45 mins] were combined and lyophilised to give a white fluffy powder (4 mg, 11.4% yield). TOF mass spectrometry gave $(M-H)^- = 1366.3$ Da; calculated (average mass) for caerulein 1,2, $(M-H)^- = 1366.4$ Da.

6.11 Solid-phase Synthesis of pEQDY(SO₃)TGAHMDF-NH₂ (caerulein 2.1)

This peptide was synthesised by using Boc-Phe-OCH₂-Pam-resin (0.25 mmol scale). The Boc group was removed using neat TFA before coupling the activated Fmoc-amide linker. The peptide chain was elongated as outlined above. The following Fmoc-amino acid derivatives were introduced: Phe, Asp(O-*t*Bu), Met, His(Trt), Ala, Gly, Thr(*t*Bu), Tyr(SO₃Ba), Asp(O-*t*Bu) and Gln(Trt). The amino acid, pGlu was the last introduced into the peptide chain. All couplings were determined by the ninhydrin test⁵⁷. Double coupling was required for each of the residues 1 and 2. After chain elongation, the resin was washed with DMF, DCM and then dried under nitrogen to give 863 mg of peptide-resin.

The peptide-resin (300 mg) was treated with aqueous TFA (54 mL) in triisopropylsilane (6 mL) (9:1, v/v) at 4°C for 2.5 hrs. The resin was removed by filtration and the TFA solution was concentrated by blowing with nitrogen. The precipitate was washed with diethyl ether (5 mL, twice), dissolved in aqueous acetonitrile (50%, 20 mL, containing 0.1% TFA) and lyophilised to give a white powder (48 mg). Crude peptide (25 mg) was subjected to reverse phase preparative HPLC [eluting with gradient 25 to 45% B over 40 mins]. The

fractions of retention time 26.5 mins [as monitored by analytical HPLC, gradient system = 0 to 45% B over 45 mins] were combined and lyophilised to give a white fluffy powder (6 mg, 24.0% yield). TOF mass spectrometry gave $(M-H)^- = 1372.4$ Da; calculated (average mass) for caerulein 2.1, $(M-H)^- = 1372.4$ Da.

6.12 Solid-phase Synthesis of pEQDY(SO₃)TGAHFDF-NH₂ (caerulein 2.2)

This synthesis was performed on a 0.25 mmol scale of a Boc-Phe-OCH₂-Pam-resin. The Boc group was removed with neat TFA and neutralised with DIEA in DMF as mentioned above. After the activated Fmoc-amide linker was coupled to the resin, the following Fmoc-amino acid derivatives were introduced to the peptide chain: Phe, Asp(O-*t*Bu), Phe, His(Trt), Ala, Gly, Thr(*t*Bu), Tyr(SO₃Ba), Asp(O-*t*Bu) and Gln (Trt). The amino acid, pGlu was the last introduced into the peptide chain. The peptide chain was elongated as outlined above. Double coupling was required for residue 2. After chain elongation, the peptide-resin was flow washed with DMF (1 min), DCM (1 min) and dried under nitrogen to give 859 mg of material.

The peptide-resin (360 mg) was treated with TFA (64.8 mL) in triisopropylsilane (7.2 mL) (9:1, v/v) at 4°C for 2.5 hrs. The resin was filtered and washed with TFA (5 mL). The TFA solution was collected and then concentrated by blowing with nitrogen. The crude peptide mixture was worked up as mentioned above and then lyophilised to give a white powder (43 mg). Crude peptide (23 mg) was purified by preparative HPLC [eluting with gradient 25 to 45% B over 40 mins]. The fractions of retention time 29.8 mins as monitored by analytical HPLC (gradient system = 0 to 45% B over 45 mins) were combined and

lyophilised to give a white fluffy powder (4 mg, 17.4% yield). TOF mass spectrometry gave $(M-H)^- = 1388.4$ Da; calculated (average mass) for caerulein 2.2, $(M-H)^- = 1388.4$ Da.

6.13 Solid-phase Synthesis of pEQDY(SO₃)GTGWMDf-NH₂ (caerulein 3.1)

This synthesis was performed on a Boc-Phe-OCH₂-Pam-resin (0.2 mmol scale) with Boc group removed prior to use. The activated Fmoc-amide linker was coupled to the resin for 3 hrs. The peptide chain was elongated as outlined above. The following Fmoc-amino acid derivatives were successively introduced: Phe, Asp(O-*t*Bu), Met, Trp(Boc), Gly, Thr(*t*Bu), Gly, Tyr(SO₃Na), Asp(O-*t*Bu), Gln(Trt), followed by the last amino acid, pGlu. All couplings were detected using the ninhydrin test⁵⁷. Double coupling was required for the introduction of each of the residues 2, 3, 4, 9 and 11. The peptide-resin was washed with DMF (1 min), DCM (1 min) and dried under nitrogen; yield 577 mg.

The peptide-resin (280 mg) was treated with a mixture of TFA (50.4 mL) in triisopropylsilane (5.6 mL) (9:1, v/v) at 4°C for 2.5 hrs. The resin was removed by filtration and the TFA solution was concentrated under nitrogen. The crude peptide was washed with diethyl ether (10 mL), dissolved in aqueous acetonitrile (50%, 20 mL, containing 0.1% TFA) and lyophilised to give a fluffy powder (30 mg). The crude peptide was purified by preparative HPLC with a linear gradient from 25 to 45% B over a 40 min period. The fractions of retention time 34.9 mins [as monitored by analytical HPLC, gradient system = 0 to 45% B over 45 mins] were combined. The solvent was removed by lyophilization to afford a white fluffy powder (4 mg, 13.3% yield). TOF mass spectrometry

gave $(M-H)^- = 1407.3$ Da; calculated (average mass) for caerulein 3.1, $(M-H)^- = 1407.5$ Da.

6.14 Solid-phase Synthesis of pEQDY(SO₃)GTGWDFD-NH₂ (caerulein 3.2)

This peptide was synthesised on Boc-Phe-OCH₂-Pam-resin (0.25 mmol scale) with the Boc group removed before adding the activated Fmoc-amide linker as outlined above. The Fmoc-amino acids were elongated to the peptide chain as follows: Phe, Asp(O-*t*Bu), Phe, Trp(Boc), Gly, Thr(*t*Bu), Gly, Tyr(SO₃Ba), Asp(O-*t*Bu) and Gln(Trt). The amino acid pGlu was the last introduced to the peptide chain. Free α -amino groups were determined by the ninhydrin test⁵⁷. Double coupling was required for residue 2. After completion of the chain assembly, the peptide-resin was washed with DMF (1 min), DCM (1 min) and dried under nitrogen to give 823 mg of peptide-resin.

The peptide-resin (358 mg) was treated with neat TFA (64.8 mL) in triisopropylsilane (7.2 mL) (9:1, v/v) at 4°C for 2.5 hrs. The resin was removed by filtration and the TFA solution was concentrated by blowing with nitrogen. The crude peptide was washed with diethyl ether (5 mL, twice), dissolved in aqueous acetonitrile (50%, 20 mL, containing 0.1% TFA) and lyophilised to afford a white powder (48 mg). Crude peptide (25 mg) was subjected to preparative HPLC [eluting at 8 mL/min with 25 to 45% B over 40 mins]. The fractions of retention time 37.7 mins [as monitored by analytical HPLC, gradient system = 0 to 45% B over 45 mins] were combined and lyophilised to give a white fluffy powder (6 mg, 24% yield). TOF mass spectrometry gave $(M-H)^- = 1423.3$ Da; calculated (average mass) for caerulein 3.2, $(M-H)^- = 1423.5$ Da.

6.15 Solid-phase Synthesis of pEQDY(SO₃)TGSHMDF-NH₂ (caerulein 4.1)

This synthesis was carried out on a Boc-Phe-OCH₂-Pam-resin (0.25 mmol scale). The Boc group was removed and neutralised as mentioned above prior to use. Activated Fmoc-amide-linker (0.53 mmol) was coupled to the resin overnight and the following Fmoc-amino acid derivatives were then respectively introduced to the peptide chain: Phe, Asp(O-*t*Bu), Met, His(Trt), Ser(*t*Bu), Gly, Thr(*t*Bu), Tyr(SO₃Ba), Asp(O-*t*Bu) and Gln(Trt). The amino acid pGlu was the last introduced to the peptide chain. The peptide chain was elongated as outlined above. All couplings were detected by the ninhydrin test⁵⁷. Double coupling was required for residue 2. After chain assembly, the peptide-resin was flow washed with DMF (1 min), DCM (1 min) and dried under nitrogen to give 879 mg of material.

The peptide-resin (430 mg) was treated with TFA (77.4 mL) in triisopropylsilane (8.6 mL) (9:1, v/v) at 4°C for 2.5 hrs. The resin was removed by filtration and the TFA solution was concentrated by blowing with nitrogen. The precipitate was washed with diethyl ether (5 mL, twice), dissolved in aqueous acetonitrile (50%, 20 mL, containing 0.1% TFA) and then lyophilised to give a white powder (62 mg). Crude peptide (29 mg) was purified by preparative HPLC [eluting with gradient 25 to 45% B over 40 mins]. The fractions of retention time 25.9 mins [as monitored by analytical HPLC, gradient system = 0 to 45% B over 45 mins] were combined and lyophilised to afford a white fluffy powder (3 mg, 10.3% yield). TOF mass spectrometry gave (M-H)⁻ = 1388.6 Da; calculated (average mass) for caerulein 4.1, (M-H)⁻ = 1388.4 Da.

6.16 Solid-phase Synthesis of pEQDY(SO₃)TGSHFDF-NH₂ (caerulein 4.2)

This peptide was synthesised using Boc-Phe-OCH₂-Pam-resin (0.25 mmol scale). After the Boc group was removed and neutralised as mentioned above, an activated Fmoc-amide linker (0.53 mmol) was coupled to the resin for a period of 2.15 hours. The peptide chain was elongated in a similar manner. All couplings were monitored using the ninhydrin test⁵⁷. The following Fmoc-amino acid derivatives were successively introduced: Phe, Asp(O-*t*Bu), Phe, His(Trt), Ser(*t*Bu), Gly, Thr(*t*Bu), Tyr(SO₃Ba), Asp(O-*t*Bu) and Gln(Trt). pGlu was the last amino acid introduced to the peptide chain. After chain assembly, the peptide-resin was washed with DMF (1 min), DCM (1 min) and dried under nitrogen; yield 883 mg.

The peptide-resin (400 mg) was treated with a mixture of TFA (72 mL) in triisopropylsilane (8 mL) (9:1, v/v) at 4°C for 2.50 hours. The resin was removed by filtration and the TFA solution was concentrated under nitrogen. The crude peptide was washed with diethyl ether (10 mL), dissolved in aqueous acetonitrile (50%, 20 mL, containing 0.1% TFA) and lyophilised to give a white powder (58 mg). The crude peptide (23 mg) was subjected to preparative HPLC [eluting with a linear gradient from 25 to 45% B over 40 mins]. Fractions at retention time 28.5 mins were combined (gradient system = 0 to 45% B over 45 mins) and lyophilised to give a white fluffy powder (4 mg, 17.4% yield). TOF mass spectrometry gave (M-H)⁻ = 1404.7 Da; calculated (average mass) for caerulein 4.2, (M-H)⁻ = 1404.4 Da.

6.17 Solid-phase Synthesis of pEQDY(SO₃)VFMHPF-NH₂ (eugenin)

This peptide was synthesised on Boc-Phe-OCH₂-Pam-resin (0.25 mmol scale). The N^α-Boc was removed with neat TFA (2 x 1 min) before adding the activated Fmoc-amide linker. The peptide chain was elongated as outlined above. The Fmoc-amino acid derivatives were respectively introduced as follows: Phe, Pro, His(Trt), Met, Phe, Val, Tyr(SO₃Na), Asp(O-*t*Bu), Gln(Trt), followed by the last amino acid, pGlu. Couplings were checked for a free-amino group using the ninhydrin test⁵⁷, except for proline, which was monitored using the isatin test^{58,119}. Double coupling was required for each of the residues 1 and 2. The peptide-resin was dried under nitrogen after flow wash with DMF (1 min) and DCM (1 min).

The peptide-resin (337 mg) was treated with TFA (61.2 mL) in triisopropylsilane (6.8 mL) (9:1, v/v) at 4°C for 2.5 hrs. The resin was removed and the TFA solution was concentrated under nitrogen. The crude peptide was washed with diethyl ether (10 mL), dissolved in aqueous acetonitrile (50%, 20 mL, containing 0.1% TFA) and lyophilised to give a white powder (28 mg). This sample was subjected to preparative HPLC, [eluting with gradient 25 to 45% B over 40 mins]. The fractions of retention time of 35.89 mins [as monitored by analytical HPLC, gradient system = 0 to 45% B over 45 mins] were combined and lyophilised to give a white fluffy powder (4 mg, 14.3% yield). TOF mass spectrometry gave (M-H)⁻ = 1371.6 Da; calculated (average mass) for eugenin, (M-H)⁻ = 1371.5 Da.

6.18 Abbreviations

APS	=	adenosine 5'-phosphosulfate
BOC	=	tert-butyloxycarbonyl
Bzl	=	benzyl
2ClBz	=	dichlorobenzyl
cm	=	centimeter
DCM	=	dichloromethane
DIC	=	diisopropylcarbodiimide
DIEA	=	N,N-diisopropylethylamine
DMF	=	dimethylformamide
DNP	=	dinitrophenyl
EDT	=	1,2-ethanedithiol
Fmoc	=	9-fluorenylmethoxycarbonyl
HF	=	hydrogen fluoride
HPLC	=	high performance liquid chromatography
Eq	=	equivalent
HBTU	=	2-(1H-benzotriazol-1-yl)-1,1,3,3-tetramethyl-uroniumhexafluorophosphate
^m Mg	=	milligram
^m Min	=	minute
^m ML	=	milliliter
Mmol	=	millimol
Mob	=	methylbenzyl
ⁿ Nm	=	nanometer

PAPS	=	3'-phosphoadenosine 5'-phosphosulfate
PEG	=	polyethylene glycol
Pmc	=	2,2,5,7,8-pentamethylcroman-6-sulfonyl
SPPS	=	solid phase peptide synthesis
t-Bu	=	tertiary-butyl
TFA	=	trifluoroacetic acid
TiPSi	=	triisopropylsilane
TOF	=	time of flight mass spectrometer
Tos	=	toluenesulfonyl
TPST	=	tyrosylprotein sulfotransferase
Trt	=	triphenylmethyl
uL	=	microliter
um	=	micrometer

6.19 References

- 1) Curtius, T. *J. Pract. Chem.* **1881**, 24, 239.
- 2) Fischer, E.; Forneau, E. *Ber. Dtsch. Chem. Ges.* **1932**, 65, 1932.
- 3) Bergmann, M.; Zervas, L. *Ber. Dtsch. Chem. Ges.* **1932**, 65, 1192.
- 4) Merrifield, B. *Methods in Enzymology*; Fields, G. B., Ed.; Academic Press: New York, 1997; Vol. 289, p 3.
- 5) Wieland, T.; Bernhard, H. *Liebigs. Ann. Chem.* **1951**, 572, 190.
- 6) Wieland, T.; Schafer, W.; Bokelmann, E. *Liebigs. Ann. Chem.* **1951**, 573, 99.
- 7) Schwyzer, R.; Feurer, M.; Iselin, B. *Helv. Chim. Acta* **1955**, 38, 83.
- 8) Bodanszky, M. *Nature* **1955**, 175, 685.
- 9) Kovacs, J.; Kisfaludy, L.; Ceprini, M. *Q. J. Am. Chem. Soc.* **1967**, 89, 183.
- 10) Sheehan, J. C.; Hess, G. P. *J. Am. Chem. Soc.* **1955**, 77, 1067.
- 11) Carpino, L. A. *J. Am. Chem. Soc.* **1957**, 79, 4427.
- 12) McKay, F. C.; Albertson, N. F. *J. Am. Chem. Soc.* **1957**, 79, 4686.
- 13) Anderson, G. W.; McGregor, A. C. *J. Am. Chem. Soc.* **1957**, 79, 6180.
- 14) Zervas, L.; Borovas, D.; Gazis, E. *J. Am. Chem. Soc.* **1963**, 85, 3660.
- 15) Sieber, P.; Isalin, B. *Helv. Chim. Acta* **1968**, 51, 622.
- 16) Merrifield, R. B.; Wooley, D. W. *J. Am. Chem. Soc.* **1958**, 80, 6635.
- 17) Merrifield, R. B. *J. Am. Chem. Soc.* **1963**, 85, 2149.
- 18) Kent, S. B. H. *Ann. Rev. Biochem.* **1988**, 57, 957.
- 19) Meldal, M.; Suendsen, I. *J. Chem. Soc. Perkin Trans 1* **1995**, 1591.
- 20) Sarin, V. K.; Kent, S. B. H.; Mitchell, A. R.; Merrifield, R. B. *J. Am. Chem. Soc.* **1984**, 106, 7845.
- 21) Pugh, K. C.; York, E. J.; Stewart, J. M. *Int. J. Pept. Protein Res.* **1992**, 40, 208.

- 22) Meldal, M. *Methods in Enzymology*; Fields, G. B., Ed.; Academic Press: New York, 1997; Vol. 289, p 83.
- 23) Arshady, R. *J. Chromatogr.* **1991**, 586, 199.
- 24) Atherton, E.; Clive, D. L. J.; Sheppard, R. C. *J. Am. Chem. Soc.* **1975**, 97, 6584.
- 25) Kanda, P.; Kennedy, R. C.; Sparrow, J. T. *Int. J. Pept. Protein Res.* **1991**, 38, 385.
- 26) Rapp, W.; Zhang, L.; Habish, R.; Bayer, E. *Peptides 1988, Proceedings of the 20th European Peptide Symposium*; Jung, G. and Bayer, E., Ed.; De Gruyter: Berlin, 1989, p 199.
- 27) Ho, D. D.; Neumann, A. V.; Perelson, A. S.; Chen, W.; Leonard, J. M.; Markowitz, M. *Nature* **1995**, 373, 123.
- 28) Meldal, M. *Tet. Lett.* **1992**, 33, 3077.
- 29) Renil, M.; Meldal, M. *Tet. Lett.* **1995**, 36, 4647.
- 30) Kempe, M.; Barany, G. *J. Am. Chem. Soc.* **1996**, 118, 7083.
- 31) Renil, M.; Meldal, M. *Tet. Lett.* **1996**, 37, 6185.
- 32) Letsinger, R. L.; Kornet, M. J. *J. Am. Chem. Soc.* **1963**, 85, 3045.
- 33) Dryland, A.; Sheppard, R. C. *J. Chem. Soc. Perkin Trans I* **1986**, 125, 1986.
- 34) Small, P. W.; Sherrington, D. C. *Chem. Commun.* **1989**, 1589.
- 35) Berg, R.; Amdal, K.; Pederson, W. B.; Holm, A.; Tam, J. P.; Merrifield, R. B. *J. Am. Chem. Soc.* **1989**, 111, 8024.
- 36) Capperucci, A.; Degl' Innocenti, A.; Funicello, M.; Mauriello, G.; Seafato, P.; Spagnolo, P. *J. Org. Chem.* **1995**, 60, 2254.
- 37) Hodge, P. *Innovation and Perspectives in Solid Phase Synthesis*; Epton, R., Ed.; SPPC: Birmingham, 1990, p 273.
- 38) Deshpande, M. S. *Tet. Lett.* **1994**, 35, 5613.
- 39) Yan, L.; Taylor, C. M.; Goodnow, J.; Kahne, D. *J. Am. Chem. Soc.* **1994**, 116, 6953.

- 40) Rinnova, M.; Lebl, M. *Coll. Czech. Chem. Commun.* **1996**, *61*, 171.
- 41) Paulsen, H.; Schleyer, A.; Mathieux, N.; Meldal, M.; Bock, K. *J. Chem. Soc. Perkin Trans 1* **1997**, 281.
- 42) Kent, S. B. H. *Ann. Rev. Biochem.* **1988**, *57*, 963.
- 43) Sarin, V. K.; Kent, S. B. H.; Merrifield, R. B. *J. Am. Chem. Soc.* **1980**, *102*, 5463.
- 44) Yajima, H.; Takeyama, M.; Kanaki, J.; Nishimura, O.; Fujino, M. *Chem. Pharm. Bull.* **1978**, *26*, 3752.
- 45) Tam, J. P.; Wong, T. W.; Riemen, M. W.; Tjoeng, F. S.; Merrifield, R. B. *Tet. Lett.* **1979**, 4033.
- 46) Barany, G.; Merrifield, R. B. *The Peptides: Analysis, Synthesis, Biology*; Gross, E. and Meienhofer, J., Ed.; Academic Press: New York, 1980; Vol. 3, p 1.
- 47) Previero, A.; Colletti-Previero, M. A.; Cavadore, J. C. *Biochem. Biophys. Acta* **1967**, *147*, 453.
- 48) Nakagawa, Y.; Nishiuchi, Y.; Emura, J.; Sakakibara, S. *Peptide Chemistry 1980, Proc. Jpn. Pept. Symp.*; Okawa, K., Ed.; Protein Res. Found.: Osaka, 1980, p 41.
- 49) Ramage, R.; Green, J. *Tet. Lett.* **1987**, *28*, 2287.
- 50) Sieber, P.; Riniker, B. *Tet. Lett.* **1987**, *28*, 6031.
- 51) White, P. *Peptide Chemistry and Biology*; Smith, J. A. and Rivier, J., Ed.; Escom Science Publishers: Leiden, Netherland, 1992, p 1537.
- 52) McCurdy, S. N. *Pept. Res.* **1989**, *2*, 147.
- 53) Sieber, P.; Riniker, B. *Tet. Lett.* **1991**, *32*, 739.
- 54) Green, J.; Ogunjobi, O. M.; Ramage, R.; Stewart, A. J. S.; McCurdy, S.; Noble, R. *Tet. Lett.* **1988**, *29*, 4341.
- 55) Knorr, R.; Trzeciak, A.; Bannwarth, W.; Gillessen, D. *Tet. Lett.* **1989**, *30*, 1927.

- 56) Kent, S. B. H.; Alewood, D.; Alewood, P.; Baca, M. *Innovation and Perspectives in Solid Phase Synthesis*; Epton, R., Ed.; Intercept Limited: Andover, UK, 1992, p 1.
- 57) Sarin, V. K.; Kent, S. B. H.; Tam, J. P.; Merrifield, R. B. *Anal. Biochem.* **1981**, *117*, 147.
- 58) Kaiser, E.; Bossinger, C. D.; Colecott, R. L.; Olser, D. D. *Anal. Chem. Acta* **1980**, *118*, 149.
- 59) Tam, J. P.; Heath, W. F.; Merrifield, R. B. *J. Am. Chem. Soc.* **1983**, *105*, 6442.
- 60) Stewart, J. M. *Methods in Enzymology*; Fields, G. B., Ed.; Academic Press: New York, 1997; Vol. 289, p 29.
- 61) Brady, S. F.; Hirschmann, R.; Veber, D. F. *J. Org. Chem.* **1977**, *42*, 143.
- 62) Lundt, B. F.; Johansen, N. L.; Volund, A.; Markussen, J. *Int. J. Pept. Protein Res.* **1978**, *12*, 258.
- 63) Tam, J. P. *Macromolecular Sequencing and Synthesis*; Schlesinger, D. H., Ed.; Alan R. Liss: New York, 1988, p 153.
- 64) Sieber, P. *Tet. Lett.* **1987**, *28*, 1637.
- 65) King, D. S.; Fields, C. G.; Fields, G. B. *Int. J. Pept. Protein Res.* **1990**, *36*, 255.
- 66) Riniker, B.; Hartmann, A. *Peptides: Chemistry, Structure, Biology*; Rivier, J. E. and Marshall, G. R., Ed.; ESCOM: Leiden, Netherland, 1990, p 950.
- 67) Ramage, R.; Green, J.; Blake, A. J. *Tetrahedron* **1991**, *47*, 6353.
- 68) Jaeger, E.; Remmer, H. A.; Jung, G.; Metzger, J.; Oberthur, W.; Rucknagel, K. P.; Schafer, W.; Sonnenbichler, J.; Zetl, I. *Biol. Chem. Hoppe-Seyler* **1993**, *374*, 349.
- 69) Riniker, B.; Florsheimer, A.; Fretz, H.; Sieber, P.; Kamber, B. *Tetrahedron* **1993**, *49*, 9307.
- 70) Hofmann, K.; Haas, W.; Smithers, M. J.; Wells, R. D.; Wolman, Y.; Yanalhora, N.; Zanetti, G. *J. Am. Chem. Soc.* **1965**, *87*, 620.

- 71) Norris, K.; Halstrom, J.; Brunfeldt, K. *Acta Chem. Scand.* **1971**, *25*, 945.
- 72) Sieber, P. *Peptide 1968*; Bricas, E., Ed.: North-Holland, Amsterdam, 1968, p 236.
- 73) Sieber, P.; Riniker, B.; Brugger, M.; Kamber, B.; Rittel, W. *Helv. Chim. Acta* **1970**, *53*, 2135.
- 74) Noble, R. L.; Yamashiro, D.; Li, C. H. *J. Am. Chem. Soc.* **1976**, *98*, 2324.
- 75) Lundt, B. F.; Johansen, N. L.; Markussen, J. *Int. J. Pept. Protein* **1979**, *14*, 344.
- 76) Atherton, E.; Cameron, L. R.; Sheppard, R. C. *Tetrahedron* **1988**, *44*, 843.
- 77) Riniker, B.; Kamber, B. *Peptide 1988*; Jung, G. and Bayer, E., Ed.; de Gruyter: Berlin, 1989, p 115.
- 78) Alakhov, Y. B.; Kirushkin, A. A.; Lipkin, V. M.; Milne, G. W. A. *Chem. Commun.* **1970**, 406.
- 79) Fontana, A.; Toniolo, C. *Progress in the Chemistry of Organic Natural Products*; Herz, W., Griseback, H. and Kirby, G. W., Ed.; Springer-Verlag: Berlin, 1976; Vol. 33, p 309.
- 80) Sakakibara, S. *Peptides: Proceedings of the 5th American Peptide Symposium*; Goodman, M. and Meienhofer, J., Ed.; Halsted Press: New York, 1977, p 436.
- 81) Wunsch, E.; Jaeger, E.; Kisfaludy, L.; Low, M. *Angrew. Chem. Int. Ed. Eng.* **1977**, *16*, 317.
- 82) Jaeger, E.; Thamm, P.; Knof, S.; Wunsch, E. *Hoppe-Seyler's Z. Physiol. Chem.* **1978**, *359*, 1629.
- 83) Jaeger, E.; Thamm, P.; Knof, S.; Wunsch, E.; Low, M.; Kisfaludy, L. *Hoppe-Seyler's Z. Physiol. Chem.* **1978**, *359*, 1617.
- 84) Low, M.; Kisfaludy, L.; Jaeger, E.; Thamm, P.; Knof, S.; Wunsch, E. *Hoppe-Seyler's Z. Physiol. Chem.* **1978**, *359*, 1637.
- 85) Low, M.; Kisfaludy, L.; Sohar, P. *Hoppe-Seyler's Z. Physiol. Chem.* **1978**, *359*, 1643.

- 86) Gausepohl, H.; Kraft, M.; Frank, R. W. *Int. J. Pept. Protein Res.* **1989**, *34*, 287.
- 87) Harrison, J. L.; Petrie, G. M.; Noble, R. L.; Beilan, H. S.; McCurdy, S. N.; Culwell, A. R. *Techniques in Protein Chemistry*; Hugli, T. E., Ed.; Academic Press: San Diego, 1989, p 506.
- 88) Sieber, P.; Riniker, B. *Innovation and Perspectives in Solid Phase Synthesis*; Epton, R., Ed.; Solid Phase Conference Coordination: Birmingham, UK, 1990, p 577.
- 89) Johnson, T.; Sheppard, R. C. *Chem. Commun.* **1991**, 1653.
- 90) Wade, J. D.; Fitzgerald, S. P.; McDonald, M. R.; McDougall, J. G.; Tregear, G. W. *Biopolymers* **1986**, *25*, 521.
- 91) Scanlon, D. B.; Eefting, M. A.; Lloyd, C. J.; Burgess, A. W.; Simpson, R. J. *Chem. Commun.* **1987**, 516.
- 92) Yajima, H.; Kanaki, J.; Kitajima, M.; Funakoshi, S. *Chem. Pharm. Bull.* **1980**, *28*, 1214.
- 93) Photaki, I.; Taylor-Papadimitriou, J.; Sakarellos, C.; Mazarakis, P.; Zervas, L. J. *Chem. Soc. C* **1970**, 2683.
- 94) Bullesbach, E. E.; Danho, W.; Helbig, H. J.; Zahn, H. *Peptide 1978*; Siemion, I. Z. and Kupryszewski, G., Ed.; Wroclaw University Press: Wroclaw, 1979, p 643.
- 95) McCurdy, S. N. *Pept. Res.* **1989**, *2*, 147.
- 96) Pearson, D. A.; Blanchette, M.; Baker, M. L.; Guindon, C. A. *Tet. Lett.* **1989**, *30*, 2739.
- 97) Scarso, A.; Brison, J.; Durieux, J. P.; Loffet, A. *Peptides 1980*; Brunfeldt, K., Ed.; Scriptor: Copenhagen, 1981, p 321.
- 98) Ramage, R.; Green, J.; Ogunjobi, O. M. *Tet. Lett.* **1989**, *30*, 2149.
- 99) Ondetti, M. A.; Pluscec, J.; Sabo, E. F.; Sheehan, J. T.; Williams, N. J. *Am. Chem. Soc.* **1970**, *92*, 195.

- 100) Moroder, L.; Wunsch, E. *Natural Product Chemistry*; Rahman, A. U., Ed.; Springer Verlag: Berlin, 1986; Vol. 26, p 255.
- 101) Kurano, Y.; Kimura, T.; Sukakibara, S. *Chem. Commun.* **1987**, 323.
- 102) Fujii, N.; Futaki, S.; Funakoshi, S.; Akaji, K.; Morimoto, H.; Doi, R.; Inour, K.; Kogire, M.; Sumi, S.; Yun, M.; Tobe, T.; Aono, M.; Matsuda, M.; Narusawa, H.; Moriga, M.; Yajima, H. *Chem. Pharm. Bull.* **1988**, 36, 3281.
- 103) Penke, B.; Rivier, J. *J. Org. Chem.* **1987**, 52, 1197.
- 104) Penke, B.; Ngyerges, L. *Peptide. Res.* **1991**, 4, 289.
- 105) Futaki, S.; Taike, T.; Akita, T.; Kitagawa, K. *Tetrahedron* **1992**, 48, 8899.
- 106) Yagami, T.; Shiwa, S.; Futaki, S.; Kitagawa, K. *Chem. Pharm. Bull.* **1993**, 41, 376.
- 107) Kitagawa, K.; Futaki, S.; Yagami, T.; Sumi, S.; Inoue, K. *Int. J. Pept. Protein Res.* **1994**, 43, 190.
- 108) Han, Y.; Bontems, S. L.; Hegyes, P.; Munson, M. C.; Minor, C. A.; Kates, S. A.; Albericio, F.; Barany, G. *J. Org. Chem.* **1996**, 61, 6326.
- 109) Kitagawa, K.; Aida, C.; Fujiwara, H.; Yagami, T.; Futaki, S.; Kogire, M.; Ida, J.; Inoue, K. *J. Org. Chem.* **2001**, 66, 1.
- 110) Penke, B.; Toth, G. K.; Zarandy, M.; Nagy, A.; Kovacs, K. *Peptide 1980, Proc. 16th Eur. Peptide Symp.*; Brunfeldt, K., Ed.; Scriptor: Copenhagen, 1981, p 253.
- 111) Brown, E.; Sheppard, R. C.; Williams, B. J. *J. Chem. Soc. Perkin Trans 1* **1983**, 1161.
- 112) Rink, H. *Tet. Lett.* **1987**, 28, 3787.
- 113) Albericio, F.; Knieb-Cordonier, N.; Biancalana, S.; Gera, L.; Masada, I. R.; Hudson, D.; Barany, G. *J. Org. Chem.* **1990**, 55, 3730.
- 114) Barlos, K.; Gatos, D.; Kallitsis, J.; Papaphotiu, G.; Sotiriu, P.; Wenqing, Y.; Schafer, W. *Tet. Lett.* **1989**, 30, 3943.

- 115) Barlos, K.; Gatos, D.; Kapolos, S.; Papaphotiu, G.; Schafer, W. *Tet. Lett.* **1989**, *30*, 3947.
- 116) Barlos, K.; Chatzi, O.; Kapolos, S.; Poulos, C.; Schafer, W.; Wenqing, Y. *Int. J. Pept. Protein Res.* **1991**, *38*, 555.
- 117) Kitagawa, K.; Aida, C.; Fujiwara, H.; Yagami, T.; Futaki, S. *Tet. Lett.* **1997**, *38*, 599.
- 118) Kitagawa, K.; Yagami, T.; Aida, C.; Fujiwara, H.; Futaki, S.; Kogire, M.; Ida, J.; Inoue, K. *Peptide Science-Present and Future*; Shimonixhi, Y., Ed.; Kluwer Academic: U.K., 1999, p 525.
- 119) Pritchard, C. I.; Auffret, A. D. *Biochem. Soc. Trans.* **1986**, *14*, 1286.
- 120) Wabnitz, P. A.; Bowie, J. H.; Tyler, M. J. *Rapid Commun. Mass Spectrom.* **1999**, *13*, 2498.
- 121) Alewood, P.; Alewood, D.; Miranda, L.; Love, S.; Meuttermans, W.; Wilson, D. *Methods in Enzymology*; Fields, G. B., Ed.; Academic Press: New York, 1997; Vol. 289, p 14.

Chapter Seven

Bioactivity of Eugenin and Caerulein-like Peptides

7.1 Introduction

Tyrosine sulfate [Tyr(SO₃)]-containing peptides have been isolated from a wide variety of natural sources. The sulfate ester formation of Tyr residues in peptides appears to be a widespread post-translational modification event in different tissues and different organisms¹⁻³.

Tyrosine sulfate was first observed over four decades ago in a peptide derived from fibrinogen⁴. Since then, many tyrosine-sulfated peptides have been discovered. Biologically active Tyr(SO₃)-containing peptides are found in a variety of organisms including insects, mammals and amphibians. Some examples are shown in *Table 7.1*.

Table 7.1: Some Tyr(SO₃)-containing peptides found in nature

Peptide	Sequence	Source
Pea-SK	EQFDDY(SO ₃)GHMRF-NH ₂	<i>Periplaneta americana</i> ⁵
Leucosulfakinin I	EQFEDY(SO ₃)GHMRF-NH ₂	<i>Leucophaea maderae</i> ⁶
Leucosulfakinin II	pESDDY(SO ₃)GHMRF-NH ₂	<i>Leucophaea maderae</i> ⁷
Sulfakinin I	FDDY(SO ₃)GHMRF-NH ₂	<i>Calliphora vomitoria</i> ⁸ <i>Lucilia cuprina</i> ⁸ <i>Drosophila melanogaster</i> ⁹ <i>Neobellieria bullata</i> ¹⁰
Gastrin	pEGPWLEEEEEAY(SO ₃)GWMD F-NH ₂	Human gut ¹¹
CCK-8	DY(SO ₃)MGWMDF-NH ₂	Sheep brain ¹²
Cionin	NY(SO ₃)Y(SO ₃)GWMDNF-NH ₂	<i>Ciona intestinalis</i> ¹³
Caerulein	pEQDY(SO ₃)TGWMDF-NH ₂	<i>Litoria caerulea</i> ¹⁴
Phyllocaerulein	pEEY(SO ₃)TGWMDF-NH ₂	<i>Phyllomedusa sauvagei</i> ¹⁵

7.2 Characterisation of Tyrosine Sulfation Sites

7.2.1 Occurrence

Tyrosine sulfate is generated by the enzyme tyrosylprotein sulfotransferase (TPST) in Golgi compartments¹⁶. Like all sulfotransferases, TPST uses 3'-phosphoadenosine 5'-phosphosulfate (PAPS) as a sulfate donor (*Figure 7.1*).

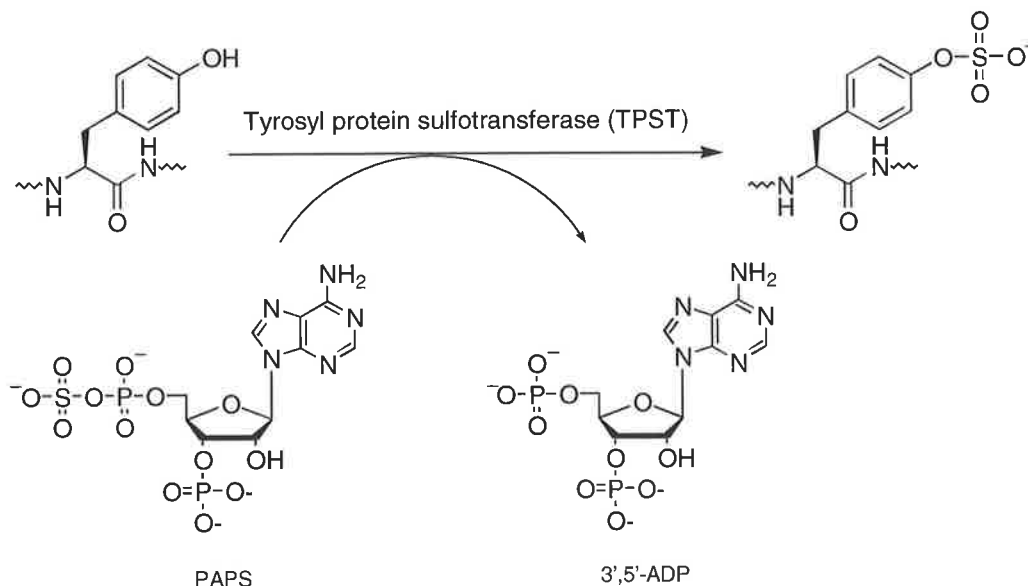


Figure 7.1: Sulfotransferases pathway

ATP and inorganic sulfate are first converted to adenosine 5-phosphosulfate (APS) by the action of ATP sulfurylase. APS kinase then phosphorylates APS to produce PAPS. Finally, PAPS is imported into the Golgi compartments by a specific transport^{17,18}.

The sulfated tyrosine residues in gastrin, CCK and caerulein are preceded by one or more acidic amino acids. These acidic amino acids may contribute to the recognition of certain peptides and proteins by TPST.

7.2.2 Roles of tyrosine sulfation

The sulfation of tyrosine residue in peptides appears to be a highly selective process. The role of this sulfate group in bioactivity is not well understood. Recent work has suggested that tyrosine sulfate is important for peptide folding and for protein-protein interactions occurring during the intracellular transport of proteins¹⁹.

7.2.3 Tyrosine sulfation and bioactivity

Tyrosine sulfation has long been known to be required for the biological activity of peptides such as caerulein, CCK and leucosulfakinin. The unsulfated form may occur following inhibition of cellular PAPS synthesis^{20,21} or site directed mutagenesis of sulfated tyrosine^{22,23}. The differences in activity between sulfated tyrosine and desulfated tyrosine containing peptides are summarised in *Table 7.2*.

Table 7.2: Examples of biological effects of desulfated tyrosine peptides

Peptides (sequences-see <i>Table 7.1</i>)	Biological activity	Reduced activity due to lack of sulfation (divided by)	References
Caerulein	Gastric acid secretion	6-20	24,25
	Pancreatic secretion	20	24,25
	Motability of the gall bladder and intestine	100	24,25
CCK-8	Stimulation of gall bladder contraction and α -amylase secretion	260	20,21
CCK-4	Hemolytic activity	2	19
Gastrin	Half-life in plasma	5	19
Leucosulfakinin	Stimulation of intestine contraction	10^4	6

7.3 Caerulein-like Peptides

7.3.1 General

Caerulein is characterised by a post-translated tyrosine sulfate residue and exhibits a spectrum of biological activities similar to those of the mammalian intestinal peptide hormones cholecystokinin (CCK) and gastrin²⁶. The question as to whether these peptides are homologous to each other or whether they merely exhibit a superficial resemblance is still unclear. The relationship of caerulein and CCK peptides is manifested primarily by the sequence similarity at the C-terminal pentapeptide sequence (WMDF-NH₂) and by the presence of a sulfated tyrosine residue. These features are reported to be necessary for biological activity²⁷. The N-terminal residue of caerulein is pyroglutamate: this may serve the function of protecting the peptide from degradation by aminopeptidases during transport *in vivo*²⁸.

The difference in structure between CCK-8, gastrin, and caerulein responsible for the selectivity in action, is that CCK-8 and caerulein are sulfated at a tyrosine in position 7 from the C-terminus, whereas gastrin has a sulfated tyrosine in position 6 (*Figure 7.2*).

CCK-8	DY(SO ₃)MGWMDF-NH ₂
Caerulein	pEQDY(SO ₃)TGWMDF-NH ₂
Gastrin	pEGPWLEEEEEAY(SO ₃)GWMDNF-NH ₂

Figure 7.2: The location of the tyrosine sulfated residue from the C-terminus of CCK, caerulein and gastrin

7.3.2 Pharmacological action

Caerulein exhibits biological activity similar to CCK and gastrin (for sequences see *Figure 7.2*). However, the cDNA encoding the amphibian peptide caerulein²⁹⁻³² is quite different from that encoding the mammalian analogues³³⁻³⁵. Preprocaerulein contains multiple copies of the caerulein sequence, accompanied by several copies of caerulein precursor fragment (CPF)³⁶, which has antibacterial activity. In contrast, gastrin and CCK do not have any DNA repeating units and have no regions encoding a peptide structurally similar to the amphibian antibiotic peptide CPF.

The biological actions of caerulein, CCK and gastrin include stimulation of pancreatic enzyme secretion and gall bladder contraction³⁷. Apart from effecting gastric acid secretion, these peptides also stimulate smooth muscle contraction, increase blood circulation and water secretion in the stomach and intestine, and stimulate pancreatic secretion⁷. They also influence calcitonin release in the thyroid gland³⁸.

Caerulein and CCK also act on the central nervous system. This includes satiety, sedation, thermoregulation and anti-nociception^{39,40}. In relation to analgesia, caerulein is 10 times as potent as CCK-8 and several thousand times more potent than morphine^{40,41}.

Caerulein shows a potent muscle stimulation effect with a consequent increase in acetylcholine release. This effect is Ca^{2+} -dependent⁴². Ca^{2+} antagonist drugs administered to the organ perfusion solution diminish this muscle stimulation. Subsequent administration of caerulein reinforces this inhibition of contraction and acetylcholine release.

Because of their potency and the long duration of their central effects, it has been proposed that caerulein-like peptides may prove to be useful in the management of certain types of pain and in the treatment of neuropsychiatric disorders⁴³.

7.3.3 Target Receptors

Caerulein and CCK receptors have been classified into peripheral (CCK-A) and central (CCK-B) types on the basis of ligand binding assays and the use of selective antagonists.

The location and major characteristics of the 2 receptor subtypes are summarised in *Table 7.3*.

7.3.

Table 7.3: Location and characteristics of the CCK-A and CCK-B receptors

Location	CCK-A receptor	CCK-B receptor
CNS		Increase anxiety Decrease dopamine release
Pancreas	Increase exocrine secretion	
Stomach	Increase gastric secretion Pyloric sphincter contraction	Increase gastric secretion
Gallbladder	Increase contraction	
Distal duodenum, jejunum, ileum and colon	Increase motility	
Proximal duodenum	Decrease motility	

CCK-A receptors occur in the peripheral tissues and have a high affinity for only sulfated CCK or caerulein. In contrast, CCK-B receptors distributed in the central nervous system have a high affinity for both the sulfated and non-sulfated forms of CCK-related peptides⁴⁴.

7.3.4 Caerulein and contraction activity

The contractile activity of caerulein is increased by parasympathetic^{§§} stimulation, but inhibited by sympathetic^{***} stimulation. Parasympathetic activities are mediated via acetylcholine action on muscarinic receptors^{†††}, while the sympathetic response is caused by noradrenaline acting on the smooth muscle⁴⁵. The contraction response to caerulein is atropine-independent⁴⁶, having a direct effect on the CCK-A receptor of smooth muscle. The CCK-A receptor is believed to be located on muscle cells, mediating contraction by direct action on the muscle cells and not via acetylcholine release.

7.3.5 Caerulein and analgaesic activity

Few studies have been performed on the possible physiological interaction between endogenous CCK and opioid systems^{47,48}. A recent study indicated that CCK modulates the spinal release of enkephalins^{‡‡‡49}. An increase in the spinal release of enkephalins

^{§§} Parasympathetic refers to the autonomic nervous system in the brain and sacral region of the spinal cord. This has long cholinergic (acetylcholine-releasing) preganglionic fibers and short postganglionic fibers.

^{***} Sympathetic refers to the autonomic nervous system in the thoracic and lumbar regions of the spinal cord. This has short cholinergic (acetylcholine-releasing) preganglionic fibers and long adrenergic (norepinephrine-releasing) postganglionic fibers.

^{†††} Muscarinic receptors are found on effector cell membranes (smooth muscle, cardiac muscle and glands). They bind with acetylcholine released from parasympathetic postganglionic fibers.

^{‡‡‡} Enkephalin is an opioid peptide, capable of binding with very high affinity. It exhibits exceptional selectivity for either μ or δ opioid receptors.

is noted upon stimulation of CCK-A receptors (*Figure 7.3*).

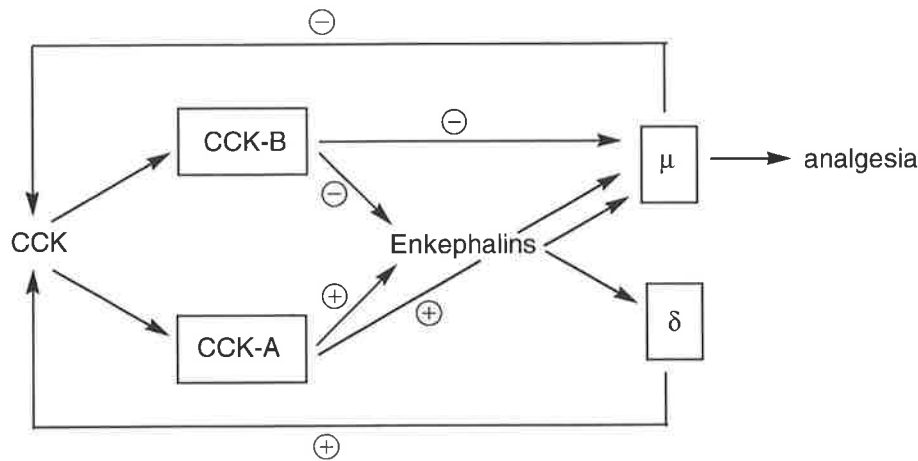


Figure 7.3: Hypothetical model of the interactions between CCK, via CCK-A and CCK-B receptors and the opioid system via δ -opioid and μ -opioid receptors. CCK agonists, endogenous and/or exogenous, stimulate the CCK-B and/or the CCK-A receptors, which can modulate the opioidergic systems, either directly (via the release of endogenous enkephalins). In addition, activation of μ -opioid receptors, which leads to antinociceptive responses, could negatively modulate the release of endogenous CCK, whereas δ -opioid receptors may enhance it.

The stimulation of CCK-A receptors enhances opioid release and/or directly improves the efficacy of transduction processes occurring at the μ -opioid receptors⁵⁰. In contrast, CCK-B receptor activation can adversely affect the modulation of the opioidergic system.

It is proposed that caerulein and CCK exert a stimulatory influence on spinal release of enkephalin through the activation of CCK-A receptors in order to enhance analgesic activity⁵¹.

7.4 Structure-activity Relationship of Caerulein-like Peptides

The relationship between chemical structure and biological activity is summarised below⁵².

Caerulein: pGlu-Gln-Asp-Tyr(SO₃)-Thr-Gly-Trp-Met-Asp-Phe-NH₂

- (i) A caerulein-like spectrum of activity depends on the C-terminal tetrapeptide (WMDF-NH₂); further lengthening of the peptide chain is of limited effect.
- (ii) The threonine residue at position 5 can be replaced by other amino acids without a significant change in activity.
- (iii) The tyrosyl sulfate residue cannot be replaced by *p*-sulphonamido-phenylalanine; however it can be replaced by a residue of the general formula X-CH-CH-CO-, where X is a substituted aromatic ring bearing either a SO₂OH or a OSO₂OH or a OPO₃H₂ group.
- (iv) The chirality of the tyrosyl sulfate amino acid residue is of limited importance.
- (v) The methionyl residue at position 8 can be replaced with the stable norleucine residue.
- (vi) Both desulfation of the tyrosyl residue and a shift of this residue toward the C-terminus produce a remarkable reduction in activity.

In conclusion, it appears that any active analogue of caerulein should (i) bear a negatively charged residue (ii) contain the C-terminal tetrapeptide (WMDF-NH₂) and (iii) a sulfated tyrosine at residue 4.

The aim of the work described in this chapter is to investigate the biological activities of eugenin and the caerulein analogues as shown in *Table 7.4*.

Table 7.4: Sequencing of eugenin and caerulein analogues

Name	Sequence
Eugenin	pEQDY(SO ₃)VFMHPF-NH ₂
Caerulein 1.2	pEQDY(SO ₃)TGWFDNF-NH ₂
Caerulein 2.1	pEQDY(SO ₃)TGAHMDF-NH ₂
Caerulein 2.2	pEQDY(SO ₃)TGAHFDF-NH ₂
Caerulein 3.1	pEQDY(SO ₃)GTGWMDNF-NH ₂
Caerulein 3.2	pEQDY(SO ₃)GTGWFDNF-NH ₂
Caerulein 4.1	pEQDY(SO ₃)TGSHMDF-NH ₂
Caerulein 4.2	pEQDY(SO ₃)TGSHFDF-NH ₂

7.5 Results and Discussion

Eugenin and the caerulein analogues were synthesised as described in *Chapter 6*. The purity of each peptide was greater than 95% as shown by HPLC.

Peptides were tested first for antibiotic activity. Neither eugenin nor caerulein analogues show antibiotic activity. As eugenin and caerulein analogues show some sequence similarities to caerulein 1.1 and CCK-8, the effect of these peptides on smooth muscle was then investigated.

Eugenin was tested for muscle contraction using CCK-8 and acetylcholine as a controller. This experiment was conducted by Dr. Ian Musgrave (Department of Pharmacology, Adelaide University, Adelaide, Australia). It was found that eugenin contracted guinea pig ileum tissue, beginning at 10⁻⁹ M. The response is atropine-dependent in contrast to the

similar activity of caerulein which is atropine independent. It is not clear whether eugenin is acting directly on muscarinic receptors or indirectly via stimulation of CCK-B receptor on nerve terminals. However, it is possible that eugenin may be acting as a CCK-B/gastrin agonist by stimulating acetylcholine release from neurons in the myenteric plexus^{§§§}.

More exciting is the observation that eugenin increases the concentration of T cells at a concentration of 10^{-6} M. At present these are only preliminary tests, and they need to be repeated. If this is correct, it explains why eugenin is present in the wallaby pouch for the first two weeks when the young has no immune system of its own. A pronounced increase in T-lymphocytes in the pouch could significantly alter the immune response of the mother. Further work on this system is underway.

The caerulein analogues listed in *Table 7.4* were investigated for contractile response in the Institute for Molecular Bioscience (Queensland University, Queensland, Australia). The results show that only caerulein 1.2 and 3.1 caused contraction and increased frequency of spontaneous activity in isolated rat pyloric sphincter at a concentration of 10^{-9} M or below. The responses of caerulein 1.2 and 3.1 are both atropine-dependent. This preliminary work needs to be repeated: the reason why the other caeruleins (shown in *Table 7.4*) are “inactive” is not clear at this time.

The active caeruleins 1.2 and 3.1 have similar sequences to caerulein 1.1 as shown below.

Caerulein 1.1	pEQDY(SO ₃)TGWMDf-NH ₂
Caerulein 1.2	pEQDY(SO ₃)TGWFDf-NH ₂
Caerulein 3.1	pEQDY(SO ₃)GTGWMDf-NH ₂

^{§§§} Myenteric plexus is a nerve between the two muscle layers of the intestine.

In caerulein 1.2, the change from a methionine to a phenylalanine residue in position 3 from the C-terminus might change the hydrophobic and possibly also the charge-charge interactions between the ligand and the receptor. Caerulein 3.1 has an extra glycine residue at position 7 from the C-terminal end. This peptide shows a slightly lower activity than caerulein 1.2.

From the results obtained here, it appears that modifications in the C-terminal amino acid sequence of a caerulein (compared with that of caerulein 1.1) lead to a decrease in smooth muscle activity. However these unusual caerulein peptides may have some other pharmacological activity which has as yet not been identified.

7.6 Conclusions

This research has investigated the biological activity of eugenin from the Tammar wallaby (*Macropus eugenii*) and caerulein analogues from the Australian tree frog (*Litoria citropa*).

Eugenin and caerulein analogues showed no significant antibacterial activity against the range of tested pathogens. Eugenin and caerulein analogues show some sequence similarities to caerulein 1.1 and CCK-8, they are likely to exhibit a similar spectrum of neurological activity.

Eugenin caused contraction in guinea pig ileum tissue. The response seems to be atropine-dependent. Eugenin is possibly acting as a CCK-B agonist by stimulating acetylcholine release from neurons in the myenteric plexus. The function of eugenin in the wallaby

pouch is still unknown. The physiological functions of eugenin are currently undergoing further investigations.

Preliminary work found that caerulein 1.2 and 3.1 caused contraction in isolated rat pyloric sphincter. The responses of caerulein 1.2 and 3.1 are atropine-dependent.

7.7 Experimental

7.7.1 Antimicrobial testing

Antimicrobial testing of synthetic peptides was carried out by the Institute of Medical and Veterinary Science (Adelaide, South Australia). The method involved the measurement of the inhibition zone produced by the applied peptide on a thin agarose plate containing the microorganisms under study. The method follows a standard testing procedure⁵³. The micro-organisms used were:- *Bacillus cereus*, *Escherichia coli*, *Leuconostoc lactis*, *Listeria innocua*, *Micrococcus luteus*, *Pasteurella multocida*, *Staphylococcus aureus*, *Staphylococcus epidermidis* and *Streptococcus uberis*. No activity below 10^{-5} M was noted, and the peptides are deemed antimicrobially inactive.

7.7.2 Contraction studies of eugenin

Contraction studies of eugenin were carried out by Dr. Ian Musgrave (Department of Pharmacology, Adelaide University, Adelaide, Australia), with the author observing, and assisting when required.

Tissue preparation

Guinea pigs weighing approximately 300 g were killed by stunning and subsequent decapitation. The ileum was dissected free and was cleaned by rinsing it with physiological salt solution (2.7 mM KCl, 1.0 mM CaCl₂, 13.0 mM NaHCO₃, 3.2 mM NaH₂PO₄, 137 mM NaCl, 5.5 mM glucose), and the mesenteric tissue was removed. Segments of about 3 cm were cut, suspended in 20 mL organ baths containing the physiological salt solution gassed with 95% O₂ and 5% CO₂, connected to a tissue holder and to an isometric force-displacement transducer. Tension was recorded via MacLab version 3.0. Segments were washed thoroughly by replacing the physiological salt solution repeatedly, and then allowed to equilibrate for a period of 30 min under 2 g of resting tension. Supply reservoirs and organ baths were maintained at 37 °C and were gassed with O₂/CO₂ as above.

Tissue viability assessment

Following the 30 min equilibration period the viability of the tissues was assessed. Tissues that failed to produce a 0.5 g increase in tension to acetylcholine (1 µM) were rejected. The tissue-bathing solution was replaced repeatedly with fresh physiological salt solution until a stable baseline tension was achieved. The tension was then readjusted to 2 g.

Contraction studies

All segment preparations were then constricted with acetylcholine (0.01-1 µM). After washout, acetylcholine (1 µM) was added again to check that the response was stable. After 5 min washout and achievement of a stable baseline, a cumulative response curve to cholecystokinin (CCK-8 0.0001-0.01 µM) was performed. After another 5 min washout and achievement of a stable baseline, a cumulative concentration response curve to eugenin (0.001-0.1 µM) was performed. Following washout, tissues were either pretreated with

atropine or the CCK-B blocker LY 225910 and CCK-8 or eugenin reapplied. Eugenin was shown, in three separate experiments, to contract smooth muscle at concentrations down to 10^{-9} M.

7.7.3 Contraction studies of caerulein analogues

Caerulein analogues were tested for contractile activity in the Institute for Molecular Bioscience (Queensland University, Queensland, Australia). The author was not involved in these experiments.

Tissue preparation

Adult Wistar rats were killed by stunning and decapitation. The pyloric sphincters were excised about 5 mm below and above the sphincter and placed in Krebs bicarbonate buffer (119 mM NaCl, 4.7 mM KCl, 1.6 mM $\text{CaCl}_2 \cdot 6\text{H}_2\text{O}$, 1.2 mM KH_2PO_4 , 1.2 mM $\text{MgSO}_4 \cdot 7\text{H}_2\text{O}$, 0.05 mM Na_2EDTA , 22.6 mM NaHCO_3 , 5 mM glucose). The buffer was aerated with gas (95% O_2 /5% CO_2) prior to the experiment, bringing the solution to pH 7.4. The preparations were cleared of fat and excess antral and duodenal tissue, rinsed with buffer to remove any chyme inside the lumen, and mounted in a 10 mL organ bath containing Krebs buffer with constant aeration (as above).

Contraction studies

A resting tension of 1 g was gradually applied to the preparation. The tissue was equilibrated for approximately 45 min until a baseline of relative constant spontaneous activity was obtained. Isometric contractions were recorded using a Narco Bio-System F-60 force transducer and a MacLab/8s data acquisition system with Chart version 3.6.4B3/s

software. Two preparations were used in each experiment. In the first experiment, the baseline spontaneous activity of the tissue was studied. The quality of the preparations was investigated by measuring the smooth muscle contractile response to barium and acetylcholine. Caerulein analogues were added as concentrated solutions to a final concentration of 0.1 μM at 37 $^{\circ}\text{C}$, and the tissue exhibited high spontaneous activity. For the second experiment, the temperature was lowered to 35 $^{\circ}\text{C}$, which gave a slight reduction of spontaneous contraction.^{****} Of the caeruleins listed in *Table 7.4*, only caerulein 1.2 and 3.1 increased smooth muscle contractions at concentrations of 10^{-9} M.

^{****} P. F. Alewood personal communication.

7.8 References

- 1) Huttner, W. B. *Nature* **1982**, 299, 273.
- 2) Huttner, W. B. *Ann. Rev. Physiol.* **1988**, 50, 363.
- 3) Huttner, W. B.; Baeuerle, P. A. *Modern Cell Biology*; Satir, B. and Alan, R., Ed.; Liss Inc.: New York, 1988; Vol. 6, p 97.
- 4) Bettelheim, F. R. *J. Am. Chem. Soc.* **1954**, 76, 2838.
- 5) Veenstra, J. A. *Neuropeptides* **1989**, 14, 145.
- 6) Nachman, R. J.; Holman, G. M.; Haddon, W. F.; Ling, N. *Science* **1986**, 234, 71.
- 7) Nachman, R. J.; Holman, G. M.; Cook, B. J.; Haddon, W. F.; Ling, N. *Biochem. Biophys. Res. Comm.* **1986**, 140, 357.
- 8) Duve, H.; Thorpe, A.; Scott, A. G.; Johnson, A. H.; Rehfeld, J. P.; Hines, E.; East, P. D. *Eur. J. Biochem.* **1995**, 232, 633.
- 9) Nicholas, R. *Mol. Cell Neurosci.* **1992**, 3, 342.
- 10) Fonagy, A.; Schoofs, L.; Proost, P.; Van Damme, J.; Loof, A. *Comp. Biochem. Physiol.* **1992**, 103c, 135.
- 11) Bentley, P. H.; Kenner, G. W.; Sheppard, R. C. *Nature* **1966**, 209, 583.
- 12) Dockray, G. J.; Gregory, R. A.; Hutchison, J. B.; Harris, J. I.; Runswick, M. J. *Nature* **1978**, 274, 711.
- 13) Johnsen, A. H.; Rehfeld, J. F. *J. Biol. Chem.* **1990**, 265, 3054.
- 14) Bertaccini, G. *Pharmacol. Rev.* **1976**, 28, 127.
- 15) Anastasi, A.; Bertaccini, G.; Cei, J. M.; De Caro, G.; Erspamer, V.; Impicciatore, M. *Brit. J. Pharmacol.* **1969**, 37, 198.
- 16) Baeuerle, P. A.; Hutter, W. B. *J. Cell Biol.* **1987**, 105, 2655.
- 17) Ozeran, J. D.; Westley, J.; Schwartz, N. B. *Biochemistry* **1996**, 35, 3695.

- 18) Hirschberg, L. B.; Robbins, P. W.; Abeijon, C. *Annu. Rev. Biochem.* **1998**, *67*, 49.
- 19) Niehrs, C.; Beisswanger, R.; Hutter, W. B. *Chem. Biol. Interact.* **1994**, *92*, 257.
- 20) Baeuerle, P. A.; Huttner, W. B. *Biochem. Biophys. Commun.* **1986**, *141*, 870.
- 21) Hortin, G. L.; Schilling, M.; Graham, J. P. *Biochem. Biophys. Res. Commun.* **1988**, *150*, 342.
- 22) Friederich, E.; Fritz, H. J.; Hutter, W. B. *J. Cell Biol.* **1988**, *107*, 1655.
- 23) Leyte, A.; Van Schijndel, H. B.; Niehrs, C.; Huttner, W. B.; Verbeet, M. P.; Mertens, K.; Van Mourik, J. A. *J. Biol. Chem.* **1991**, *266*, 740.
- 24) Johnson, L. R.; Stening, G. F.; Grossman, M. I. *Gastroenterology* **1969**, *56*, 1255.
- 25) Erspamer, V.; Falconieri Erspamer, G. *Brit. J. Pharmacol.* **1972**, *45*, 333.
- 26) Lazarus, L. H.; Attila, M. *Prog. Neurobiol.* **1993**, *41*, 473.
- 27) Dockray, G. J. *Nature* **1976**, *264*, 568.
- 28) Gregory, H.; Hardy, P. M.; Jones, D. S.; Kenner, G. W.; Sheppard, R. C. *Nature* **1964**, *204*, 931.
- 29) Hofmann, W.; Bach, T. C.; Seliger, H.; Kreil, G. *EMBO J.* **1983**, *2*, 111.
- 30) Wakabayashi, T.; Kato, H.; Tachibana, S. *Gene* **1984**, *31*, 295.
- 31) Wakabayashi, T.; Kato, H.; Tachibana, S. *Nucleic Acids Res.* **1985**, *13*, 1817.
- 32) Richter, K.; Egger, R.; Kreil, G. *J. Biol. Chem.* **1986**, *261*, 3676.
- 33) Deschenes, R. J.; Lorenz, L. J.; Haun, R. S.; Roos, B. A.; Collier, K. J.; Dixon, J. E. *Proc. Natl. Acad. Sci. USA* **1984**, *81*, 726.
- 34) Gubler, U.; Chua, A. O.; Hoffman, B. J.; Collier, K. J.; Eng, J. *Proc. Natl. Acad. Sci. USA* **1984**, *81*, 4307.
- 35) Friedman, J.; Schneider, B. S.; Powell, D. *Proc. Natl. Acad. Sci. USA* **1985**, *82*, 5593.
- 36) Bevins, C. L.; Zasloff, M. *Annu. Rev. Biochem.* **1990**, *59*, 395.
- 37) Deutsh, J. A. *Prog. Neurobiol.* **1983**, *20*, 313.

- 38) Erspamer, V.; Melchiorri, P. *Pure Appl. Chem.* **1973**, *35*, 463.
- 39) De Castiglione, R. *Farmaco* **1982**, *37*, 305.
- 40) Erspamer, V.; Melchiorri, P. *Neuroendocrine Perspectives*; Muller, E. E. and MacLeod, R. M., Ed.; Elsevier: Amsterdam, 1983; Vol. 2, p 37.
- 41) Faris, P. L.; Komisaruk, B. R.; Watkins, L. R.; Mayer, D. J. *Science* **1983**, *219*, 310.
- 42) Mantovani, P.; Valoti, M.; Rakowska, A.; Adorni-Ugolotti, M. C. *Methods Find. Exp. Clin. Pharmacol.* **1995**, *17*, 321.
- 43) Zetler, G. *Neuropharmacology* **1982**, *21*, 295.
- 44) Innis, R. B.; Synder, S. H. *Proc. Natl. Acad. Sci. USA* **1980**, *77*, 6917.
- 45) Sherwood, L. *Human Physiology from Cell to Systems*; Wadsworth Publishing Company: USA, 1997; Vol. 3, p 204.
- 46) Bertaccini, G.; De Cara, G.; Endean, R.; Erspamer, V.; Impicciatore, M. *Br. J. Pharmacol.* **1968**, *34*, 291.
- 47) Derrien, M.; Noble, F.; Maldonado, R.; Roques, B. P. *Neurosci. Lett.* **1993**, *160*, 193.
- 48) Noble, F.; Derrien, M.; Roques, B. P. *Br. J. Pharmacol.* **1993**, *109*, 1064.
- 49) Cesslin, F.; Bourgoin, S.; Artaud, F.; Hamon, M. J. *Neurochem.* **1984**, *43*, 763.
- 50) Magnuson, D. S. K.; Sullivan, A. F.; Simonnet, G.; Roques, B. P.; Dikenson, A. H. *Neuropeptides* **1990**, *16*, 213.
- 51) Salem, A., (Department of Pharmacology, Adelaide University, Adelaide, Australia), Personal Communication.
- 52) Bernardi, L.; Bertaccini, G.; Bosisio, G.; Bucci, R.; De Castiglione, R.; Erspamer, V.; Goffredo, O.; Impicciatore, M. *Experientia* **1972**, *28*, 7.
- 53) Jorgensen, J. H.; Cleeland, R.; Craig, W. A.; Doern, G.; Ferraro, M. J.; Finegold, S. M.; Hansen, S. L.; Jenkins, S. G.; Novick, W. J.; Pfaller, M. A.; Preston, D. A.; Reller, L.

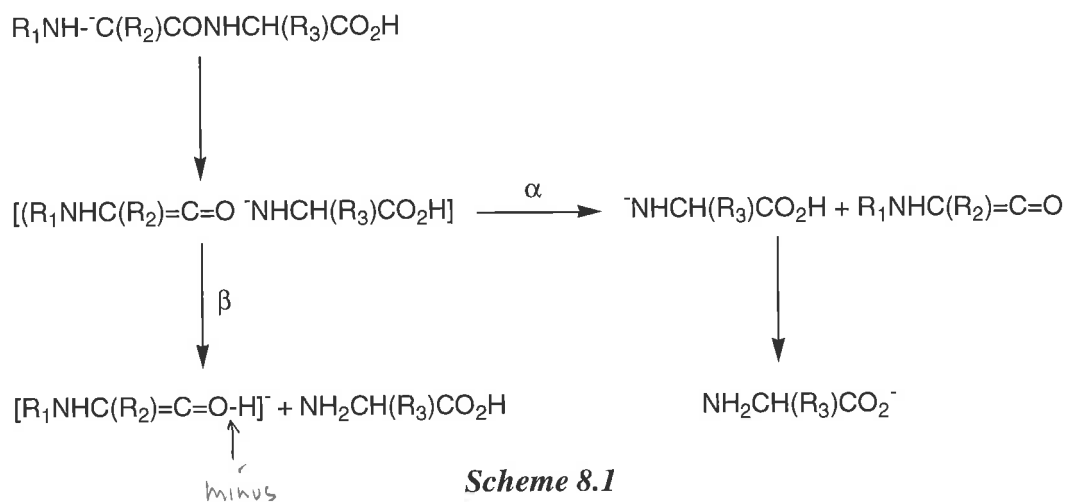
B.; Swenson, J. M. *National Committee for Clinical Laboratory Standards Document M7-A3* **1993**, 13, 1.

Chapter Eight

Comparison of the Positive and Negative Ion Electrospray Mass Spectra of Small Peptides Containing Pyroglutamate

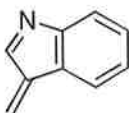
During the last decade, our group has been interested in the fragmentation of (M-H)⁻ ions of small synthetic peptides and natural peptides using fast atom bombardment (FAB) mass spectrometry^{1,2}.^{*} Recently, we have studied the negative ion cleavages of some amphibian peptides using the Micromass QTOF 2 mass spectrometer³. There are many types of backbone cleavages in the negative ion spectra, which provide sequencing information. Two backbone cleavages involving fragmentations of the amide moieties provide sequence information: these are α and β cleavages. α -Cleavages give sequence information from the N-terminal end of the peptide, while β -cleavages give sequence information from the C-terminal end of the peptide (*Scheme 8.1*).

* Full details of the operation of the VG ZAB JHF instrument are given in Stringer, M. B., Bowie, J. H., and Holmes, J. L., *J. Am. Chem. Soc.* 1986, 108, 3888 - see also p 195, this thesis



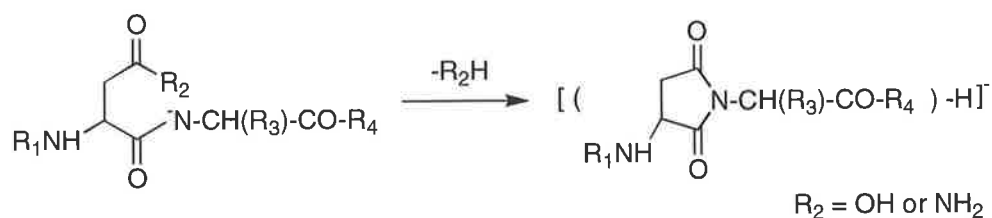
In addition to the backbone cleavages, there are side-chain cleavages, which identify particular residues as shown in *Table 8.1*.

Table 8.1: Characteristic negative ion fragmentations of side-chain of amino acid residues from $(M-H)^-$ ions of small peptides

Residue	Loss (or formation)	Mass
Ala	Me [•]	15
Val	Pr [•]	43
Leu (Ile)	Bu [•]	57
Phe	PhCH ₂ ⁻	91
Tyr	<i>p</i> -HOC ₆ H ₄ CH ₂ ⁻	107
	O=C ₆ H ₄ =CH ₂	106
Trp		129
Ser	CH ₂ O	30
Thr	MeCHO	44
Cys	H ₂ S	34
Met	MeSH	48
	MeSMe	62
	[•] CH ₂ CH ₂ SMe	75
Asp	H ₂ O	18

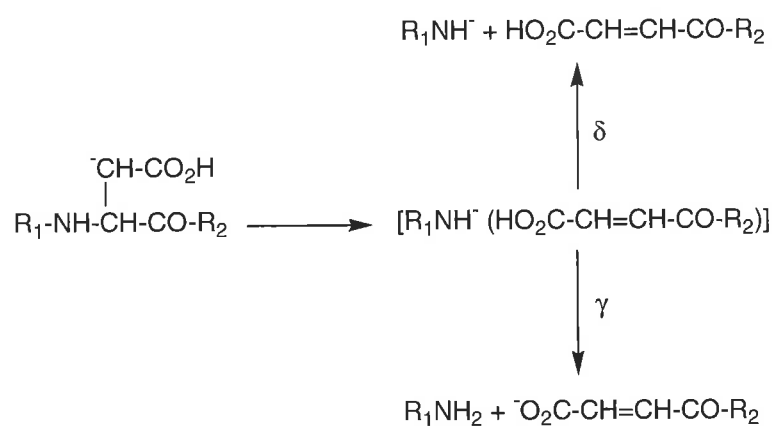
Glu	H ₂ O	18
Arg	NH=C=NH	42

Many of these side chain fragmentations become less pronounced or disappear as the size of the peptide increases. However, some of the side chain fragmentations dominate the negative ion spectrum regardless of the size of the peptide. The processes are pronounced for Ser (-CH₂O), Thr (-MeCHO), Asp (-H₂O), Glu (-H₂O), Asn (-NH₃) and Gln (-NH₃). As examples, the losses of H₂O from Asp and NH₃ from Asn can be rationalised as shown in *Scheme 8.2*^{1,4}.



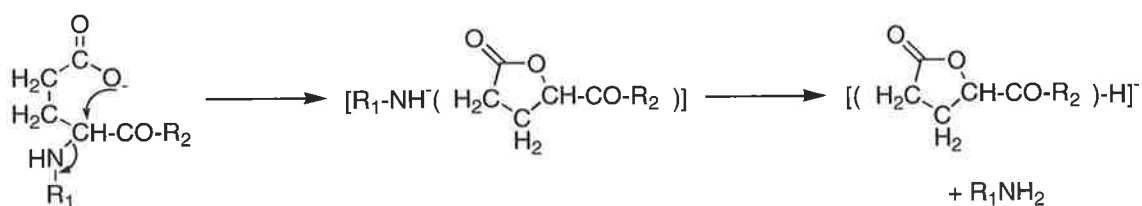
Scheme 8.2

There is another type of backbone cleavage which can occur when Asp, Asn, Glu and Gln residues are present in the peptide^{2,4}. For Asp and Asn, the process occurs via an enolate anion as shown for Asp in *Scheme 8.3*.

**Scheme 8.3**

In general, the major fragment ion is that formed by loss of the amine R_1NH_2 (called a γ cleavage), in some instances the ion corresponding to R^1-NH^- (called a δ cleavage ion) is occasionally observed. In small peptides of six residues or less, similar fragmentations may occur with Phe, Tyr and His where the δ , γ cleavages are initiated by a carbanion ($^-\text{CH}-\text{R}$; $\text{R} = \text{C}_6\text{H}_5$, $-\text{C}_6\text{H}_4\text{OH}$ or $-\text{C}_3\text{H}_3\text{N}_2$) adjacent to the peptide backbone.

The residues Glu and Gln can also initiate γ type cleavage fragmentation. Theoretical calculations of a Glu model system suggest that the mechanism involves the cyclisation of the carboxylate anion via a five-centre transition state (*Scheme 8.4*)⁴.

**Scheme 8.4**

It is feasible that the negative ion spectrum of a peptide may provide sequence information, and it would appear that the negative ion spectrum may yield data complementary with that provided by the ubiquitous positive ion fragmentation data (see e.g. *Chapter 1, section 1.7.1*).

The aim of the research presented in this chapter is to

- (i) compare the positive and negative ion electrospray mass spectra of some small synthetic peptides containing pyroglutamate, and
- (ii) investigate the negative ion fragmentations of some caerulein-like peptides isolated from skin secretions of the Australian Blue Mountain tree frog *Litoria citropa*.

8.1 Comparison of Positive and Negative Ion Mass Spectra of Peptides Containing Pyroglutamate

8.1.1 General

We have isolated some unusual small compounds from the pouch secretion of the female Tammar wallaby (*Macropus eugenii*) (*Chapter 4*). We thought initially that these were peptides containing a pyroglutamic acid residue. A number of peptides were synthesised which contain N-terminal pyroglutamate residues, in order to assist with the structure determination of the natural compounds. We showed subsequently that these pouch components were not peptides. The sequences of the synthetic peptides are listed below:

- | | |
|----------------------------------|-----|
| pGlu Pro Gln Val-OH | (1) |
| pGlu Pro Gln Val-NH ₂ | (2) |

pGlu Pro Gln Val Gln Val-OH (3)

pGlu Pro Gln Val Phe Val-OH (4)

pGlu Pro Gln Val Phe Val-NH₂ (5)

As part of our continuing study of the negative ion mass spectra of peptides it was decided to

- (i) sequence these small peptides by mass spectrometry, since Edman sequencing is not possible because of the presence of the blocked N-terminal group.
- (ii) compare the negative ion spectra of small peptides containing C-terminal CO₂H and CONH₂ groups and to ascertain whether the spectra are comparable, and
- (iii) investigate the backbone cleavages in the negative ion spectra of the five peptides.

8.1.2 Results and discussion

The collision-induced (CID) MS/MS spectra of the (MH)⁺ and (M-H)⁻ ion of peptide (1) are shown in *Figures 8.1a* and *8.1b*, respectively. The characteristic positive ion dissociation of peptides has been previously reported^{5,6}. In the positive ion spectra, the B and Y+2 fragmentations⁵ (see *Chapter 1, section 1.7.1*) define the sequence, but do not

differentiate between the isobaric residues, Lys and Gln^{†††}. The positive ion spectrum not only shows B and Y+2 cleavage ions, but there is also pronounced peaks at m/z 181, 229 and 408 originating from A₁ and Z₂ cleavages^{‡‡‡‡5}.

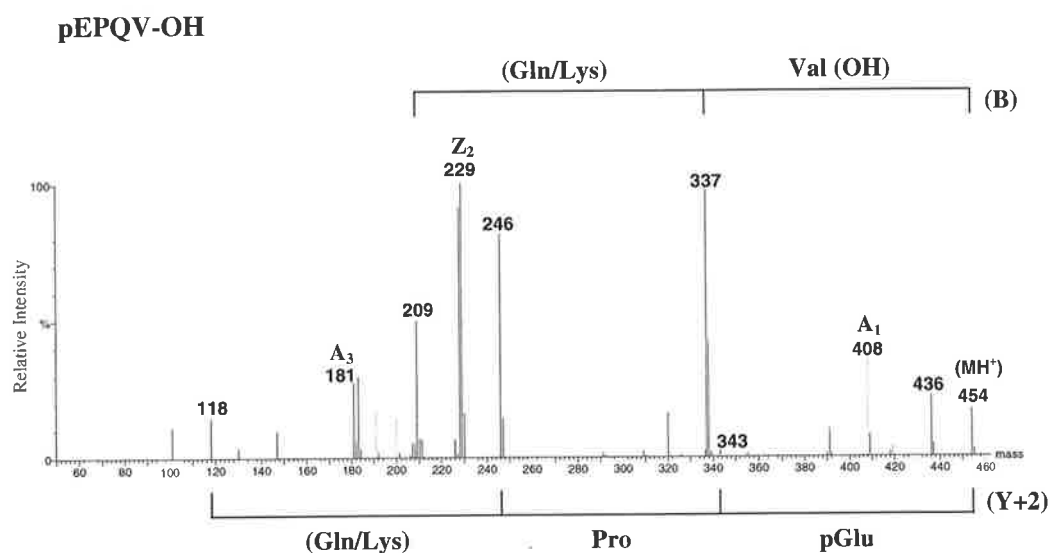
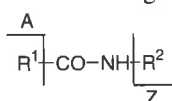


Figure 8.1a: CID electrospray mass spectrum (MS/MS) of the (MH)⁺ ion of pGlu Pro Gln Val-OH: B cleavages are drawn schematically above the spectrum, while Y+2 cleavages are shown schematically underneath the spectrum.

^{†††} The QTOF 2 will allow differentiation between Lys and Gln using the “high-resolution” capability of the instrument. However, this requires calibration of the instrument. It is more efficient to use the negative ion spectrum to distinguish between the residues Lys and Gln.

^{‡‡‡‡} A and Z fragmentations are shown below⁵:



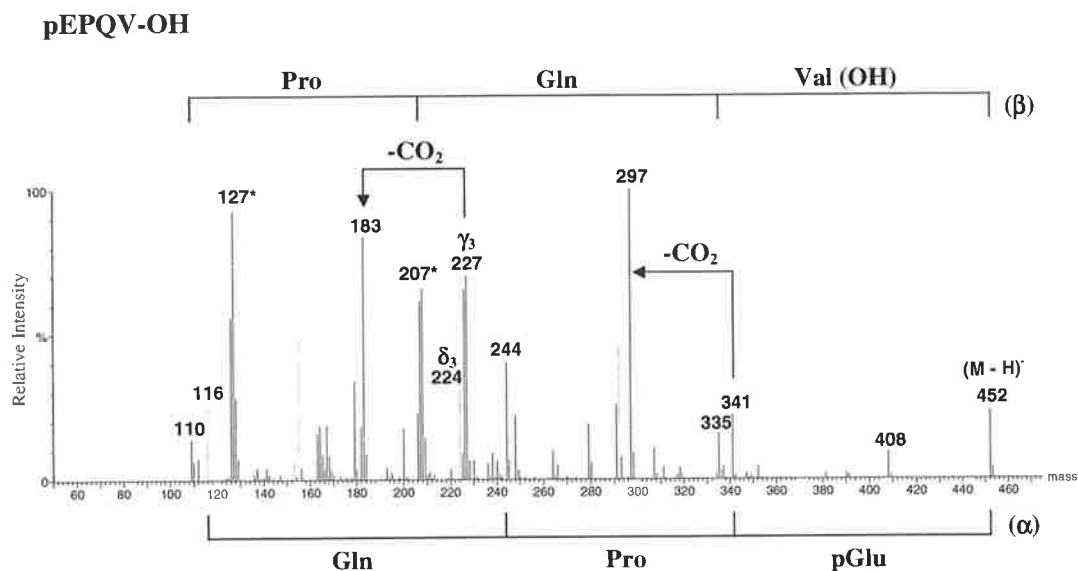
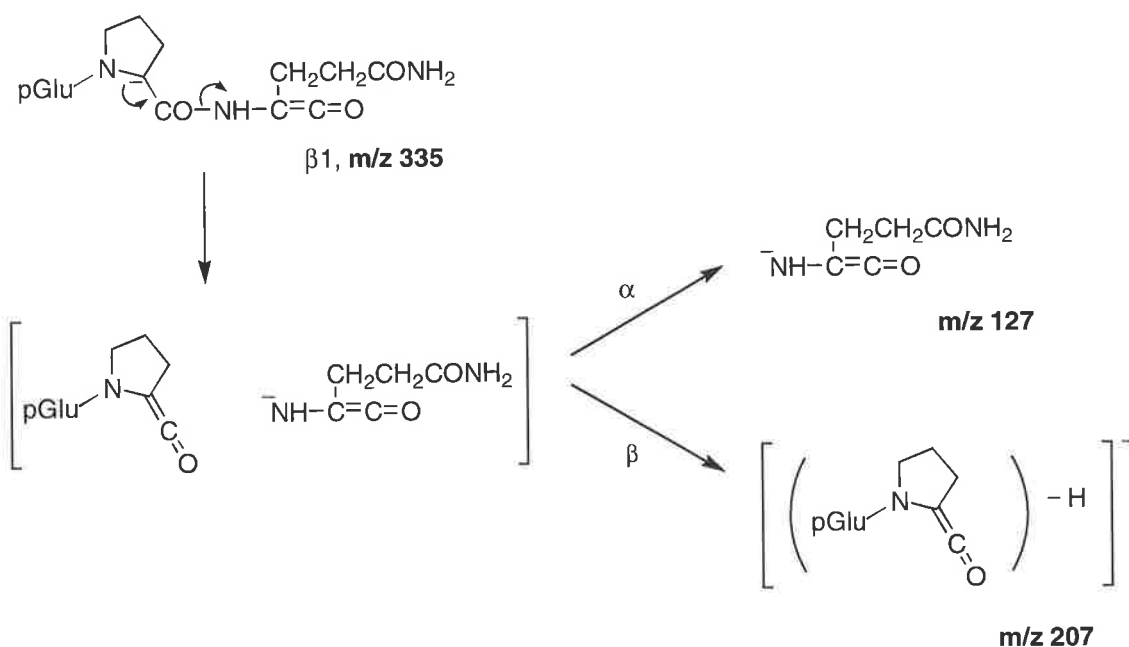


Figure 8.1b: CID electrospray mass spectrum (MS/MS) of the $(M-H)^-$ ion of pGlu Pro Gln Val-OH: α and β cleavage sequences are indicated schematically below and above the spectrum respectively, while δ and γ cleavages are shown on the spectrum. Peaks marked with an asterisk (*) are α and β granddaughter ions originating from the $\beta 1$ ion.

The negative ion spectrum of (1) is shown in *Figure 8.1b*. The sequence of (1) is determined by the α and β cleavages. The peaks at m/z 224 and 227 correspond to the δ_3 and γ_3 cleavage ions (cf. *Scheme 8.4*) which originate from Gln_3 . These cleavage ions identify this residue as Gln rather than Lys. Negative ion MS/MS data indicate that the pronounced peaks at m/z 127 and 207 are α and β granddaughter ions originating from the $\beta 1$ ion (m/z 335). The fragmentations are rationalised as α and β cleavages of the enolate anion m/z 335 (*Scheme 8.5*).

**Scheme 8.5**

The positive and negative ion spectra of the corresponding amide (2) are listed in *Table 8.2*. The fragmentations of (2) are similar to both the negative and positive cleavages of (1): in these cases the negative ion cleavages are similar for both the C-terminal CO_2H and CONH_2 containing peptides.

Table 8.2: Positive and negative ion mass spectra of peptide (2), (3) and (4)

pEPQV-NH ₂ (2)	
(A) Positive ion spectrum of [(MH) ⁺ , m/z 453] (only characteristic B and Y+2 ions are listed)	
B ions;	m/z 436, 337 and 209 [QV-NH ₂]
Y+2 ions;	m/z 342, 245 and 117 [pEPQ]
(B) Negative ion spectrum of [(M-H) ⁻ , m/z 451] (only characteristic α , β , δ and γ fragment ions are listed)	
α ions;	m/z 340, 243 and 115 [pEPQ]
β ions;	m/z 335, 207 and 110 [PQV-NH ₂]
δ and γ ions;	m/z 224 (δ , Gln ₃) and 226 (γ , Gln ₃)

pEPQVQV-OH (3)	
(A) Positive ion spectrum of [(MH) ⁺ , <i>m/z</i> 681] (only characteristic B and Y+2 ions are listed)	
B ions;	<i>m/z</i> 663, 564, 436, 337 and 209 [QVQV-OH]
Y+2 ions;	<i>m/z</i> 473, 345 and 246 [(pEP)QV]
pEPQVQV-OH (4)	
(A) Positive ion spectrum of [(MH) ⁺ , <i>m/z</i> 700]	
B ions;	<i>m/z</i> 682, 583, 436, 337 and 209 [QVQV-OH]
Y+2 ions;	<i>m/z</i> 492, 364 and 265
(B) Negative ion spectrum of [(M-H) ⁻ , <i>m/z</i> 698]	
α ions;	<i>m/z</i> 587, 490, 362, 263 and 116 [pEPQVQV]
β ions;	<i>m/z</i> 335 and 207 [363 Q]
δ and γ ions;	<i>m/z</i> 224 (δ, Gln ₃), 246 (γ, Phe ₄), 451 (δ, Phe ₄), 473 (γ, Gln ₃)

The characteristic peaks in the positive ion spectrum of (3) are listed in *Table 8.2*. The positive ion spectrum provides the sequence, except that it does not differentiate between Lys and Gln at residues 3 and 5. The negative ion spectrum of (3), shown in *Figure 8.2*, gives five α ions and three β ions. The δ and γ cleavages of Gln₃ yield *m/z* 224 (δ₃) and 454 (γ₃) respectively. The peak at *m/z* 227 corresponds to the γ cleavage initiated by Gln₅. Thus residues 3 and 5 are identified as Gln.

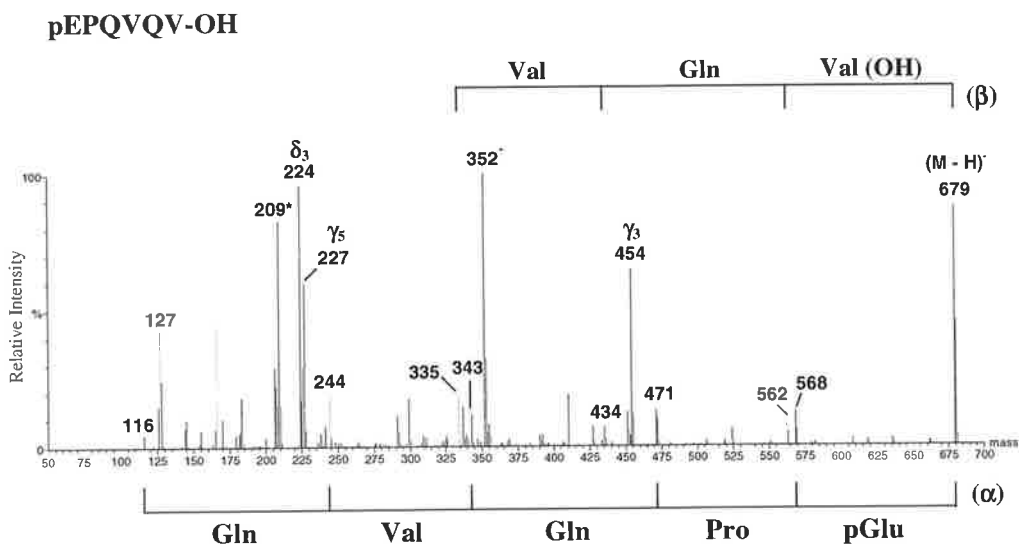
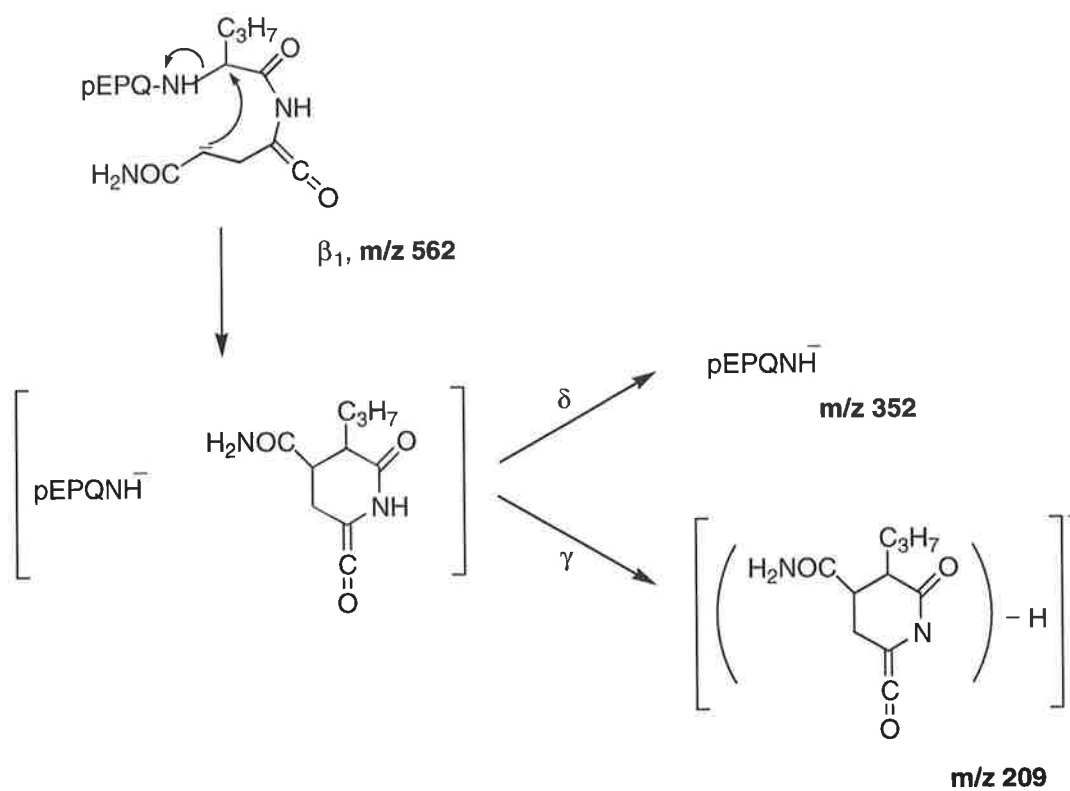


Figure 8.2: CID electrospray mass spectrum (MS/MS) of the (M-H)⁻ ion of pGlu Pro Gln Val Gln Val-OH: α and β cleavage sequences are indicated schematically below and above the spectrum, respectively, while δ and γ cleavage ions are shown on the spectrum. Peaks marked with an asterisk (*) are δ and γ granddaughter ions originating from the β ion.

In addition, MS/MS data indicate that m/z 352 and 209 originate from the β 1 ion at m/z 562; these are δ and γ cleavage ions respectively. These processes are rationalised in *Scheme 8.6*. This negative ion spectrum provides the full sequence of (3).



Scheme 8.6

The positive and negative ion MS/MS data of (4) are shown in Figure 8.3a and 8.3b, respectively. The positive ion spectrum gives a partial sequence but does not differentiate between Lys and Gln at residue 3.

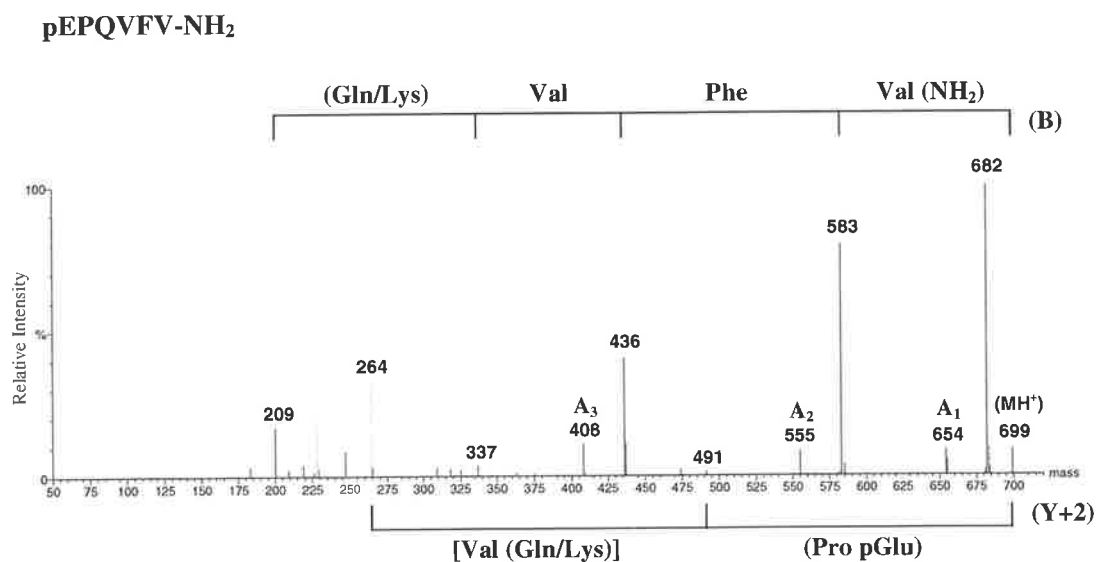


Figure 8.3a: CID electrospray mass spectrum (MS/MS) of the $(MH)^+$ ion of pGlu Pro Gln Val Phe Val-NH₂: B cleavages are drawn schematically above the spectrum, while Y+2 cleavages are shown schematically underneath the spectrum.

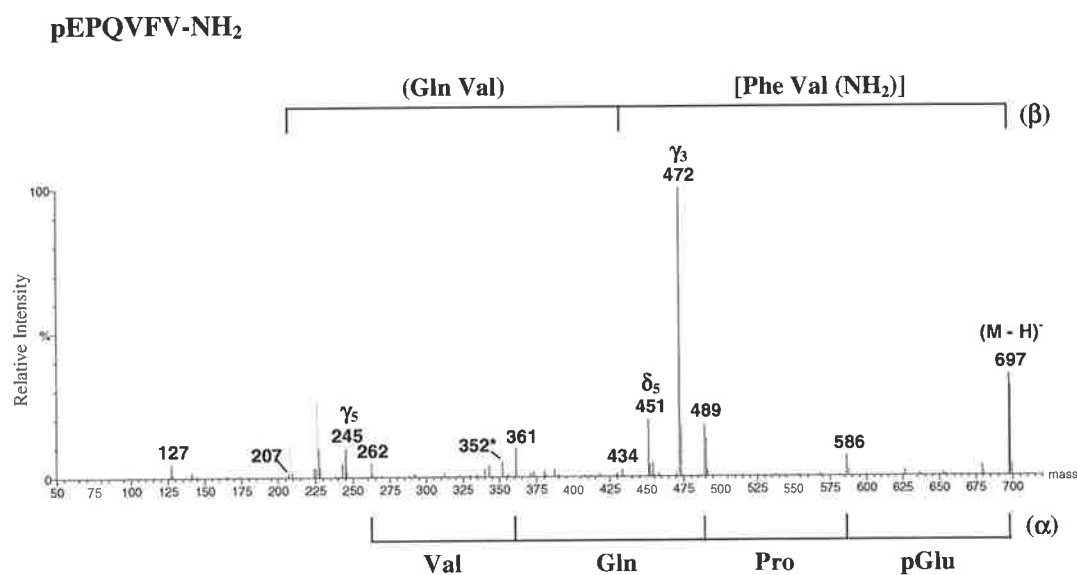
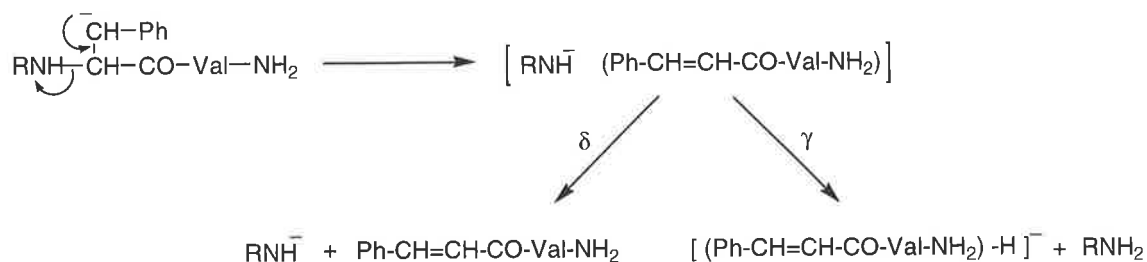


Figure 8.3b: CID electrospray mass spectrum (MS/MS) of the $(M-H)^-$ ion of pGlu Pro Gln Val Phe Val-NH₂: α and β cleavage sequences are indicated schematically below and above the spectrum, respectively, while δ and γ cleavages are shown on the spectrum. The peak marked with an asterisk (*) is the δ granddaughter ion originating from the β 1 ion.

The negative ion spectrum provides full sequencing information. The base peak m/z 472 corresponds to the γ cleavage ion of Gln₃. A δ cleavage process analogous to that shown in Scheme 8.6 forms the fragment ion m/z 352. The peaks at m/z 245 and 451 in Figure 8.3b

correspond to the Phe₅ γ and δ cleavage ions. The Phe₅ δ and γ cleavages are shown in *Scheme 8.7*.



Scheme 8.7

Conclusions

- (i) The fragmentation data for both positive and negative ions of these small peptides provide amino acid sequencing information. The negative ion spectra of these peptides often provide more sequencing data than given by the corresponding positive ion spectra.
- (ii) The negative ion backbone cleavages of these small peptides with C-terminal CO₂H or CONH₂ groups are the same.
- (iii) The negative ion spectra of Gln containing peptides show characteristic δ and/or γ backbone cleavage processes initiated by Gln residue. Such fragmentations can be used to differentiate between isobaric Gln and Lys residues.
- (iv) Small peptides containing Phe show δ and γ backbone cleavages initiated from the Phe side chain.

- (v) There are some unusual granddaughter fragments in some of the negative ion spectra. The granddaughter anions originate from the β 1 cleavage anion, which undergoes further fragmentations either by α and β or by δ and γ processes.

8.2 Negative Ion Spectra of Caerulein-Like Peptides

8.2.1 General

During the last decade, we have isolated and identified host-defence peptides from the skin secretion of a number of Australian amphibians. Frogs of the genus *Litoria* often produce the neuropeptide caerulein [pEQDY(SO₃)TGWMDf-NH₂]. Caerulein shows potent smooth muscle activity. It is also an analgaesic several thousand times more potent than morphine⁷. A number of peptides of the caerulein family have been isolated from *Litoria citropa*⁸. Each caerulein peptide is accompanied in the glandular secretion by the non-sulfated analogue. Non-sulfated caerulein is known to show much reduced smooth muscle activity in comparison with caerulein itself^{7,9}. We have synthesised all of these peptides and are currently investigating their bioactivity¹⁰. ^{(see also Chapter 7} All of the caerulein analogues have a pyroglutamate residue, so they cannot be sequenced using automated Edman sequencing. Fragmentations in the positive ion electrospray mass spectra of [(MH)⁺-SO₃]⁺ ions of these caerulein analogues were used to determine the sequences of the caerulein-type peptides⁸. The molecular weights were determined from the mass of the (M-H)⁻ ion. The LCQ instrument was used to provide both molecular weight and sequencing data. Peaks corresponding to both (M-H)⁻ and [(M-H)⁻-SO₃]⁻ were also observed, but few negative ion fragmentations were observed using the LCQ instrument.

Previously, the negative ion spectrum was only used to identify the presence of the tyrosine sulfate residue of caerulein peptide by identification of the molecular weight via the $(M-H)^-$ ion⁸. In this section we record the collision induced negative ion electrospray mass spectra of caerulein analogues using the Micromass QTOF 2 instrument, and compare the negative and positive ion MS/MS data for these peptides. The caerulein peptides used in this study are shown in *Table 8.3*. Most of the peptides contain (i) Ser or Thr, (ii) Asp and Gln, and (iii) tyrosine sulfate residues: residues which should be readily identified using negative ion mass spectrometry.

Table 8.3: Sequences of caerulein peptides used in this study.

Caerulein	Sequence
2.2	pEQDY(SO ₃)TGAHFDF-NH ₂
2.2Y ⁴	pEQDY TGAHFDF-NH ₂
3.1	pEQDY(SO ₃)GTGWMDf-NH ₂
3.1Y ⁴	pEQDY GTGWMDf-NH ₂
3.2	pEQDY(SO ₃)GTGWFDF-NH ₂
3.2Y ⁴	pEQDY GTGWFDF-NH ₂
4.1	pEQDY(SO ₃)TGSHMDF-NH ₂
4.1Y ⁴	pEQDY TGSHMDF-NH ₂
4.2	pEQDY(SO ₃)TGSHFDF-NH ₂
4.2Y ⁴	pEQDY TGSHFDF-NH ₂

8.2.2 Results and discussion

The positive ion mass spectrum (MS/MS) of the $[(MH)^+ - SO_3]^+$ ion of caerulein 2.2 (i.e the $(MH)^+$ ion of desulfated caerulein 2.2Y⁴), $[(MH)^+ = 1310 \text{ Da}]$ is shown in *Figure 8.4*.

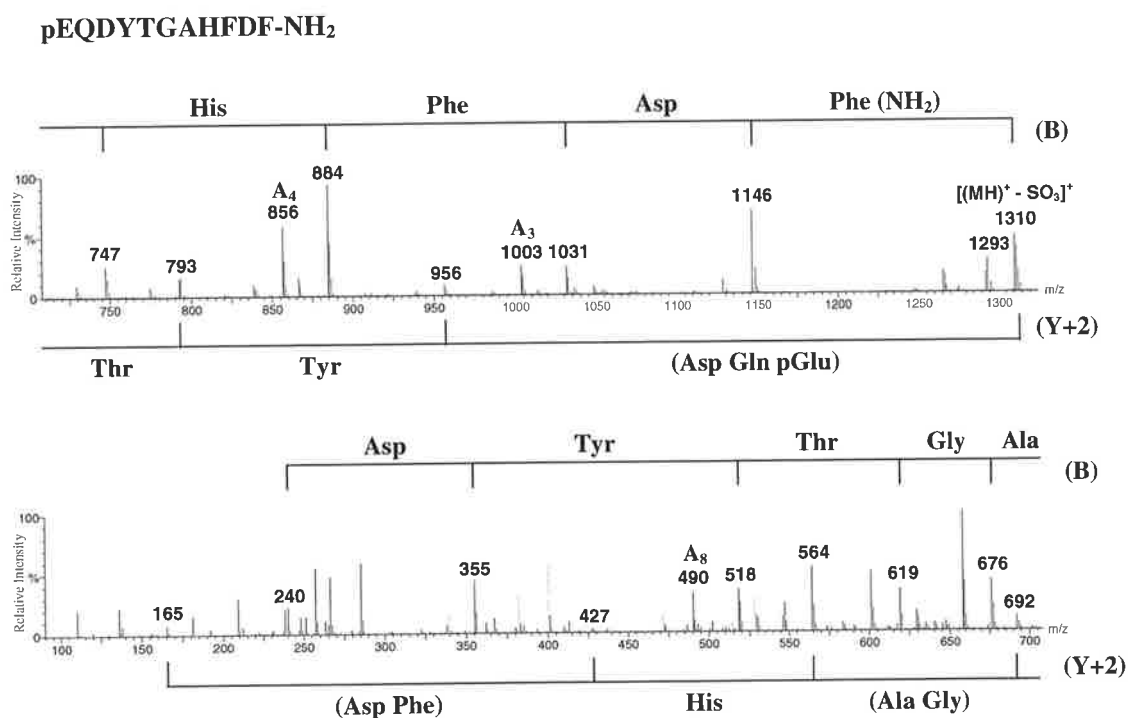


Figure 8.4: Positive ion electrospray mass spectrum (MS/MS) of the $[(MH)^+ - SO_3]^+$ ion of caerulein 2.2. B and Y+2 sequences are indicated schematically above and below the spectrum.

Positive ion MS/MS data for the $[(MH)^+ - SO_3]^+$ species from caerulein 2.2 are identical to those obtained from the $(MH)^+$ ion of caerulein 2.2Y⁴. The positive ion spectrum (MS/MS) shows three A, nine B and six Y+2 fragment peaks, with the B and Y+2 type cleavage ions together providing the amino acid sequence information. This low-resolution spectrum however cannot distinguish between Gln and Lys at position 2. All the positive ion spectra of these peptides listed in *Table 8.3* provide similar information to that shown in *Figure 8.1*. They are not considered further here.

The negative ion spectra of the $[(M-H)^-SO_3]^-$, and $(M-H)^-$ ions from caerulein 2.2 are shown in *Figure 8.5a* and *8.5b*, respectively.

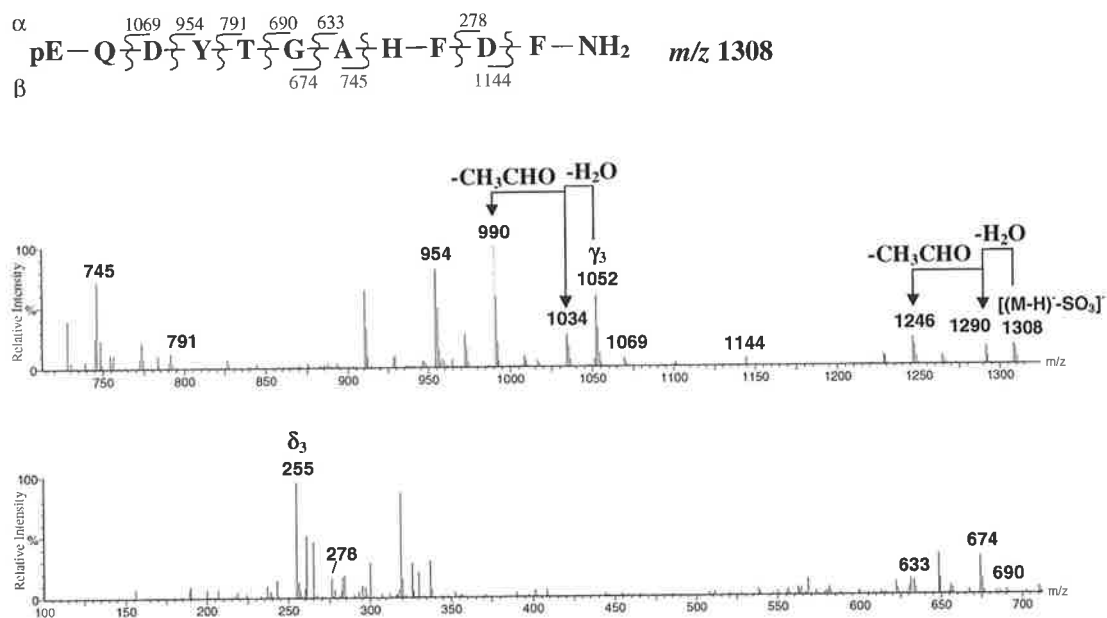


Figure 8.5a: Negative ion electrospray mass spectrum (MS/MS) of the $[(M-H)^-SO_3]^-$ ion of caerulein 2.2.

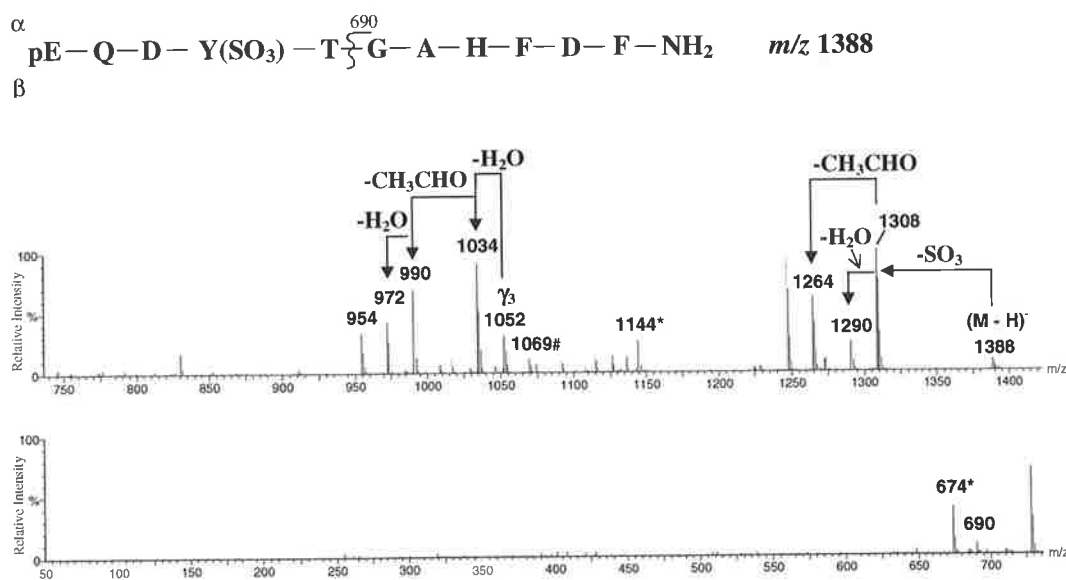


Figure 8.5b: Negative ion electrospray mass spectrum (MS/MS) of the $(M-H)^-$ ion of caerulein 2.2. Peak marked with (#) is the $\alpha 2$ ion originating from the $[(M-H)^-SO_3]^-$. Peaks marked with (*) are $\beta 1$ and $\beta 2$ ions originating from the $[(M-H)^-SO_3]^-$ ion.

Figure 8.5a shows six α and three β backbone cleavages, which provide the partial sequence as summarised on the structural formula drawn above the spectrum in *Figure 8.5a*. The various losses of H_2O (18 Da) and MeCHO (44 Da) shown in *Figure 8.5a* are characteristic of Asp and Thr respectively. δ and γ backbone cleavages of Gln_2 and Asp_{10} are not observed in this spectrum, but the δ and γ cleavages of Asp_3 yield m/z 255 and 1052, respectively.

The negative ion spectrum of the sulfate of caerulein 2.2, $[(\text{M-H})^- = 1388 \text{ Da}]$ is shown in *Figure 8.5b*. Comparison of *Figures 8.5a* and *8.5b* show the presence of peaks corresponding to both $(\text{M-H})^-$ and $[(\text{M-H})^- \text{-SO}_3]^-$ ions in *Figure 8.5b*, but α and β cleavage peaks are generally absent. Major fragmentation proceeds via γ cleavage of Asp_3 . Loss of H_2O and MeCHO are characteristic of Asp and Thr side chain cleavages respectively. The peaks at m/z 1144 and 674 are β_1 and β_5 ions of the $[(\text{M-H})^- \text{-SO}_3]^-$ ion (m/z 1308). The peak at m/z 1052 is the γ_3 cleavage ion originating from the $[(\text{M-H})^- \text{-SO}_3]^-$ ion. The peak at m/z 1069 corresponds to the α_2 cleavage ion originating from the $[(\text{M-H})^- \text{-SO}_3]^-$ ion. Other sulfated caeruleins listed in *Table 8.3* give similar negative ion spectra, and are not examined further.

The negative ion spectra of the $[(\text{M-H})^- \text{-SO}_3]^-$ ions from caerulein 3.2, $[(\text{M-H})^- = 1343 \text{ Da}]$ and 4.2, $[(\text{M-H})^- = 1324 \text{ Da}]$ peptides are listed in *Table 8.4*.

Table 8.4: Negative ion mass spectra of caerulein 3.2 and 4.2

Caerulein 3.2: pEQDY(SO ₃)GTGWFDNF-NH ₂	
[(M-H) ⁻ -SO ₃] ⁻ ; <i>m/z</i> 1343, MS/MS 1343	
α ions;	<i>m/z</i> 1104, 989, 826, 278 [pEQDY-548-DF-NH ₂]
β ions;	<i>m/z</i> 1179, 573 [573-606-F-NH ₂]
δ and γ ions;	<i>m/z</i> 1087 (γ ₃), 255 (δ ₃)
Sequence;	pEQDYG-491-DF-NH ₂
Caerulein 4.2: pEQDY(SO ₃)TGSHFDF-NH ₂	
[(M-H) ⁻ -SO ₃] ⁻ ; <i>m/z</i> 1324, MS/MS 1324	
α ions;	<i>m/z</i> 1085, 970, 807, 562 and 425 [pEQDY-245-H(FDF)-NH ₂]
β ions;	<i>m/z</i> 1160, 898, 761 and 674 [674-SH(FD)F-NH ₂]
δ and γ ions;	<i>m/z</i> 1068 (γ ₃), 255 (δ ₃)
Sequence;	pEQDY(TG)SH(FD)F-NH ₂

The negative ion spectrum of caerulein 3.1Y⁴, [(M-H)⁻ = 1327 Da] is shown in *Figure 8.6*.

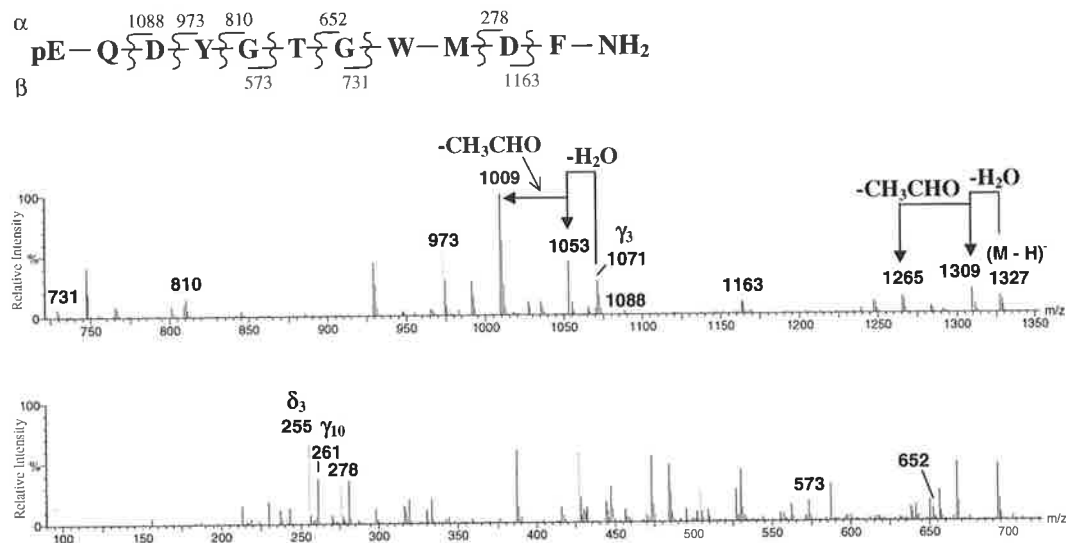


Figure 8.6: Negative ion electrospray mass spectrum (MS/MS) of the (M-H)⁻ ion of caerulein 3.1Y⁴.

Eight backbone cleavages, five α and three β cleavage ions, are shown on the structural formula above the spectrum. There are also δ and γ cleavage ions of Asp₃, *m/z* 255 (δ₃) and

m/z 1071 (γ_3) respectively. The peak at m/z 261 is produced by the γ cleavage originating from Asp₁₀. Losses of H₂O (18 Da) and CH₃CHO (44 Da) are characteristic of Asp and Thr respectively: these cleavages occur from both the parent (M-H)⁻ and γ_3 fragment anions.

The spectrum of caerulein 4.1Y⁴, [(M-H)⁻ = 1308 Da] is shown in *Figure 8.7*.

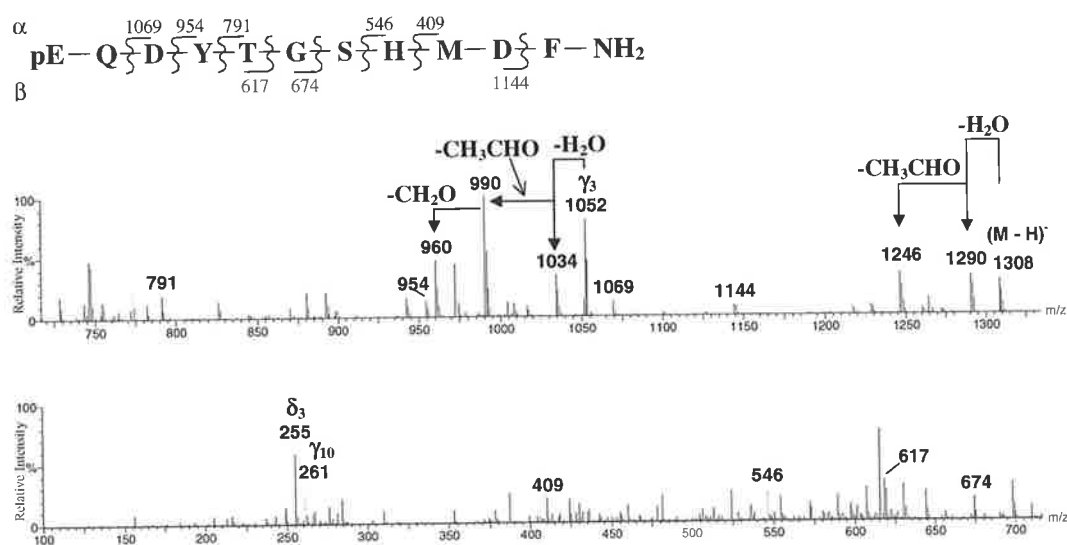


Figure 8.7: Negative ion electrospray mass spectrum (MS/MS) of the (M-H)⁻ ion of caerulein 4.1Y⁴.

The spectrum shows five α and three β cleavages which provide much of the sequence. Peaks at m/z 255 and 1052 correspond to the Asp₃ δ and γ cleavage ions. The Asp₁₀ γ-cleavage gives the peak at m/z 261. Neither δ nor γ ions from Gln₂ are observed in this spectrum. The γ_3 cleavage ion fragments further by the sequence [- H₂O - CH₃CHO - CH₂O]: these losses are the characteristic side chain cleavages of the residues Asp, Thr and Ser, respectively.

Conclusions

- (i) The negative ion electrospray mass spectra of desulfated caeruleins identify at least 80% of the amino acid sequence from a combination of α , β , δ and γ backbone cleavage ions. The most informative negative ion spectrum is that of caerulein 4.1Y (*Figure 8.7*), but even this spectrum does not distinguish between Lys and Gln at residue 2.
- (ii) Asp, Ser and Thr undergo the characteristic losses of H₂O, CH₂O and CH₃CHO, respectively: (these fragmentations compete with the α , β , δ and γ backbone cleavages).
- (iii) δ and/or γ backbone cleavages are observed only for the Asp residues in the caerulein peptides: similar cleavages are not noted for Gln and Phe residues.

8.3 Conclusions

It can be concluded that the negative ion electrospray mass spectra of the peptides considered in this study provide significant sequencing data arising from identification of the α , β , δ and γ backbone cleavage ions. The negative ion spectra also indicate the presence of specific amino acid side chains (like Ser and Thr) by side-chain cleavages: there are no counterparts of these in positive ion spectra.

8.4 Experimental

8.4.1 Preparation of synthetic peptides

The small peptides containing pyroglutamate residues were synthesised by Mimotopes (Clayton, Victoria) using L-amino acids via the standard N- α -Fmoc procedure. Full details, including protecting groups and deprotection, have been reported¹¹.

Caerulein analogues were synthesised as described in *Chapter 6*.

8.4.2 Mass spectrometry

Electrospray mass spectra were measured with a Micromass QTOF 2 orthogonal acceleration time of flight mass spectrometer with a mass range to 10,000 Da. The QTOF 2 is fitted with an electrospray source in an orthogonal configuration with the ZSPRAY interface. Samples were dissolved in acetonitrile/water (1:1) and infused into the electrospray source at a flow rate of 5 μ L/min. Conditions were as follows: capillary voltage 2.43 kV, source temperature 80°C, desolvation temperature 150°C and cone voltage 50-100 V. MS/MS data were acquired with the argon collision gas energy set to ca. 50 eV to give optimal fragmentation.

8.5 References

- 1) Waugh, R. J.; Bowie, J. H. *Rapid Commun. Mass Spectrom.* **1994**, *8*, 169.
- 2) Bradford, A. M.; Waugh, R. J.; Bowie, J. H. *Rapid Commun. Mass Spectrum.* **1995**, *9*, 677.
- 3) Micromass *Model QTOF 2*: Manchester, UK.
- 4) Brinkworth, C. S.; Dua, S.; McAnoy, A. M.; Bowie, J. H. *Rapid Commun. Mass Spectrum.* **2001**, *15*, 1965.
- 5) Biemann, K.; Martin, S. *Mass Spectrom. Rev.* **1987**, *6*, 1.
- 6) Biemann, K. *Biomed. Environ. Mass Spectrom.* **1988**, *16*, 99.
- 7) Erspamer, V. *Bioactive Secretions of the Amphibian Integument, in Amphibian Biology*; Heatwole, H. and Barthalmus, G. T., Ed.; Surrey Beatty and Sons: Chipping North, NSW, Australia, 1994; Vol. 1, p 214.
- 8) Wabnitz, P. A.; Bowie, J. H.; Wallace, J. C.; Tyler, M. J. *Rapid Commun. Mass Spectrom.* **1999**, *13*, 1724.
- 9) Lazarus, L. H.; Attila, M. *Prog. Neurobiol.* **1993**, *41*, 473.
- 10) Boontheung, P.; Baudinette, R. V.; Alewood, P. F.; Bowie, J. H. *unpublished work*
- 11) Maeji, N. J.; Bray, A. M.; Valerio, R. M.; Wang, W. *Pept. Res.* **1995**, *8*, 33.

Summary and Conclusions

Skin secretions of *Litoria alboguttata* have revealed three distinct groups of guttatin peptides, namely, the guttatins 1, 2 and 3. These peptides showed no significant antibacterial activity. *Litoria alboguttata* produces the guttatin 1 peptide that may correspond to a peptide (MH⁺) 715 obtained from *Cyclorana australis*. It is possible that *Litoria alboguttata* should be reclassified as a member of the *Cyclorana* genus.

The secretions from the pouch of the pregnant Tammar wallaby, Brush-tailed Rock wallaby and Yellow-footed Rock wallaby have been investigated. Eugenin was found in the pouch secretion of pregnant Tammar wallabies during the first two weeks of occupancy by the young. This peptide was not found in pouch secretions of the other wallabies. Eugenin contains an N-terminal pyroglutamic acid and tyrosine sulfated residue at position 4, suggesting that it may be a neuropeptide. Eugenin causes contraction of smooth muscle cells via acetylcholine release. Eugenin is now currently undergoing further evaluation in the Department of Pharmacology (The University of Adelaide).

A novel approach for the Fmoc-chemistry solid phase peptide synthesis of tyrosine sulfated containing peptides was developed. The vital points of our strategy are the use of an acid sensitive Pam-resin as a solid support, and the final deprotection with 90% TFA/TIPSi at low temperature to minimise the hydrolysis of the tyrosine sulfated residue. The effectiveness of this approach was evaluated through the synthesis of eugenin and a number of caerulein analogues.

Pharmacological studies of seven different caerulein analogues using isolated rat sphincter were performed. Only caerulein 1.2 and 3.1 show contractile activity on the smooth muscle cell. The response seems to be atropine-dependent.

The collision induced dissociation (CID) negative ion electrospray mass spectra (MS/MS) of selected pyroglutamate containing peptides were investigated. The negative ion electrospray mass spectra provide significant sequencing information compared with the corresponding positive ion spectra. MS/MS data derived from the $(M-H)^-$ ions provide (i) sequencing information from a combination of α , β and γ backbone cleavage ions, and (ii) identification of specific amino acid side chain (eg. Ser and Thr) by side chain cleavages: these fragmentations are not observed in the corresponding positive ion spectra.

Publications

Journals Related to Thesis

Boontheung, P.; Brinkworth, C. S.; Baudinette, R. V. and Bowie, J. H. (2002) Comparison of the positive and negative ion electrospray mass spectra of some small peptides containing pyroglutamate, *Rapid Commun. Mass Spectrom.* 16, 287-292.

Boontheung, P.; Alewood, P. F.; Brinkworth, C. S.; Bowie, J. H.; Wabnitz, P. A. and Tyler, M. J. (2002) Negative ion electrospray mass spectra of caerulein peptides: an aid to structural determination, *Rapid Commun. Mass Spectrom.* 16, 281-286.

Additional Journals

Boontheung, P.; Perlmutter, P. and Puniani, E. (2001) Base-promoted acetal formation employing aryl salicylates, *Arkivoc.* 8, 95-103

Boontheung, P. and Perlmutter, P. (1998) A highly-efficient synthesis of benzoxazine-2,4-diones, *Tet. Lett.* 39, 2629-2630.

Boontheung, P., Brinkworth, C.S., Bowie, J.H. & Baudinette, R.V. (2002) Comparison of the positive and negative ion electrospray mass spectra of some small peptides containing pyroglutamate. *Rapid Communications in Mass Spectrometry*, v. 16(4), pp. 287-292

NOTE:

This publication is included after page 199 in the print copy of the thesis held in the University of Adelaide Library.

It is also available online to authorised users at:

<http://doi.org/10.1002/rcm.576>

Boontheung, P., Alewood, P.F., Brinkworth, C.S., Bowie, J.H., Qabnitz, P.A. & Tyler, M.J. (2002)
Negative ion electrospray mass spectra of caerulein peptides: an aid to structural determination.
Rapid Communications in Mass Spectrometry, v. 16(4), pp. 281-286

NOTE:

This publication is included after page 199 in the print copy
of the thesis held in the University of Adelaide Library.

It is also available online to authorised users at:

<http://doi.org/10.1002/rcm.577>

Base-promoted Acetal Formation Employing Aryl Salicylates.

Pinmanee Boontheung, Patrick Perlmutter* and Evaloni Puniani

School of Chemistry, Monash University, PO Box 23, Victoria 3800 Australia

E-mail: Patrick.perlmutter@sci.monash

Dedicated to Professor T. R. Govindachari on the occasion of his 85th birthday.

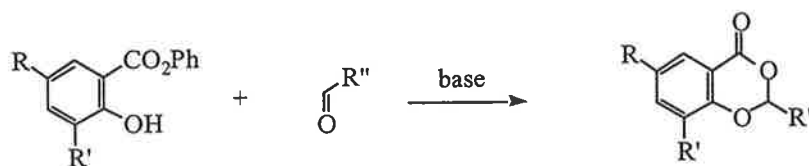
Abstract

New examples of base-promoted acetal formation in the reactions of aryl salicylate and salicylate-type esters 1 to 3 with aldehydes are reported.

Keywords: Oxo-acetals, aldehydes, salicylate, DABCO

Introduction

Recently we reported that aryl esters of 2-hydroxybenzoic acids (i.e. salicylates) form cyclic acetals with a variety of aldehydes (scheme 1) under base-catalyzed conditions.¹ Key aspects of the process were that the reactions worked best under neat conditions or, where necessary, with minimal solvent to effect dissolution. This is in contrast to most methods for acetal formation which usually employ acid-catalyzed conditions.



Scheme 1

Herein we provide further examples of this process as well full experimental details for these new cases as well as the first successful reaction with an aromatic aldehyde.

Results and Discussion

Oxo-acetal formations of esters 1 to 3 were investigated. The structures of the starting materials and products are shown in Figure 1. Most reactions were carried out neat except where either, or both, the aldehyde and salicylate were solids. In those cases a very small volume of chloroform was added to effect solution. The ratio of reactants was salicylate: aldehyde: base = 1 : 5 : 1.

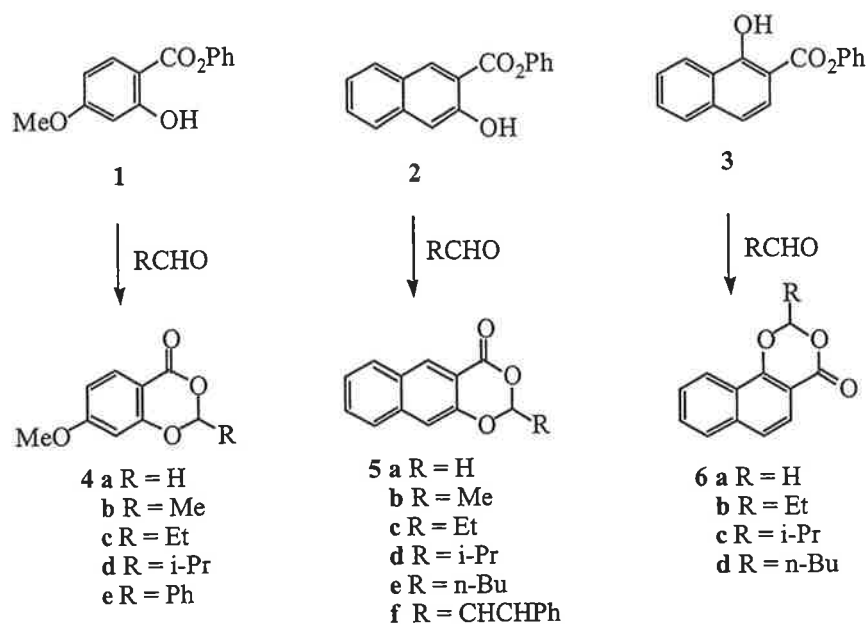
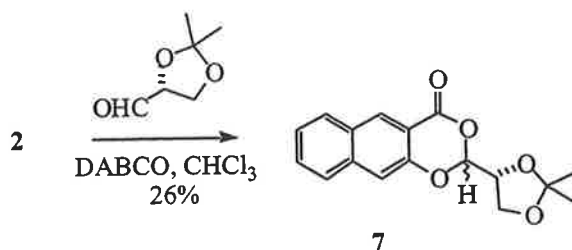


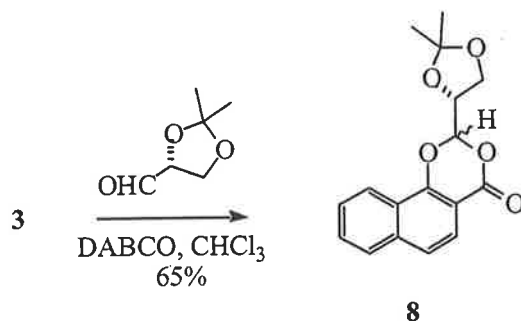
Figure 1

As before aliphatic aldehydes, solid paraformaldehyde and chloral all reacted well with esters 1 to 3. In our previous report we noted that the use of aromatic aldehydes did not lead to successful reaction. Interestingly we have now discovered one exception to this, namely reaction of phenyl 4-methoxysalicylate (1). Reaction with benzaldehyde under standard conditions gave oxo-acetal 4e in 49% yield. Only in one case, that of salicylate 5 was any product formed in a reaction with an unsaturated aldehyde (cinnamaldehyde). The yield was very low (8%). Hence it can be concluded that, in general, unsaturated aldehydes (including aromatic aldehydes) are not usually good substrates for this process.

A brief investigation was carried out to examine whether any diastereoselectivity would occur in reactions with the chiral, non-racemic aldehyde, D-glyceraldehyde acetonide². Hence 2 was reacted with D-glyceraldehyde acetonide. This provided an essentially 1:1 diastereomeric mixture of acetals 7. Unfortunately this mixture proved to be inseparable.



Similar reaction of 3 led to another inseparable 1:1 mixture of acetals 8.



In conclusion, this facile process represents one of the very few base-promoted methods for acetal formation.³ In this report, we have successfully extended the range of salicylate and salicylate-type esters which undergo this reaction.⁴

Acknowledgements

E. P. thanks the Australian Agency for International Development for an overseas research scholarship.

Experimental

General methods and materials

Melting points were determined on a Kofler hotstage and are uncorrected. Elemental microanalyses were performed by the Australian Microanalytical Service, National Analytical Laboratories, Melbourne and the University of Otago, Dunedin, New Zealand. Optical rotations were recorded on a Perkin Elmer Model 141 Polarimeter. Infrared (IR) spectra were recorded on a Perkin-Elmer 1600 Series Fourier Transform spectrophotometer (cm^{-1} scale) and refer to thin films of liquids (neat) or paraffin (Nujol) mulls of solids between NaCl plates. High resolution hydrogen-1 nuclear magnetic resonance (^1H NMR) spectra were recorded at 300 MHz on a Bruker DPX-300 spectrometer or 400 MHz on a Bruker Avance DRX 400 spectrometer. The ^1H NMR spectral data refer to deuteriochloroform solutions (CDCl_3) using tetramethylsilane (TMS) as internal reference (δ 0.00 ppm). Carbon-13 nuclear magnetic resonance (^{13}C NMR) spectra were recorded at 75 MHz on a Bruker APX-300 spectrometer or 100 MHz on a Bruker Avance DRX 400 spectrometer. Mass spectrometry (ESI) was performed using samples in methanol on a Micromass Platform QMS Electrospray mass spectrometer. High resolution mass spectra (HRMS) for accurate mass determinations were recorded on a Bruker BioApex 47e FTMS fitted with an Analytica electrospray source using NaI for accurate mass calibration (accuracy \pm 3 ppm). Low resolution mass spectra were recorded on a VG micromass 70/70F or a VG TRIO-1 mass spectrometer with an ion source temperature of 200 °C and electron impact energy of 70 eV. Esters 2 and 3 were purchased from Aldrich Chemical Company.

General procedure for preparation of cyclic oxo-acetals.

Unless otherwise indicated, a solution of salicylate ester, aldehyde (5 mol equivalent) and base (1.0 mol equivalent) was stirred at room temperature and allowed to react until TLC

analysis indicated complete consumption of starting material. In those cases where one of the starting materials was a solid, and hence the reaction mixture was heterogeneous, a small amount of chloroform (usually about 0.2 mL) was added to effect dissolution. The reaction mixture was then dissolved in diethyl ether (20 mL) and the ethereal solution was then washed with water (3x5 ml). The organic layer was dried (MgSO₄), filtered and concentrated under reduced pressure. Purification of the crude product was carried out either by recrystallization, flash column chromatography or preparative TLC (eluant 1:4, ethyl acetate/light petroleum). Most reactions were carried out using 500mg of the salicylate ester in each case. In the following only reaction times, chromatography details (eluant, Rf), isolated yield, physical constants and spectroscopic data are given.

2-Hydroxy-4-methoxybenzoic acid⁵

To a solution of (15.4 g, 0.1 mol) of 2,4-dihydroxybenzoic acid in 20% NaOH (50 mL) was added (10.41 mL, 0.11 mol) of dimethyl sulfate. The resulting orange solution was stirred at room temperature for 20 hours before being neutralized with concentrated HCl. The mixture was extracted with ether (3x100 ml) and the aqueous layer was acidified to pH~1 with concentrated HCl, resulting in white precipitate. The precipitate was collected by filtration, washed with water and dried (under vacuum). Recrystallization from ethanol and water afforded (9.7 g, 58%) of product as cream solid. m.p. 145-146 °C (lit.⁵ 157-159 °C). IR (Nujol) 3050-2554b, 1649s, 1624s, 1576m, 1504m, 1465m, 1436s, 1348m, 1360m, 1316m, 1261m, 1250m, 1226m, 1205m, 1176m, 1150m, 1095m, 1025m, 966m, 962m cm⁻¹; ¹H NMR (200 MHz, CDCl₃) δ 10.69 (s, 1H, OH), 7.82 (d, J=9.26 Hz, 1H, H5), 6.49 (d, 1H, H6), 6.47 (s, 1H, H3), 3.85 (s, CH₃); ¹³C NMR (50 MHz, CDCl₃) δ 172.5 (CO), 166.9 (C-Ar), 165.3 (C-Ar), 132.6 (C-Ar), 107.9 (C5), 106.0 (C6), 101.5 (C3), 55.9 (CH₃).

Phenyl 2-hydroxy-4-methoxybenzoate 1. 2-Hydroxy-4-methoxybenzoic acid (3.00 g, 17.86 mmol), phenol (1.68 g, 17.86 mmol) and POCl₃ (2.34 ml) were heated at 120-130° C for 45 minutes. The mixture was dissolved in diethyl ether and then extracted with water. The ether layer was dried over MgSO₄ and evaporated in vacuo to give a red oil. The crude material was purified by flash column chromatography (1:4, ethyl acetate/light petroleum). Fractions containing material of Rf=0.46 were combined and concentrated to afford the product as white solid (4.28 g, 98%). m.p. 41-42°. IR (Nujol) 2924.5s, 2854.0s, 1686.2m, 1625.0m, 1589.8m, 1459.1s, 1376.6s, 1273.9m, 1254.2m, 1194.2m, 1163.4m, 1128.2m, 1070.7m, 1030.1m, 963.2m, 856.7m, 836.4m, 773.8m, 744, 721.8m, 687.8m cm⁻¹; ¹H NMR (200 MHz, CDCl₃) δ 10.73 (s, 1H, OH), 7.96 (d, J=0.84 Hz, 1H, H5), 7.23 (m, 5H, Ph), 6.55 (d, J=8.45 Hz, 1H, H6), 6.51 (s, 1H, H3), 3.87 (s, 3H, CH₃); ¹³C NMR (50 MHz, CDCl₃) δ 168.7 (CO), 166.2 (C-Ar), 164.4 (C-Ar), 150.1 (C-Ar), 131.7 (C5), 129.5 (2xCH-Ph), 126.2 (C6), 121.7 (2xCH-Ph), 108.0 (C3), 104.8 (C-Ph), 100.8 (CH-Ph), 55.6 (CH₃); MS *m/z* 245.14 (M+H)⁺.

7-Methoxy-4-oxo-1,3-benzodioxane 4a. 6 d, (Rf=0.25), 79%, colourless crystals (diethyl ether), m.p. 67-68 °C. IR (Nujol) 2922.8s, 2853.6s, 2358.4m, 1742.3m, 1624.6m, 1458.5s, 1376.8m, 1254.8m, 1180.0w, 1110.6w, 1063.6w, 1014.4w, 982.1w, 929.0w, 832.5w, 739.7w, 668.0w, 667.9w cm⁻¹; ¹H NMR (200 MHz, CDCl₃) δ 7.9 (d, J=8.87 Hz, 1H, H5), 6.73 (dd, J=6.42 Hz, 1H, H6), 6.51 (s, 1H, H8), 5.63 (s, 2H, CH₂), 3.86 (s, 3H, CH₃O); ¹³C NMR (50 MHz, CDCl₃) δ 166.0 (CO), 161.3 (C-Ar), 160.2 (C-Ar), 131.8 (C5), 111.4 (C6), 107.3 (C-Ar), 100.3 (C8), 91.0 (C2), 55.7 (CH₃O); HRMS calcd. for C₉H₈O₄: *m/z* 180.0423, found 180.0421; MS *m/z* 180 (58), 150 (100), 122 (66).

2-Methyl-7-methoxy 4-oxo-1,3-benzodioxane 4b. 2 d, (Rf=0.16) (94%), white crystals (diethyl ether), m.p. 59-60 °C. IR (Nujol) 3436.0b, 2923.7s, 2853.5s, 1741.1m, 1616.4m, 1460.1s, 1376.9s, 1263.0m, 1094.0m, 1025.6m, 929.4w, 847.9w, 767.9w, 734.4w, 688.2w cm^{-1} ; ^1H NMR (200 MHz, CDCl_3) δ 7.89 (d, J=8.87 Hz, 1H, H5), 6.71 (dd, J=2.39, 6.44 Hz, 1H, H6), 6.48 (d, J=2.38 Hz, 1H, H8), 5.73 (q, J=5.17 Hz, 1H, H2), 3.86 (s, 3H, CH_3O), 1.73 (d, J=5.17 Hz, 3H, CH_3); ^{13}C NMR (50 MHz, CDCl_3) δ 166.1 (CO), 162.2 ($\underline{\text{C}}\text{-Ar}$), 160.3 ($\underline{\text{C}}\text{-Ar}$), 131.7 (C5), 111.2 (C6), 106.9 ($\underline{\text{C}}\text{-Ar}$), 100.2 (C8), 98.9 (C2), 55.8 (CH_3O), 19.9 ($\underline{\text{CH}}_3$); HRMS calc'd for $\text{C}_{10}\text{H}_{10}\text{O}_4$: m/z 194.0579, found 194.0562; MS m/z 195.06 (M+H) $^+$.

2-Ethyl-7-methoxy 4-oxo-1,3-benzodioxane 4c. 28 h, (Rf=0.25), (86%), yellow oil. IR (neat) 3458.6w, 3079.7w, 2979.0s, 2942.1s, 2844.1m, 2364.1w, 2017.7w, 1744.1s, 1614.7s, 1584.9s, 1501.0s, 1451.3s, 1395.1s, 1332.1m, 1258.8s, 1201.6s, 1169.9s, 1133.9s, 1088.6s, 1050.7s, 1022.9s, 985.8w, 964.1s, 930.5m, 838.6s, 800.4w, 769.9s, 690.0s, 665.2w, 649.3m, 611.6w, 573.1s cm^{-1} ; ^1H NMR (200 MHz, CDCl_3) δ 7.9 (d, J=8.83 Hz, 1H, H5), 6.71 (dd, J=2.39, 6.33 Hz, 1H, H6), 6.50 (d, J=2.37 Hz, 1H, H8), 5.56 (m, 1H, H2), 3.87 (s, 3H, CH_3O), 2.04 (m, 2H, CH_2), 1.4 (t, J=7.46, 7.54 Hz, 3H, CH_3); ^{13}C NMR (50 MHz, CDCl_3) δ 165.9 (CO), 162.1 ($\underline{\text{C}}\text{-Ar}$), 160.1 ($\underline{\text{C}}\text{-Ar}$), 131.4 (C5), 110.9 (C6), 106.7 ($\underline{\text{C}}\text{-Ar}$), 101.9 (C8), 100.0 (C2), 55.6 (CH_3O), 26.6 ($\underline{\text{CH}}_2$), 6.9 ($\underline{\text{CH}}_3$); HRMS calc'd for $\text{C}_{11}\text{H}_{12}\text{O}_4$: m/z 208.0736, found 208.0739; MS m/z 209.09 (M+H) $^+$.

2-Isopropyl-7-methoxy 4-oxo-1,3-benzodioxane 4d. 4 d, (Rf=0.27), (87%), yellow oil. IR (neat) 3462.2w, 2972.3m, 2844.0m, 2362.3m, 1742.8s, 1618.3s, 1584.9s, 1500.3s, 1448.8s, 1397.2s, 1375.6s, 1332.3m, 1261.3s, 1201.7s, 1167.2s, 1110.5s, 1079.3m, 1048.3m, 1020.4m, 982.6m, 959.5m, 837.8m, 768.4m, 691.9m, 699.9w, 652.2w, 617.6w cm^{-1} ; ^1H NMR (200 MHz, CDCl_3) δ 7.89 (d, J=8.81 Hz, 1H, H5), 6.72 (dd, J=2.39 Hz, 1H, H6), 6.67 (d, J=2.39 Hz, 1H, H8), 5.36 (d, J=4.22 Hz, 1H, H2), 3.86 (s, 3H, CH_3O), 2.39 (m, 1H, $\underline{\text{CH}}$), 1.14 (d, J=6.89 Hz, 6H, $2\times\text{CH}_3$); ^{13}C NMR (50 MHz, CDCl_3) δ 165.9 (CO), 162.3 ($\underline{\text{C}}\text{-Ar}$), 160.3 ($\underline{\text{C}}\text{-Ar}$), 131.4 (C5), 111.0 (C6), 106.8 ($\underline{\text{C}}\text{-Ar}$), 104.4 (C8), 100.1 (C2), 55.6 (CH_3O), 31.6 ($\underline{\text{C}}\text{-iPr}$), 15.9 ($2\times\text{CH}_3$); HRMS calc. for $\text{C}_{12}\text{H}_{14}\text{O}_4$: m/z 222.0892, found 222.0897; MS m/z 223.10 (M+H) $^+$.

2-Phenyl-7-methoxy 4-oxo-1,3-benzodioxane 4e. 5 d, 60 °C, (Rf=0.24), (49%), brown solid, m.p. 75-76 °C. IR (Nujol) 2920.5s, 2725.8w, 1759.8m, 1726.0m, 1618.03m, 1582.2m, 1463.0s, 1376.9s, 1315.0m, 1260.4m, 1197.7m, 1116.5m, 1074.1m, 1016.1m, 944.8m, 889.1m, 833.7m, 794.7w, 722.4m, 697.0w, 668.0w cm^{-1} ; ^1H NMR (200 MHz, CDCl_3) δ 7.94 (d, J=8.82 Hz, 1H, H5), 7.64-7.47 (m, 5H, Ph), 6.74 (dd, J=2.39, 6.37 Hz, 1H, H6), 6.56 (d, J=2.37 Hz, 1H, H8), 6.51 (s, 1H, H2), 3.85 (s, 3H, CH_3O); ^{13}C NMR (300 MHz, CDCl_3) δ 166.1 (CO), 161.65 ($\underline{\text{C}}\text{-Ar}$), 159.9 ($\underline{\text{C}}\text{-Ar}$), 134.1 ($\underline{\text{C}}\text{-Ph}$), 131.7 (C5), 130.2 (C6), 128.5 ($2\times\text{CH-Ph}$), 126.5 ($2\times\text{CH-Ph}$), 111.5 ($\underline{\text{CH}}\text{-Ph}$), 107.0 ($\underline{\text{C}}\text{-Ar}$), 100.6 (C8), 100.4 (C2), 55.9 (CH_3O); HRMS calc. for $\text{C}_{15}\text{H}_{12}\text{O}_4$: m/z 256.0736, found 256.0739; MS m/z 262 (M+Na) $^+$.

4-Oxo-1,3-(b)-naphthodioxane 5a. 2 d, (Rf=0.84), (44%), white crystals (diethyl ether), m.p. 105-106 °C. IR (Nujol) 2922.1s, 2852.8s, 1749.7m, 1638.4w, 1608.5w, 1560.2w, 1460.2s, 1376.9s, 1345.3m, 1277.6w, 1257.4m, 1205.4m, 1155.9w, 1124.4w, 1042.8w, 1019.7w, 995.0m, 951.6m, 915.7w, 881.8m, 853.9m, 773.0m, 738.1m, 722.2m cm^{-1} ; ^1H NMR (300 MHz, CDCl_3) δ 8.66 (s, 1H, H5), 7.95 (d, J=8.28 Hz, 1H, H6), 7.81 (d, J=8.32 Hz, 1H, H9), 7.62 (t, J=1.17, 1.27 Hz, 1H, H7), 7.48 (t, J=1.14 Hz, 1H, H8), 7.46 (s, 1H, H10), 5.74 (s, 2H, $\underline{\text{CH}}_2$); ^{13}C NMR (50 MHz, CDCl_3) δ 161.7 (CO), 153.3 ($\underline{\text{C}}\text{-Ar}$), 137.3 ($\underline{\text{C}}\text{-Ar}$), 133.0 (C5),

129.8 (C6), 129.6 (C9), 129.4 (C-Ar), 127.0 (C7), 125.7 (C8), 115.1 (C-Ar), 112.3 (C10), 91.4 (C2); MS m/z 200 (51), 170 (100), 142 (89), 114 (74); Anal. Calc. for $C_{12}H_8O_3$: C, 71.99, H, 4.03. Found: C, 71.60; H, 3.81.

2-Methyl 4-oxo-1,3-(b)-naphthodioxane 5b. 2 d, rt, K_2CO_3 in place of DABCO, ($R_f=0.27$), (14%), white solid, m.p. 90-91 °C. IR (Nujol) 2923.1s, 2854.1s, 1726.4m, 1636.1m, 1608.1m, 1504.4m, 1463.7s, 1270.6s, 1255.0s, 1215.3s, 1135.9m, 1084.9m, 1029.4s, 934.0s, 881.8s, 781.7s, 754.1s, 720.2m cm^{-1} ; 1H NMR (300 MHz, $CDCl_3$) δ 8.63 (s, 1H, H5), 7.92 (d, $J=8.3$ Hz, 1H, H6), 7.78 (d, $J=8.3$ Hz, 1H, H9), 7.59 (t, $J=7.50$ Hz, 1H, H7), 7.46 (t, $J=7.60$ Hz, 1H, H8), 7.40 (s, 1H, H10), 5.8 (m, 1H, H2), 1.8 (d, $J=5.2$ Hz, 3H, CH_3); ^{13}C NMR (50 MHz, $CDCl_3$) δ 162.4 (CO), 153.1 (C-Ar), 137.2 (C-Ar), 132.7 (C5), 129.6 (C6), 129.5 (C9), 129.2 (C-Ar), 127.0 (C7), 125.5 (C8), 114.5 (C-Ar), 112.0 (C10), 99.2 (C2), 20.1 (CH_3); MS m/z 214 (100), 171 (50), 170 (77), 143 (47), 142 (84), 115 (39), 114 (67), 113 (74), 88 (46), 87 (27), 86 (19), 76 (11), 75 (77), 74 (23), 71 (24), 63 (49), 62 (29), 57 (13).

2-Ethyl 4-oxo-1,3-(b)-naphthodioxane 5c. 2 d, ($R_f=0.35$), (75%), colourless crystals (diethyl ether), m.p. 81-82 °C. IR (Nujol) 2851.1s, 2725.4w, 1762.2w, 1728.1m, 1637.4m, 1607.2w, 1463.1s, 1377.1s, 1310.2w, 1271.1w, 1244.4m, 1207.1m, 1148.6w, 1033.0w, 947.8m, 896.4w, 873.3w, 846.7w, 817.7w, 779.3w, 722.2m cm^{-1} ; 1H NMR (300 MHz, $CDCl_3$) δ 8.63 (s, 1H, H5), 7.93 (d, $J=8.34$ Hz, 1H, H6), 7.78 (d, $J=8.34$ Hz, 1H, H9), 7.59 (t, $J=1.21$ Hz, 1H, H7), 7.46 (t, $J=1.15, 1.09$ Hz, 1H, H8), 7.42 (s, 1H, H10), 5.64 (t, $J=4.92$ Hz, 1H, CH), 2.12 (m, $J=4.94$ Hz, 2H, CH_2), 1.18 (t, $J=7.49, 7.60$ Hz, 3H, CH_3); ^{13}C NMR (50 MHz, $CDCl_3$) δ 162.6 (CO), 153.3 (C-Ar), 137.3 (C-Ar), 132.7 (C5), 129.6 (C6), 129.5 (C9), 129.3 (C-Ar), 127.0 (C7), 125.5 (C8), 114.7 (C-Ar), 112.1 (C10), 102.5 (C2), 27.1 (CH_2), 7.2 (CH_3); MS m/z 228 (18), 170 (100), 142 (54), 114 (53), 113 (20); Anal. Calc. for $C_{14}H_{12}O_3$: C, 73.60, H, 5.30. Found: C, 73.13; H, 5.23.

2-Isopropyl 4-oxo-1,3-(b)-naphthodioxane 5d. 3 d, ($R_f=0.42$), (87%), white crystals (diethyl ether), m.p. 58-59 °C. IR (Nujol) 2923.9s, 2854.0s, 2280.6w, 1760.5m, 1639.5m, 1609.4w, 1460.3s, 1377.1s, 1344.3m, 1296.9m, 1268.2m, 1245.5m, 1209.6m, 1135.8w, 1062.1m, 986.3m, 961.5m, 917.4m, 875.9m, 831.0w, 807.5w, 776.4m, 745.9m, 722.6m cm^{-1} ; 1H NMR (300 MHz, $CDCl_3$) δ 8.63 (s, 1H, H5), 7.92 (d, $J=8.32$ Hz, 1H, H6), 7.78 (d, $J=8.39$ Hz, 1H, H9), 7.59 (t, $J=1.24, 1.30$ Hz, 1H, H7), 7.46 (t, $J=1.22, 6.78$ Hz, 1H, H8), 7.42 (s, 1H, H10), 5.45 (d, $J=4.30$ Hz, 1H, H2), 2.29 (m, 1H, CH), 1.18 (d, $J=6.92$ Hz, 6H, $2 \times CH_3$); ^{13}C NMR (50 MHz, $CDCl_3$) δ 162.8 (CO), 153.4 (C-Ar), 137.4 (C-Ar), 132.7 (C5), 129.6 (C6&C9), 129.3 (C-Ar), 127.0 (C7), 125.5 (C8), 114.8 (C-Ar), 112.2 (C10), 104.9 (C2), 31.9 (CH), 16.1 ($2 \times CH_3$); MS m/z 242 (12), 171 (16), 170 (100), 142 (48), 114 (24); Anal. Calc. for $C_{15}H_{14}O_3$: C, 74.36, H, 5.82. Found: C, 74.42; H, 5.64.

2-Butyl 4-oxo-1,3-(b)-naphthodioxane 5e. 3 d, ($R_f=0.39$), (83%), colourless crystals (diethyl ether), m.p. 85-86 °C. IR (Nujol) 2850.8s, 2724.7w, 1762.6m, 1744.7w, 1637.4m, 1608.6w, 1462.8s, 1377.2s, 1270.9m, 1249.8m, 1202.0m, 1137.8w, 1087.5w, 1004.4w, 970.9m, 914.0w, 791.2w, 770.2m, 722.2s cm^{-1} ; 1H NMR (200 MHz, $CDCl_3$) δ 8.63 (s, 1H, H5), 7.93 (d, $J=7.59$ Hz, 1H, H6), 7.79 (d, $J=7.59$ Hz, 1H, H9), 7.62 (t, $J=1.28, 1.30$ Hz, 1H, H7), 7.46 (d, $J=5.50$ Hz, 1H, H8), 7.41 (s, 1H, H10), 5.68 (t, $J=5.07, 5.01$ Hz, 1H, H2), 2.09 (m, 2H, CH_2), 1.60 (m, 2H, CH_2), 1.43 (m, 2H, CH_2), 0.99 (t, $J=7.08$ Hz, 3H, CH_3); ^{13}C NMR (50 MHz, $CDCl_3$) δ 162.5 (CO), 153.2 (C-Ar), 137.2 (C-Ar), 132.6 (C5), 129.6 (C6), 129.5 (C9), 126.9 (C7), 125.4 (C8), 114.7 (C-Ar), 112.1 (C10), 102.5 (C2), 33.4 (CH_2), 24.9 (CH_2), 22.2

($\underline{\text{CH}}_2$), 13.8 ($\underline{\text{CH}}_3$); MS m/z 256 (14), 171 (17), 170 (100), 142 (56), 114 (50), 115 (20), 113 (15); Anal. Calc. for $\text{C}_{16}\text{H}_{16}\text{O}_3$: C, 74.98. H, 6.29. Found: C, 73.79; H, 6.97.

2-Trichloromethyl 4-oxo-1,3-(b)-naphthodioxane 62f. 0.5 h, ($R_f=0.30$), (45%), pale yellow crystals (diethyl ether), m.p. 179-180 °C. IR (Nujol) 3433.3b, 2921.5s, 1753.6m, 1632.1m, 1609.0w, 1462.6s, 1377.1s, 1341.5m, 1270.0w, 1241.4m, 1203.9m, 1141.5m, 1099.4w, 1059.8w, 1015.8m, 910.5w, 882.2w, 864.4w, 835.4m, 765.9m, 722.2m cm^{-1} ; ^1H NMR (300 MHz, CDCl_3) δ 8.66 (s, 1H, H5), 7.96 (d, $J=8.34$ Hz, 1H, H6), 7.83 (d, $J=8.25$ Hz, 1H, H9), 7.65 (t, $J=6.97$, 7.07 Hz, 1H, H7), 7.58 (s, 1H, H10), 7.52 (t, $J=8.10$, 7.02 Hz, 1H, H8), 5.95 (s, 1H, H2); ^{13}C NMR (50 MHz, CDCl_3) δ 159.2 (CO), 150.9 ($\underline{\text{C}}\text{-Ar}$), 137.5 ($\underline{\text{C}}\text{-Ar}$), 133.1 (C5), 130.3 (C6), 129.7 (C9), 129.7 ($\underline{\text{C}}\text{-Ar}$), 127.2 (C7), 126.3 (C8), 113.3 ($\underline{\text{C}}\text{-Ar}$), 112.9 (C10), 100.9 (C2), 94.4 ($\underline{\text{C}}\text{Cl}_3$); MS m/z 316 (9), 200 (9), 199 (65), 171 (33), 170 (100), 142 (74), 115 (37), 114 (81), 113 (35), 88 (22), 86 (11), 63 (23); Anal. Calc. for $\text{C}_{13}\text{H}_7\text{O}_3\text{Cl}_3$: C, 49.17. H, 2.22. Found: C, 49.38; H, 2.21.

2-Cinnamal 4-oxo-1,3-(b)-naphthodioxane 5g. 3 d, ($R_f=0.32$), (8%), white needles (diethyl ether), m.p. 163-164 °C. IR (Nujol) 3329.6w, 2926.0s, 1729.7m, 1711.8m, 1693.9m, 1668.9m, 1637.8m, 1536.4m, 1463.0s, 1377.1s, 1254.6m, 1207.5w, 1144.6w, 1050.0w, 1018.3w, 979.6m, 953.4m, 879.4w, 772.6w, 722.3m, 693.6w cm^{-1} ; ^1H NMR (300 MHz, CDCl_3) δ 8.67 (s, 1H, H5), 7.94 (d, $J=8.36$ Hz, 1H, Ha), 7.80 (d, $J=7.69$ Hz, 1H, H9), 7.60 (t, $J=1.30$, 7.03 Hz, 1H, H7), 7.49 (m, 5H, Ph), 7.37 (t, $J=1.64$, 1.69 Hz, 1H, H8), 7.35 (s, 1H, H10), 7.06 (d, $J=15.95$ Hz, 1H, H6), 6.45 (dd, $J=5.24$, 37.92, 5.13 Hz, 1H, Hb), 6.27 (d, $J=1.16$ Hz, 1H, H2); ^{13}C NMR (50 MHz, CDCl_3) δ 162.2 (CO), 152.9 ($\underline{\text{C}}\text{-Ar}$), 137.5 ($\underline{\text{C}}\text{-Ar}$), 136.8 (Ca), 134.9 ($\underline{\text{C}}\text{-Ar}$), 132.9 (C5), 129.8 (C6), 129.7 (C9), 129.4 ($\underline{\text{C}}\text{-Ar}$), 129.2 ($\underline{\text{C}}\text{H-Ph}$), 128.8 ($2\times\underline{\text{C}}\text{H-Ph}$), 127.2 ($2\times\underline{\text{C}}\text{H-Ph}$), 127.1 (C7), 125.7 (C8), 121.2 (Cb), 114.9 ($\underline{\text{C}}\text{-Ar}$), 112.6 (C10), 100.4 (C2); HRMS calc. for $\text{C}_{20}\text{H}_{14}\text{O}_3$: m/z 302.0943, found 302.0948; MS m/z 303.1 ($\text{M}+\text{H}$) $^+$.

2-Isopropylidene glycerol 4-oxo-1,3-(b)-naphthodioxane 7. 3 d, ($R_f=0.80$), (26%), colorless crystals (diethyl ether), m.p. 163-164 °C, $[\alpha]_D^{20}$ 14.192 (c 2.5, CHCl_3). IR (Nujol) 2925.3s, 2280.8w, 1749.1m, 1637.1m, 1462.6s, 1377.1s, 1347.1m, 1303.8m, 1252.1w, 1210.6m, 1151.4w, 1080.9w, 1019.6m, 889.6w, 843.1w, 775.9w, 722.0m cm^{-1} ; ^1H NMR (300 MHz, CDCl_3) δ 8.63 (s, 1H, H5), 7.93 (d, $J=8.28$ Hz, 1H, H6), 7.78 (d, $J=8.28$ Hz, 1H, H9), 7.61 (t, $J=1.16$ Hz, 1H, H7), 7.48 (t, $J=7.07$ Hz, 1H, H8), 7.44 (s, 1H, H10), 5.69 (d, $J=4.35$ Hz, 1H, H2), 4.52 (m, 1H, $\underline{\text{C}}\text{H}$), 4.29 (m, 2H, $\underline{\text{C}}\text{H}_2$), 1.50 (d, $J=33.80$ Hz, 6H, $2\times\underline{\text{C}}\text{H}_3$); ^{13}C NMR (50 MHz, CDCl_3) δ 161.3 (CO), 152.5 ($\underline{\text{C}}\text{-Ar}$), 137.3 ($\underline{\text{C}}\text{-Ar}$), 132.9 (C5), 129.9 (C6), 129.7 (C9), 129.5 ($\underline{\text{C}}\text{-Ar}$), 127.1 (C7), 125.8 (C8), 114.6 ($\underline{\text{C}}\text{-Ar}$), 112.5 (C10), 110.9 ($\underline{\text{C}}\text{-iPr}$), 99.8 (C2), 75.02 ($\underline{\text{C}}\text{H}$), 64.6 ($\underline{\text{C}}\text{H}_2$), 26.3 ($\underline{\text{C}}\text{H}_3$), 25.5 ($\underline{\text{C}}\text{H}_3$); MS m/z 301.2 ($\text{M}+\text{H}$) $^+$; Anal. Calc. for $\text{C}_{17}\text{H}_{16}\text{O}_5$: C, 67.99. H, 5.37. Found: C, 68.13; H, 5.30.

2-Dihydro 4-oxo-1,3-(a)-naphthodioxane 6a. 1 d, ($R_f=0.40$), (62%), cream solid, m.p. 208-209 °C. IR (Nujol) 3329.1m, 2855.0s, 1753.2m, 1729.7m, 1712.0m, 1694.1m, 1661.0m, 1631.3m, 1578.4m, 1536.5m, 1513.9m, 1463.6s, 1377.2s, 1352.7m, 1282.2m, 1254.1w, 1220.6m, 1151.8m, 1102.8m, 1048.3m, 1029.7m, 980.3m, 922.1w, 861.7w, 820.9m, 792.2m, 762.2s, 722.4m, 698.1w, 647.9w cm^{-1} ; ^1H NMR (300 MHz, CDCl_3) δ 8.17 (d, $J=7.59$ Hz, 1H, H5), 7.87 (d, $J=8.69$ Hz, 1H, H6), 7.84 (d, $J=7.95$ Hz, 1H, H10), 7.66 (d, $J=1.27$ Hz, 1H, H7), 7.58 (m, 2H, H8&H9), 5.84 (s, 2H, $\underline{\text{C}}\text{H}_2$); ^{13}C NMR (50 MHz, CDCl_3) δ 161.6 (C=O), 156.9 ($\underline{\text{C}}\text{-Ar}$), 137.2 ($\underline{\text{C}}\text{-Ar}$), 130.1 (C5), 127.9 (C6), 126.9 (C10), 123.7 (C7), 123.0 (C8),

129.9 (C-Ar), 122.7 (C9), 109.0 (C-Ar), 91.2 (C2); HRMS calc. for C₁₂H₈O₃: *m/z* 200.0473, found 200.0488; MS *m/z* 201 (M+1)⁺.

2-Ethyl 4-oxo-1,3-(a)-naphthodioxane 6b. 2 d, (Rf=0.42), (38%), colourless crystals (diethyl ether), m.p. 81-82 °C. IR (Nujol) 2846.7s, 2724.6w, 1759.2m, 1721.2m, 1631.2m, 1581.3m, 1513.9m, 1463.3s, 1376.8s, 1311.3m, 1281.3m, 1247.7m, 1213.1m, 1141.7w, 1020.6m, 961.5m, 934.9m, 889.8m, 821.1m, 791.8m, 763.2m, 722.3m cm⁻¹; ¹H NMR (200 MHz, CDCl₃) δ 8.25 (d, J=0.62 Hz, 1H, H5), 7.87 (dd, J=8.69, 6.18 Hz, 2H, H6&H10), 7.68 (d, J=1.48 Hz, 1H, H7), 7.59 (m, 2H, H8&H9), 5.75 (t, J=4.93, 4.97 Hz, 1H, H2), 2.23 (m, 2H, CH₂), 1.25 (t, J=7.47, 7.56 Hz, 3H, CH₃); ¹³C NMR (50 MHz, CDCl₃) δ 162.7 (C=O), 156.8 (C-Ar), 137.3 (C-Ar), 129.9 (C5), 127.9 (C10), 126.8 (C6), 123.7 (C7), 123.1 (C9), 122.8 (C-Ar), 122.7 (C8), 108.6 (C-Ar), 102.5 (C2), 26.9 (CH₂), 7.4 (CH₃); MS *m/z* 228 (11), 171 (15), 170 (100), 115 (19), 114 (91), 113 (27), 88 (18), 63 (17); Anal. Calc. for C₁₄H₁₂O₃: C, 73.67. H, 5.30. Found: C, 73.87; H, 5.38.

2-Isopropyl 4-oxo-1,3-(a)-naphthodioxane 6c. 2 d, (Rf=0.40), (32%), colourless crystals (diethyl ether), m.p. 69-70 °C. IR (Nujol) 2924.4s, 1757.9m, 1720.6m, 1630.0m, 1581.0m, 1513.7m, 1462.8s, 1377.0s, 1294.0m, 1277.0m, 1248.5m, 1217.1m, 1133.8m, 1111.0m, 1051.7m, 1020.1m, 984.2m, 957.7m, 867.0w, 820.4m, 790.1m, 724.3m, 649.3w cm⁻¹; ¹H NMR (200 MHz, CDCl₃) δ 8.23 (d, J=0.85 Hz, 1H, H5), 7.88 (dd, J=8.66, 7.67 Hz, 2H, H6&H10), 7.70 (d, J=1.46 Hz, 1H, H7), 7.58 (m, 2H, H8&H9), 5.56 (d, J=4.50 Hz, 1H, H2), 2.41 (m, 1H, CH), 1.26 (d, J=5.27 Hz, 6H, 2xCH₃); ¹³C NMR (50 MHz, CDCl₃) δ 162.8 (C=O), 156.9 (C-Ar), 137.3 (C-Ar), 129.9 (C5), 128.0 (C10), 126.8 (C6), 123.8 (C7), 123.2 (C9), 122.7 (C-Ar), 122.6 (C8), 108.6 (C-Ar), 104.9 (C2), 31.9 (CH-ⁱPr), 16.3 (CH₃), 16.2 (CH₃); MS *m/z* 242 (9), 171 (15), 170 (100), 115 (12), 114 (43), 113 (12), 72 (9); Anal. Calc. for C₁₅H₁₄O₃: C, 74.36. H, 5.82. Found: C, 74.14; H, 5.71.

2-Butyl 4-oxo-1,3-(a)-naphthodioxane 6d. 2 d, (Rf=0.35), (38%), colourless crystals (diethyl ether), m.p. 60-62 °C. IR (Nujol) 2851.0s, 1757.7s, 1633.1m, 1582.1m, 1514.0m, 1463.2s, 1376.9s, 1278.6m, 1208.9m, 1138.6w, 1108.3w, 1021.8w, 970.2w, 823.8m, 793.3w, 762.5m, 722.3m cm⁻¹; ¹H NMR (200 MHz, CDCl₃) δ 8.24 (d, J=0.66 Hz, 1H, H5), 7.87 (dd, J=8.67, 5.94 Hz, 2H, H6&H10), 7.84 (d, J=1.51 Hz, 1H, H7), 7.63 (m, 2H, H8&H9), 5.78 (t, J=5.1, 5.14 Hz, 1H, H2), 2.20 (m, 2H, CH₂), 1.66 (m, 2H, CH₂), 1.48 (m, 2H, CH₂), 1.00 (t, J=7.17, 7.21 Hz, 3H, CH₃); ¹³C NMR (50 MHz, CDCl₃) δ 162.6 (C=O), 156.7 (C-Ar), 137.2 (C-Ar), 129.9 (C5), 127.9 (C10), 126.7 (C6), 123.7 (C7), 123.1 (C-Ar), 122.6 (C9), 122.3 (C8), 108.6 (C-Ar), 101.8 (C2), 33.2 (CH₂), 25.1 (CH₂), 22.3 (CH₂), 13.8 (CH₃); MS *m/z* 256 (16), 171 (16), 170 (100), 115 (11), 114 (42), 113 (10); Anal. Calc. for C₁₆H₁₆O₃: C, 74.98. H, 6.29. Found: C, 75.05; H, 6.37.

2-Isopropylidene glycerol 4-oxo-1,3-(a)-naphthodioxane 8. 1 d, (Rf = 0.22), (65%), colourless crystals (diethyl ether), m.p. 105-106 °C, [α]_D⁰ 4.9 (C 3, CHCl₃). IR (Nujol) 3329.6m, 2922.4s, 2853.8s, 1729.4m, 1711.7m, 1694.1m, 1680.9m, 1536.4m, 1462.7s, 1377.0s, 1291.0w, 1254.0m, 1164.6w, 1054.3w, 979.6m, 763.7w, 722.2m, 702.0w cm⁻¹; ¹H NMR (200 MHz, CDCl₃) δ 8.22 (d, J=0.90 Hz, 1H, H5), 7.89 (m, 2H, H6&H10), 7.72 (d, J=5.43 Hz, 1H, H7), 7.63 (m, 2H, H8&H9), 5.83 (d, J=4.09 Hz, 1H, H2), 4.62 (m, 1H, CH), 4.38 (m, 2H, CH₂), 1.55 (d, J=28.04 Hz, 6H, 2xCH₃); ¹³C NMR (50 MHz, CDCl₃) δ 161.4 (C=O), 137.4 (C-Ar), 130.2 (C5), 128.1 (C10), 127.1 (C6), 123.7 (C7), 123.3 (C9), 123.1 (C-Ar), 122.7 (C8), 111.0 (C-Ar), 108.8 (C-Ar), 99.8 (C2), 95.4 (C-ⁱPr), 74.9 (CH), 64.6 (CH₂),

26.5 ($\underline{\text{C}}\text{H}_3$), 25.2 ($\underline{\text{C}}\text{H}_3$); HRMS calc. for $\text{C}_{17}\text{H}_{16}\text{O}_5$: m/z 300.0998, found 300.1008; MS m/z 301.1 ($\text{M}+\text{H}$)⁺.

References

1. Perlmutter, P.; Puniani, E. *Tetrahedron Lett.* **1996**, *37*, 1715.
2. Jackson, D. Y. *Synth. Commun.* **1988**, *18*, 337.
3. Kocienski, P. J. *Protecting Groups* Thieme, Stuttgart, 1994.
4. Khan, A. A.; Emslie, N. D.; Drewes, S. E.; Field, J. S.; Ramesar, N. *Chem. Ber.* **1993**, *126*, 1477.
5. Evans, J. C.; Klix, R. C.; Bach, R. D. *J. Org. Chem.* **1988**, *53*, 5519.
6. Jadhav, G. V.; Thakkar, R. M. *J. Univ. Bombay Sect. A* **1949**, *18*, 29.

Boontheung, P. & Perlmutter, P. (1998) A highly-efficient synthesis of benzoxazine-2, 4-diones.
Tetrahedron Letters, v. 39(17), pp. 2629-2630

NOTE:

This publication is included after page 199 in the print copy
of the thesis held in the University of Adelaide Library.

It is also available online to authorised users at:

[http://doi.org/10.1016/S0040-4039\(98\)00223-8](http://doi.org/10.1016/S0040-4039(98)00223-8)

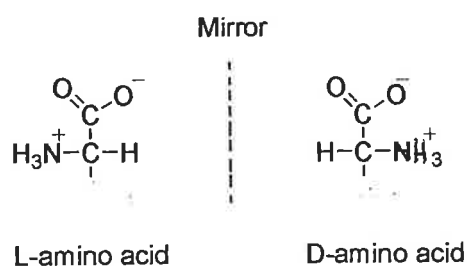


Figure A.2: *A pair of enantiomers*

All amino acid except glycine can exist in D and L forms. Glycine does not have chirality because two of the groups on the α -carbon are H.

A.1.2 D-amino acid containing peptides

Most amino acids found in peptides or proteins occur in the L-configuration at the α -carbon atom. No one knows why this is the case. It is possibly L-amino acids have no obvious inherent superiority over their D isomers for biological function¹. D-amino acids are not involved in the metabolic pathways of eukaryotic organisms, although it was demonstrated that D-amino acids are used for certain purposes in unicellular organisms. For example, the cell wall of bacteria contains D-alanine and D-glutamic acid, while D-tyrosine is a constituent of the wall of yeast spores². Moreover, antibiotics such as penicillins contain D-valine moiety and cycloserine derived from D-serine and gramicidin S contains D-phenylalanine in the structure of cyclic decapeptide³.

In additional, D-amino acids have been detected in a variety of peptides synthesized by animal cells. These are opiate and antimicrobial peptides from amphibian skin, neuropeptides from snail ganglia, a hormone from crustacean and a constituent of spider

venom. The D-amino acids are derived from the corresponding L forms by a post-translational modification, the mechanism of which is still unclear⁴. An example of D-amino acid containing peptides in animal cells is shown in *Table A.1*.

Table A.1: An example of D-amino acid containing peptides^a

Peptides	Sequence	Source	References
Dermorphin	Y A FGYPS-NH ₂	<i>Phyllomedusa sauvagei</i>	5
Deltorphin A	Y M FHLMD-NH ₂	<i>Phyllomedusa bicolor</i>	6
Deltorphin S	Y A FXaaVVG-NH ₂ ^b	<i>Phyllomedusa bicolor</i>	7
Bombinin H3	I I GPVLGMVGSALG G LLKKI-NH ₂	<i>Bombina variegata</i>	8
Bombinin H4	L I GPVLGLVGSALG G LLKKI-NH ₂	<i>Bombina variegata</i>	8
Bombinin H5	I I GPVLGLVGSALG G LLKKI-NH ₂	<i>Bombina variegata</i>	8
Bombinin H7	I L GPILGLVSNALG G LL-NH ₂	<i>Bombina orientalis</i>	9
Fulicin	F N EF-NH ₂	<i>Achatina fulica</i>	10

Note: (a) D-amino acids are boldfaced. **I**, allo-isoleucine. (b) Xaa is either Asp or Glu.

A.1.3 Configuration determination of amino acid residues

Several methods have been adopted to determine the configuration of amino acid residues in these peptides such as compare the retention time of HPLC or the biological activity between the isolated peptide and the synthesized optically active peptides¹¹ and D-amino acid oxidase assay¹¹. Moreover, the combined use of Edman degradation and amino acid configuration analysis after acid hydrolysis of peptides was also reported for the configuration determination of amino acid residues¹². The combination of HPLC and mass spectrometry has also used for determination of the absolute configuration of constituent amino acids in peptide¹³. However, there is no reported on the configuration determination of amino acids in peptides by mass spectrometry alone. To date, the distinction of amino acid enantiomers by use of chiral crown ethers¹⁴ or cyclodextrins¹⁵ as host molecules and

the detection of the formed diastereomeric complex by mass spectrometry has attracted a lot of attention.

A.1.4 References

- 1) Mathews, C. K.; van Holde, K. E. *Biochemistry*; The Benjamin/Cummings: Redwoodcity, California, 1990, p 135.
- 2) Kreil, G. *J. Biol. Chem.* **1994**, *269*, 10967.
- 3) Kleinkauf, H.; Dohren, H. V. *Eur. J. Biochem.* **1996**, *236*, 335.
- 4) Simmaco, M.; Mignogna, G.; Barra, D. *Biopolymers (Peptide Science)* **1998**, *47*, 435.
- 5) Montecucchi, P. C.; Castiglione, R. D.; Piani, S.; Gozzini, L.; Erspamer, V. *Int. J. Pept. Prot. Res.* **1981**, *17*, 275.
- 6) Kreil, G.; Barra, D.; Simmaco, M.; Erspamer, V.; Erspamer, G. F.; Negri, L.; Severini, C.; Corsi, R.; Melchiorri, P. *Eur. J. Pharm.* **1989**, *162*, 123.
- 7) Erspamer, V.; Melchiorri, P.; Falconieri-Erspamer, G.; Negri, L.; Corsi, R.; Severini, C.; Barra, D.; Simmaco, M.; Kreil, G. *Proc. Natl. Acad. Sci. USA* **1989**, *86*, 5188.
- 8) Mignogna, G.; Simmaco, M.; Kreil, G.; Barra, D. *EMBO J.* **1993**, *12*, 4829.
- 9) Gibson, B. W.; Tang, D.; Mandrell, R.; Kelly, M.; Spindel, E. R. *J. Biol. Chem.* **1991**, *266*, 23103.
- 10) Ohta, N.; Kubota, I.; Takao, T.; Shimonishi, Y.; Yasud-Kamatani, Y.; Minakata, H.; Nomoto, K.; Muneoka, Y.; Kobayashi, M. *Biochem. Biophys. Res. Commun.* **1991**, *178*, 486.
- 11) Iida, T.; Santa, T.; Toriba, A.; Imai, K. *Biomed. Chromatogr.* **2001**, *15*, 319.
- 12) Scaloni, A.; Simmaco, M.; Bossa, F. *Anal. Biochem.* **1991**, *197*, 305.
- 13) Fujii, K.; Ikai, Y.; Oka, H.; Suzuki, M.; Harada, K. *Anal. Chem.* **1997**, *69*, 5146.

- 14) Sawada, M.; Takai, Y.; Yamada, H.; Nishida, J.; Kaneda, T.; Arakawa, R.; Okamoto, M.; Hirose, K.; Tanaka, T.; Naemura, K. *J. Chem. Soc. Perkin Trans* **1998**, *2*, 701.
- 15) Ramirez, J.; He, F.; Lebrilla, C. B. *J. Am. Chem. Soc.* **1998**, *120*, 7387.

A.2 Table of Common Amino Acids and their Masses

Amino Acid	Symbol	Mass
Glycine	Gly - G	57.06
Alanine	Ala - A	71.08
Serine	Ser - S	87.08
Proline	Pro - P	97.12
Valine	Val - V	99.14
Threonine	Thr - T	101.11
Cysteine	Cys - C	103.14
Isoleucine	Ile - I	113.17
Leucine	Leu - L	113.17
Asparagine	Asn - N	114.11
Aspartic acid	Asp - D	115.09
Glutamine	Gln - Q	128.14
Lysine	Lys - K	128.18
Glutamic acid	Glu - E	129.12
Methionine	Met - M	131.21
Histidine	His - H	137.15
Phenylalanine	Phe - F	147.18
Arginine	Arg - R	156.20
Tyrosine	Tyr - Y	163.18
Trptophan	Trp - W	186.21